Identification of Blast Resistance Genes in Aegilops tauschii and Triticum aestivum.

Thomas Edward O'Hara
100202802

A thesis submitted to the University of East Anglia for the degree of Doctor of Philosophy (PhD)

John Innes Centre
Department of Crop Genetics
Norwich Research Park, Colney Lane, Norwich, NR4 7UH

March 2023

I. ABSTRACT

As the world's most widely grown crop, wheat contributes to 20% of the daily protein and calorie intake for 4.5 billion people. Wheat blast disease, caused by the fungal pathogen *Magnaporthe oryzae* pv. *tritici* (*MoT*), is a relatively recent disease threatening global wheat production. In February 2016, wheat blast made the headlines with a severe outbreak reported in Bangladesh. The presence of wheat blast in Bangladesh is of immense concern as it could act as a gateway for wheat blast to spread throughout South Asia. Despite continuous breeding efforts over the past 30 years to improve blast resistance in wheat, only a handful of resistance genes have been discovered. Moreover, wheat blast resistance has been overcome in some regions in Brazil. It is therefore crucial that new resistance genes are discovered to control this devastating disease. Crop wild relative species are potential sources of novel resistances, as they often have greater genetic variation than cultivated crops.

The resistance genes *Rmg7* and *Rmg8* map to 2A and 2B respectively in wheat and both recognise the *Avr-Rmg8* effector. In the present study, a rapid GWAS based gene cloning approach was used to identify D genome resistance against the *Avr-Rmg8* effector using a diversity panel of *Aegilops tauschii*, the D genome progenitor of hexaploid wheat. An association spanning 162kb on chromosome 7D, containing seven candidates in the resistant haplotype was investigated. Landraces also capture genetic diversity lost through breeding. Similar methods were used to exploit the genetic diversity within 320 Watkins landrace accessions. This resulted in the identification and validation of a serine/threonine kinase as *Rmg7*; the first *R* gene cloned for wheat blast. The gene was identical to the race specific gene wheat powdery mildew (*Blumeria graminis* f.sp. *tritici*) gene *Pm4*. The work carried out within this study demonstrates the power of combining genome-based GWAS with isolate-specific phenotyping in the identification of loci and genes conferring resistance to *MoT*.

II. ACKNOWLEDGEMENTS

Firstly, I would like to express my immense gratitude to my supervisors Paul Nicholson, Brande Wulff and Cristobal Uauy for their continued support, encouragement and expertise over the past four and a half years. I would especially like to thank Andrew Steed, Dr Rachel Goddard, Roshani Badgami, Dr Catherine Chinoy and Martha Nicholson for their invaluable help with the detached leaf and spike assays, without which this work would not have been possible.

I am also grateful to Dr Sreya Ghosh, Dr Clemence Marshal, Dr Sanu Arora, Dr Kumar Gaurav and Dr Burkhard Steuernagel for their bioinformatics help and to Francesca Minter and Matt Downie for sharing their time and expertise. Additionally, I would like to thank Jesus Quiroz-Chavez for generously running the IBSpy analysis despite being busy writing his own thesis. Members of the Nicholson and Brown groups past and present welcomed me into the legendary and religiously observed tea-time discussions; an honour and a privilege. I was fortunate to share this time with fellow students and friends for life Alan Houghton, Dr Lauran Mills, Dr Jonathan Ford, Dr Ocean Ellis, David Gilbert, Joshua Joyce, Samuel Warner, Dr Sebastian Samwald, Kelly Robinson, Dr Miguel Santos and Dr Amber Hafeez, who made my time in and outside of work so enjoyable. Finally, I would like to thank my family for their unwavering belief in me, and Chris, whose love and support I could not do without.

III. ABBREVIATIONS

°C	degrees Celsius
[Chromosome]L	long arm of chromosome
%	percentage
aa	amino acid
AgRenSeq	association genetics with *resistance* gene enrichment sequencing
Avr	pathogen avirulence genes
A-WSOW	*Ae. tauschii*-wheat synthetic octoploid wheat
bp	base pair
CC	coiled coil
CIMMYT	International Maize and Wheat Improvement Center
CFEM	conserved fungi-specific extracellular membrane spanning
CL2	containment level two
cm	centimetre
CWR	crop wild relatives
DAMP	damage-associated molecular patterns
dH_2O	distilled water
DNA	deoxyribonucleic acid
dsDNA	double stranded DNA
dpi	days post infection
DLA	detached leaf assay
DSA	detached spike assay
EMS	ethyl methanesulfonate
ER	endoplasmic reticulum
EIHM	extra-invasive hyphal membrane
ETI	effector-triggered immunity
ETS	effector-triggered susceptibility
Gb	gigabase
GPCRs	G protein-coupled receptors
GTPases	guanosine triphosphatases
HMA	heavy metal-associated
HR	hypersensitive response
HVG	spike virulence group
IBS	identical by state
IBSpy	Identity By State in python
IGV	Integrative Genomics Viewer
INDEL	insertion-deletion
IH	Invasive hyphae
JIC	John Innes Centre
JG30	rice cultivar Jingang 30
kb	kilobases
KDE	Kernel Density Estimation

kg	kilogram
L	litre
L1	*Ae. tauschii* lineage 1
L2	*Ae. tauschii* lineage 2
L3	*Ae. tauschii* lineage 3
LD	linkage disequilibrium
LRR	leucine rich repeat
LRR-RLK	leucine rich repeat receptor like protein
m	metre
MAMP	microbial-associated molecular patterns
Mb	megabases
ml	millilitre
MLMG	multilocus microsatellite genotype
Mo	*Magnaporthe oryzae*
MoA	*Magnaporthe oryzae* pv. *Avena*
MoE	*Magnaporthe oryzae* pv. *Elusine*
MoL	*Magnaporthe oryzae* pv. *Lolium*
MoO	*Magnaporthe oryzae* pv. *Oryza*
MoS	*Magnaporthe oryzae* pv. *Setaria*
MoSt	*Magnaporthe oryzae* pv. *Stenotaphrum*
MoT	*Magnaporthe oryzae* pv. *Triticum*
MoU	*Magnaporthe oryzae* pv. *Urochloa*
MPa	megapascal
NBS	nucleotide binding site
Nep1	necrosis and ethylene-inducing peptide 1
NLPs	necrosis and ethylene-inducing peptide 1 like proteins
NGS	next generation sequencing
NIAB	National Institute of Agricultural Botany
NIL	near-isogenic line
NLR	nucleotide-binding leucine-rich repeat receptor
NRPS	non-ribosomal peptide synthase
ORF	open reading frame
OWWC	Open Wild Wheat Consortium
PAMP	pathogen-associated molecular patterns
PCA	principle component analysis
PEX	*P. infestans* extracellular
PexRD	*P. infestans* extracellular Arginine-(any AA)-Leucine-Arginine-DEER
Pmk1	Pathogenicity MAP Kinase 1
PKS	polyketide synthase
PRR	pattern recognition receptor
PRT_C	plant phosphoribosyltransferase C-terminal domain
PTI	pamp triggered immunity
QoI	quinone outside inhibitor

R	disease *resistance* gene
rcf	relative centrifugal force
RefSeq	reference sequence
RenSeq	*R* gene enrichment sequencing
RLK	receptor-like kinase
RLP	receptor-like protein
Rmg	resistance to *Magnaporthe grisea*
RNA	ribonucleic acid
RNAseq	RNA sequencing
RP	pool of DNA from resistant accessions
RPW8	RESISTANCE TO POWDERY MILDEW 8
RQA	reference-quality pseudomolecule assembly
RXLR	Arginine-(any Aaa)-Leucine-Arginine
S	disease *susceptibility* gene
SA	salicylic acid
SOW	synthetic octoploid wheat
SP	pool of DNA from susceptible accessions
STK	serine/threonine protein kinase
S_TKc	serine/threonine protein kinase catalytic domain
SNB	*Septoria nodorum* blotch
SHW	synthetic hexaploid wheat
SNP	single nucleotide polymorphism
spp.	species
SSR	simple sequence repeats
SVG	seedling virulence group
SWRH	Susceptible with resistant haplotype
TIR	Toll, interleukin-1 receptor, resistance protein
TKP	tandem kinase-pseudokinase
TM	transmembrane
WGS	whole genome shotgun
WTK	wheat tandem kinase
WSSM	rice cultivar Wushansimiao

IV. TABLE OF CONTENTS

V. TABLE OF FIGURES

Figure 39: Representative leaves from the differential temperature leaf assay with NO6047+*Avr-Rmg8* and SRA, for Arina, Mattis, Claire and Stanley at 20 and 26 ^{o}C. Pictures were taken at 5 and 6 dpi.

Figure 40: Cluster heat map for the IBSpy haplotype analysis of the 5.2Mb interval, using Mattis as the reference. Each 50kb window within a genotype is represented as a coloured square; the darker the colour the closer that region is to being identical by state to Mattis (purple arrow). WATDE0571 is resistant but lacks the last 200kb of the *Region 1* (blue box), and WATDE048 and WATDE0720 are susceptible but lack the first 400kb of *Region 2* (yellow box). *T. timopheevii* is shown in the green. Resistant/susceptible accessions are highlighted in green/red respectively.

Figure 41: Representative expression profile of *MA4* for the Mattis RNAseq data mapped to Mattis. Red arches within the 'Splice junctions' track show predicted intron/exon boundaries on the forward strand.

Figure 42: Expression profile of *MA5* for the Mattis RNAseq data mapped to Mattis. Red arches within the 'Splice junctions' track show predicted intron/exon boundaries on the forward strand.

Figure 43: Representative expression profiles of (**A**) *MA6* (**B**) *MA7* for the Mattis RNAseq data mapped to Mattis. Red and blue arches within the 'Splice junctions' track show predicted intron/exon boundaries on the forward and reverse strand respectively. Black rectangles below the 'Splice junctions' track indicate regions where read covered exceeded 100 reads and so was down-sampled.

Figure 44: Representative expression profiles of (**A**) *MA8* (**B**) *NLR2* for the Mattis RNAseq data mapped to Mattis. Red and blue arches within the 'Splice junctions' track show predicted intron/exon boundaries on the forward and reverse strand respectively. Black rectangles below the 'Splice junctions' track indicate regions where read covered exceeded 100 reads and so was down-sampled.

Figure 45: Domain structure of the two transcripts of MA4. Both transcripts have identical predicted domains at the N terminus: PKc_like = Protein Kinases catalytic_like family, PknB_PASTA_kin = serine/threonine kinase with penicillin-binding protein and serine/threonine kinase associated domain family, PLN00034 = provisional mitogen-activated protein kinase kinase family. S_TKc = Serine/Threonine protein kinase catalytic domain, SPS1 = Serine/threonine protein kinase domain, STKc_IRAK = Catalytic domain of the Serine/Threonine kinases, Interleukin-1 Receptor Associated Kinases and Pkinase_Tyr = Protein tyrosine kinase domain. Transcript one has a protein kinase C conserved region (C2) at the C terminus, with a non-specific hit for a 'C2 domain third repeat found in multiple C2 domain and transmembrane region proteins' (C2C_MCTP_PRT_plant) domain. Transcript two has a similar C2 domain downstream of the STK domain, with a non-specific hit for a 'C2 domain fourth repeat found in multiple C2 domain and transmembrane region proteins' (C2D_MCTP_PRT_plant) domain. Transcript two had an additional domain at the C terminus: PRT_C = plant phosphoribosyltransferase C-terminal domain.

Figure 46: Detached leaf assay to validate the recognition of *Avr-Rmg8* by *Pm4*, using NO6047+*Avr-Rmg8* and SRA. (**A**) *Pm4b* overexpression lines in the susceptible Bobwhite background. 'Nr#' = transgenics, 'S#' = sister lines originating from the same

VI. TABLE OF TABLES

VII. TABLE OF SUPPLEMENTARY FIGURES

VIII. TABLE OF SUPPLEMENTARY TABLES

1. GENERAL INTRODUCTION

1.1 Evolution of wheat

Wheat was first cultivated approximately 12,000 years ago in the fertile crescent, an area spanning modern-day Israel, Jordan, Lebanon and Syria, into southeast Turkey and areas of Iraq and western Iran (Salamini et al. 2002). Einkorn wheat (*Triticum monococcum*), domesticated from *T. boeoticum*, was the first wheat to be cultivated and has a diploid AA genome. During the Bronze Age, cultivation of polyploid wheats were favoured, likely due to being better adapted to warmer climates and having beneficial harvesting traits such as naked seeds and soft glumes. All tetraploid species of domesticated wheat originated from the wild tetraploid *T. dicoccoides*. Bread wheat (*T. aestivum*) is an allohexaploid (6n = 42) with three subgenomes AA, BB and DD donated by three related diploid grass species (Marcussen et al. 2014).

Extensive genetic analyses comparing the genomes of progenitor species and domesticated wheat suggest that *T. aestivum* arose via sequential natural hybrid speciation events, two polyploid and one homoploid. The first polyploidisation event occurred around 0.8 million years ago between the diploid A and B genome progenitors, *T. urartu* (AA) and an unknown wheat closely related to *Aegilops speltoides* (BB) (Marcussen et al. 2014). This produced the exant tetraploid Emmer wheat lineage (*T. turgidum*; AABB) and would later give rise to pasta wheat (*T. turgidum L.* subsp*. durum*). A second polyploidisation event between *T. turgidum* and the D genome progenitor (*Ae. tauschii)* resulted in modern hexaploid bread wheat (*T. aestivum*; AABBDD) (Petersen et al. 2006). *T. aestivum* originated around 10,000 to 430,000 years ago, and only a few *Ae. tauschii* accessions are thought to have been involved (Petersen et al. 2006; Cox 1997; Marcussen et al. 2014). *Ae. tauschii* resulted from homoploid hybrid speciation between the A and B donors, approximately 5.5 million years ago (Marcussen et al. 2014).

Wheat is highly agronomically adaptable and able to grow from near arctic regions to the equator and from 0 to 4000m above sea level (NABIM 2019). As such wheat is the world's most widely grown crop and contributes 20% of the daily protein and calorie intake for 4.5 billion people, and is the primary source of carbohydrate in a majority of countries (NABIM 2019; GCARD 2012). It is grown on over 218 million hectares, yielding 759.4 million tonnes in 2017 (NABIM 2019; FAO 2019). Around 95% of wheat produced is hexaploid bread wheat (NABIM 2019; Shewry 2009). The world population is expected to reach 9 billion by 2050, with wheat demands predicted to rise by 60%. To meet this shortfall, annual yield increases must exceed 1.6%, compared to less than 1% currently. A major limiting factor to

obtaining a state of food security is disease. Oerke reported total wheat yield losses of 12.1% between 2001 and 2003, equating to 340kg/hectare, with estimated potential losses due to pathogens (including viruses) of 18-21% without disease prevention measures (Oerke 2006; Nelson 2017). Disease losses increase with attainable yield, highlighting the increasing importance of disease management as crop productivity increases. A relatively recent disease threatening global wheat production is wheat blast, caused by the ascomycete fungal pathogen *Magnaporthe oryzae*. Within the literature, *Magnaporthe oryzae*, *Pyricularia oryzae* and *Pyricularia grisea* are often used interchangeably. To maintain clarity, throughout this report I will refer to the pathogen as *Mo* (*M. oryzae*). Species adapted lineages will be denoted by *'Mo'* followed by the first letter of the host species name, for example *MoT* corresponds to *Magnaporthe oryzae Triticum*-adapted lineage.

1.2 Emergence of wheat Blast

Wheat blast was first reported on wheat in Paraná state, Southern Brazil in 1985 (Igarashi et al. 1986). Having invaded the neighbouring states of São Paulo and Mato Grosso do Sul in 1986 (Goulart, Paiva, and de Mesquita 1990), followed by Rio Grande do Sul in 1987 (Igarashi 1990), the pathogen migrated into warmer areas 1200 km north and 1700 km northwest towards Brasília and Santa Cruz in Bolivia respectively. By 2007, the disease had also spread 1200 km south west into Northern Argentina, firmly establishing the disease throughout South America (Ceresini, Castroagudin, Rodrigues, Rios, Aucique-Perez, Moreira, Croll, et al. 2018).

In February 2016, wheat blast made the headlines with severe outbreaks reported in Bangladesh (Callaway 2016). Nearly 15,000 hectares were affected across eight districts, with yields reduced by 5 - 51% (Islam et al. 2016). This was the first reported incidence of the disease in Asia, which accounts for around 42% of world wheat production (Islam, Kwang-Hyung Kim, and Jaehyuk Choi 2019). A study using phylogenomic and population genomic data concluded that the outbreak in Bangladesh in 2016 was most likely caused by isolates of a South American lineage (Islam et al. 2016). Isolates collected from Bangladesh clustered as a near clonal genotype, in stark contrast to the genetic diversity observed in South America. Blast has since been reported in a further 14 districts (Islam, Kwang-Hyung Kim, and Jaehyuk Choi 2019; Singh et al. 2021). Bangladesh shares a border of over 2000km with west Bengal, India, cutting through the lower portion of the Indio gangetic-plains (IGP) (Mottaleb et al. 2018); an intensely cultivated region that runs from West Bengal, up through North Western India to Pakistan (Erenstein and Thorpe 2011). This area adopts a wheat rice rotation system covering around 13.5 million hectares of the IGP (Samra and Kumar 2003). This may not only facilitate the spread of the disease, but also allow more inoculum to persist from one wheat growing season to another,

making epidemics more likely. In 2017 wheat blast was reported in Zambia, the first instance of the disease in Africa (Tembo et al. 2020).

1.3 Rice blast

The first report of blast disease was recorded on rice (*Oryza sativa*) in China about 400 years ago, and rice blast remains one of the most devastating diseases of rice, with 10 to 30% crop losses reported annually (Savary et al. 2000; Talbot 2003; Devanna et al. 2022). Yield losses are associated with leaf and neck infection, with neck blast causing significantly higher losses (Savary et al. 2000). The relationship between leaf and neck resistance remains unclear, however some degree of tissue specific resistance is seen, where some cultivars are relatively resistant/susceptible to the disease on one organ compared to the other. Ghatak and colleagues showed that isolates are not specialised to infect a certain tissue, and that leaf infection can act as source of inoculum for neck infection (Ghatak et al. 2013). The rice/*MoO* pathosystem is used as a model for molecular pathology (Valent 1990), and *MoO* was the first fungal plant pathogen to have its genome sequenced (Dean et al. 2005). As a consequence, many genetic analyses have been carried out to identify blast resistance in rice.

Couch et al. suggest that rice infecting stains are virulent on rice due to loss of the avirulence gene (*Avr*) *Avr-CO39*, which is common amongst strains that infect other hosts (2005). Function was disrupted in rice-infecting strains, but retained in all haplotypes from other hosts, making it a host specificity gene. As expected, most rice cultivars have *Pi-CO39,* the cognate resistance gene to *Avr-CO39* in rice (Chauhan et al. 2002; Zheng et al. 2011). They hypothesised that the domestication of rice combined with clonal propagation and strong selection pressure due to rice being grown over large continuous areas, resulted in genetic isolation and divergence from strains pathogenic to other hosts. Several studies have verified that while rice isolates can be pathogenic to wheat, wheat isolates cannot infect rice (Prabhu, Filippi, and Castro 1992; Urashima, Igarashi, and Kato 1993).

More than 500 quantitative trait loci (QTL) have been mapped in rice for blast resistance, and over 100 genes have been mapped, of which 38 have been cloned (Li et al. 2019; Devanna et al. 2022) (Wang, Ebbole, and Wang 2017). In addition, around 26 *Avr* genes have been mapped, 14 of which have been cloned. However, despite the low levels of genetic diversity within *MoO* races, resistance introduced into rice cultivars is frequently broken down by new races (Zhou et al. 2007). It has been argued that this observed breakdown of resistance could be due to deployed resistance (*R*) genes being involved in gene-for-gene interactions that are overcome by new races (Ceresini et al. 2018).

Plants rely on a two-tiered innate immune system to detect and respond to pathogens. The first uses plasma membrane associated pattern recognition receptors (PRRs) to recognise conserved microbial-/pathogen-/damage-associated molecular patterns (MAMPs/PAMPs/DAMPs). PRRs are usually either receptor-like proteins (RLPs) or receptor-like kinases (RLKs) (Ngou, Ding, and Jones 2022). Recognition of PRRs activates PAMP triggered immunity (PTI), which limits pathogenicity. Successful pathogens have evolved secreted effector molecules to evade or supress PTI, resulting in effector-triggered susceptibility (Giraud, Gladieux, and Gavrilets). In response to pathogen effectors, plants evolved nucleotide-binding leucine-rich repeat receptors (NLRs) which, on recognising a given effector, initiate effector-triggered immunity (ETI); the second tier. *Resistance* (*R*) genes constitute PRRs and NLRs that provide resistance. ETI often causes a localised hypersensitive cell death response (HR) at the point of infection (Jones and Dangl 2006). Pathogens may regain virulence by diversifying or losing the recognised effector or gaining new effectors that supress ETI, hence gene for gene interactions are often non-durable. Perception of PAMPs and effectors may be through direct (physical interaction) or indirect (recognition of modified host targets, or guardee) mechanisms (Kourelis and Van Der Hoorn 2018; Van Der Biezen and Jones 1998). In rice seven *MoO R-Avr* gene pairs have been characterised. Five interact directly (*Pi-ta*/*Avr-Pita*, *Pik*/*Avr-Pik*, *Pia*/*Avr-Pia*, *Pi-CO39*/*Avr1-CO39*, and *Pi54*/*Avr-Pi54*) and two indirectly (*Piz-t*/*AvrPiz-t* and *Pii*/*Avr-Pii*) (Devanna et al. 2022). Gene for gene interactions are often race specific. Several race specific rice genes that provide partial resistance to *MoO* have been described including *Pif* (Yunoki et al. 1970), *Pi21* (Fukuoka and Okuno 1997) and *PbL* (Zenbayashi-Sawata, Ashizawa, and Koizumi 2005). Eight *MoO R* genes give broad spectrum durable resistance: *Pi9* (Liu et al. 2002), *Pi54* (Sharma et al. 2005), *pi21* (Fukuoka et al. 2009), *Pi50* (Su et al. 2015), *Pi7* (Chaipanya et al. 2017), *Pi57* (Dong et al. 2017), *Pigm* (Deng et al. 2017) and *Ptr* (Zhao et al. 2018).

The majority of plant immune receptors encode nucleotide-binding site (NBS) domain and leucine-rich repeat proteins (NLRs) which are classified by their N-terminal domains: coiled coil (CC), Toll, interleukin-1 receptor, resistance protein (TIR), or RESISTANCE TO POWDERY MILDEW 8 (RPW8)-like CC domain (Ngou, Ding, and Jones 2022). Of the 140 plus cloned NLR *R* genes with a proposed mechanism, a majority of perceive their elicitor indirectly (Ngou, Ding, and Jones 2022). Alternatively, fusion events can integrate guardees within the open reading frame (ORF) of NLRs, giving rise to noncanonical domains; the integration model (Cesari 2018; Cesari et al. 2014). Integrated NLRs usually require a second NLR to initiate the defence response. A single NLR can interact with several guardees to enable recognition of multiple effectors, even from different pathogens (Brabham et al. 2022). Indeed the vast majority of the cloned rice blast *R* genes encode NLRs. Three CC-NLR gene pairs act via a guard mechanism: *RGA4*/*RGA5*, *Pik-1*/*Pik-2*, and *Pi5-1*/*Pi5-2* (Okuyama et al. 2011; Ashikawa et al. 2008; Lee et al. 2009; Yuan et al. 2011; Zhai et al. 2014).

Only three of the cloned *MoO R* genes encode non-NLRs. *pi21* encodes a recessive proline-rich protein with a putative heavy metal-binding domain (Chen et al. 2006; Fukuoka et al. 2009) and *Ptr* encodes a protein with four Armadillo repeats and is required for broad-spectrum resistance mediated by NLR *R* genes *Pi-ta* and *Pi-ta2* (Zhao et al. 2018). The third atypical rice blast resistance gene, *Pi-d2,* encodes a serine/threonine RLK (STK) (Chen et al. 2006). RLKs are the second largest class of *R* genes. Plant RLKs have undergone extensive gene expansions (increase in number of kinases per genome) and diversification (increase in number of domain combinations) (Dievart et al. 2020). This has resulted in many different classes of RLK, most of which contain a transmembrane domain (TM), extracellular domain and cytoplasmic kinase domain (Ngou, Ding, and Jones 2022). Kinases catalyse the transfer of phosphoryl groups, with serine/threonine phosphorylation being the most common. It is therefore reasonable to assume that many wheat blast resistance genes may also encode NLRs and RLKs.

Additional classes of *R* genes include detoxification enzymes, for example homologous genes *Hm1* and *Hm2* encode HC toxin reductase enzymes which provide resistance against the fungal pathogen *Cochliobolus carbonum*, the causal agent of southern corn leaf blight (Johal and Briggs 1992). *Hm1* and *Hm2* detoxify a cyclic tetrapeptide toxin (HC toxin) which is essential for pathogenicity. Transporter proteins can also act as *R* genes, for example the leaf rust resistance gene *Lr34* encodes an ABC transporter which transports phospholipids from the cytoplasmic to the exoplasmic membrane (Krattinger et al. 2009; Deppe et al. 2018). In barley, transgenic lines overexpressing *Lr34* show up regulation of several stress-responsive genes without being exposed to pathogens (Hulbert et al. 2007; Chauhan et al. 2015). This suggests that the transporter mimics abiotic and biotic stress exposure, activating stress response pathways which provide broad spectrum resistance. Similarly, the hexaploid wheat locus *Lr67*/*Yr46* on 4DL encodes a putative hexose sugar transporter and provides resistance against leaf and yellow rusts (Moore et al. 2005; Herrera-Foessel et al. 2011; Hiebert et al. 2010). In maize, a caffeoyl-CoA *O*-methyltransferase, *CCoAOMT2,* gives quantitative resistance to the necrotropic diseases southern leaf blight and grey leaf spot (Yang et al. 2017). *CCoAOMT2* is associated with the phenylpropanoid pathway and increased lignin synthesis, which has been positively correlated with disease resistance to many plant pathogens (Wan et al. 2021). For example the transcription factor *OsMYB30* activates expression of lignin biosynthesis-associated genes *Os4CL3* and *Os4CL5* in rice which results in the accumulation of lignin subunits G and S (Li, Wang, et al. 2020). This strengthens the sclerenchyma cell wall and prevents *MoO* penetration. Another class of *R*-gene are the WRKY-type transcription factors (Nelson et al. 2018). The WRKY domain consists of a 60 aa region containing the conserved sequence WRKYGQK at the N terminus

and a zinc-finger-like motif. *WRKY13* in rice gives partial resistance to both *MoO* and *Xanthomonas oryzae pv. Oryzae* (rice bacterial blight) (Hu et al. 2008). Additionally, the TIR-NBS-LRR type *R*-gene *RRS1-R* in *Arabidopsis* also contains a WRKY domain (Deslandes et al. 2002).

1.4 The *M. oryzae* genome

To date more than 74 *Mo* strains have had their genomes' sequenced, with an average size of 40.12 Mb and a predicted proteome of between 11,109 and 12,841 proteins (Devanna et al. 2022; Dean et al. 2005; Soanes et al. 2008). Different isolates have similar genomic sizes and are transposon-rich however some contain hundreds of isolate-specific genes and several duplication events (Zhang, Zheng, and Zhang 2016; Xue et al. 2012). Thus far over 1600 *Mo* genes have been functionally characterised, more than 10% of the *Mo* genome (Foster et al. 2021). A secretome of up to 1546 proteins has been predicted, significantly higher than closely related fungal species for example *Neurospora crassa* (Dean et al. 2005; Soanes et al. 2008; Cornell et al. 2007). The secretome includes plant cell wall degrading enzymes such as glucanses, xylanases and cutinases (Soanes et al. 2008; Soanes, Richards, and Talbot 2007) as well as putative effector proteins including a protein family with similarity to necrosis-inducing peptides from *Phytophthora infestans*, the causal agent of potato late blight, and three protein families of cysteine-rich polypeptides (Collemare et al. 2008). A recent transcriptional profiling study identified 863 genes encoding putative secreted proteins that show differential expression at specific stages of the *Mo* life cycle, 546 of which were annotated as effectors (Yan et al. 2023). Investigating the distribution of the full set of 863 potential effectors revealed that loci were present across all seven chromosomes, with statistically significant enrichment of effector loci in sub-telomeric regions. In addition to the seven chromosomes, Peng et al., found that when assembling the genome sequence of *MoT* isolate B71, some reads also formed a dispensable mini-chromosome containing repetitive sequences and sequences encoding effector genes taken from the ends of chromosomes (Peng et al. 2019). The authors suggested that the mini chromosome may contribute to the evolution of the pathogens' effector set. The *Mo* genome also contains a high proportion of genes encoding secondary metabolites including eight non-ribosomal peptide synthases (NRPSs), 22 polyketide synthases (PKSs) and ten hybrid PKS-NRPS enzymes (Collemare et al. 2008). Sixty-one G protein-coupled receptors (GPCRs) are also predicted (Dean et al. 2005). GPCRs are the biggest class of fungal cell surface receptors and are involved in sensing environmental signals (Brown et al. 2018) Of the 61 GPCRs in *Mo*, 12 contain a conserved fungi-specific extracellular membrane spanning (CFEM) domain, all of which are expressed during infection-related processes (Dean et al. 2005; Kulkarni, Kelkar, and Dean 2003). One CFEM GPCR gene, Pth11, is a virulence factor that is essential for appressorium development (DeZwaan et al. 1999). Curiously, CFEM GPCR genes are not

present in hemi-ascomycete yeasts or basidiomycete fungi and only one has been reported in *N. crassa* and *Aspergillus nidulans*, both saprophytic ascomycetes (Wilson and Talbot 2009). The abundance of extracellular GPCRs in filamentous fungi reflects the increased ability of some species such as *Mo* to sense and respond to a changing environment during the different stages of disease development.

1.5 Host specificity

Mo has over 50 wild and cultivated grass hosts, including oats (*Avena* sativa), barley (*Hordeum vulgare*) and foxtail millet (*Setaria italica*) (Castroagudín et al. 2016; Takabayashi et al. 2002; Murakami et al. 2000). *Mo* is widely classified as a single species, split into host adapted lineages with restricted host ranges, limited to members of the same genus (Gladieux, Ravel, et al. 2018). A study using whole genome data from 76 *Mo* isolates across 12 host genera, identified 10 lineages within *Mo* (Gladieux, Condon, et al. 2018). Discriminant analysis of principle components (DAPC) was carried out to infer population subdivision and then gene genealogies were created using both maximum likelihood (ML) and neighbour-joining (NJ) methods. Both trees validated lineage groupings observed from the DAPC (**Figure 1**). Gladieux et al., found that individual lineages tend to be isolated from a single host, suggesting that ecological barriers may significantly reduce gene flow between lineages (Gladieux, Condon, et al. 2018). Additionally, the fact that sexual reproduction likely takes place within host tissues (Silué and Nottéghem 1990) may contribute to the maintenance of different lineages by decreasing the amount of mating between isolates from different hosts (Giraud, Gladieux, and Gavrilets 2010). Moreover, loss of sexual fertility may also help maintain lineages. This is particularly apparent in the rice lineage which is female sterile and has a single mating type across most of its range, which would greatly reduce the chance of outcrossing with other lineages (Saleh et al. 2012).

Host species specificity is not ubiquitously upheld however, and there is conflict within the literature regarding the extent of non-host specificity and the degree to which these lineages are maintained. Many strains have been identified with broader host ranges (Kato et al. 2000; Castroagudin et al. 2017). For example, *MoT* isolates can cause blast on barley and oats and at least 12 other grass species (Urashima, Igarashi, and Kato 1993; Castroagudín et al. 2016), while *Lolium* (*MoL*) pathotypes (which include *Avena* (*MoA*) pathotypes) can infect wheat varieties that lack the host specificity gene *Rwt3* (Oh et al. 2002; Inoue et al. 2017). Previous studies suggest that matings between most pairs of lineages result in high numbers of viable ascospores and that pre or post mating reproductive barriers do not contribute to relative isolation of lineages (Kato et al. 2000; Urashima, Igarashi, and Kato 1993; Vy et al. 2014). Gladieux and colleagues found evidence supporting significant and relatively recent

gene flow and admixture between wheat and other host infecting isolates (Gladieux, Condon, et al. 2018). Many hosts of *M. oryzae* are either widely cultivated crops, such as barley and ryegrass, or are forage/weed species with wide distributions that provide niches for sexual reproduction. This may increase the chances of matings between isolates with shared host ranges, possibly facilitating gene flow between lineages. Similarly, Castroagudin et al., found evidence for high levels of historic and continuing gene flow between wheat infecting populations and grass infecting populations, biased towards transfer from grass populations into wheat populations (2017).

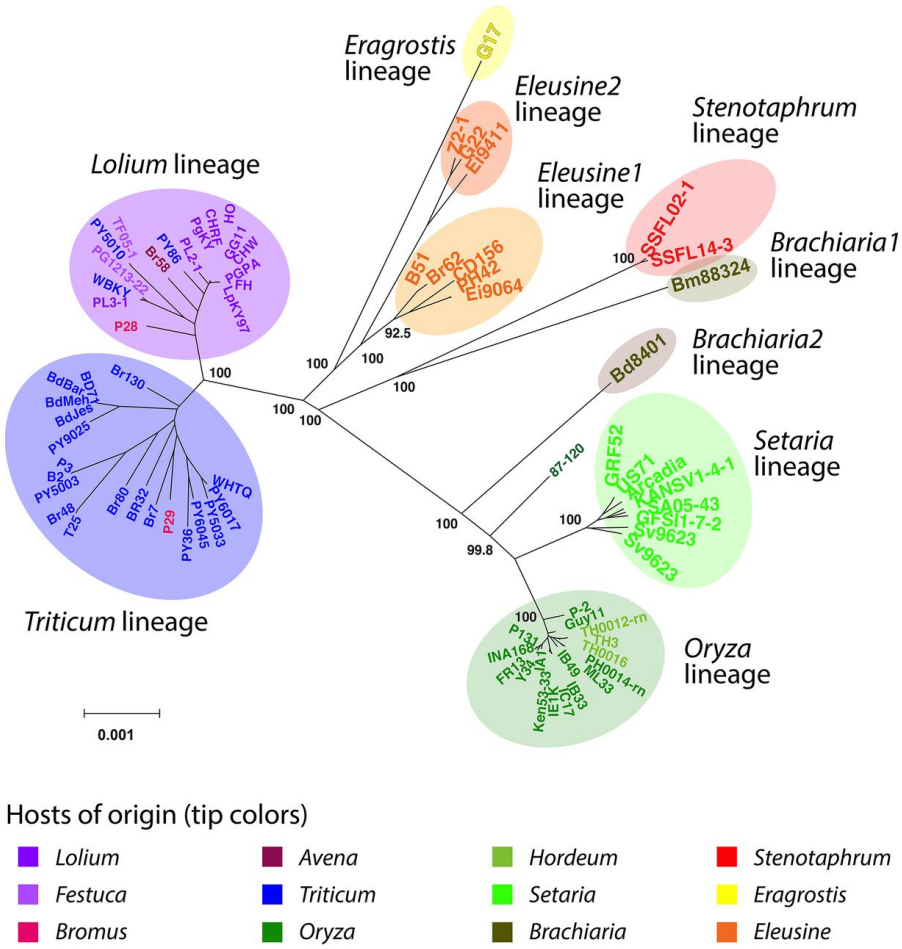

Figure 1: Total-evidence neighbour-joining distance tree using pairwise distances (number of differences per kilobase) calculated from analysis of pairwise BLAST alignments between repeat-masked genomes. Only nodes with confidence of >80% are labelled. Adapted from Gladieux, Condon et al. 2018.

1.6 Origins of *M. oryzae* pv. *tritici*

As with the rice/*MoO* pathosystem, genetic analyses have shown that resistance to wheat blast conforms to the gene-for-gene model where resistance genes in the host have corresponding genes conditioning pathogenicity in the pathogen (Anh et al. 2015; Anh et al. 2018; Hirata et al. 2005; Vy et al. 2014). Inoue et al., proposed that *Mo* made the host jump from *Lolium* to wheat due to the loss of two host specificity genes (Inoue et al. 2017).

Takabayashi et al. observed that an *MoA* isolate, Br58, was virulent on oat, but avirulent on wheat at 20°C, whilst a *MoT* isolate, Br48, was virulent on wheat but avirulent on oat under the same conditions (2002). The authors used this model to investigate genetic mechanisms of host specificity in the *Mot*-plant system using segregation analyses of progeny from crosses between the two isolates. At 20°C the isolates showed different virulences to two cultivars of wheat (Chinese Spring and Norin 4). Br48 was virulent to both cultivars, producing large green/pale green water-soaked lesions (virulent), whereas Br58 produced just a few small necrotic spots (avirulent). At 25°C, Br48 maintained virulence to both cultivars however Br58 gained virulence to Chinese Spring and became virulent. This suggested that the genetic mechanisms of host specificity were different among cultivars. They identified two avirulence genes in Br58 responsible for the isolates avirulence on wheat; *PWT3* (operating on both cultivars) and *PWT4* (operating only on Norin 4) (Takabayashi et al. 2002). Utilising the cultivar specificity of *PWT4,* they were able to identify its corresponding resistance gene in Norin 4 and designated it *Rmg1* (syn *Rwt4*) - the first resistance gene to be found against wheat blast. *Rwt3* was temperature dependent, functioning at 20°C but not at 25°C. Similarly, a study in 2014 identified two genes (*A1* and *A2*) that conditioned the avirulence of the *MoL* isolate TP2 to wheat cultivars Chinese Spring, Norin 4 and Shin-chunaga (Vy et al. 2014). *A1* was highly effective and its corresponding resistance gene was designated *Rmg6*. *A2* resulted in moderate resistance.

Following on from these studies, allelism tests showed that *A1* and *PWT3* are at the same locus, and that *Rwt3* is equivalent to *Rmg6* (Inoue et al. 2017). This suggested that the *PWT3/Rmg6* (syn. *Rwt3*) gene pair has a role in the incompatibility on wheat of both *MoL* and *MoA* isolates. To better understand the role of *PWT3* and *PWT4* during field infections, Inoue and colleagues used Br48 and transformants with either *PWT3* or *PWT4* to inoculate spikes from four cultivars containing both, one or neither of the corresponding resistance genes *Rwt3* and *Rwt4*. Results showed that the interactions of *PWT3-Rwt3* and *PWT4-Rwt4* play crucial roles in seedling leaf and spike infection and that disruption or loss of *PWT3* and *PWT4* would result in a gain of virulence on most wheat cultivars. To investigate whether mutation or loss of *PWT3* and *PWT4* events were important in wheat blast

evolution, the genotypes of a diverse group of 60 *Mo* strains were determined. Two *PWT4* homologues were found but were considered non-functional. All of the isolates tested contained *PWT3* homologs, which could be classified into four types, A – D, based on their open reading frame sequence. The A type could be further divided based on upstream sequence variation into Ao (Br58 homologue), Ao' and Atm subtypes. However, the Ao carriers were avirulent on *Rwt3* cultivars Norin 4 and Chinese Spring, which presented the question how have strains with functional type Ao *PWT3* been identified as *MoT* isolates?

In Brazil in the late 1970's and early 1980's, the most widely grown what cultivar was IAC-5, which carried *Rwt3* (Bonjean and Angus, 2001, as referenced in Inoue et al. 2017). In 1980 a new cultivar, Anahuac 75, was introduced and became very popular as it was well adapted to non-acidic soils, however it did not carry *Rwt3*. The authors proposed a model whereby the extensive cultivation of *rwt3* cultivars enabled strains carrying Ao type *PWT3* to colonise wheat and produce a large source of inoculum. The minority of wheat varieties containing *Rwt3* in cultivation may have imposed strong selection for the deletion or mutation of *PWT3*, giving rise to *pwt3* strains that eventually caused the epidemic in South America. Unfortunately, despite being highly susceptible to *Mot*, Anahuac was still officially recommended to farmers until 1999, further facilitating the spread of this devastating disease (Embrapa, 1999, as referenced in Urashima et al., 2004). However, this model does not account for the extreme genetic divergence reported to have accompanied *Mo* adaption to wheat (Gladieux, Condon, et al. 2018).

Rahnama et al. performed a haplotype analysis of *MoL* and *MoT* isolates which revealed regions of complete haplotype identity interspersed with regions of high diversity (2021). This contrasted alignments between *MoO* isolates which showed evenly distributed variation (Rahnama et al. 2021). Phylogenetic analyses using CH7BAC7 and MPG1 markers confirmed that *MoL* and *MoT* had four alleles at each locus, suggesting that these lineages contained introgressions from a minimum of five pre-existing *Mo* lineages: *Elusine* (*MoE1*), *Urochloa* (*MoU1*) *Stenotaphrum* (*MoSt*), a variant of *MoSt* (*MoU3*) and a lineage closely related to *MoO* and *Setaria* (*MoS*). Furthermore, examining the *MoT* reference assembly, B71, revealed that the entire genome is a medley of pre-existing lineages, predominantly those highlighted from the phylogenetic analyses. The authors proposed that *MoT*/*MoL* represent a multi-hybrid swarm; populations where hybrid individuals constituting a diverse genetic pool, through subsequent intermating and backcrossing, assort and recombine chromosomes resulting in an adaptive radiation. In this model *MoT* and *MoL* lineages co evolved to be preadapted to wheat infection through standing variation and were not the result of driving selection from the host. A fertile *Mo* strain on *Urochloa* imported into Brazil for cattle fodder may have sparked the

hybrid swarm event (Rahnama et al. 2021). This model reconciles observations of gene flow between wheat pathotypes and other host infecting pathotypes, previously attributed to recent and continued sexual reproduction, that contradicted the limited host range seen in other *Mo* lineages (Gladieux, Ravel, et al. 2018; Castroagudin et al. 2017).

1.7 Wheat blast symptoms

MoO symptoms are observed on all parts of the plant, however in wheat symptoms are limited to the aerial parts of the plant (Marcel et al. 2010; Cruz and Valent 2017). The most apparent symptom of *MoT* is the premature bleaching of spikelets and entire heads (Malaker et al. 2016). Infection in the heads occurs in the base or upper part of the rachis and affects grain development above the point of infection. A study into disease symptoms during the Bangladesh epidemic found that the stage of head development at the point of infection was crucial (Islam et al. 2016). Infection during the grain filling stage resulted in small shrivelled grains, whereas no grain was produced if infection occurred at the flowering stage. On leaves, the first sign of infection is the appearance of diamond shaped, water-soaked lesions. After several days, these turn into eye-shaped lesions with a grey/tan coloured center during and after sporulation, respectively (Cruz and Valent 2017). During late stages of infection, the spots enlarge and in severe cases cover the whole leaf, resulting in leaf death (Islam et al. 2016).

1.8 Optimum conditions for wheat blast

MoT favours high temperatures ranging from 18°C - 30°C and high humidity, specifically wetting of plants for at least 10 hours during infection (Cardoso, Reis, and Moreira 2008). In addition to Bangladesh's geographical proximity to central India, alarmingly the agro-climatic conditions may be ideal for blast. A recent ex-ante analysis based on conditions in Bangladesh during the 2016 outbreak, identified vulnerable areas in India, Bangladesh and Pakistan totaling seven million hectares (Mottaleb et al. 2018). A conservative yield loss of 5 - 10% due to blast in these areas would equate to 0.81 - 1.61 million tonnes. Furthermore, climate change could exacerbate the situation, allowing conditions for blast epidemics to occur more frequently, and making areas previously unsuitable for blast vulnerable (Maciel 2011; Hossain and Teixeira da Silva 2013). Combined, the presence of wheat blast in Bangladesh is of immense concern as it could act as a gateway for blast to spread throughout South Asia, posing a threat to global food security, not least because China and India are the world's largest wheat producers, yielding 134.3 and 98.5 million tonnes per annum, respectively (WorldAtlas 2019).

1.9 Life cycle of *M. oryzae* pv. *tritici*

The main mechanism of spread is widely considered to be the transport of infected seed, which provides inoculum for either local or long-distance dispersal (Urashima, Leite, and Galbieri 2007). This has been stated as being the mechanism behind wheat blast's spread from its origin in Paraná to the rest of South America and into Bangladesh (Ceresini, Castroagudin, Rodrigues, Rios, Aucique-Perez, Moreira, Croll, et al. 2018). The fungus may also spread locally via airborne spores (Ceresini, Castroagudin, Rodrigues, Rios, Aucique-Perez, Moreira, Alves, et al. 2018). Using the combined knowledge of *Mo* biology and epidemiology, Castroagudin and colleagues suggested a provisional lifecycle for wheat blast, reconfigured in **Figure 2** (2017). Crop residues that remain post-harvest may create a niche for sexual reproduction of the fungus (Castroagudin et al. 2017). Mature perithecia release ascospores, which germinate to give rise to new colonies. Vegetative growth followed by conidiogenesis results in the release of primary conidia which likely go on to infect the leaves of wheat in nearby fields and other poaceous hosts (Moreira, Ceresini, and Alves 2015; Urashima, Igarashi, and Kato 1993; Papaïx et al. 2015). In turn, conidia released from these leaf lesions contribute to inoculum for wheat head infection (Urashima, Igarashi, and Kato 1993; Urashima and Kato, 1998, as referenced in Castroagudin et al. 2017). Biological evidence suggests that sexual reproduction occurs predominantly on dying stems of wheat and alternative grass hosts (Castroagudin et al. 2017). These findings suggest that pasture grasses act as a major sources of wheat blast inoculum and form spacial and temporal bridges connecting wheat fields across Brazil.

Cruz et al. found that the production of conidia on the lower leaves of some wheat cultivars coincided with spike infection, and proposed that inoculum produced from the lower canopy may be important in the development of wheat blast epidemics (Cruz et al. 2015). The authors also reported higher instances of disease on old wheat leaves compared to on young expanding leaves, in contrast to the rice blast pathosystem where younger leaves are more susceptible (Ghatak et al. 2013). Indeed, in rice, conidia on young leaves provide inoculum for succeeding disease outbreaks.

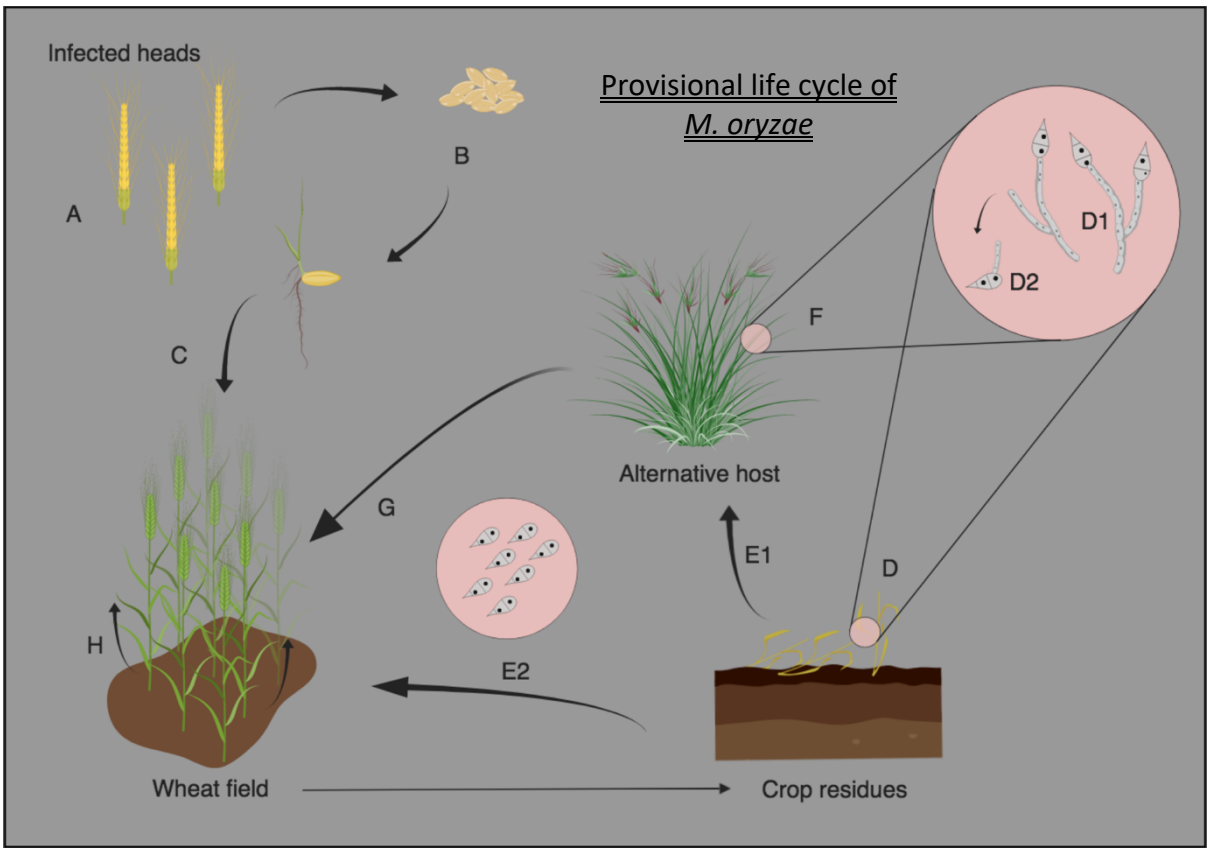

Figure 2: Provisional life cycle of wheat infecting strains of *M. oryzae*. At the end of the growing season, wheat blast infection on heads (**A**) results in seed infection (**B**), which provides inoculum for either local or long-distance dispersal (Urashima, Leite, and Galbieri 2007). This causes primary infections in new wheat crops (**C**). Crop residues that are left in the field post-harvest (**D**) may create a niche for sexual reproduction. Mature perithecia release ascospores, which germinate to give rise to new colonies. Vegetative growth followed by conidiogenesis (**D1**) (Moreira, Ceresini, and Alves 2015) result in the release of primary conidia (**D2**), which likely contribute to inoculum for leaf infection of alternative poaceous hosts (**E1**), and subsequent/nearby wheat crops (**E2**). Sexual reproduction may also occur within alternative poaceous hosts (**F**), releasing conidia from leaf lesions that further contribute to inoculum for wheat blast on heads (**G**) (Urashima, Igarashi, and Kato 1993) (Urashima and Kato, 1998, as referenced in Castroagudin et al. 2017). Conidia production from leaf lesions in some wheat cultivars coincides with head infection (**H**).

1.10 Infection cycle of *M. oryzae*

Mo is a hemibiotrophic plant pathogen meaning the fungus initially has a biotrophic phase where the host immune system is suppressed, facilitating the uptake of nutrients from living cells via invasive hyphae (IH), followed by a necrotrophic stage that promotes cell death (Fernandez and Orth 2018). The infection cycle starts when three celled asexual spores, conidia, land on the leaf cuticle and adhere by releasing spore tip mucilage (Hamer et al. 1988). The conidium subsequently germinates to produce a polarised germ-tube that grows apically across the leaf surface. After four hours the germ tube switches to isotropic growth during a process called 'hooking', regulated by Pathogenicity MAP Kinase 1 (Pmk1) (Xu and Hamer 1996; Wilson and Talbot 2009). The tip of the germ tube differentiates into an appressorium, a dome shaped infection structure deployed by many pathogenic fungi to enter and colonise the host cell (Fernandez and Orth 2018; Ryder and Talbot 2015). During appressorium maturation, melanin deposits form in the appressorium cell wall which prevent the exodus of compatible solutes but permit osmosis and the contents of the conidium are recycled into the appressorium (Chumley and Valent 1990; de Jong et al. 1997). The accumulation of high concentrations of polyols, such as glycerol, draw water into cell via osmosis generating tremendous turgor of up to 8.0 MPa (de Jong et al. 1997; Foster et al. 2017). The base of the appressorium lacks melanin and forms the point at which the penetration peg emerges; the appressorium pore (Dagdas et al. 2012; Gupta et al. 2015). Remodelling of the actin cytoskeleton at the pore forms a toroidal F-actin network, scaffolded by Septin guanosine triphosphatases (GTPases) which give cortical stability and serve as a lateral diffusion barrier to organise polarity determinants and secretion proteins. Turgor is applied at the appressorial pore as mechanical force, enabling the penetration peg to puncture the leaf cuticle and invade plant tissue (Bourett and Howard 1990). Cytoskeletal rearrangement and formation of the septin ring only occurs once a threshold of turgor is reached, controlled by a sensor histidine-aspartate kinase (Sln1) (Ryder et al. 2019). Once inside the plant cell, the penetration peg differentiates from filamentous to pseudo-hyphal primary IH (Veses and Gow 2009; Khang et al. 2010). A plant membrane-rich cap forms at the tip of the peg known as the biotrophic interfacial complex (BIC). The IH expand by budding into bulbous IH and rapidly colonise the cell (Kankanala, Czymmek, and Valent 2007).

Only once the primary infected cell is fully invaded does the fungus spread to neighbouring cells (Cruz-Mireles et al. 2021). Whilst not fully understood, it is thought that IH transverse cells via plasmodesmata by forming a structure similar to appressorium; transpressorium (Kankanala, Czymmek, and Valent 2007; Cruz-Mireles et al. 2021). This requires a switch back to the narrower primary IH in order to pass into the adjoining cell before becoming bulbous IH once more. This cycle

continues, again mediated by Pmk1, during the biotrophic phase (Sakulkoo et al. 2018; Fernandez and Wilson 2014). New BICs are formed in each colonised cell (Khang et al. 2010). Fluorescent tagging suggests that primary BICs within the first colonised cells are removed once the secondary BICs are formed, correlating with the switch from filamentous IH to bulbous IH.

In order to supress the plant innate immune system, effectors are secreted into the cytoplasm by the BIC or into the apoplast from the hyphal tip via discrete mechanisms (Khang et al. 2010; Fernandez and Wilson 2014; Yan et al. 2023). Studies using live cell imaging to monitor the localisation of fluorescently labelled effectors during infection have shown that many effectors, such as *Avr-Pita1*, *PWL1*, *PWL2*, *Bas1* and *Avr-Pizt*) initially accumulate in the BIC at the primary IH before translocating into the cytoplasm (Khang et al. 2010; Park et al. 2012). *PWL2* and *Bas1* have been shown to be continuously secreted into the BIC whilst bulbous IH colonise the cell (Khang et al. 2010). The authors also suggest that host immunity is decreased in neighbouring cells prior to IH invasion by effectors such as *PWL2* by movement through plasmodesmata (Khang et al. 2010). Fluorescently labelled PWL2 was observed in both the cytoplasm and nuclei within neighbouring cells two to four cells deep surrounding the primary invaded cell. Following invasion into neighbouring cells, accumulation of effectors at secondary BICs is also observed. Furthermore, Yan et al., characterised 32 *Mo* effector proteins and found that the majority were targeted to the cytoplasm via the BIC (2023). In contrast, apoplastic effectors do not associate with the BIC. For example, apoplastic effectors *Slp1* and *Bas4* accumulate between the fungal cell wall and the extra-invasive hyphal membrane (EIHM), the apoplastic matrix, which surrounds the IH (Mentlak et al. 2012; Khang et al. 2010).

Whist significant advances in understanding how *Mo* invades and colonises host tissue have been made in recent years, much is unclear. For example, how does the BICs facilitate the delivery of effectors into the cytoplasm and what are the mechanisms behind effector driven suppression of the host immune system? Additionally, the signals that lead to both appressorium and transpressorium morphogenesis, and the cues that enable *Mo* to switch from the biotrophic to necrotrophic phase are unknown.

1.11 Genetic diversity of *M. oryzae* pv. *tritici*

Mo has a highly dynamic genome, resulting in high population diversity and the frequent emergence of new races (Singh et al. 2014; Van de Wouw et al. 2010). This has been shown to be the main cause of the rapid breakdown of *R* gene resistance observed in rice (Devanna and Sharma 2018). Maciel et al. used 11 simple sequence repeat loci to investigate population structure and genotype diversity of *MoT* in Brazil, 25 years after the first epidemic (Maciel et al. 2014). Eight to 30 isolates were collected per site, and each given a multilocus microsatellite genotype (MLMG). 48 MLMGs were identified, of which 13 were shared between populations. Wheat and rice infecting populations showed the highest population differential, with no MLMGs in common, and showed very little historical migration.

The degree of pathotype diversity (virulence spectrum) and distribution was also investigated, by measuring the virulence of 69 *MoT* isolates, representing 38 MLMG, on seven wheat cultivars. The isolates were split into 14 seedling virulence groups (SVGs), designated A - U. SVG A was virulent on all seven cultivars and consisted of 36% of the isolates. Virulence was also tested on detached spikes which were divided into eight detached spike virulence groups (HVG), A' - T', of which HVG A' was virulent on all seven cultivars. Only five HVG A' isolates showed a strong relationship between seedling and spike virulences, although compete and partial resistance was observed at both stages. It is therefore important to investigate resistance in early and late stages of plant development in order to ensure resistance is maintained at the crucial spike development stage. Combined, these results indicate that there is a high gene and genotype flow within *MoT,* and significant pathotype diversity.

Castroagudin et al. continued this work, using 173 isolates covering 80 unique MLMGs which could be grouped into 25 SVGs and 9 HVGs using 10 wheat cultivars (Castroagudin et al. 2017). As with the previous study, they identified cultivars that were resistant at the seedling stage, but susceptible at the head stage, and again found SVG A and HVG A were virulent on all cultivars. These isolates were designated as a 'super race' on Brazilian wheat and were also found on many invasive grass species including *Digitaria sanguinalis*, *Avena sativa* and *Eragrostis plana*. HVG A was found in 80% of the isolates and was present in all populations, and in relatively high frequency. The ubiquitous presence of this super race across Brazil may confound breeding efforts for durable resistance.

1.12 Wheat blast disease management

1.12.1 Wheat blast resistance

Despite continuous breeding efforts over the past 30 years to improve blast resistance in wheat, there has only been limited success (Urashima et al. 2004; Cruz et al. 2010; Prestes et al. 2007). In contrast to rice blast, where many rice lines have been shown to provide strong resistance to blast, resistance to wheat blast has been limited to a few lines that show only low to moderate resistance (Devanna and Sharma 2018). To date BR18 Terena, BRS 229, and MGS 3 Brilhante have been the most commonly used cultivars in breeding programmes in Brazil due to their relatively high levels of resistance to spike blast in the field, with BR18 Terena showing the highest resistance (Urashima et al. 2004; Sousa 2002). However, these cultivars have become susceptible in some regions of Brazil, likely due to the local emergence of new pathogen isolates through sexual reproduction (Urashima, Bruno, and Lavorenti 2001; Urashima, Galbieri, and Stabili 2005). Furthermore, so called 'resistant' cultivars exhibit varying levels of resistance depending on the isolate they are exposed to, and where they are deployed (Urashima et al. 2004). This was highlighted in a study into the resistance spectra of wheat cultivars against 72 *MoT* isolates collected from the Mato Grosso do Sul and Paraná regions of Brazil (Urashima et al. 2004). Twenty cultivars were chosen based on reported resistance to wheat blast or because they were officially recommended, of which 14 showed resistance against only 20% or less of the 72 isolates used in the study. As expected, BR18 Terena was the most consistently resistant cultivar across both regions, however even this variety was only resistant to an average of 51% of the isolates. Variation in BR18 Terena resistance has been corroborated in other studies (Arruda 2005; Sousa 2002).

Whilst many blast *R* genes have been discovered in rice, they seem rare in wheat with only nine identified to date (**Table 1**). Of these, only five show resistance against *MoT*: *Rmg2*, *Rmg3*, *Rmg7*, *Rmg8* and *RmgGR119* (Zhan, Mayama, and Tosa 2008; Tagle, Chuma, and Tosa 2015; Anh et al. 2015; Wang et al. 2018). *Rmg2* and *Rmg3* were found in the cultivar 'Thatcher' and convey seedling resistance to Brazilian isolates collected in the early 1990's (Zhan, Mayama, and Tosa 2008). However highly virulent strains isolated since 2011 devastate Thatcher so both genes appear to have been overcome (Cruz and Valent 2017). Furthermore, both *Rmg2* and *Rmg3* are temperature sensitive and ineffective in spike blast, so have very limited use for breeding (Zhan, Mayama, and Tosa 2008). *Rmg4* and *Rmg5* were identified as *R* genes to the crab grass (*Digitaria sanguinalis*) specific blast pathogen *M. grisea* in common wheat cultivars (Nga, Hau, and Tosa 2009). As mentioned in **Section 1.5** '**Origins of *M. oryzae* pv. *tritici***', *Rmg1* (*Rwt4*) and *Rmg6* (*Rwt3*) were identified as resistance genes to corresponding *Avr* genes *PWT4* and *PWT3* (*A1*), and convey resistance to *MoA* isolate Br58 and *MoL*

isolate TP2 respectively (Takabayashi et al. 2002; Vy et al. 2014). *Rmg7* was identified in the tetraploid wheat accession KU120 using an aggressive *MoT* isolate, Br48, collected from Mato Grosso do Sul in Brazil, 1990 (Tagle, Chuma, and Tosa 2015). Three cultivars resistant to Br48 (KU112, KU120 and KU122) were crossed with the susceptible *T. paleocolchicum* accession Tat14 and selfed to produce F_2 seed. On inoculating all three populations with Br48 at the seedling stage, resistant and susceptible seedlings for each population segregated in a 3:1 ratio indicating that a single gene was responsible for resistance, designated *Rmg7*. To identify the corresponding avirulence gene, an F_1 population was generated by crossing Br48 with a Japanese *MoE* isolate (avirulent on wheat), MZ5-1-6, to produce 76 progeny strains. The three resistant cultivars were inoculated with the F_1 strains and showed identical segregation patterns with a 1:1 ratio of virulent and avirulent strains. This indicated that a single gene conditioned the avirulence of Br48 on the three cultivars and was designated *Avr-Rmg7.* The F_2 population for KU120 x Tat14 was taken forward to F_3 and Simple Sequence Repeat (SRR) markers were used to map *Rmg7* to the distal region of chromosome 2A (Anh et al. 2015).

Building upon this work Anh et al. identified *Rmg8* (2015). Hexaploid wheat cultivars S-615 and Shin-chunaga were inoculated with Br48 and phenotyped as resistant and susceptible respectively. An F_2 population (S-615 x Shin-chunaga) was then inoculated with Br48 and these segregated in a 3:1 ratio as resistant or susceptible. In F_3 populations, non-segregating resistant, segregating, and non-segregating susceptible lines displayed a 1:2:1 ratio suggesting that a single dominant gene in S-615 provided resistance to Br48; designated *Rmg8*. Molecular mapping via bulked segregant analysis with SRR markers assigned *Rmg8* to the distal region of chromosome 2B. To identify the corresponding avirulence gene one of the F_1 strains from the Br48 x MZ5-1-6 population described above, 200R29 *(avr-Rmg8)*, was crossed with Br48 to create a BC_1F_1 population of 73 hybrid strains (**Figure 3**). S-615 was inoculated with the strains and the 1:1 segregation ratio of avirulent and virulent strains suggested avirulence was controlled by a single gene; *Avr-Rmg8*. The BC_1F_1 mapping population was expanded to 449 cultures, 58 of which were used to fine map *Avr-Rmg8* to a 45kb interval on chromosome 7, containing five genes: 755.4, 755.2, 2570.1, 4315.4 and 1106.3 (Anh et al. 2018). Ten stable transformants of 200R29 (virulent on *Rmg8*) were produced for each gene and used to inoculate S-615. Six of the ten transformants carrying 4315.4 were avirulent while all remaining transformants were virulent suggesting that 4315.4 corresponds to *Avr-Rmg8.* Crucially, the tetraploid KU120 carrying *Rmg7* showed the same response to the transformants suggesting that *Avr-Rmg7* and *Avr-Rmg8* are the same effector (hereafter referred to as *Avr-Rmg8)* recognised by both *Rmg7* and *Rmg8*. As such they can be considered as the same gene for the purposes of breeding resistance. Whilst both *Rmg7* and *Rmg8* confer resistance at the seedling and spike stages, *Rmg7* is not effective

in the spike at high temperatures (26°C) (Anh et al. 2018). Additionally, *Rmg7* is also ineffective against isolates recently obtained in Paraguay so *Rmg7* and *Rmg8* are no longer useful for South American wheat breeders (Cruz and Valent 2017; Cazal-Martínez, Reyes-Caballero, and Kohli 2022). A new gene, *RmgGR119*, has been identified in an Albanian wheat accession that works synergistically with *Rmg8* resulting in high resistance against Br48 (Wang et al. 2018). This gene combination may be of use against Bangladesh isolates and is already being backcrossed into Japanese varieties as a preventative measure (Islam, Kwang-Hyung Kim, and Jaehyuk Choi 2019; Wang et al. 2018).

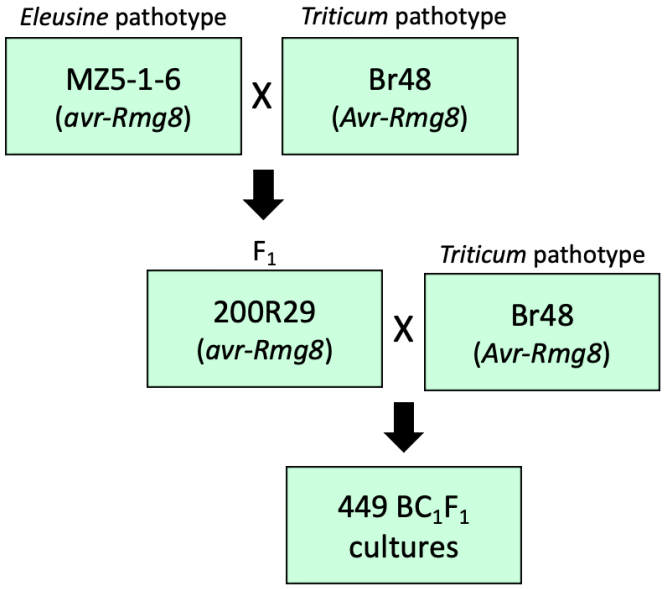

Figure 3: Pedigree of *Magnaporthe oryzae* strains used to identify *Rmg8* and it's effector *Avr-Rmg8*.

Table 1. List of blast resistance genes identified and mapped in wheat.

Gene	Source cultivar	Effective against	*Avr* genes	Chromosome	References
Rmg1 (Rwt4)	Norin 4	*Avena* isolate Br58	*PWT4*	1D	(Takabayashi et al. 2002; Arora et al. 2023)
Rmg2	Thatcher	*Triticum* isolate Br48	Not known	7A	(Zhan et al. 2008)
Rmg3	Thatcher	*Triticum* isolate Br48	Not known	6D	(Zhan et al. 2008)
Rmg4	P168, Shin-chunaga, Norin 4, Norin 26, Norin 29	*Digitaria* isolate	Not known	4A	(Nga et al. 2009)
Rmg5	Red Egyptian and Salmon	*Digitaria* isolate	Not known	6D	(Nga et al. 2009)
Rmg6 (Rwt3)	Chinese Spring, Shin-chunaga and Norin 4	*Lolium* isolate TP2	*PWT3* (or *A1*)	1D	(Vy et al. 2014; Arora et al. 2023)
Rmg7	St24, St17, St25	*Triticum* isolate Br48	*Avr-Rmg7*	2A	(Tagle et al. 2015)
Rmg8	S-615	*Triticum* isolate Br48	*Avr-Rmg8* (=*Avr-Rmg7*)	2B	(Anh et al. 2015; Anh et al. 2018)
RmgGR119	GR119	*Triticum* isolate Br48	Not known	-	(Wang et al.. 2018)

1.12.2 2NS translocation

Cruz et al. showed that the presence of the 2NS segment from *Ae. ventricosa* associates with wheat spike blast resistance (Cruz et al. 2016). This segment is on a 25 to 38 Mb region from *Ae. ventricosa* which translocated to the distal region of chromosome 2AS in wheat. Seventy-six of the 418 cultivars tested possessed the translocation and showed 50% to 72% less spike blast symptoms when inoculated with isolate T-25 (collected in Panara in 1988) in growth chamber conditions (Cruz et al. 2016; Cruz et al. 2012). Newer isolates collected from South America between 2011 and 2014 were also tested; however, not all cultivars with 2NS showed significantly less spike blast suggesting that genetic background and/or the environment may alter the expression of resistances within 2NS. The most aggressive of the new isolates was B-71, isolated from Bolivia in 2012, which caused significantly more disease in all of the cultivars compared to T-25. Nonetheless, those carrying 2NS were still much more resistant than susceptible cultivars lacking 2NS. Six pairs of near isogenic lines (NILs) differing in presence and absence of 2NS were also used to test the effect of the translocation in different genetic backgrounds of spring and winter wheat (Cruz et al. 2016). In greenhouse conditions, when inoculated with the T-25 isolate, and the more recent isolate B-2 (collected in Bolivia in 2011), all NILs with 2NS showed a significant reduction in spike blast. In contrast, lines with 2NS did not show a reduction in spike blast with B-71 and P-3 (collected in Paraguay 2012). It is not yet clear why 2NS resistance to B-71 and P-3 is reduced in some genetic backgrounds however four of the NILs were tested under natural epidemic conditions in field sites in Bolivia in 2014 and 2015 and gave convincing evidence that 2NS conferred spike blast resistance.

Cruz et al. also showed that the CIMMYT (International Maize and Wheat Improvement Center) line 'Milan' contains the 2NS translocation (2016). Milan derived cultivars such as CD116 and Sausal CIAT have previously been shown to have high levels of blast resistance in the field and are widely cultivated in South America (Kohli et al. 2011). The 2NS segment also contains *R* genes against root-knot and cereal cyst nematodes, and against certain strains of wheat leaf, stem and stripe rust (Williamson et al. 2013; Jahier et al. 2001; Helguera et al. 2003). However, it is uncertain how durable this resistance will be. In fact, the 2NS resistance in the French cultivar 'Renan' may already be overcome by a third of wheat blast virulence groups found in Brazil, including the widespread HVGA super-race (Castroagudín et al. 2015). As such, while it is recommended that breeders use 2NS in their cultivars, parent lines should be chosen with caution, and additional sources of resistance are still required (Cruz et al. 2016; Cruz and Valent 2017).

1.12.3 Fungicides

The very limited availability of cultivars with resistance to wheat blast has forced farmers to depend on alternative methods to protect crops. In South America farmers typically apply up to three applications of fungicide at spike emergence (Cruz et al. 2015). This however is proving ineffective as commercially available fungicides are only 50% efficient in the field (Maciel 2011). When weather conditions are favourable for the development of the disease, efficiency is reduced much further. In addition, the narrow window between leaf and spike infection in wheat makes it difficult to detect the disease in time for fungicides to be applied and be effective (Devanna and Sharma 2018). As seed borne inoculum is a major cause of disease spread, fungicide treatment of seed could offer an alternative. Toledo et al., reported that this approach can eradicate blast primary inoculum and recommend that treatment of seed from infected fields should become standard practice (Toledo et al. 2015, as referenced in Cruz and Valent, 2017).

Triazoles and combinations of triazole and quinone outside inhibitor (QoI) fungicides are the most common fungicides marketed for wheat blast in Brazil (MAPA, 2017, as referenced in Ceresini et al. 2018). One possible reason for the inefficiency is fungicide resistance. For example, a study by Castroagudín and colleagues found that resistance to QoIs increased from 36 to 90% from 2005 to 2012 (Castroagudín et al. 2015). This suggests that existing fungicides cannot be relied upon to provide efficient and durable control of blast in Brazil, and those to which resistance has been seen in Brazil are unlikely to provide durable control of blast in Asia or elsewhere.

In summary, the extremely limited number of wheat blast resistance genes identified so far, the limited effectiveness of fungicides, and the fact that some races of *M. oryzae* are already virulent on the 2NS translocation segment highlights the immense importance of finding new genes effective against blast. Furthermore, genetic analyses show that blast *Avr* proteins are the major cause of host species specificity in both rice and wheat, and the identification of *Avr* genes and cognate resistances in the rice-blast system has helped scientists to understand co-evolutionary dynamics (Valent and Khang 2010; Couch et al. 2005; Tosa et al. 2016). Additionally, studying *Avr* genes from strains isolated across different regions has helped breeders select the best *R* gene combinations against rice blast (Valent and Khang 2010; Cruz and Valent 2017). *R* gene mediated resistance has proved one of the best strategies for managing blast in rice, further advocating the cloning and characterization of *R* genes for blast in wheat (Devanna and Sharma 2018). However, with such low D genome diversity within hexaploid wheat, alternative sources of resistance need to be identified and utilized. In order for an introduced *R* gene to be effective, its associated *Avr* gene must exist in the *Mo* population, therefore understanding the *Avr* gene repertoire of current isolates is crucial for breeding (Islam,

Kwang-Hyung Kim, and Jaehyuk Choi 2019). Given the high genetic diversity of *Mo*, it is vital that resistances are tested against local races to ensure they will be effective in natural epidemic conditions (de Paula et al. 2019).

1.13 Crop wild relatives as additional sources of genetic variation

Crop wild relative (CWR) species usually have greater genetic variation than cultivated crops, where variation has been lost through genetic bottle neck events caused by domestication, and offer a rich source of diversity which can be exploited for crop improvement (Maxted et al. 2012; Brozynska, Furtado, and Henry 2016). As such, CWRs have been used to introduce biotic and abiotic resistance into crops, most notably with respect to pest and disease resistance (Maxted et al. 2012; Maxted et al. 2006). For example, Witek et al. cloned a broad-spectrum resistance gene to potato late blight (*Phytophthora infestans*), *RPi-amr3i*, from the wild, non-tuber forming species *Solanum americanum* (Witek et al. 2016). CWR are widely used for crop improvement in many different species, most extensively in rice and wheat, but also in barley (*Hordeum vulgare*), tomato (*Solanum lycopersicum*) and cassava (*Manihot esculenta*) to name a few (Maxted et al. 2012).

1.13.1 *Aegilops tauschii*

During the polyploidisation events between *T. turgidum* and the D genome progenitor, *Ae. tauschii,* that formed hexaploid bread wheat, only a few *Ae. tauschii* accessions are thought to have been involved (Giles and Brown 2006; Cox 1997). This bottle neck event resulted in very low D genome variation within hexaploid wheat (Reif et al. 2005). Furthermore, during domestication the occasional *T. durum* introgression increased diversity within the A and B genomes. Combined, the wheat D genome has the lowest variation relative to the other genomes, at approximately 16% of the A and B genomes (Voss-Fels et al. 2015; Pont et al. 2019; Zhou et al. 2020).

Ae. tauschii may therefore offer a source of blast resistance genes that have been lost through bottlenecks and conventional breeding. Genetic classification divided *Ae. tauschii* into two lineages, lineage one (L1) made up of spp. *tauschii*, and lineage two (L2) containing spp. *strangulata* (Wang et al. 2013; Mizuno et al. 2010). These lineages have been further subdivided into 1E, 1W, 2E and 2W (Wang et al. 2013). Based on SNP data, a L2E population from the southern and southwestern Caspian was found to be the main donor of the D genome, while L1 contributed only 0.8%. An additional lineage was recently identified using short-read whole genome sequence data from 242 *Ae. tauschii* accessions (Gaurav et al. 2022). 100,000 random *k*-mers (51bp in length) were selected to generate a

phylogeny with 28 *T. aestivum* cultivars based on the presence/absence of *k*-mers. A discrete clade closely related to L2 was observed and designated lineage 3 (L3), comprising 5/242 accessions. The L3 contribution to the D genomes of 11 reference *T. aestivum* genomes ranged from 0.5 to 1.9%.

As with many CWR, *Ae. tauschii* has high genetic diversity. Luo et al. showed that *Ae. tauschii* chromosomes have been evolving an order of magnitude faster than in other grasses and hypothesized that large amounts of very similar repeated sequences result in frequent recombination errors (Luo et al. 2017). This facilitated rapid genome evolution by causing structural chromosome changes and an unprecedented number of dispersed duplicated genes, which in addition to being excluded from human driven genetic bottle necks resulted in high genetic diversity. A rapidly evolving genome, paired with high levels of genetic diversity provides an excellent basis to maintain an evolutionary arms race against pests and pathogens, and may explain the multiple resistances found within *Ae. tauschii* (Bergelson et al. 2001). *Ae. tauschii* has already been shown to be a valuable source of variation for many agronomically important traits, including abiotic stress such as drought and water logging, disease resistance and grain yield (Börner et al. 2015; Saeidi et al. 2008; Zhang et al. 2012; Villareal et al. 2001). Indeed, resistance genes for leaf, stripe and stem rusts have already been introgressed from *Ae. tauschii* into wheat (Olson et al. 2013; Ma, Singh, and Mujeeb-Kazi 1995; Kerber 1987). Taken together, it is therefore reasonable to assume that *Ae. tauschii* may also be a reservoir for wheat blast resistance genes (Kerber 1987; Bockus et al. 2012).

Cloning genes from hexaploid wheat is compounded by its large genome size (17Gb) and high proportion of repetitive DNA (81%), making assembly and genetic mapping very difficult (Wulff and Moscou 2014; International Wheat Genome Sequencing 2014) *Ae. tauschii* has a relatively small diploid genome of around 4.3GB and is therefore much more amenable to genetic analysis (Luo et al. 2017). Furthermore, variation in *Ae. tauschii* may be introgressed into wheat by forming 'synthetics', negating the need for genetic modification.

1.14 Synthetic wheat

There are two main approaches used to introgress *Ae. tauschii* diversity into cultivated wheat. The most common method involves crossing tetraploid wheat (*T. turgidum* or *T. dicoccoides*) with *Ae. tauschii* to form a triploid, and then doubling the chromosome set. This is called artificial hexaploid wheat synthesis and is not limited to the D genome as segments from the A and B genomes may also be introduced. The resulting artificial hexaploid wheat lines are called synthetic hexaploid wheat

(SHW) and have been widely exploited for the enhancement of bread wheat (Börner et al. 2015). The second approach involves direct introgression where *Ae. tauschii* is crossed with bread wheat, and the resulting progeny repeatedly backcrossed to produce a stable bread wheat derived line containing 42 chromosomes (Gill and Raupp 1987).

To increase the D genome diversity available to breeders, the world's largest collection of SHW was generated by CIMMYT more than two decades ago. Around 50 elite durum wheat lines and 900 *Ae. tauschii* accessions were used to produce 1300 lines, which have been used extensively to characterise and exploit abiotic, biotic and yield affecting traits (Ogbonnaya et al. 2013). However, generating synthetic wheat lines, and introgressing traits of interest into agronomically important cultivars is time consuming and resource demanding (Arora et al. 2017). Issues associated with gene introgression can be further compounded by linkage drag, where valuable genes are linked with unfavourable traits which can take many years to remove (Börner et al. 2015). Furthermore, the usefulness of introduced alleles only becomes clear post transfer, as traits in *Ae. tauschii* may not correlate with those in their derived SHW lines (Ogbonnaya et al. 2013). This can be caused by changes in gene expression via unwanted genomic alterations during artificial hybridization, or epistatic interactions between homoeologues in the A and B genomes (Dreisigacker et al. 2008). Expression may also be reduced due to partial or complete suppression in SHW, where resistance genes on one genome are inhibited by genes on another (Kema, Lange, and Van Silfhout 1995). In addition, as with conventional hexaploid wheat, cloning resistance genes from SHW is immensely costly and time consuming due to its large genome size.

1.15 Rapid cloning of *R* genes

1.15.1 RenSeq and MutRenSeq

Conventional map-based cloning has been used to clone numerous R genes however it can be time and resource demanding as several generations are required to generate a segregating population (Bettgenhaeuser and Krattinger 2019). Map-based cloning also relies on recombination and may fail if the casual gene is in an area of strong linkage disequilibrium (LD). An alternative is a direct cloning approach using complexity reduction sequencing which targets only a subset of the genome. Exome capture enriches for the protein coding portion of the genome, or exome, which in hexaploid wheat constitutes just 1-2% of the genome (Paux et al. 2006). This is commonly achieved by creating RNA baits complementary to the exome target sequences, which are hybridised to a next generation sequencing (NGS) library. Hybrid molecules are then removed via binding to a streptavidin coated

magnetic bead, creating a sample highly enriched in sequences of expressed genes. This method can be taken further and used to target a specific gene family of interest. Jupe et al. developed *R* gene enrichment sequencing (RenSeq) to capture the NLR gene repertoire of potato (Jupe et al. 2013). NLRs are the most common class of resistance genes in plants and thus are frequently targeted for breeding disease resistant crops (Jones and Dangl 2006). RenSeq enabled Jupe et al. to identify SNPs that segregated with resistance to potato late blight, however they were unable to pinpoint individual genes responsible for resistance due to the high sequence diversity between *R* genes in the biparental population. Steuernagel et al. overcame this problem by introducing a mutagenesis step to generate and screen for susceptible mutants prior to sequencing (2016). A single highly homozygous mutant was used to generate a near isogenic mutant population, facilitating the mapping of the short reads to the assembly of the resistant mutant parent. This modified approach enabled the isolation of two wheat stem rust resistance genes (*Sr22* and *Sr45*) without fine mapping and was termed MutRenSeq. However, in order to clone a resistance gene using MutRenSeq, the gene of interest must exist in an otherwise susceptible background to the pathogen isolate of interest, which may take many generations to accomplish, and only allows for one gene to be cloned at a time.

1.15.2 RenSeq combined with association genetics

The need for mutagenesis was removed by using a sequence-configured diversity panel to exploit pre-existing recombination events (Arora et al. 2019). The diversity panel consists of 151 accessions of *Ae. tauschii* L2, from around the Caspian Sea. Each accession in the panel was genotyped by RenSeq (in this case enriching for the NLR compliment of the genome) and then the panel was subjected to association genetics, resulting in the association genetics with RenSeq (AgRenSeq) pipeline (**Figure 4**). The diversity panel was phenotyped using six stem rust races. As NLR genes are highly diverse thus complicating the conventional alignment of raw reads and SNP-calling against a reference genome, overlapping *k*-mers (sub-sequences) rather than SNPs were used in the association analysis. *k*-mers were filtered according to the correlation of presence/absence to the degree of resistance or susceptibility within the diversity panel. A linear regression model was used to predict the phenotype with each remaining *k*-mer, using principal component analysis (PCA) to control the population structure. *k*-mers were then mapped against the RenSeq assembly of a resistant accession and plotted in an association matrix. Using this method, four stem rust resistance genes were identified in just a few months: *Sr33*, *Sr45*, *Sr46* and *SrTA1662*. *Sr46* and *SrTA1662* had been identified in previous studies, validating the reliability of AgRenSeq (Yu et al. 2015; Olson et al. 2013). The sequenced NLR contigs constitute an extremely valuable resource, as the panel may be phenotyped with other pathogens again and again without the need to generate a new population of plants, or for further

sequencing to potentially identify resistance genes against other diseases. However, all iterations of RenSeq are limited to identifying NLR genes, and so exome capture or whole genome sequencing would be required to identify atypical *R* genes. To facilitate this, Gaurav et al. generated a whole genome shotgun (WGS) based pipeline using WGS data for the *Ae. tauschii* diversity panel generated through the Open Wild Wheat Consortium (OWWC) (2022). A similar approach to AgRenSeq was used to develop an NLR RenSeq pipeline for 320 wheat lines from the Watkins collection, discussed further in **Sections 1.13.2 and 2.5.3** (Arora et al. 2023).

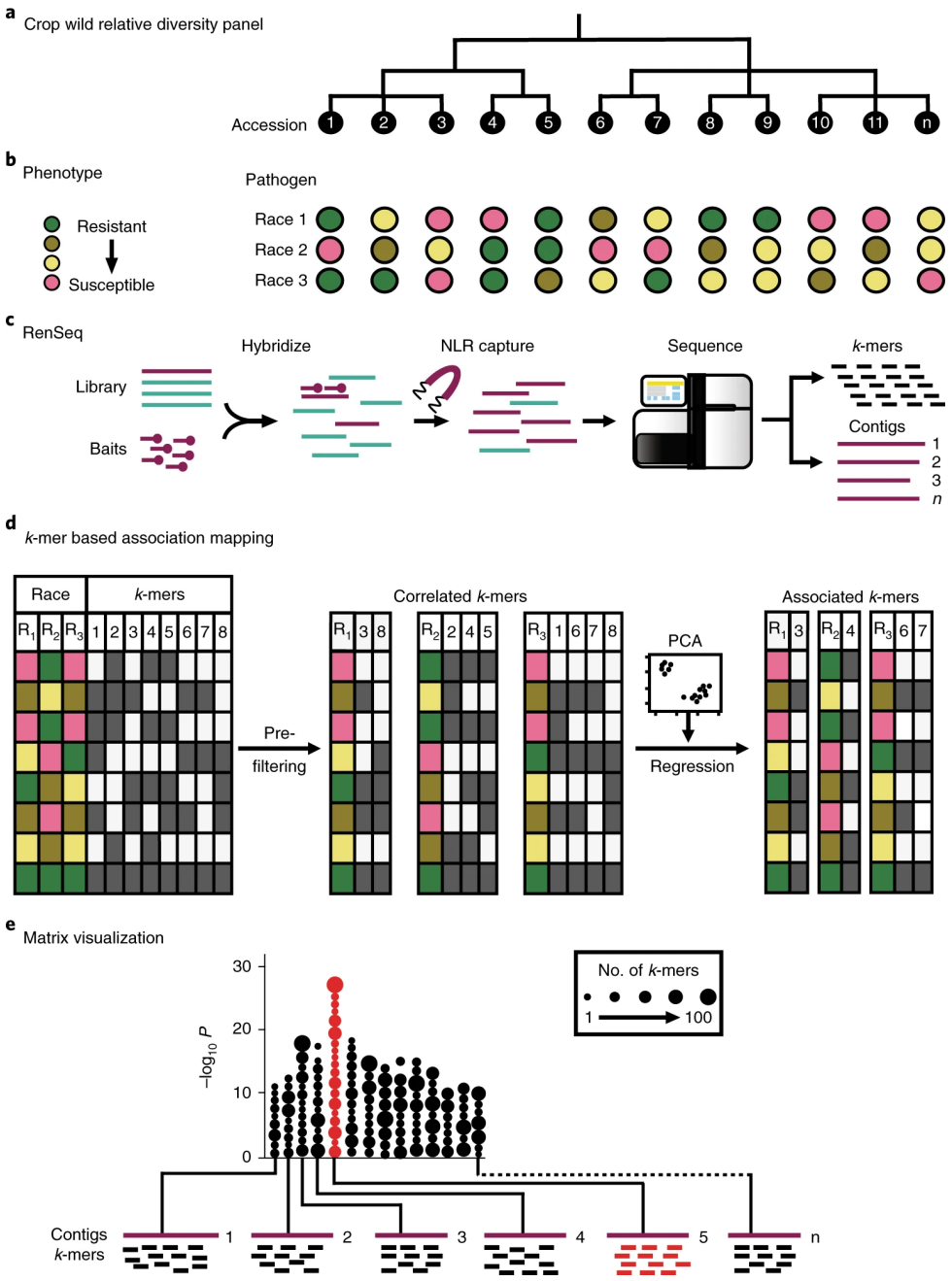

Figure 4: Schematic of the AgRenSeq pipeline: (**a**) A genetically diverse panel of accessions is (**b**) phenotyped with different pathogen races and (**c**) subjected to RenSeq followed by assembly of the NLR repertoire and extraction of NLR *k*-mers for each accession. (**d**) *k*-mers are pre-filtered based on the correlation of their presence/absence to the level of resistance or susceptibility in the phenotyped panel. Each pre-filtered *k*-mer is given a *P* value based on its ability to predict the phenotype using linear regression, with PCA dimensions as covariates to control for population structure. Phenotypes are color-coded as in (**b**), and the presence and absence of *k*-mers is indicated by dark gray and white, respectively. (**e**) *k*-mers are then plotted in an association matrix according to their sequence identity to NLRs from a given accession (*x* axis) and the measure of their association with phenotype (*y* axis). A candidate R gene contig is illustrated by a red-dot column. Figure adapted from Figure 1 of Arora et al. (2019).

1.16 Introduction to the current study

In this project resistance to *MoT* was explored using two diversity panels. The first, *Ae. tauschii* is discussed in Chapter 3. *MoT* resistance genes *Rmg7* and *Rmg8* both recognise the *Avr-Rmg8* effector and map to 2AL and 2BL in wheat respectively (Anh et al. 2015; Anh et al. 2018). *Rmg7* and *Rmg8* are thought to be homoeologous so this chapter aimed to investigate if a homeolog also exists on the D genome.

The objectives of this work were to:

1. Phenotype the *Ae. tauschii* diversity panel using a wildtype Brazilian isolate (NO6047), and a transformed isolate (NO6047+*Avr-Rmg8*) to identify resistance recognising the *Avr-Rmg8* effector.
2. Use a *k*-mer based GWAS approach (AgRenSeq) to map loci associated with resistance to *Avr-Rmg8*.
3. Identify markers that segregate with the loci to determine if they confer resistance in a synthetic hexaploid wheat background.

In Chapters 4 and 5, the second diversity panel is introduced, the Watkins collection of wheat landraces, with the aim of determining if the 2A (*Rmg7*) and 2B (*Rmg8*) genome resistances reported for *Avr-Rmg8* could be detected using the WatRenSeq pipeline.

The objectives of this work were to:

1. Phenotype the Watkins core collection using the transformed isolate NO6047+*Avr-Rmg8* and a recent Brazilian isolate, Py15.1.018 that contains *Avr-Rmg8* to identify if resistance recognising the *Avr-Rmg8* effector is present within the Watkins collection.
2. Run the phenotype data through the WatRenSeq pipeline to identify loci associated with recognition of *Avr-Rmg8*. It was hypothesised that an association would be seen on chromosomes 2A and/or 2B.
3. Utilise gene annotation models and RNAseq data to interrogate intervals associated with resistance to identify candidate genes suitable for functional validation.
4. Identify markers that can be used by wheat breeders to determine if their breeding material contains the resistance.

2. GENERAL MATERIALS AND METHODS

2.1 Culturing, conidia harvesting and storage of *MoT* isolates

Isolates were cultured from filter paper in 9 cm Petri dishes on either complete media agar (CMA) or oatmeal agar (**Section 2.1.1**) plates depending on which media produced the most conidia. Plates were incubated for two weeks at 22°C under a 16 h/8 h light-dark photoperiod. Plates were then sub-cultured onto fresh oatmeal agar and incubated for a further two weeks under the same conditions. Conidia were harvested using a glass spreader and approximately 3ml sterile distilled water (dH_2O) per plate and filtered through a single layer of muslin. The conidial suspension was determined using a haemocytometer under a Vickers M17 optical microscope at 125x magnification.

To store cultures, a 3 to 5 mm^2 piece of mycelium from the growing margin of a 7 to 14-day-old culture was transferred to a fresh agar plate using a flame-sterilised scalpel. 5 to 7 mm^2 pieces of sterile filter paper were placed evenly around the piece of mycelium using flame-sterilised forceps. Plates were incubated at 22°C under a 16 h/8 h light-dark photoperiod, for a maximum of two weeks, until the mycelia had grown through the paper. The filter papers were then transferred into empty 9 cm Petri dishes using a scalpel, taking care not to transfer the agar, sealed with micropore tape and placed in a Boehringer box containing approximately 1 cm silica gel to desiccate for 14 days at room temperature. The filter papers were then transferred into Eppendorf tubes using flame-sterilised forceps and stored at -20°C.

2.1.1 Oatmeal media

Powdered oats (40g) were added to 500ml of dH_2O and placed in a water bath at 65°C for one hour, and then filtered through two layers of muslin. As much liquid was extracted from the oats as possible before dividing equally between two 1L Schott bottles. Agar (10g) (Sigma Aldrich) and 2.5g sucrose were added to each bottle and the volume was made up to 500ml before autoclaving. This media is prone to boiling over so was autoclaved standing in water.

2.1.2 Biological containment precautions

As a non-native plant pathogen of a major UK crop, *Mo* is classed as a medium risk biological agent and assigned to containment level two (CL2). All work with *Mo* was carried out within a circulating

Class II flow hood which was decontaminated with UV light after use. Isolates were stored at -20°C under Plant Health License 51908/198798. All waste material was autoclaved prior to disposal.

2.2 Detached leaf assays

Seeds were incubated for 48 hours in the dark at 4°C in 9 cm Petri dishes containing filter paper and 4ml of 2µM GA_3 (Sigma Aldrich). Seeds were transferred to 20°C for 24 hours and then grown for 14 days in peat-based compost at 22/18°C under a 16/8 hour light-dark photoperiod. Agar (50ml of 1%) was dispensed into square clear plastic plates (10 x 10 cm) (Thermofisher Scientific). Two rectangular strips (2 x 10 cm) were cut from the centre of the agar. The second leaf of each seedling was detached, cut into 8 cm sections and placed adaxial side upwards across the plate, bridging the cut portion, taking care to handle the leaf sections as little as possible. The 2 x 10 cm strips of agar were then laid over the cut edges of the leaf sections to hold them in place. A total of seven leaves were included per plate, including a susceptible control, the tetraploid wheat cultivar Kronos. Five biological replicates were used per accession, with each replicate on a different plate. To delay senescence 1 ml of dH_2O was pipetted into the gap between the leaf sections and the agar strip on each side. Leaves were spray inoculated with *M. oryzae* conidial suspension at a concentration of 0.3 – 0.45 x 10^6 conidia per ml using a Clarke Wiz Mini Air Compressor spray gun kit (Clarke Tools, Dunstable, England). Isolates were passaged a maximum of five times when used for plant inoculations. The lids of the plates were misted with sterile dH_2O to increase humidity, and then laid flat in plastic trays lined with blue roll drenched in water to create a humid environment. The plates were randomised across the trays and then placed into an autoclave bag and kept in the dark for 24 hours after inoculation and incubated at 22°C under a 16/8 hour light-dark photoperiod (**Figure 5**). Leaves were scored for disease symptoms at three to seven days post infection (dpi). Images were taken using an OLYMPUS CAMEDIA C-750 UZ digital camera using the 'macro' feature with an aperture of '7'.

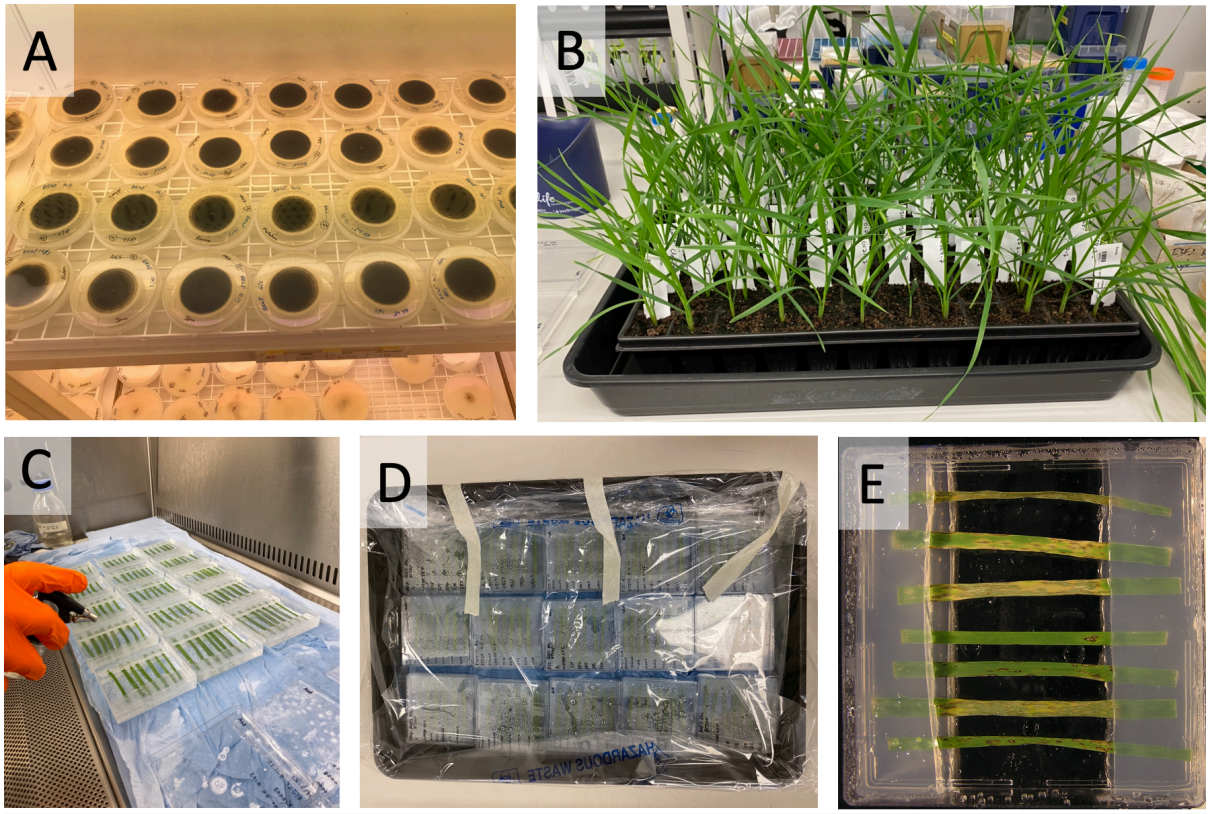

Figure 5: Photos of some steps involved in detached leaf *M. oryzae* assays. **(A)** *M. oryzae* being cultured on agar plates. **(B)** Two week old seedlings. **(C)** Inoculation. **(D)** Plates post inoculation, misted and covered ready to be incubated. **(E)** Representative plate with Kronos as the negative control (top leaf).

2.2.1 Leaf phenotype data collection

Leaves were scored two to three times at intervals of one to two days over a period of three to seven dpi, depending on the disease progress. A seven point scale was used ranging from 0 – 6 (fully resistant to fully susceptible respectively) (**Figure 6**).

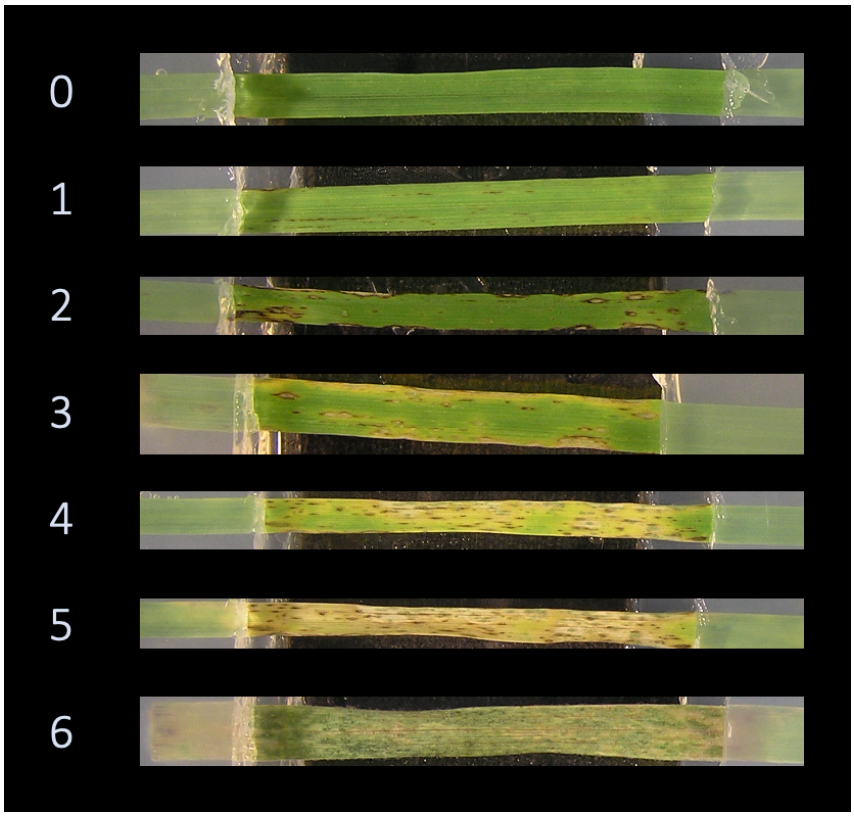

Figure 6: *M. oryzae* detached leaf assay disease scale. 0 = completely resistant, no sign of infection. 1 = minor necrotic flecking. 2 = moderate, stronger necrotic flecking. 3 = some chlorosis, small grey lesions. 4 = intermediate phenotype with moderate flecking and moderate chlorosis. 5 = complete collapse with some flecking indicating initial host detection of the pathogen, but insufficient to provide resistance. 6 = complete collapse with no necrosis.

2.3 Detached *Ae. tauschii* spike assays

Seeds were prepared as described in **Section 2.2** '**Detached leaf assays**'. The seedlings were then vernalised for eight weeks at 4°C under a 16/8 hour light-dark photoperiod. The strongest seedling per accession was then potted up into a 1 litre pot and transferred to either an unheated Keder polytunnel during the summer, or a heated glass house over winter (19°C day/15°C night temperature with a 16 hour daylength. Three spare seedlings were potted together into a three litre pot and kept under the same conditions. John Innes Centre 'Cereals Mix' compost was used, comprising of 65% peat, 25% loam and 10% grit, plus additives (3kg/m^3 Dolomitic limestone, 1.3kg/m^3 PG mix and 3kg/m^3 osmocote exact). Detached spikes were placed in 200 □l StarLab tip boxes, with the yellow inserts kept in place. The top and bottom two rows of holes were covered with a double layer of masking tape to hold the tips securely. 200 □l tips were cut to remove the bottom 2.5 cm and pushed through the tape into alternate holes in the outermost rows. The tips keep the detached spikes upright during inoculation and photographing (**Figure 7**). Spikes were harvested pre anthesis as this improves the infection rate. The boxes were prefilled with water and placed in trays lined with blue roll drenched in water to create a humid environment. To prevent air bubbles forming in the xylem vessels the spikes were cut twice; once to remove them from the plant, and a second time with the stem underwater, leaving approximately 4 cm of stem remaining. Once a tray was full, they were covered with a clear plastic propagator lid to maintain humidity. Three biological replicates were used per accession which were placed together in the same box. A susceptible control was included in each assay. The spikes were spray-inoculated with *M. oryzae* conidial suspension at a concentration of 0.2 to 0.3 x 10^6 conidia per ml using a Clarke Wiz Mini Air Compressor spray gun kit (Clarke Tools, Dunstable, England). Isolates were passaged a maximum of five times when used for plant inoculations. Approximately 25 ml of inoculum was used per five boxes of spikes (60 spikes in total). The lids of the propagators were misted with dH_2O to increase humidity. Trays were kept in the dark for 24 hours after inoculation and incubated thereafter at 22°C under a 16/8 hour light-dark photoperiod. Spikes were scored for disease symptoms at nine to twelve dpi using a 0 – 6 scale (fully resistant to fully susceptible) (**Figure 8**). Images were taken using an OLYMPUS CAMEDIA C-750 UZ digital camera with an aperture of '7'.

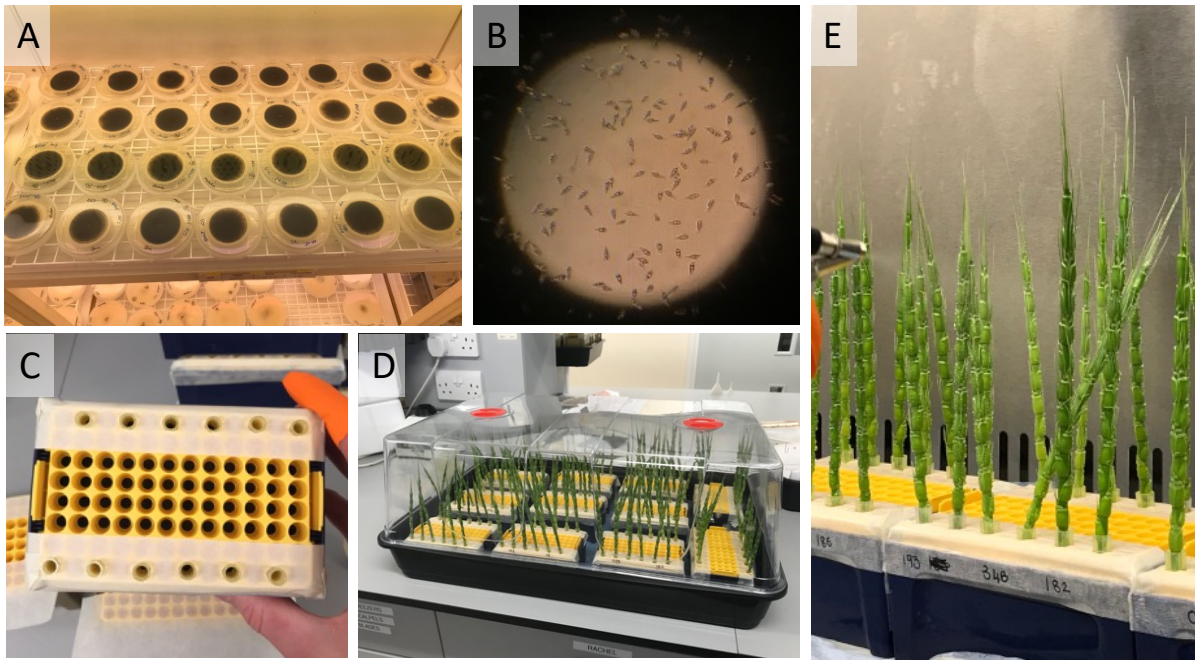

Figure 7: Photos of some steps involved in detached spike *M. oryzae* assays. **(A)** *M. oryzae* being cultured on agar plates. **(B)** *M. oryzae* spores under a compound microscope at 125x magnification. **(C)** StarLab tip box prepared to hold the detached spikes. **(D)** Boxes ready for inoculation. **(E)** *Ae. tauschii* spikes being inoculated.

2.3.1 *Ae. tauschii* spike phenotype data collection

Spikes were scored two to three times at intervals of one to two days over a period of five to nine dpi, depending on the disease progress. A seven point scale was used ranging from 0 – 6 (fully resistant to fully susceptible respectively) (**Figure 8**).

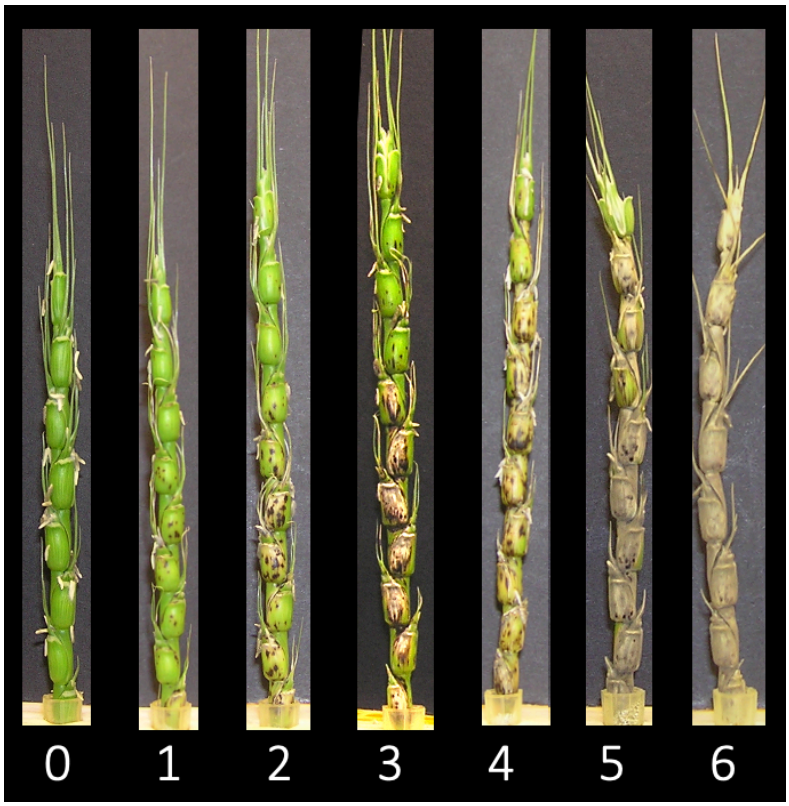

Figure 8: *M. oryzae* detached *Ae. tauschii* spike assay disease scale. 0 = completely resistant, no sign of infection. 1 = minor necrotic flecking. 2 = moderate necrotic flecking. 3 = some flecking, some grey lesions. 4 = intermediate phenotype with moderate flecking and moderate chlorosis. 5 = some flecking however overcome with sporulation and some bleaching, indicating initial host detection of the pathogen but insufficient to provide resistance. 6 = complete collapse with bleaching and sporulation covering the entire spike.

2.4 Detached wheat spike assays

Seeds and seedlings were prepared as described in **Section 2.3**: '**Detached *Ae. tauschii* spike assays**'. Three to five seedlings per accession were potted up individually into 1 litre pots of John Innes Centre 'Cereals Mix' compost, comprising of peat, sterilised soil and grit (40:40:20). and transferred to an unheated heated glass over summer, or a heated glass house over winter (19°C day/15°C night temperature with a 16 hour daylength. Spikes were harvested and spray-inoculated as described in **Section 2.3**. Three biological replicates were used per accession which were placed together in the same box. Trays were kept in the dark for 24 h after inoculation and incubated thereafter at 20, 22 or 26°C (depending on the experiment) under a 16 h/8 h light-dark photoperiod.

2.4.1 Wheat spike phenotype data collection

Spikes were scored for disease symptoms at intervals of one to two days, over a period of three to nine dpi. A seven point scale was used ranging from 0 – 6 (fully resistant to fully susceptible respectively) (**Figure 9**).

Figure 9: *M. oryzae* detached wheat spike assay disease scale. 0 = completely resistant, no sign of infection. 1 = minor necrotic flecking. 2 = moderate necrotic flecking. 3 = some flecking, some grey lesions. 4 = intermediate phenotype with moderate flecking and moderate chlorosis. 5 = some flecking however overcome with sporulation, indicating initial host detection of the pathogen but insufficient to provide resistance. 6 = complete collapse with bleaching and sporulation covering the entire spike.

2.5 Association Mapping

2.5.1 AgRenSeq

Arora et al. combined association genetics with R gene enrichment sequencing (AgRenSeq) to exploit pre-existing recombination events in *Ae. tauschii* (2019). A sequence-configured diversity panel consisting of 151 accessions of *Ae. tauschii* L2, from around the Caspian Sea was developed. As NLR genes are highly diverse thus complicating the conventional alignment of raw reads and SNP-calling against a reference genome, *k*-mers (sub-sequences) were subjected to association analysis, filtered for *k*-mers with high association scores, and then mapped against the RenSeq assembly of a resistant accession (**Figure 4**). In this study the presence and absence of overlapping *k*-mers were mapped against a range of resistant and susceptible accessions to identify *k*-mers associated with resistance. The pipeline was run in Python using the code available at https://github.com/steuernb/AgRenSeq.

2.5.2 OWWC

The Open Wild Wheat Consortium (OWWC) pipeline uses *Ae. tauschii* whole genome data and so can detect associations with non-NLR resistance genes (Gaurav et al. 2022). Associated *k*-mers were mapped to reference assemblies of AL8/78, Chinese Spring and the AL8/78-anchored assembly of BW_01111 using a pre-publication version of the pipeline (curtesy of Kumar Gaurav). The assemblies were prepared for *k*-mer mapping by either splitting the reference into equal sequences of 10000bp or by mapping a non-reference assembly to the reference genome and retaining the longest hit. The assembly files were then split into multiple files which could be processed in parallel to speed up the association mapping. The association script was run on each assembly file using a *k*-mer matrix generated by Kumar Gaurav, and the outputs merged together before generating a Manhattan plot. The pipeline was run in Python using the code available at https://github.com/kgaurav1208/AgRenSeq_GLM.

2.5.3 WatRenSeq

Arora at al. used a *Triticeae* bait library to capture and sequence the NLR complements of the 320 wheat lines described in **Section 4.2.1.2** (2022). Mapping and association steps were carried out as described in **Section 2.5.2**, using the NLR compliments of multiple resistant and susceptible Watkins lines. In this study the cultivar Mattis was used as the reference accession. The pipeline was run in Python using the code available at https://github.com/arorasanu/watkins_renseq.

2.6 NLR-Parser and NLR-Annotator

Given the high proportion of cloned *R* genes that are NLRs, the software tools NLR-Parser and NLR-Annotator were used to predict putative NLR loci (Kourelis and Van Der Hoorn 2018; Steuernagel 2020; Steuernagel et al. 2015). First the input sequence was split into 20kb fragments overlapping by 5kb. Then NLR-Parser preselected fragments containing a series of consecutive motifs associated with the NB-ARC domain. NLR-Annotator then searched for additional motifs associated with the pre-NB region and LRRs. The presence, position and combination of motifs identified was evaluated to generate a list of predicted NLR loci. NLR-Annotator does not predict ORFs.

2.7 DNA extraction

DNA was extracted from three week old seedlings (third leaf) using the oKtopure bead based automated DNA extraction system (LGC Biosearch Technologies) following manufacturer's instructions. Samples were stored at -20^{o}C.

2.8 Kompetitive allele-specific PCR assays

Kompetitive Allele-Specific PCR (KASP™) genotyping assays enable bi-allelic discrimination of single nucleotide polymorphisms (SNPs) and insertions and deletions (Indels) at specific loci. The assays are high throughput as can be performed in 384 well plates.

Three assay-specific primers are used: two allele-specific forward primers that target the selectable polymorphism (SNP/INDEL) and one common reverse primer (allele specific reverse/common forward primer sets can also be generated). A unique tail sequence is added to the allele-specific primers that corresponds with a universal FRET (fluorescence resonant energy transfer) cassette (**Table 2**). The FRET cassette is labelled with either a FAM™ or HEX™ tag. During the reaction, the appropriate allele-specific primer anneals to the template and elongates, incorporating the tail. The complement of the tail sequence is then generated during subsequent rounds of PCR, allowing the FRET cassette to bind to the DNA. The FRET cassette is now free to emit fluorescence, which can be detected on a plate reader (PHERAstar, BMG LABTECH) using the genotyping data analysis software KlusterCaller (LGC Genomics). If the genotype at a given SNP is heterozygous, a mixed fluorescent signal will be generated. Note, if a genotype lacks the selectable polymorphism (eg doesn't contain the gene the KASP primers have been designed within), the datapoints will segregate along with the 'no template' contols (NTCs), thus allowing the assay to distinguish between three different genotypes in one reaction (**Figure 10**).

All reactions were run on a Mastercycler pro 384 PCR thermocycler (Eppendorf®) using the following touchdown PCR programme:

1. 94°C for 15 minutes
2. 94°C for 20 seconds
3. 65°C for 1 minute (repeat steps 2 to 3 ten times, decreasing by 0.8°C each cycle to 57°C)
4. 94°C for 20 seconds
5. 57°C for 1 minute (repeat steps 4-5 30x)
6. Hold at 16°C
    - an additional 5 – 10 cycles may be required for full separation of the signals from the different genotypes)

Table 2: HEX and FAM tail nucleotide sequences

Tail	Sequence
HEX	GAAGGTCGGAGTCAACGGAT
FAM	GAAGGTGACCAAGTTCATGCT

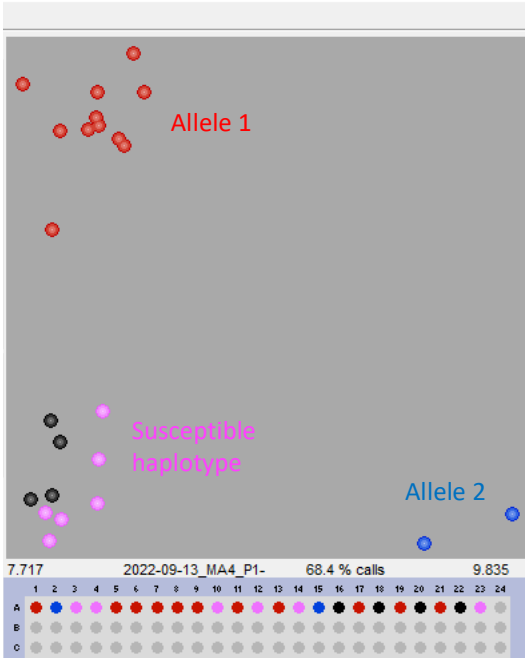

Figure 10: Example KlusterCaller cluster plot. Allele specific markers designed to a SNP in a resistance gene. Blue data points are homozygous for the allele associated with FAM Red data points are homozygous for the allele associated with HEX. The black data points represent the no template controls (NTC). In this example, pink data points represent genotypes that lack the resistance gene and so segregate with the NTC.

3. IDENTIFYING D GENOME RESISTANCE TO Avr-Rmg8

3.1 Introduction

This chapter focuses on efforts to identify resistance in the D genome effective against *MoT* isolates utilising the *Ae. tauschii* AgRenSeq pipeline. *MoT* resistance genes *Rmg7* and *Rmg8* both recognise the *Avr-Rmg8* effector and map to 2AL and 2BL in wheat respectively (Anh et al. 2015; Anh et al. 2018). *Rmg7* and *Rmg8* are thought to be homoeologous which raised the possibility that a homeolog might also exist on the D genome.

A recent Brazilian *MoT* isolate, NO6047, has been shown to be virulent on S-615 and so does not contain an *Avr-Rmg8* effector that recognises *Rmg8* (Jensen et al. 2019). The isolate NO6047 was transformed with the *Avr-Rmg8* type eI effector from the Bangladeshi isolate BTJ4P-1 downstream of the PWL2 promoter from *M. oryzae* to drive expression of the transgene (Jensen and Saunders 2023). This provided a pair of isolates differing in a single effector (NO6047 and NO6047+*Avr-Rmg8*). It was hypothesised that by phenotyping the *Ae. tauschii* diversity panel using the wildtype NO6047 and transformed NO6047+*Avr-Rmg8* isolates and comparing the disease scores it would be possible to identify accessions that recognise eI allele of *Avr-Rmg8.* It is assumed that differences in disease scores between the two assays would be due to recognition of *Avr-Rmg8* and the 'differential' dataset could be used to perform GWAS to identify loci associated with recognition of *Avr-Rmg8*. This approach should eliminate or minimise any background effects arising from resistance(s) to NO6047, increasing the likelihood of identifying an association relating specifically with resistance to *Avr-Rmg8,* which if present was expected to be on 2D.

Within the literature there are three alleles described for *Avr-Rmg8;* type eI, eII, and eII', differing in just a few amino acids (aa) (**Figure 11**) (Wang et al. 2018). Whilst *Rmg8* has been overcome in Brazil, Jensen et al. found that the Bangladesh isolate, BTJ4P-1 was avirulent on S-615, which contains *Avr-Rmg8* (2019). As isolates in Bangladesh are believed to be clonally derived from a single South American strain, this suggests that resistance to *Avr-Rmg8* could be of use in Bangladesh (Malaker et al. 2016; Cruz and Valent 2017). Indeed, Horo et al found that all of the Bangladeshi isolates tested carry the same allele of *Avr-Rmg8,* type eI (2020). Given the scarcity of wheat blast resistance that functions in the spike, and the immediate need for genetic resistance to delay the spread of the pathogen from Bangladesh through South Asia, the potential benefit of identifying resistance to *Avr-Rmg8* that could be deployed in Bangladesh is immense.

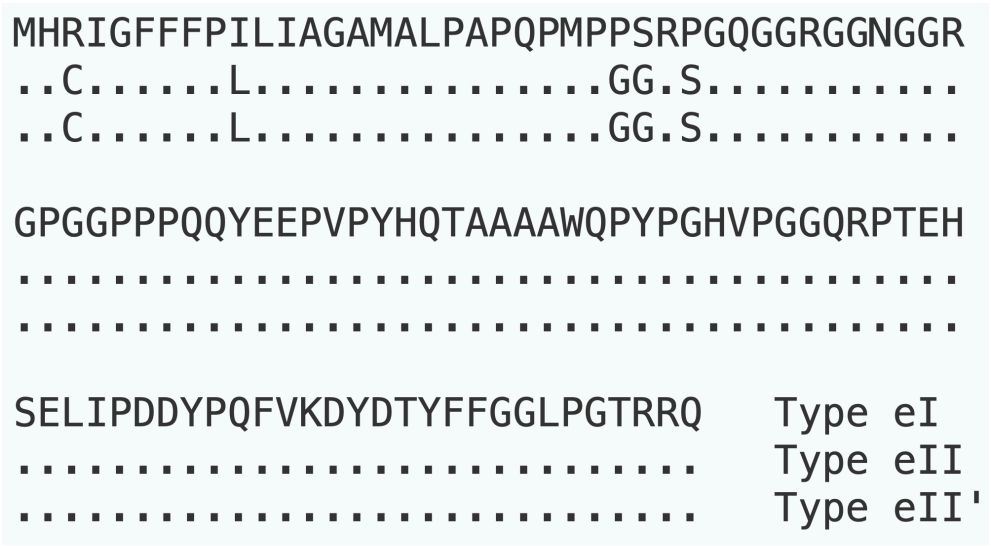

Figure 11. Amino acid sequence alignment of the three alleles of *Avr-Rmg8* effector: type eI, eII, and eII'.

3.2 Materials and methods

3.2.1 Plant and pathogen material

3.2.1.1 Ae. tauschii core diversity panel

The sequence-configured diversity panel of 151 *Ae. tauschii* ssp. *strangulata* accessions developed by Arora et al., (2019) was used in this study (**Sup. table S1**). These accessions originate from around the Caspian Sea and are non-redundant.

3.2.1.2 Synthetic hexaploid wheat lines

A number of SHW lines have been generated by the National Institute of Agricultural Botany (NIAB) by crossing of accessions of *Ae. tauschii* (D donor) to tetraploid wheats. Twenty-seven SHW lines and their tetraploid and D genome donors were used in this study (**Table 3**).

Table 3: NIAB Synthetic lines with their tetraploid and D Genome donors.

Synthetic	Tetraploid Donor	D Donor
NIAB-SHW012	Hoh-501-P14-1	BW_26040
NIAB-SHW018	Hoh-506-P9-1	BW_26041
NIAB-SHW042	Hoh-506-30	BW_26060
NIAB-SHW043	Hoh-501-P14-35	BW_26047
NIAB-SHW051	Hoh-501-P14-23	BW_26041
NIAB-SHW070	Hoh-506-P6	BW_26051
NIAB-SHW071	Hoh-501-P14	BW_20607
NIAB-SHW072	Hoh-501-P14-11	BW_26060
NIAB-SHW073	Hoh-501-P14-11	BW_20718
NIAB-SHW075	Hoh-501-P14	BW_26066
NIAB-SHW076	Hoh-501-P14	BW_26067
NIAB-SHW077	Hoh-501-P14	BW_26065
NIAB-SHW080	Hoh-501-P14	BW_26057
NIAB-SHW083	Hoh-501-P14	BW_26046
NIAB-SHW084	Hoh-501-P14	BW_20622
NIAB-SHW085	Hoh-501-P14	BW_26062
NIAB-SHW086	Hoh-501-P14	BW_26050
NIAB-SHW087	Hoh-501-P14	BW_20745
NIAB-SHW088	Hoh-501-P14	BW_25578
NIAB-SHW089	Hoh-501-P14	BW_26045
NIAB-SHW090	Hoh-501-P14	BW_26048
NIAB-SHW091	Hoh-501-P14	BW_26055
NIAB-SHW092	Hoh-501-P14	BW_20726
NIAB-SHW093	Hoh-501-P14	BW_26058
NIAB-SHW094	Hoh-501-P14	BW_20749
NIAB-SHW095	Hoh-501-P14	BW_20608
NIAB-SHW099	Hoh-501-P14	BW_26069

3.2.1.3 Recombinant inbred line populations

NIAB have created Recombinant Inbred Line (RIL) populations by backcrossing a selection of SHW lines into the spring hexaploid wheat cultivar Paragon, and the winter wheat Robigus, and selfing of progeny to F5. Two Paragon populations generated with resistant synthetic wheat lines carrying the 7D resistant haplotype, SHW031 (Population A) and SHW029 (Population B) were used in this study (**Table 4**). Seed was provided by Richard Horsnell, NIAB.

3.2.1.4 Isolates

Two isolates were used for phenotyping in this chapter, a wildtype Brazilian isolate collected in 2006 (NO6047; provided by Diane Saunders, JIC), and a transformed isolate (NO6047+*Avr-Rmg8*) generated by Cassandra Jensen, JIC, NO6047+*Avr-Rmg8* (Islam et al. 2016; Jensen et al. 2019) (**Sup. table S2**). Both isolates were cultured on oatmeal media plates as described in **Section 2.1.1**.

Table 4: NIAB backcross populations used in this study.

NIAB Population	Population nickname	Population size	Synthetic parent	*Ae. tauschii* Donor	Tetraploid Donor
NIAB SHW BC 585	A	61	SHW031	BW_26041	?
NIAB SHW BC 582	B	51	SHW029	BW_26042	Sculpture

3.2.2 Detached leaf and spike assays

Detached leaf and spike assays were performed as described in **Sections 2.2 and 2.3**. The inoculum concentrations, scoring day(s) and relevant section describing the results of each DLA and DSA in this chapter are listed in **Table 5.**

3.2.2.1 Statistics

A Welch's t-test was performed to determine if there was a statistically significant difference in mean spike scores between sampling days. The sample size for sample one and sample two was 14 and nine accessions respectively.

Table 5: Detached leaf and spike assays described in this chapter.

Isolate	Test*	Inoculum [x 10^6/ml]	Scoring day (dpi)	Section
NO6047	*Ae. tauschii* core panel DLA	0.43	4 & 5	3.3.1.1
NO6047+*Avr-Rmg8*	*Ae. tauschii* core panel DLA	0.10	5	3.3.1.2
	Ae. tauschii DSA	0.23	5 & 7	3.3.1.3
	Ae. tauschii DLA of SWRH	0.22	5	3.3.1.8
	NIAB SHW DLA	0.28	5	3.3.1.10
	NIAB SHW DSA	0.28	5 & 7	3.3.1.10
	NIAB RILs DLA	0.35	6	3.3.1.11
	NIAB RILs DSA	0.11 - 0.14	6 & 7	3.3.1.11

* DLA = detached leaf assay. DSA = detached spike assay. SWRH = susceptible with the resistant haplotype

3.2.3 Melt curve analysis for differentiating resistant and susceptible genotypes

Melt-curve analysis was used to genotype resistant and susceptible samples. This approach uses real time (q)PCR to assess the dissociation characteristics of double stranded DNA (dsDNA) and is used to distinguish between different PCR products within the same reaction. The temperature dependent dissociation of dsDNA is measured using an intercalating fluorophore which will only fluoresce when bound to dsDNA. Once the amplification cycles are completed the amount of fluorescence is measured, and then recorded as the temperature increases incrementally until the dsDNA dissociates. The decrease in fluorescence is then plotted to produce a melt curve. Two PCR products with different melting temperatures will produce distinct melt curves which can be used to genotype the sample. In this study the SYBR® green fluorophore was used (Merk). 20µl reactions comprising; 0.8µl each of the forward and reverse primers (**Table 6**), 4.4µl ddH_2O, 4µl DNA (at a concentration of between 10 to 30ng and 10µl SYBR® Green jumpstart Taq (Merck) were made per sample.

All reactions were run using the following qPCR programme:

7. 95°C for 2 minutes
8. 95°C for 10 seconds
9. 60°C for 30 seconds
10. 72°C for 30 seconds (repeat steps 2 to 4, 39 times)
11. 65 to 95°C (melt-curve step; 5 seconds at each temperature, increasing by 0.5°C increments)

Table 6: Melt-curve primers.

	Forward primer	Reverse Primer	Product length (bp)	Melting temperature (°C)
Kinase 1	GGCCACCCCACATAGTCG	CAACGGTGGTGAGGTCTGG	107	85
Kinase 4	CCCAAAGCAACAGATGGC	TATGGGTAATGGGATCCTCTAAC	126	81.5

3.3 Results

3.3.1 Phenotyping the *Ae. tauschii* diversity panel

3.3.1.1 NO6047 detached leaf assay

To determine if any of *Ae. tauschii* panel accessions possessed resistance to the wildtype NO6047 isolate a detached leaf assay was performed. There was a little resistance observed within the panel against NO6047, with only 20 accessions classed as resistant (scores ≤ 3), using averaged data for four and five dpi (**Sup. table S3**). Of the 148 accessions tested, only 40 accessions had scores less than 4. Scores from 5 dpi and the combined score dataset were run though the AgRenSeq pipeline using four resistant (BW_01004, BW_01039, BW_01050 and BW_01148), and two susceptible reference accessions (BW_01025 and BW_01107). No strong associations were identified. A representative Manhattan plot for BW_01039 (score of 2.4) is shown in (**Figure 12**).

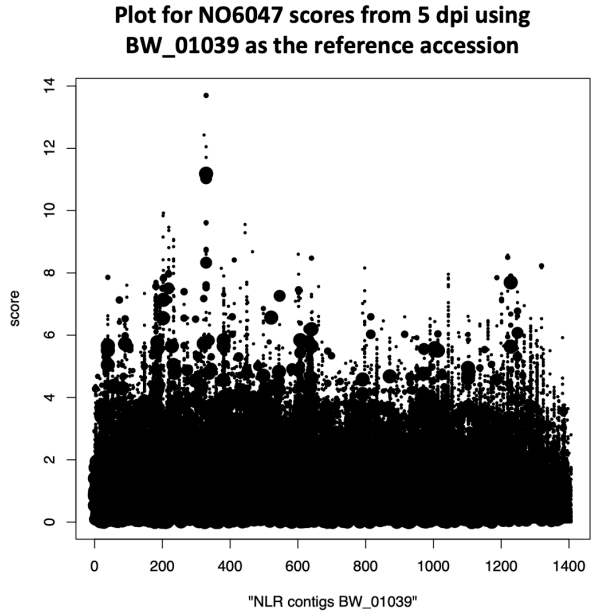

Figure 12: Representative AgRenSeq Manhattan plot for the NO6047 data for *Ae. tauschii* detached leaves. Each dot column on the x-axis represents an NLR contig from the RenSeq assembly of BW_01039. Each dot on the y-axis represents one or more RenSeq *k*-mers associated with resistance. The association score is defined as the negative log of P value obtained using likelihood ratio test for nested models. Dot size is proportional to the number of *k*-mers associated with resistance.

Accessions that were highly resistant to NO6047 were excluded from the NO6047+*Avr-Rmg8* assay to increase the likelihood of identifying a genuine association for resistance to NO6047+*Avr-Rmg8*. It was hypothesised that accessions that show strong resistance to NO6047+*Avr-Rmg8*, but that are susceptible to NO6047, with large positive differential may possess a *Rmg8* D genome homeologue.

3.3.1.2 NO6047+Avr-Rmg8 detached leaf assay

Ninety-four accessions highly susceptible to NO6047 were included in the NO6047+*Avr-Rmg8* DLA. The hexaploid wheat cultivar, S-615 which was used to identify *Rmg8*, was also included. Unfortunately, the titre of conidia harvested was low and the final inoculum concentration was only $0.1x10^6$ conidia per ml. Disease advanced more slowly than in previous experiments, likely due to the low numbers of conidia. In addition, some accessions produced anthocyanins suggesting that they had experienced stress while growing. The anthocyanin pigmentation masks disease symptoms making it difficult to accurately score these accessions.

Raw phenotype scores ranged from 0.8 to 6, with 59 accessions classed as resistant (scores ≤ 3) at 5 dpi. S-615 was highly resistant. Leaf images representative of the range of phenotypes observed are in shown in **Figure 13**. There was very little susceptibility, with just 4 accessions scoring 4 or more, with a mean score of 2.5. Differential scores (NO6047 score minus the NO6047+*Avr-Rmg8* score) ranged from -1.8 to 4.9 (**Sup. table S3**). An extreme scoring system was also used, where 11 accessions with an intermediate *Avr-Rmg8* phenotype were removed (raw score of ≥ 2 and ≤ 2.6). The remaining scores were then reclassed as either resistant or susceptible and given a score of 6 or 0 respectively. This resulted in 36 resistant accessions and 47 susceptible accessions. Data from a total of 84 accessions was used for association genetics analysis. See **Table 7** for examples of how the differential and extreme scores were calculated. To visualise the distribution of observations in the DLA a Kernel Density Estimation (KDE) plot was generated (**Figure 14**).

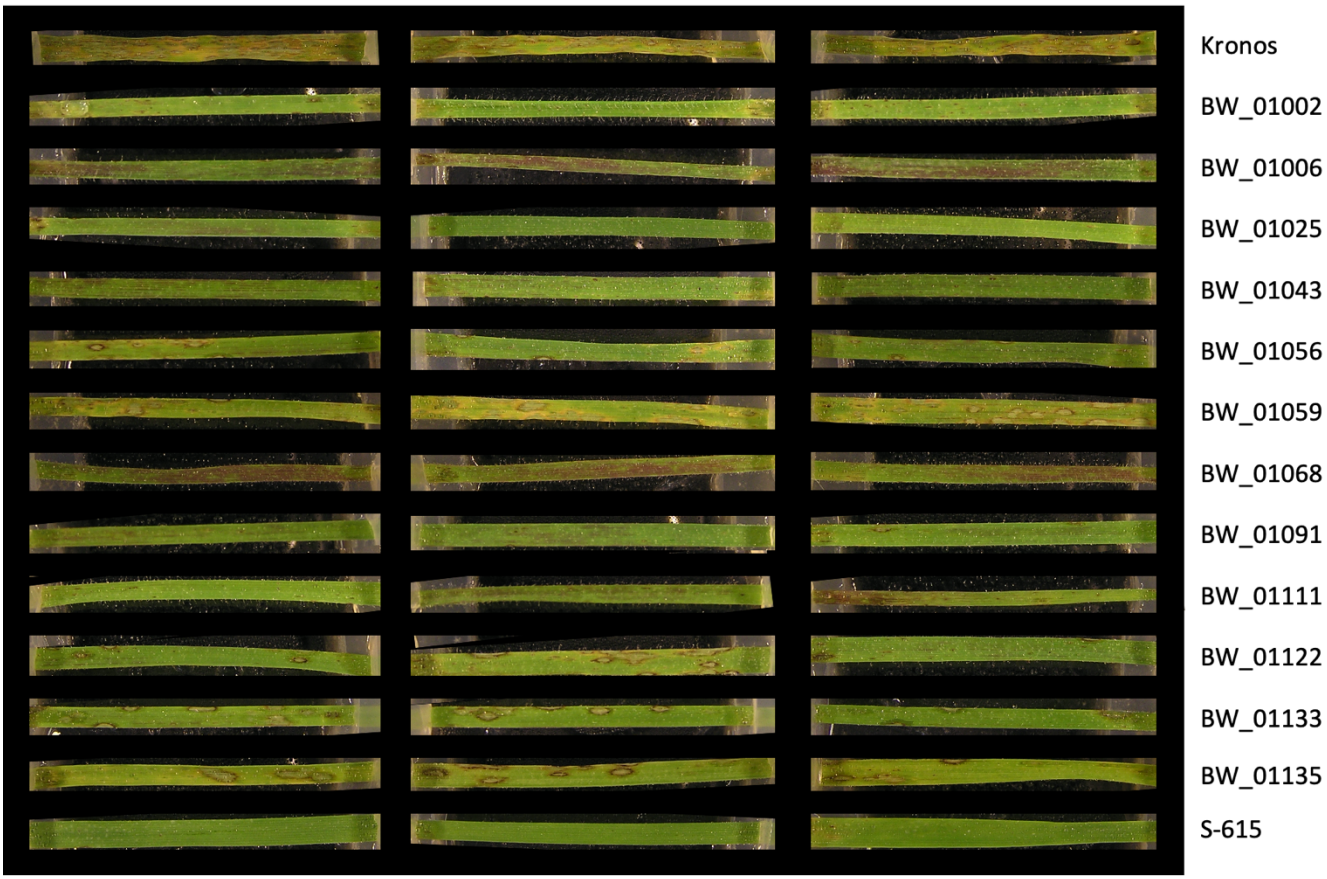

Figure 13: Representative leaf images from the *Ae. tauschii* NO6047+*Avr-Rmg8* detached leaf assay. Kronos was included as a susceptible control. Images were taken at 5 dpi.

Table 7: Table showing the reference accessions used for AgRenSeq for NO6047+*Avr-Rmg8* detached leaf assay data, and the different scoring systems used.

GRU number	Old number	Scores				Phenotype
		NO6047 mean	Avr8* mean	Differential (NO6047 - Avr8)	Avr8 Extreme	
TOWWC044	BW_01043	4.9	1.0	3.9	6	Resistant
TOWWC108	BW_01107	5.9	1.0	4.9	6	
TOWWC112	BW_01111	5.4	1.0	4.4	6	
TOWWC129	BW_01128	5.4	1.0	4.4	6	
TOWWC148	BW_01147	4.0	5.8	-1.8	0	Susceptible
TOWWC163	BW_01162	4.5	3.6	0.9	0	

* Avr8 = NO6047+*Avr-Rmg8*

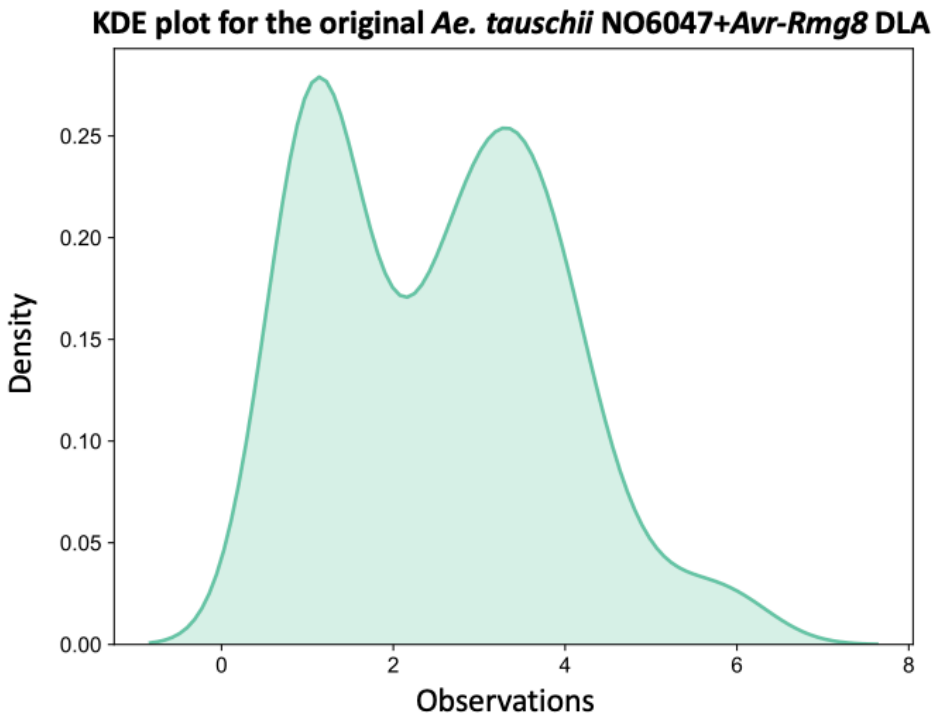

Figure 14: Kernel Density Estimation (KDE) plots for the NO6047+*Avr-Rmg8 Ae. tauschii* DLA. Scores were taken at 5 dpi.

AgRenSeq (NO6047+*Avr-Rmg8*)

The mean, differential and extreme scores from the NO6047+*Avr-Rmg8* DLA were run through the AgRenSeq pipeline, using four resistant (BW_01043, BW_01107, BW_01111 and BW_01128), and two susceptible reference accessions (BW_01147 and BW_01162) (**Table 7**). Manhattan plots for raw and differential data were almost identical. The extreme phenotype data gave the same peaks as the raw data, however the peaks were slightly more significant, with a log score of ~34 (**Figure 15**). A single clear peak was seen for each of the four resistant accessions (**Figure 16**). The contigs underlying the peaks sharing 95.62% to 99.98% sequence identity. This indicated that the peaks represented the same association (**Table 8**). However, this peak was also present in BW_01162, one of the susceptible accessions, but absent in the other (BW_01147). This could be because BW_01162 contains a non-functional allele of the resistance gene. Note in the version of the AgRenSeq pipeline used to generate the Manhattan plots, the NLR contigs were not mapped to the reference accession. This meant that the same peak could appear at different points along the x-axes for different reference accessions.

The contigs underlying the peaks for accessions BW_01128 and BW_01111 were extracted and the sequences were analysed using 'NLR-Annotator' to identify potential NLR genes. The analysis concluded that these sequences contained a single partial NLR, with only coiled coil and NB-ARC domains present. To check if there was a complete NLR present, the partial NLR sequence was BLASTed into the BW_01111 assembly, which hit scaffold17204 with 100% identity. NLR annotator was re-run on the whole scaffold but again, only a partial NLR was identified. The partial NLR was not detected by NLR annotator in the resistant accessions BW_01190 and BW_01106. This NLR fragment sequence is absent in the *Ae. tauschii* reference genome, AL8/78, which is susceptible to NO6047+*Avr-Rmg8.*

Table 8: Percent identity matrix for the contigs underlying the AgRenSeq peaks.

	BW_01107 Contig15387	**BW_01162 Contig4802**	**BW_01128 Contig63**	**BW_01043 Contig9577**	**BW_01111 Contig1626**
BW_01107 Contig15387	100.00%	96.77%	96.81%	95.62%	95.66%
BW_01162 Contig4802	96.77%	100.00%	99.15%	97.96%	97.96%
BW_01128 Contig63	96.81%	99.15%	100.00%	98.87%	98.84%
BW_01043 Contig9577	95.62%	97.96%	98.87%	100.00%	99.89%
BW_01111 Contig1626	95.66%	97.96%	98.84%	99.89%	100.00%

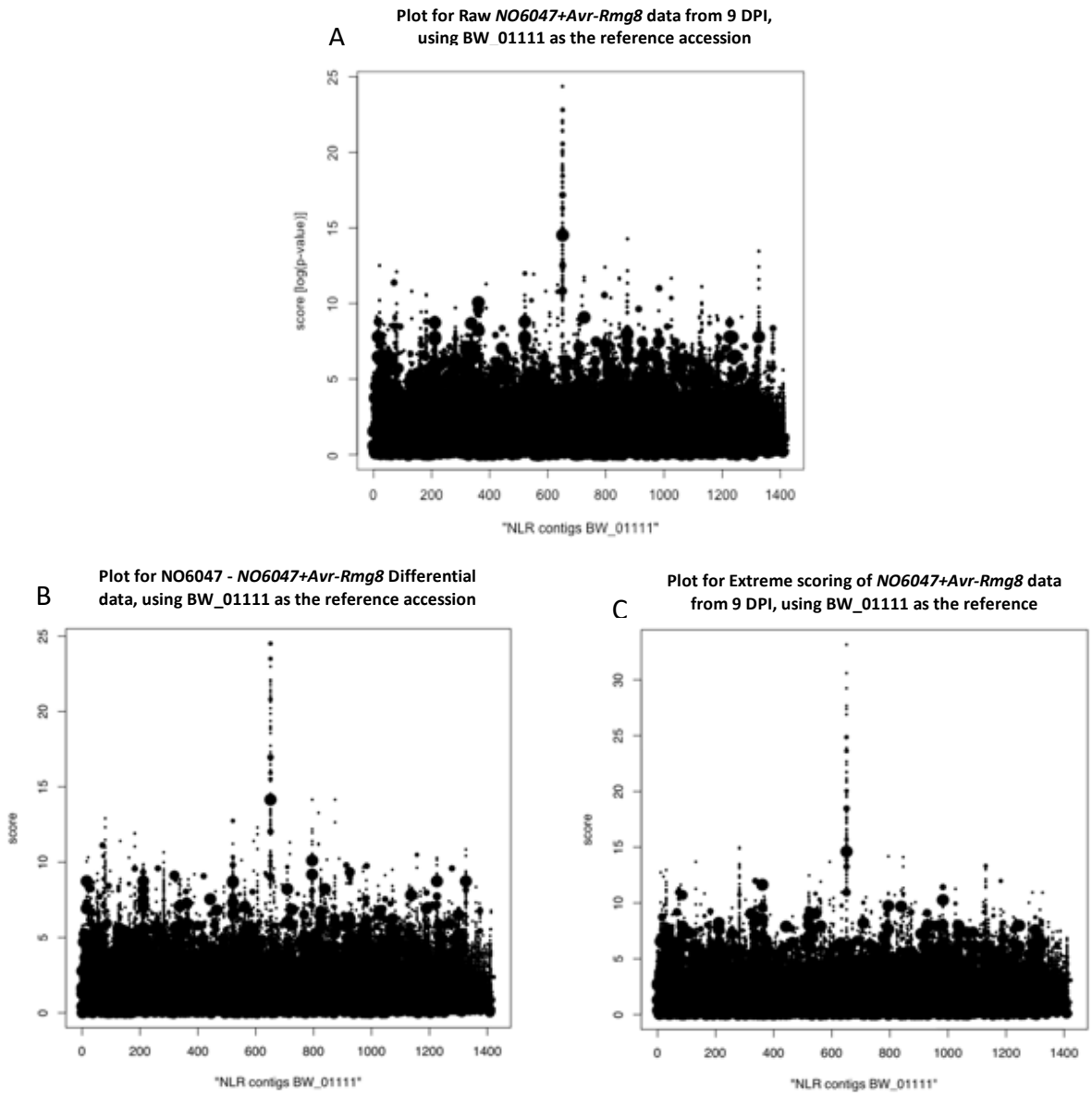

Figure 15: Comparing AgRenSeq Manhattan plots for the three different datasets for NO6047+*Avr-Rmg8* original score data for *Ae. tauschii* detached leaves. Each dot column on the x-axis represents an NLR contig from the RenSeq assembly of BW_01111. (**A**) = plot using raw scores. (**B**) = plot using NO6047 – NO6047+*Avr-Rmg8* differential scores. (**C**) = plot using extreme phenotype scores. Each dot on the y-axis represents one or more RenSeq *k*-mers associated with resistance. The association score is defined as the negative log of P value obtained using likelihood ratio test for nested models. Dot size is proportional to the number of *k*-mers associated with resistance.

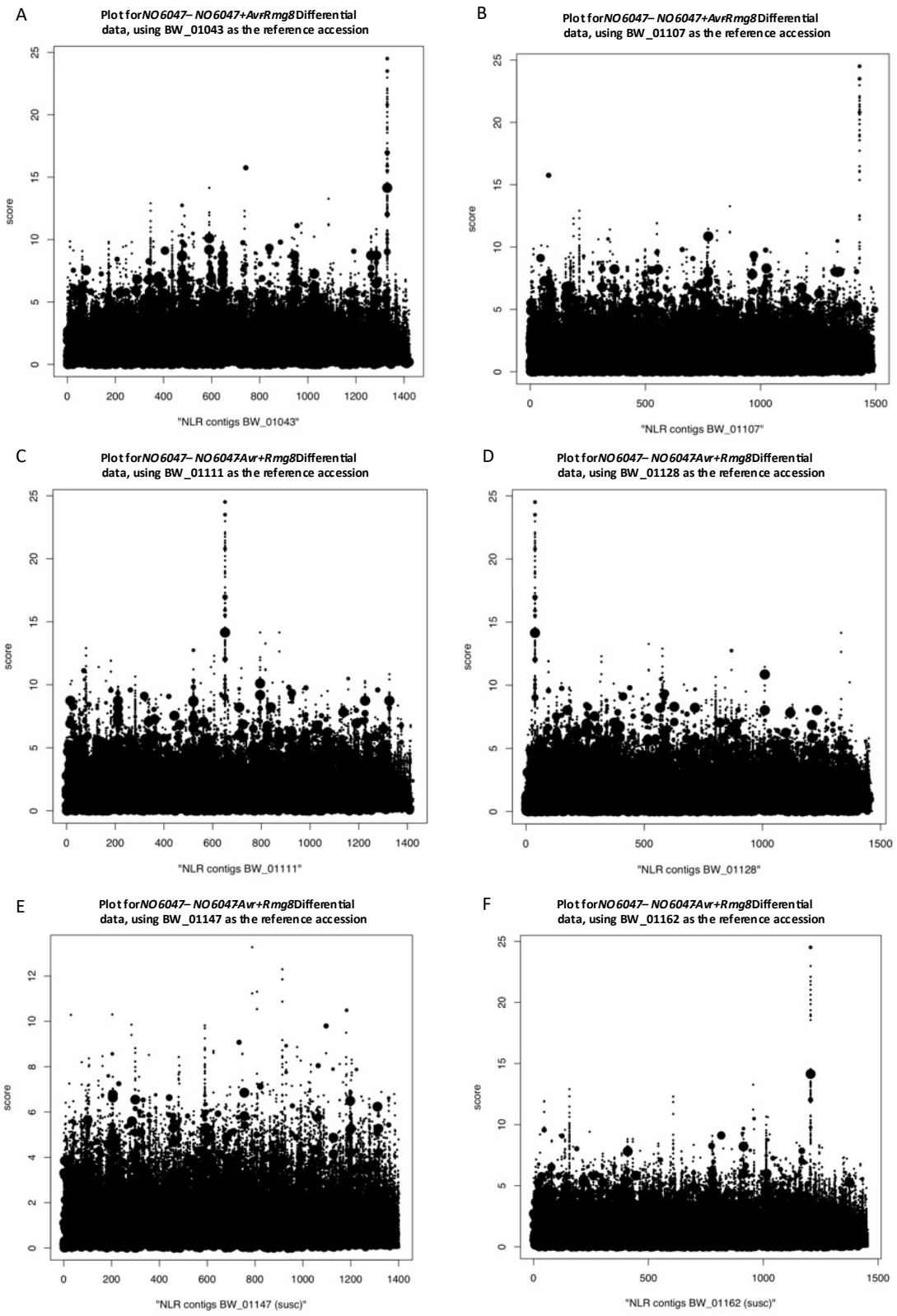

Figure 16: Comparing AgRenSeq Manhattan plots for the NO6047 – *NO6047+Avr-Rmg8* differential score data. Each dot column on the x-axis represents an NLR contig from the RenSeq assembly of (**A**) BW_01043, (**B**) BW_01107, (**C**) BW_01111, (**D**) BW_01128, (**E**) BW_01147 and (**F**) BW_01162. Each dot on the y-axis represents one or more RenSeq *k*-mers associated with resistance. The association score is defined as the negative log of P value obtained using likelihood ratio test for nested models. Dot size is proportional to the number of *k*-mers associated with resistance.

OWWC analysis (NO6047+*Avr-Rmg8*)

In parallel, the differential data was analysed using the Open Wild Wheat Consortium (OWWC) pipeline by Kumar Gaurav (JIC) (Gaurav et al. 2022). This pipeline uses whole genome data and so can detect associations with non-NLR resistance genes. Unlike AgRenSeq, positive and negative associations can be distinguished, presented within Manhattan plots as blue and red respectively. Using the differential dataset, associated *k*-mers were mapped to reference assemblies of AL8/78, Chinese Spring and the AL8/78-anchored assembly of BW_01111. On mapping the associated *k*-mers to BW_01111 two peaks were identified; one on 2DL and one on 7DL. Further analysis revealed that the 2DL peak was miss-anchored due to the presence of multiple regions of ambiguous sequence data ('Ns') in the corresponding sequence (personal communication with Kumar Gaurav, JIC). These regions represent where the sequencing software was unable to assign bases so 'Ns' were called instead. The 2DL peak truly anchors with the 7DL peak, resulting in a single association. Three scaffolds were found to be highly and positively associated with resistance: scaffold_17204, scaffold_27471 and scaffold_11603 (**Figure 17**). Note scaffold_17204 is the scaffold that has sequence similarity to the contig identified using AgRenSeq, however all three scaffolds are in linkage disequilibrium (LD) and equally likely to contain the causal gene. Mapping to AL8/78 and the Chinese Spring D genome, resulted in a discrete red peak (*i.e.* negatively associated *k*-mers) on chromosome 7DL indicative of an association with susceptibility (**Figure 18**). The coordinates of the associated interval are 622.15 – 622.24 Mb (90 kb) with respect to the Chinese Spring reference sequence (RefSeq) v1.0, and 626.90 – 627.11 Mb (210 kb) with respect to AL8/78. Both AL8/78 and Chinese Spring are susceptible to NO6047+*Avr-Rmg8.*

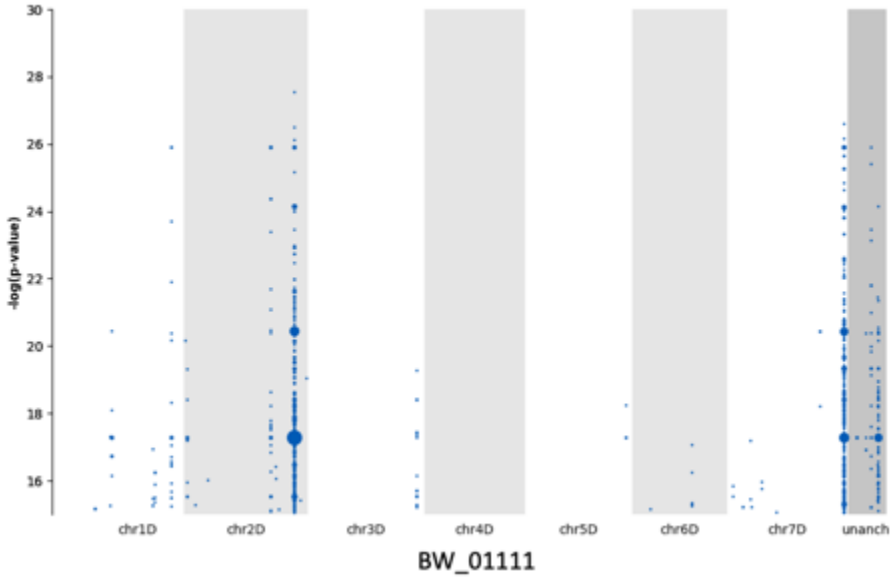

Figure 17: OWWC Manhattan plot for NO6047 - NO6047+*Avr-Rmg8* differential data. Mapping of positively associated k-mers to BW_01111. The 2DL peak was miss-anchored due to the presence of multiple regions of ambiguous sequence data ('Ns') in the corresponding sequence. The 2DL peak truly anchors with the 7DL peak, resulting in a single association. Courtesy of Kumar Gaurav.

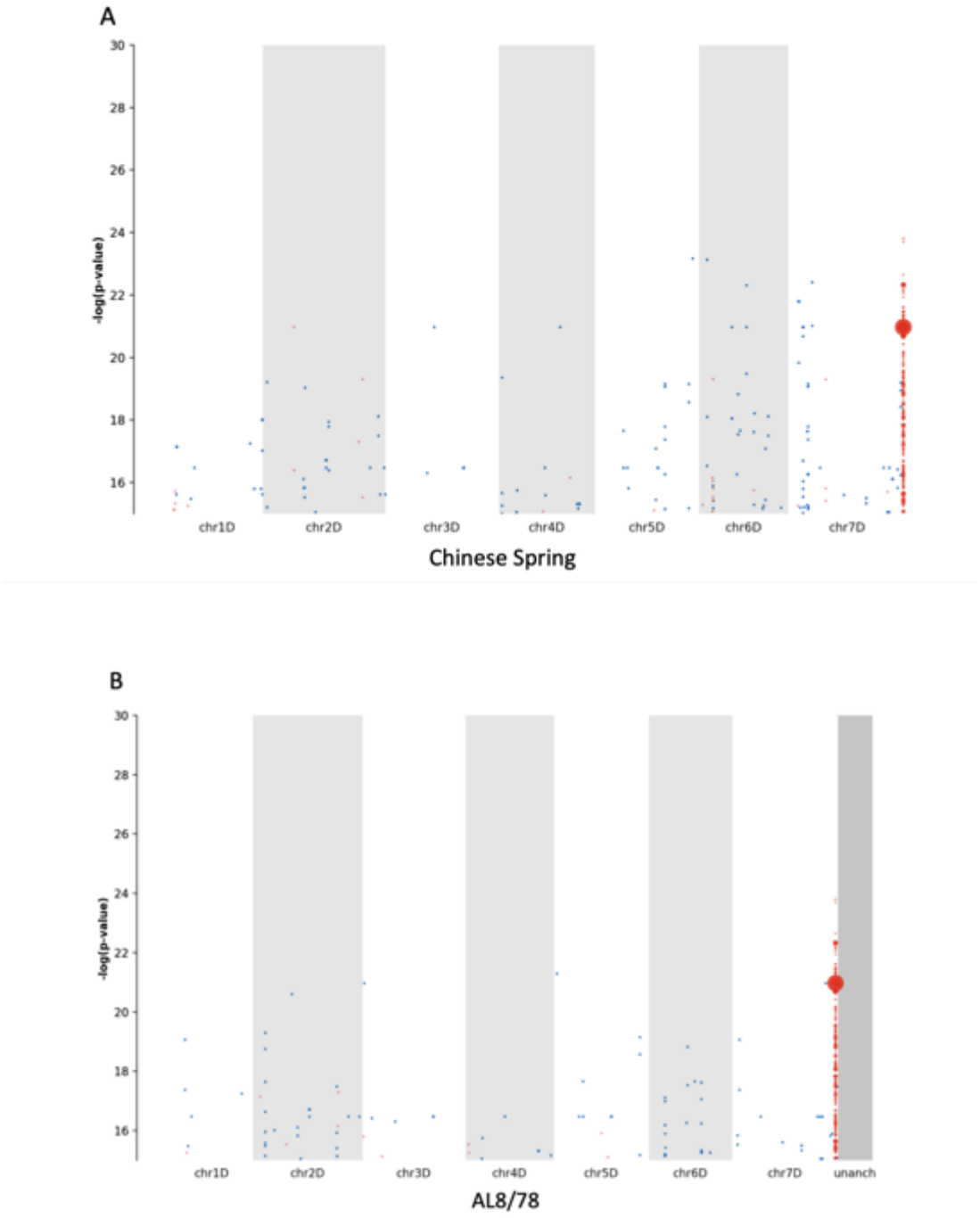

Figure 18: OWWC Manhattan plots for NO6047 - NO6047+*Avr-Rmg8* differential data. Mapping of negatively associated *k*-mers to (**A**) the Chinese Spring D genome and (**B**) and the *Ae. tauschii* reference genome, AL8/78. Courtesy of Kumar Gaurav.

3.3.1.3 Ae. tauschii NO6047+Avr-Rmg8 detached spike assay

To determine whether the 7D seedling leaf resistance also functions in the spikes, a DSA was carried out using a subset of the *Ae. tauschii* panel with the NO6047+*Avr-Rmg8* isolate, as described in **Section 2.3**. Spikes were sampled at a stage post full emergence and shortly before anthesis. Sampling occurred on two days, one week apart. Scoring was performed at 5 dpi and 7 dpi for the first and second sampling days. A Welch's t-test revealed that there was no statistically significant difference in mean scores between the two sampling days ($t = 1.426$, $p = 0.170$). Where accessions were sampled across both sampling days the scores were averaged. The disease pressure in this experiment was very high and symptoms developed rapidly, indicating that the inoculum load was excessive. Although some accessions exhibited resistance in the spikes, most accessions were moderately to severely affected resulting in a lack of correlation between the leaf and spike phenotypes (**Table 9**).

Table 9: Detached spike scores from the *Ae. tauschii* assay with NO6047+*Avr-Rmg8,* compared to detached leaf assay scores. Green = resistant, red = susceptible.

Accession	DLA (5 dpi)	Detached spike assay		
		Sample 1*	Sample 2**	Average
BW_01008	2.80	4.00	-	4.00
BW_01011	2.80	5.30	4.60	5.00
BW_01015	2.80	5.00	-	5.00
BW_01019	4.80	5.00	-	5.00
BW_01020	2.50	3.67	3.00	3.30
BW_01027	3.50	-	3.67	3.66
BW_01105	-	4.00	4.00	4.00
BW_01111	1.00	3.78	-	3.78
BW_01126	2.80	4.83	-	4.83
BW_01128	1.00	3.67	-	3.67
BW_01129	2.60	-	3.33	3.33
BW_01159	3.00	5.00	-	5.00
BW_01161	3.20	3.33	-	3.33
BW_01162	3.60	-	4.67	4.67
BW_01163	3.80	-	3.83	3.83
BW_01170	3.80	-	3.33	3.33
BW_01175	4.00	4.67	-	4.67
BW_01176	3.20	3.50	-	3.50
BW_01178	2.60	3.67	-	3.67
BW_01192	3.20	-	4.33	4.33

* Sample 1 was scores at 5 dpi

** Sample 2 was scored at 7 dpi

3.3.1.4 Iso008 spike data

A research group at Kansas State University, USA, had also performed a wheat blast spike assay of the *Ae. tauschii* panel (J. Poland, personal communication) under glasshouse conditions in Bolivia using isolate iso008, collected from Bolivia in 2015 (Cruppe et al. 2019). Data was collected from spikes of intact pot-grown plants inoculated two days after full spike emergence (**Sup. table S3**). Despite the different approach, using a SNP based association genetics pipeline they identified the same 7D resistance interval. The Pearson's correlation between the NO6047+*Avr-Rmg8* DLA and the iso008 spike data was 0.71, indicating a strong positive correlation between the two datasets (p-value of 1.4398E-11). There were some notable exceptions however: BW_01126, BW_01138, BW_01140, BW_01159, BW_01161, BW_01176 and BW_01171 were susceptible in the NO6047+*Avr-Rmg8* DLA but showed resistance in the spike. Conversely, BW_01106, BW_01111 and BW_01151 were highly resistant in the DLA assay but had an intermediate phenotype in the spike.

To visualise the difference in scores between the NO6047+*Avr-Rmg8* leaf dataset and the iso008 spike data, line graphs were plotted (**Figure 19**). The scores for the two datasets were first normalised by subtracting the sample mean for the relevant dataset and then dividing by the standard deviation of that dataset (also known as 'standard' or 'z scores'). These plots were used solely to visualise the data and so the lines do not infer a relationship between datapoints. To visualise the distribution of observations in the iso008 spike data a KDE plot was generated (**Figure 20**).

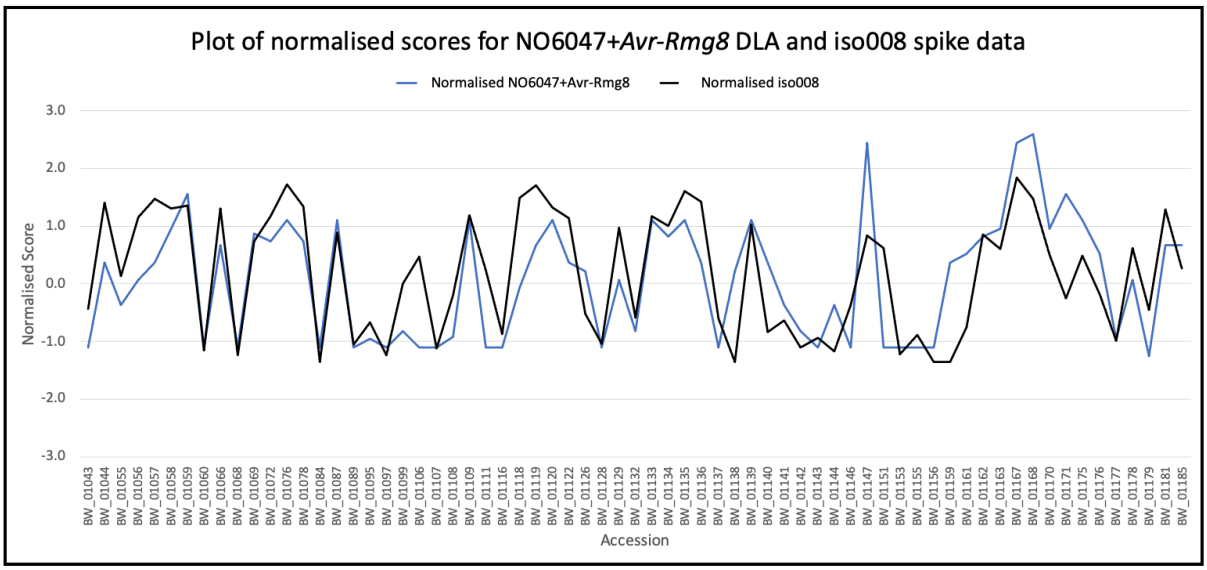

Figure 19: Line graphs comparing the normalised phenotype scores for the NO6047+*Avr-Rmg8* DLA and iso008 spike data Scores were normalised by subtracting the sample mean for the relevant dataset and then dividing by the standard deviation of that dataset. These plots were used solely to visualise the data and so the lines do not infer a relationship between datapoints.

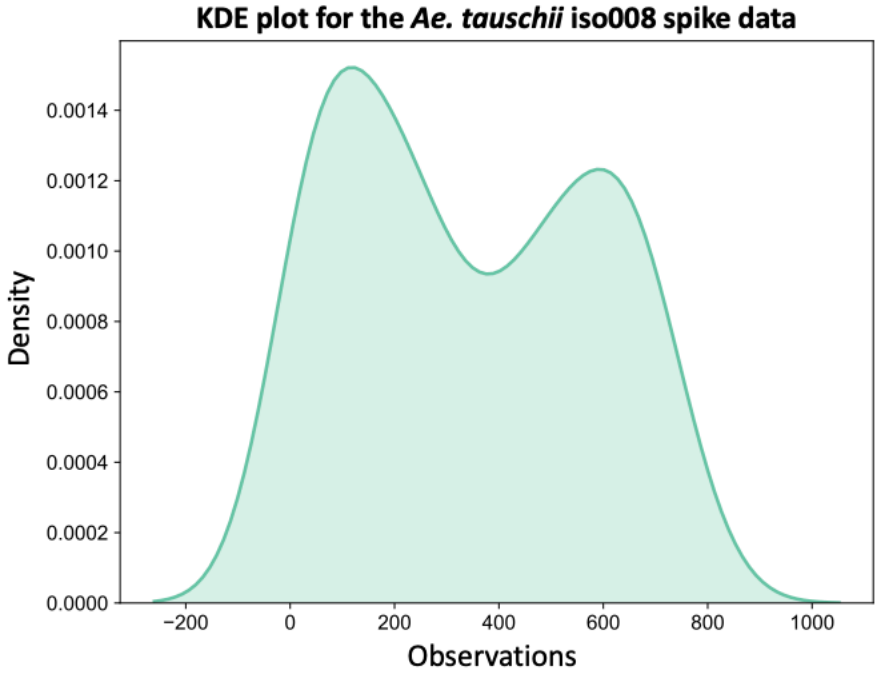

Figure 20: Kernel Density Estimation (KDE) plot for the iso008 *Ae. tauschii* detached spike data.

AgRenSeq (iso008)

The spike assay data for the 122 accessions phenotyped by the Poland group were analysed using the AgRenSeq pipeline to establish whether the 7D peak was also detected using this analysis. The NLR compliments of accessions BW_01106, BW_01111 and BW_01151 (resistant in the NO6047+*Avr-Rmg8* DLA, intermediate phenotype in the spike), in addition to BW_01159 and BW_01161 (susceptible in the original NO6047+*Avr-Rmg8* DLA, resistant in the spike) were used in these analyses. A single peak was identified in all five accessions, corresponding to the same 7D interval as identified in the NO6047+*Avr-Rmg8* DLA (**Figure 21**).

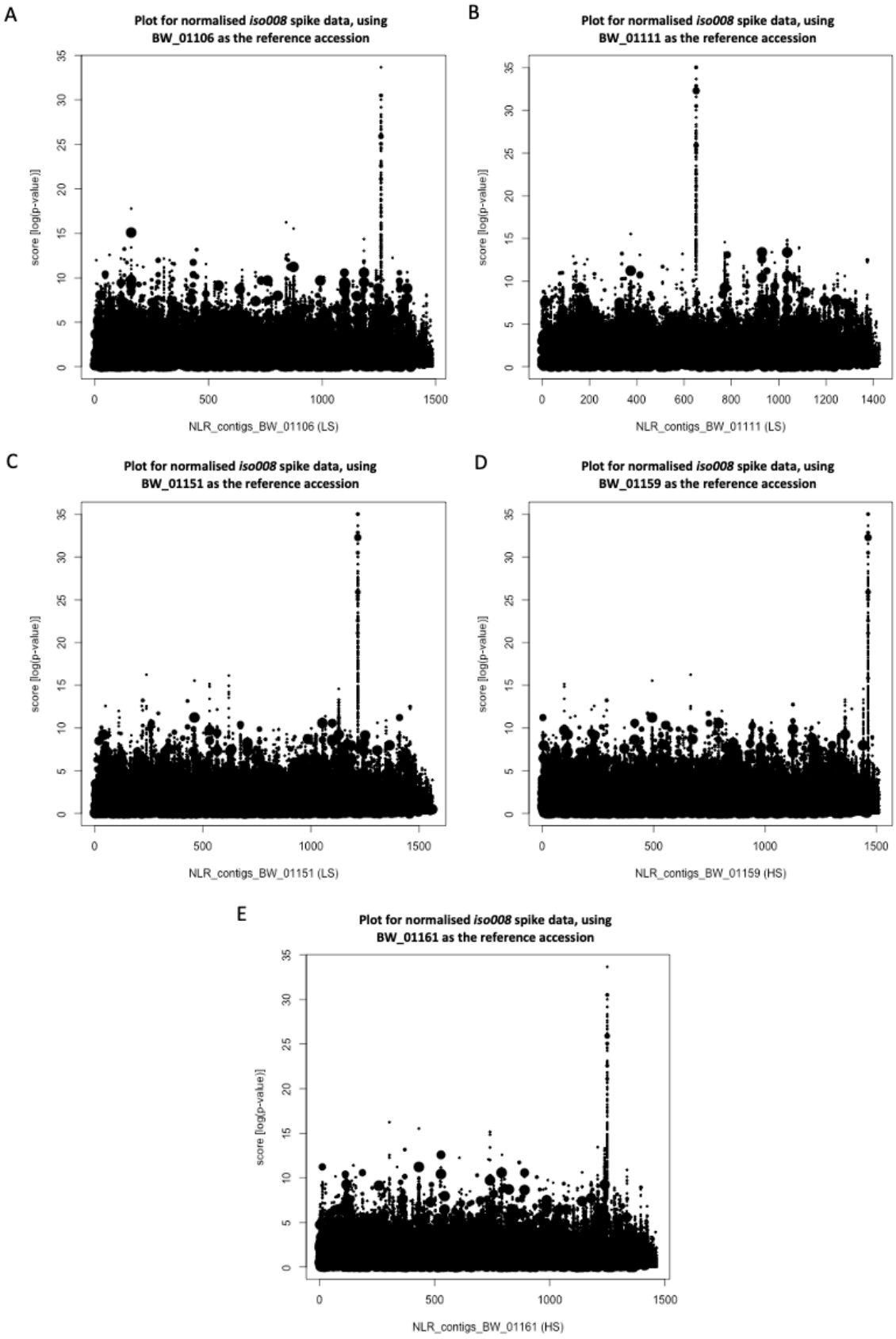

Figure 21: AgRenSeq Manhattan plots for normalised iso008 spike data. Each dot column on the x-axis represents an NLR contig from the RenSeq assembly of (A) BW_01106, (B) BW_01111, (C) BW_01151, (D) BW_01159 and (E) BW_01161. Each dot on the y-axis represents one or more RenSeq *k*-mers associated with resistance. The association score is defined as the negative log of P value obtained using likelihood ratio test for nested models. Dot size is proportional to the number of *k*-mers associated with resistance.

3.3.1.5 Resistant and susceptible 7D intervals

The coordinates of the associated interval with respect to the *Ae. tauschii* RefSeq AL8/78 were 626.90 – 627.11 Mb (210 kb). According to Ensembl, the LD block in AL8/78 contains seven genes: three kinases (AetAet7Gv21304800, Aet7Gv21305100 and Aet7Gv21305400), two NLRs (Aet7Gv21305200 and Aet7Gv21305300), a gene involved in transcription regulation (Aet7Gv21305800) and a gene of unknown function (Aet7Gv21305500) (**Figure 22**) (Yates et al. 2019; Cunningham et al. 2022). Note Aet7Gv21305300 is nested within Aet7Gv21305200, so there are actually six genes in the AL8/78 interval. The genes Aet7Gv21304800, Aet7Gv21305100, Aet7Gv21305200/5300 and Aet7Gv21305400 in the interval all have orthologues on 7D in Chinese Spring while Aet7Gv21305500 has an orthologue on 7B and no orthologue exists in Chinse spring for Aet7Gv21305800 (**Table 10**).

Figure 22: Schematic showing the gene content in the *Ae. tauschii* reference genome, AL8/78, of the interval negatively associated with resistance to *NO6047+Rmg-Avr8*. Figure from Ensembl (Yates et al. 2019).

Table 10: Gene content of the 7D AL8/78 interval and their closest orthologue in Chinese spring

AL8/78 gene ID	Closest orthologue in Chinese Spring	Gene function
Aet7Gv21304800	TraesCS7D02G527000	Kinase
Aet7Gv21305100	TraesCS7D02G527100	Kinase
Aet7Gv21305200/5300	TraesCS7D02G527200	NLR
Aet7Gv21305400	TraesCS7D02G526500	Kinase
Aet7Gv21305500	TraesCS7B02G463100	No ontology
Aet7Gv21305800	-	Transcription regulator

As AL8/78 was susceptible, it was crucial to investigate the LD block in a resistant accession to identify the resistant alleles of these genes, and any additional genes present only in resistant accessions. The three scaffolds from BW_01111 mapped to the LD block in AL8/78; scaffold_11603 which is 102 kb in length, scaffold_17204 which is 68 kb and scaffold_27471 which is 37 kb (giving a total sum of 207 kb).

These sequences contained many Ns where bases were unable to be called, so the sequences were BLASTed into a high quality assembly of BW_01105, available within the group of B. Wulff (JIC). The hits for scaffold_11603, scaffold_17204 and scaffold_27471 were 57 kb, 50 kb and 28 kb respectively, and spanned a 161 kb region within scaffold tig00002586 (approximately 119 - 281 kb) (**Figure 23**).

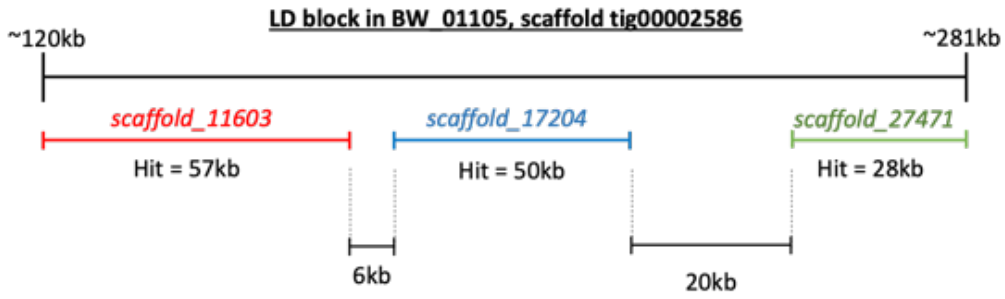

Figure 23: Schematic showing where the three scaffolds that positively associate with resistance in BW_01111 map to in the BW_01105 assembly. All three scaffolds hit tig00002586, spanning ~161 kb, from ~120 kb to ~281 kb. Scaffold_11603 = ~102 kb, scaffold_17204 = ~68 kb and scaffold_27471 = ~37 kb in length.

To determine the gene content in the respective interval of a resistant accession, the BW_01105 tig00002586 119 - 281 kb interval was analysed using FGenesh+, a hidden Markov model and similar protein-based gene prediction program (www.softberry.com). The software predicted 35 possible genes in the interval. The 35 putative genes were assessed using the NCBI Conserved Domain predictor to verify which gene predictions were genuine (Marchler-Bauer and Bryant 2004; Marchler-Bauer et al. 2010). Only 16 out of 35 had predicted domains, three of which corresponded to genes already identified in the AL8/78 interval; Aet7Gv21304800, Aet7Gv21305400 and Aet7Gv21305500 **Table 11**). The remaining nine proteins all contain domains for transposable elements, including: Group specific antigen (GAG: structural protein for virus-like particles); Reverse transcriptase (RT: DNA synthesis using an RNA template); RNase H (RNaseH: degrades the RNA template in a DNA-RNA molecule); integrase (INT: catalyse the insertion of retrotransposon cDNA into the genome) and

Transposase (TRAN: catalyse the movement of transposons without RNA intermediates) (Hickman and Dyda 2015; Orozco-Arias, Isaza, and Guyot 2019) (**Table 11**). Transposable elements do not encode proteins with functions that enable them to persist via natural selection and so can be discounted as resistance gene candidates (Wicker et al. 2018). Two additional serine/threonine kinases (STK), designated 'Kinase 1' and 'Kinase 5' were also identified, along with the partial NLR present in BW_01111 and a protein with a domain of unknown function designated 'No ontology 2' (orthologue in Chinese Spring: TraesCS7D02G527300). Kinases 1 and 5 are present in BW_01111 on scaffold_17204 and scaffold_11603 respectively. Having identified genes seemingly unique to resistant accessions, it was important to identify any genes that were only present in susceptible accessions as this would eliminate them as *R* gene candidates.

Table 11: List of genes and putative genes in the BW_01105 tig00002586 119 - 281 kb interval and their predicted protein domains.

Query from FGenesh	Number of domain hits	Key domains*	AL8/78 gene ID/ novel gene ID
1		*No domain hits*	
2		*No domain hits*	
3		*No domain hits*	
4		*No domain hits*	
5		*No domain hits*	
6	8	GAG/INT/RT/RNaseH	
7		*No domain hits*	
8	327	STK	Aet7Gv21304800
9	528	STK/RNaseH/RT	Kinase 5
10	5	RT	
11	6	RT	
12	1	RT	
13		*No domain hits*	
14		*No domain hits*	
15		*No domain hits*	
16	395	STK	Kinase 1
17	3	GAG/RT/RNaseH	
18	3	Partial NLR	Partial NLR
19		*No domain hits*	
20	80	STK/RT	Aet7Gv21305400
21		*No domain hits*	
22	4	TRAN	
23		*No domain hits*	
24		*No domain hits*	
25		*No domain hits*	
26	1	RNaseH	
27		*No domain hits*	
28	2	RT/GAG	
29		*No domain hits*	
30		*No domain hits*	
31	2	unknown	Aet7Gv21305500
32		*No domain hits*	
33	1	GAG	
34	1	Unknown function	No ontology 2
35		*No domain hits*	

*GAG = Group specific antigen, INT = Integrase, RT = Reverse transcriptase, STK = Serine/Threonine Kinase, TRAN = Transposase.

3.3.1.6 Resistant and susceptible haplotypes

To narrow down the number of candidates, the sequences of the six genes present in the AL8/78 interval were BLASTed back into all the accessions used in the NO6047+*Avr-Rmg8* DLA to see which genes could resolve the phenotype. Sequences for the six genes from resistant accessions were also examined so as not to bias the results by only using the susceptible alleles. Resistant alleles were taken from either BW_01025 or BW_01190 as both are highly resistant accessions which have been sequenced to 30X coverage and assembled. The same analysis was performed for Kinase 1 and Kinase 5. Interestingly, Aet7Gv21305100 and Aet7Gv21305200 showed a presence/absence polymorphism, and were only present in accessions with the AL8/78 (susceptible) alleles of the other genes in the AL8/78 interval. Conversely, Kinase 1 and Kinase 5 also showed presence/absence, but they were only present in accessions with the resistant version of the genes (*i.e.,* when Aet7Gv21305100 and Aet7Gv21305200 were absent).

To establish whether these observations matched the phenotype, the accessions were ordered according to their differential DLA score. Indeed, there was a cluster of the 34 most resistant accessions (the highest differential scores (>=2.5)) that all contained the resistant versions of the AL8/78 genes and lack Aet7Gv21305100 and Aet7Gv21305200, with Kinase 1 and Kinase 5, in their place. This is the ***resistant haplotype*** (**Figure 24**). In contrast, accessions with the AL8/78 version of Aet7Gv21304800, Aet7Gv21305400 and Aet7Gv21305500 lacked Kinase 1 and 5 – the ***susceptible haplotype*** (**Figure 24**)**.** The presence/absence of Aet7Gv21305800 did not follow the pattern observed for either the resistant or susceptible haplotypes and so was removed from further consideration as a candidate for *Avr-Rmg8* resistance. It was hypothesised that a non-reciprocal translocation had occurred in this region, resulting in the loss/gain of two genes in both susceptible and resistant accessions. The Chinese Spring orthologues for Kinase 1 and Kinase 5 (TraesCS7B02G462900 and TraesCS7B02G463000 respectively) are on chromosome 7B, whereas the surrounding candidates have orthologues on 7D which supports this hypothesis. **Table 12** shows all the genes present in the resistant and susceptible haplotypes, with their coordinates in BW_01105, and their closest Chinese Spring orthologue.

Table 12: Full list of genes in the resistant and susceptible haplotypes.

Gene shorthand	AL8/78 gene ID	~Coordinates in BW_01105 scaff_tig00002586 (kb)	Closest orthologue in Chinese Spring
Kinase 3	Aet7Gv21304800	136 - 145	TraesCS7D02G527000
Kinase 5	*Only present in resistant accessions*	146 - 155	TraesCS7B02G462900
Kinase 1		182 - 192	TraesCS7B02G463000
NLR Fragment		200 - 201	-
Kinase 4	Aet7Gv21305100	*Only present in susceptible accessions*	TraesCS7D02G527100
NLR	Aet7Gv21305200/5300		TraesCS7D02G527200
Kinase 2	Aet7Gv21305400	211 - 219	TraesCS7D02G526500
No ontology 1	Aet7Gv21305500	263 - 268	TraesCS7B02G463100
No ontology 2	-	276 - 280	TraesCS7D02G527300
Transcription regulator	Aet7Gv21305800	321 - 322	-

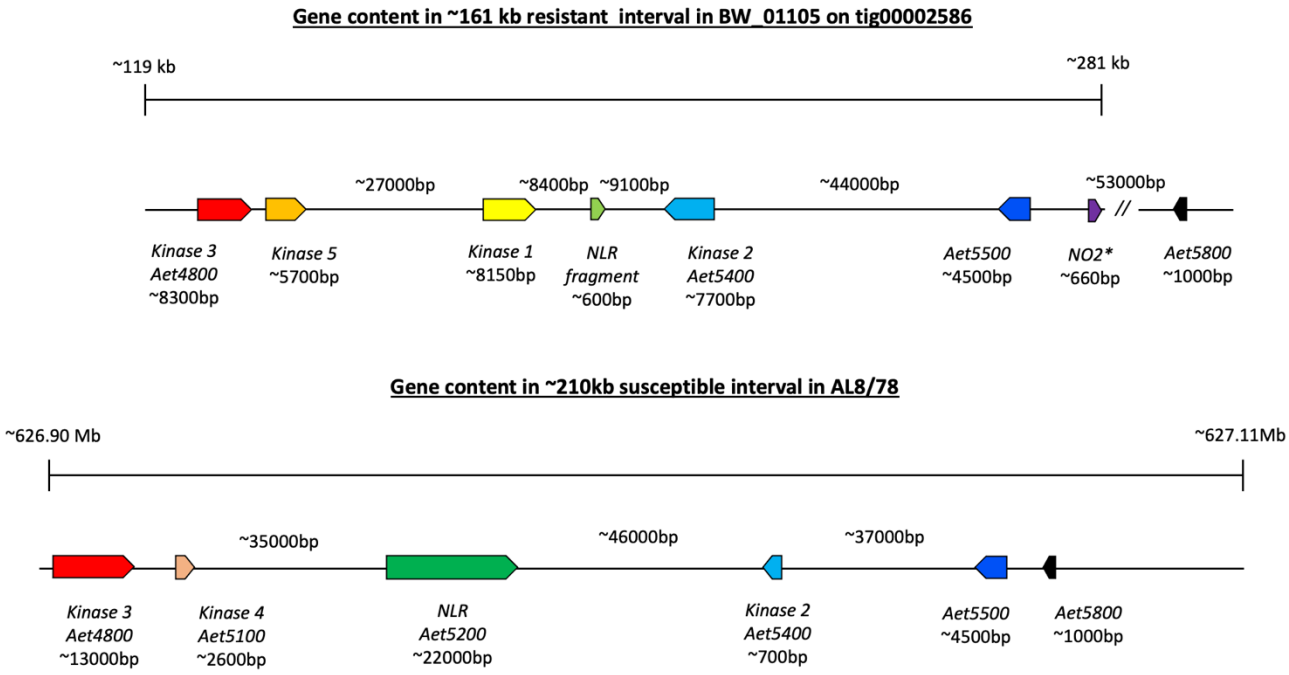

Figure 24: Schematic showing the gene content of the resistant and susceptible haplotypes. Aet5800 is outside of LD block in the resistant accessions however is included in this figure to show its position relative to the other genes. 'Aet' is short for 'Aet7Gv2130'.
* NO = No Ontology

3.3.1.7 RNAseq and cDNA RenSeq expression analysis

Alongside the comparative BLAST analysis between resistant and susceptible accessions, another approach to try to reduce the number of high confidence candidate genes was to determine which genes are expressed. NLRs are often very lowly expressed (Steuernagel 2020), to the extent that they may not be detected in conventional RNAseq data. Therefore, cDNA RenSeq data which allows detection of lowly expressed NLRs was also examined (Steuernagel 2020). Both pre-existing RNAseq and cDNA RenSeq data available from the Wulff group were analysed. It is worth noting that the seedling leaf tissue used was not exposed to wheat blast when the data was captured. To check expression of genes in resistant accessions, for both the RNAseq and cDNA RenSeq data the data for BW_01105 was mapped to itself, as well as BW_01111. For BW_01111 the reads were also mapped to BW_01190 as the BW_01111 assembly contains many 'N's. To check the expression of genes in susceptible accessions the RNAseq and cDNA RenSeq data for BW_01019 was mapped to BW_01019 and AL8/78 and cDNA RenSeq expression data for AL8/78 was mapped to AL8/78 and BW_01019. The data were visualised using the Integrative Genomics Viewer (IGV) tool (Robinson et al. 2011). The RNAseq data showed moderate levels of expression for Kinase 1, for both BW_01111 and BW_01105. Mapping to both BW_01105 and BW_01190 revealed clear and consistent intron/exon boundaries. The gene has 16 exons, spanning 8135 bp. Kinase 5 also showed moderate/high levels of expression, with clear and consistent intron/exon boundaries when mapped to both BW_01105 and BW_01190. The gene has 14 exons, spanning across 5700 bp. Whilst there was some evidence for expression of Aet7Gv21305500 in the RNAseq data of both the resistant and susceptible accessions, the sequence was peppered with stop codons and so no ORF was identified. Aet7Gv21305500 was therefore not considered further as a high confidence gene candidate. All the remaining genes in the interval showed negligible, if any expression in the RNAseq data sets making Kinase 1 and Kinase 5 the most probable resistance gene candidates. The cDNA RenSeq showed negligible expression for all of the candidates. **Figure 25** shows the expression profiles of Kinase 1 and Kinase 5 for the BW_01105 RNAseq data mapped to BW_01105.

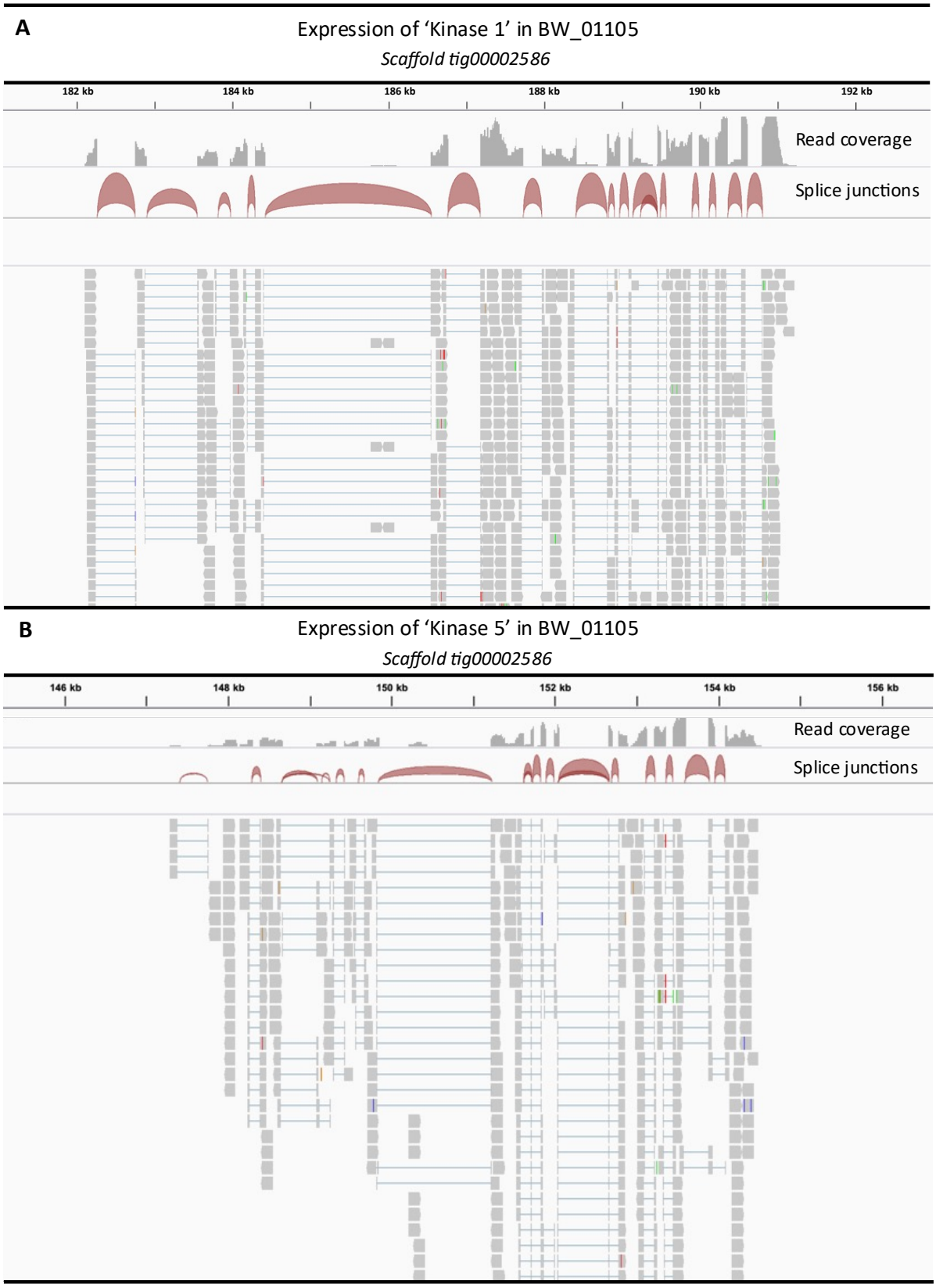

Figure 25: Expression profiles of (**A**) Kinase 1 (**B**) Kinase 5 for the BW_01105 RNAseq data mapped to BW_01105. Red arches within the 'Splice junctions' tracks show predicted intron/exon boundaries on the forward strand.

3.3.1.8 Polymorphism analysis

Disconcertingly there were 17 accessions that were phenotyped as susceptible (score greater than 2) but which contained the resistant haplotype (SWRH). To verify the phenotype of the 17 SWRH accessions a repeat DLA was performed for the 49 accessions with the resistant haplotype, including three accessions that were not included in the original assay (BW_01102, BW_01105 and BW_01190) (**Tables 5 and 13**). All accessions had a higher disease score than in the original assay (except for BW_01175 which scored 4.00 in both assays), with an average differential (repeat score – original score) of 2.56. Given the increased disease response in the retest accessions were classed as resistant if they scored 4 or less. Two SWRH accessions (BW_01008 and BW_01175) showed a gain in resistance however seven accessions that originally phenotyped as resistant were susceptible in the retest (BW_01128, BW_01146, BW_01153, BW_01155, BW_01177, BW_01108, BW_01055 and BW_01144).

The RNAseq data was re-examined to find the open reading frame of the two kinase genes that were expressed. The nucleotide and aa sequences were examined in these accessions to identify polymorphisms in the SWRH that would explain their susceptible phenotype, thus revealing a clear resistance gene candidate.

Table 13: The 49 *Ae. tauschii* accessions with the resistant haplotype and their phenotype scores for the original and repeat DLAs with NO6047+*Avr-Rmg8* at 5 dpi. resistance was classed as 2 or less and 4 or less for the original and repeat DLAs respectively. Green = resistant, red = susceptible.

Accession	NO6047+*Avr-Rmg8* DLAs		Differential*
	Original	Retest	
BW_01179	0.80	4.00	3.20
BW_01022	1.00	4.00	3.00
BW_01025	1.00	4.50	3.50
BW_01043	1.00	2.80	1.80
BW_01060	1.00	3.40	2.40
BW_01068	1.00	3.60	2.60
BW_01084	1.00	4.80	3.80
BW_01089	1.00	3.60	2.60
BW_01097	1.00	3.80	2.80
BW_01106	1.00	4.40	3.40
BW_01107	1.00	4.75	3.75
BW_01116	1.00	3.00	2.00
BW_01128	1.00	5.00	4.00
BW_01146	1.00	5.00	4.00
BW_01151	1.00	4.20	3.20
BW_01153	1.00	5.40	4.40
BW_01155	1.00	5.25	4.25
BW_01156	1.00	3.60	2.60
BW_01095	1.20	2.80	1.60
BW_01177	1.20	5.40	4.20
BW_01002	1.25	2.60	1.35
BW_01108	1.25	5.67	4.42
BW_01010	1.33	3.80	2.47
BW_01006	1.40	3.20	1.80
BW_01099	1.40	4.50	3.10
BW_01132	1.40	4.50	3.10
BW_01100	1.67	-	-
BW_01055	2.00	5.80	3.80
BW_01144	2.00	5.60	3.60
BW_01021	2.20	5.00	2.80
BW_01118	2.40	4.60	2.20
BW_01020	2.50	4.75	2.25
BW_01129	2.60	5.00	2.40
BW_01178	2.60	5.00	2.40
BW_01008	2.80	3.80	1.00
BW_01015	2.80	5.00	2.20
BW_01126	2.80	4.25	1.45
BW_01159	3.00	5.60	2.60
BW_01161	3.20	4.33	1.13
BW_01176	3.20	5.20	2.00
BW_01066	3.40	5.20	1.80
BW_01027	3.50	5.60	2.10
BW_01162	3.60	4.25	0.65
BW_01163	3.80	4.67	0.87
BW_01175	4.00	4.00	0.00
BW_01011	5.20	6.00	0.80
BW_01102	-	5.20	-
BW_01105	-	4.40	-
BW_01190	-	3.00	-

* Differential score was calculated by subtracting the original score from the repeat score

Kinase 1

The ORF of Kinase 1 for all 49 accessions with the resistant haplotype was mapped to resistant accession BW_01025 (**Table 14**), and 16 polymorphisms were identified. BW_01111 was excluded from this analysis as there were numerous 'N's in the sequence. Exons 3, 5, 14, 15, and 16 all contained a non-synonymous polymorphism. Exon 12 contained four non-synonymous polymorphisms plus a single synonymous polymorphism. Exons 7 and 13 also contained a single synonymous polymorphism. Crucially, exons 6, 7 and 9 all contained an insertion or deletion (INDEL): an A insertion, CT deletion and G deletion respectively. The INDELs all caused a sequence frameshift that would result in a truncated protein. INDELs are present in accessions BW_01179, BW_01022, BW_01107 and BW_01132 that consistently phenotype as resistant across the original leaf and spike datasets. This indicates that Kinase 1 is highly unlikely to be the causal resistance gene.

Table 14: Alignment of the ORF of Kinase 1 for all resistant accessions plus the 17 susceptible accessions that have the resistant haplotype to BW_01025. Accessions are sorted by their phenotype from the original DLA. 'Phenotype' is based on the scores from the original DLA. Polymorphisms highlighted in grey are synonymous.

	EXON 2	EXON 3	EXON 5	EXON 6	EXON 7		EXON 9	EXON 12					EXON 13	EXON 14	EXON 15	EXON 16	PHENOTYPE*	Avr8				JP 008	
	G	A	Y	A	CT	V	G	G	R	L	H	A	A	I	L	Q		ORIGINAL		RETEST			
	gly - ser	ala - val	phe - tyr	INSERTION	DELETION	val - val	DELETION	gly - glu	arg - cys	syn - leu	his - asn	ala - ala	ala - ala	ile - thr	leu - phe	gln - his		5 DPI	Norm	5 DPI	Norm	AUDPC	Norm
CONSENSUS	G G C	G C G	T T T			G T C		G G A	C G T	T T G	C A T	G C C	G C C	A T T	C T T	C A A							
BW_01179	- - -	- - -	- - -	A	-	- - -	-	- - -	- - -	- - -	- - -	- - T	- - -	- - -	- - -	- - T	R	0.80	-1.30	4.00	-0.61	232.44	-0.46
BW_01022	A - -	- - -	- - -	-	CT	- - G	-	- A -	- - -	- - -	A - -	- - T	- - T	- - -	T - -	- - -	R	1.00	-1.16	4.00	-0.61		
BW_01025	- - -	- - -	- - -	-	-	- - -	-	- - -	- - -	- - -	- - -	- - -	- - -	- - -	- - -	- - -	R	1.00	-1.16	4.50	-0.04		
BW_01043	- - -	- - -	- - -	-	-	- - -	-	- - -	- - -	- - -	- - -	- - -	- - -	- - -	- - -	- - -	R	1.00	-1.16	2.80	-1.99	239.13	-0.43
BW_01060	- - -	- - -	- - -	-	-	- - -	-	- - -	- - -	- - -	- - -	- - T	- - -	- - -	- - -	- - T	R	1.00	-1.16	3.40	-1.30	67.62	-1.15
BW_01068	- - -	- - -	- - -	-	-	- - -	-	- - -	- - -	- - -	- - -	- - -	- - -	- - -	- - -	- - -	R	1.00	-1.16	3.60	-1.07	47.57	-1.23
BW_01084	- - -	- - -	- A -	-	-	- - -	-	- - -	- - -	- - -	- - -	- - T	- - -	- - -	- - -	- - -	R	1.00	-1.16	4.80	0.31	17.99	-1.36
BW_01089	- - -	- - -	- - -	-	-	- - -	-	- - -	- - -	- - -	- - -	- - T	- - -	- - -	- - -	- - T	R	1.00	-1.16	3.60	-1.07	88.15	-1.06
BW_01097	- - -	- - -	- - -	-	-	- - -	-	- - -	- - -	- - -	- - -	- - T	- - -	- - -	- - -	- - T	R	1.00	-1.16	3.80	-0.84	46.52	-1.24
BW_01106	- - -	- T -	- - -	-	-	- - -	-	- A -	- - -	- - -	- - -	- - T	- - -	- C -	- - -	- - -	R	1.00	-1.16	4.40	-0.15	452.43	0.47
BW_01107	A - -	- - -	- - -	-	CT	- - G	-	- A -	- - -	- - -	A - -	- - T	- - T	- - -	T - -	- - -	R	1.00	-1.16	4.75	0.25	75.81	-1.11
BW_01116	- - -	- - -	- - -	-	-	- - -	-	- - -	- - -	- - -	- - -	- - -	- - -	- - -	- - -	- - -	R	1.00	-1.16	3.00	-1.76	132.64	-0.88
BW_01128	- - -	- - -	- A -	-	-	- - -	-	- - -	- - -	- - -	- - -	- - T	- - -	- - -	- - -	- - -	R	1.00	-1.16	5.00	0.54	92.84	-1.04
BW_01146	- - -	- - -	- A -	-	-	- - -	-	- - -	- - -	- - -	- - -	- - T	- - -	- - -	- - -	- - -	R	1.00	-1.16	5.00	0.54	251.47	-0.38
BW_01151	- - -	- - -	- A -	-	-	- - -	-	- - -	- - -	- - -	- - -	- - T	- - -	- - -	- - -	- - -	R	1.00	-1.16	4.20	-0.38	489.00	0.62
BW_01153	- - -	- - -	- - -	-	-	- - -	-	- - -	- - -	- - -	- - -	- - T	- - -	- - -	- - -	- - T	R	1.00	-1.16	5.40	0.99	50.67	-1.22
BW_01155	- - -	- - -	- - -	-	-	- - -	-	- - -	- - -	- - -	- - -	- - T	- - -	- - -	- - -	- - T	R	1.00	-1.16	5.25	0.82	130.48	-0.88
BW_01156	- - -	- - -	- - -	-	-	- - -	-	- - -	- - -	- - -	- - -	- - T	- - -	- - -	- - -	- - T	R	1.00	-1.16	3.60	-1.07	19.37	-1.35
BW_01095	- - -	- - -	- - -	-	-	- - -	-	- - -	T - -	- C -	- - -	- - T	- - -	- - -	- - -	- - -	R	1.20	-1.01	2.80	-1.99	181.45	-0.67
BW_01177	- - -	- - -	- - -	A	-	- - -	G	- - -	- - -	- - -	- - -	- - T	- - -	- - -	- - -	- - -	R	1.20	-1.01	5.40	0.99	106.63	-0.99
BW_01002	- - -	- - -	- A -	-	-	- - -	-	- - -	- - -	- - -	- - -	- - T	- - -	- - -	- - -	- - -	R	1.25	-0.98	2.60	-2.22		
BW_01108	- - -	- - -	- - -	-	-	- - -	-	- - -	- - -	- - -	- - -	- - -	- - -	- - -	- - -	- - -	R	1.25	-0.98	5.67	1.30	291.88	-0.21
BW_01010	- - -	- T -	- - -	-	-	- - -	-	- A -	- - -	- - -	- - -	- - T	- - -	- C -	- - -	- - -	R	1.33	-0.92	3.80	-0.84		
BW_01006	- - -	- - -	- A -	-	-	- - -	-	- - -	- - -	- - -	- - -	- - T	- - -	- - -	- - -	- - -	R	1.40	-0.87	3.20	-1.53		
BW_01099	- - -	- - -	- - -	-	-	- - -	-	- A -	- - -	- - -	- - -	- - T	- - -	- C -	- - -	- - -	R	1.40	-0.87	4.50	-0.04	339.39	-0.01
BW_01132	- - -	- - -	- - -	A	-	- - -	-	- - -	- - -	- - -	- - -	- - T	- - -	- - -	- - -	- - T	R	1.40	-0.87	4.50	-0.04	203.18	-0.58
BW_01100	- - -	- - -	- A -	-	-	- - -	-	- - -	- - -	- - -	- - -	- - T	- - -	- - -	- - -	- - -	R	1.67	-0.68			73.45	-1.12
BW_01055	- - -	- - -	- A -	-	-	- - -	-	- - -	- - -	- - -	- - -	- - T	- - -	- - -	- - -	- - -	R	2.00	-0.43	5.80	1.45	371.90	0.13
BW_01144	- - -	- - -	- - -	-	-	- - -	-	- - -	- - -	- - -	- - -	- - T	- - -	- - -	- - -	- - T	R	2.00	-0.43	5.60	1.22	63.84	-1.16
BW_01021	- - -	- T -	- - -	-	-	- - -	-	- A -	- - -	- - -	- - -	- - T	- - -	- C -	- - -	- - -	SWRH	2.20	-0.29	5.00	0.54		
BW_01118	- - -	- T -	- - -	-	-	- - -	-	- A -	- - -	- - -	- - -	- - T	- - -	- C -	- - -	- - -	SWRH	2.40	-0.14	4.60	0.08	693.63	1.48
BW_01020	- - -	- T -	- - -	-	-	- - -	-	- A -	- - -	- - -	- - -	- - T	- - -	- C -	- - -	- - -	SWRH	2.50	-0.07	4.75	0.25		
BW_01129	- - -	- - -	- - -	A	-	- - -	-	- - -	- - -	- - -	- - -	- - T	- - -	- - -	- - -	- - T	SWRH	2.60	0.00	5.00	0.54	570.24	0.96
BW_01178	- - -	- - -	- - -	-	-	- - -	-	- - -	- - -	- - -	- - -	- - T	- - -	- - -	- - -	- - T	SWRH	2.60	0.00	5.00	0.54	487.11	0.61
BW_01008	- - -	- - -	- - -	-	-	- - -	-	- - -	- - -	- - -	- - -	- - -	- - -	- - -	- - -	- - -	SWRH	2.80	0.14	3.80	-0.84		
BW_01015	- - -	- - -	- - -	-	-	- - -	-	- - -	- - -	- - -	- - -	- - T	- - -	- - -	- - -	- - T	SWRH	2.80	0.14	5.00	0.54		
BW_01126	- - -	- - -	- - -	A	-	- - -	-	- - -	- - -	- - -	- - -	- - T	- - -	- - -	- - -	- - T	SWRH	2.80	0.14	4.25	-0.33	219.33	-0.51
BW_01159	- - -	- - -	- - -	-	-	- - -	-	- - -	- - -	- - -	- - -	- - T	- - -	- - -	- - -	- - T	SWRH	3.00	0.29	5.60	1.22	19.67	-1.35
BW_01161	- - -	- T -	- - -	-	-	- - -	-	- A -	- - -	- - -	- - -	- - T	- - -	- C -	- - -	- - -	SWRH	3.20	0.43	4.33	-0.23	161.32	-0.76
BW_01176	- - -	- - -	- - -	A	-	- - -	-	- - -	- - -	- - -	- - -	- - T	- - -	- - -	- - -	- - T	SWRH	3.20	0.43	5.20	0.76	296.19	-0.19
BW_01066	- - -	- T -	- - -	-	-	- - -	-	- A -	- - -	- - -	- - -	- - T	- - -	- C -	- - -	- - -	SWRH	3.40	0.58	5.20	0.76	652.72	1.31
BW_01027	- - -	- T -	- - -	-	-	- - -	-	- A -	- - -	- - -	- - -	- - T	- - -	- C -	- - -	- - -	SWRH	3.50	0.65	5.60	1.22		
BW_01162	- - -	- - -	- - -	-	-	- - -	-	- A -	- - -	- - -	- - -	- - T	- - -	- C -	- - -	- - -	SWRH	3.60	0.72	4.25	-0.33	544.25	0.85
BW_01163	- - -	- - -	- - -	-	-	- - -	-	- A -	- - -	- - -	- - -	- - T	- - -	- C -	- - -	- - -	SWRH	3.80	0.87	4.67	0.15	482.92	0.60
BW_01175	- - -	- - -	- - -	A	-	- - -	-	- - -	- - -	- - -	- - -	- - T	- - -	- - -	- - -	- - T	SWRH	4.00	1.01	4.00	-0.61	457.96	0.49
BW_01011	- - -	- T -	- - -	-	-	- - -	-	- A -	- - -	- - -	- - -	- - T	- - -	- C -	- - -	- - -	SWRH	5.20	1.88	6.00	1.68		
BW_01102	- - -	- - -	- - -	-	-	- - -	-	- - -	- - -	- - -	- - -	- - -	- - -	- - -	- - -	- - -	??			5.20	0.76		
BW_01105	- - -	- T -	- - -	-	-	- - -	-	- A -	- - -	- - -	- - -	- - T	- - -	- C -	- - -	- - -	??			4.40	-0.15		
BW_01190	- - -	- - -	- - -	-	-	- - -	-	- - -	- - -	- - -	- - -	- - T	- - -	- - -	- - -	- - T	??			3.00	-1.76		

* R = Resistant, SWRH = Susceptible with resistant haplotype.

Kinase 5

The ORF of Kinase 5 for all 49 accessions was mapped with the resistant haplotype resistant accession BW_01025. BW_01111 was excluded from this analysis as there were numerous 'N's in the sequence. Nine polymorphisms were identified. Exons 3, 5 and 14 contained 1, 3 and 2 non-synonymous polymorphisms respectively. Exons 2 and 4 contain 2 and 1 synonymous polymorphisms respectively. None of the polymorphisms result in a frameshift or premature stop codon so no single or combination of polymorphisms resolve the phenotype using either the original or retest scores (**Table 15**). Some accessions carrying an allele of this gene are susceptible which could indicate that the gene is required but not sufficient for resistance.

Table 15: Alignment of the ORF of Kinase 5 for all resistant accessions plus the 17 susceptible accessions that have the resistant haplotype to BW_01025. Accessions are sorted by their phenotype from the original DLA**. '**Phenotype' is based on the scores from the original DLA. Polymorphisms highlighted in grey are synonymous.

	EXON 2						EXON 3			EXON 4			EXON 5									EXON 14						PHENOTYPE*	Avr8				JP 008	
	A			S			S			S			N			V			E			V			S				ORIGINAL		RETEST			
	ala -ala			ser - ser			ser - ile			ser - ser			asp -asn			val - leu			glu - asp			val - gly			ser - gly								
CONSENSUS	G	C	G	T	C	A	A	G	T	T	C	A	G	A	C	T	G	T	G	A	G	G	T	C	A	G	T		5 DPI	Norm	5 DPI	Norm	AUDPC	Norm
BW_01002	-	-	A	-	-	-	-	-	-	-	-	-	A	-	-	-	-	-	-	-	-	-	-	-	-	-	-	R	1.25	-0.98	2.60	-2.22		
BW_01006	-	-	-	-	-	-	-	-	-	-	-	-	-	-	-	-	-	-	-	-	-	-	-	-	-	-	-	R	1.40	-0.87	3.20	-1.53		
BW_01010	-	-	-	-	-	-	-	-	-	-	-	G	-	-	-	-	-	-	-	-	-	-	-	-	-	-	-	R	1.33	-0.92	3.80	-0.84		
BW_01022	-	-	-	-	-	-	-	-	-	-	-	G	-	-	-	-	T	-	-	-	-	-	G	-	-	-	-	R	1.00	-1.16	4.00	-0.61		
BW_01025	-	-	-	-	-	-	-	-	-	-	-	-	-	-	-	-	-	-	-	-	-	-	-	-	-	-	-	R	1.00	-1.16	4.50	-0.04		
BW_01043	-	-	A	-	-	-	-	-	-	-	-	G	A	-	-	-	-	-	-	-	-	-	-	-	-	-	-	R	1.00	-1.16	2.80	-1.99	239.13	-0.43
BW_01055	-	-	-	-	-	-	-	-	-	-	-	G	-	-	-	-	-	-	-	-	-	-	-	-	-	-	-	R	2.00	-0.43	5.80	1.45	371.90	0.13
BW_01060	-	-	-	-	-	-	-	-	-	-	-	G	-	-	-	-	-	-	-	-	-	-	-	-	-	-	-	R	1.00	-1.16	3.40	-1.30	67.62	-1.15
BW_01068	-	-	-	-	-	-	-	-	-	-	-	-	-	-	-	-	-	-	-	-	-	-	-	-	-	-	-	R	1.00	-1.16	3.60	-1.07	47.57	-1.23
BW_01084	-	-	-	-	-	-	-	-	-	-	-	-	-	-	-	-	-	-	-	-	-	-	-	-	-	-	-	R	1.00	-1.16	4.80	0.31	17.99	-1.36
BW_01089	-	-	-	-	-	-	-	-	-	-	-	G	-	-	-	-	-	-	-	-	-	-	-	-	-	-	-	R	1.00	-1.16	3.60	-1.07	88.15	-1.06
BW_01095	-	-	-	-	-	-	-	-	-	-	-	-	-	-	-	-	-	-	-	-	-	-	-	-	-	-	-	R	1.20	-1.01	2.80	-1.99	181.45	-0.67
BW_01097	-	-	-	-	-	-	-	-	-	-	-	G	-	-	-	-	-	-	-	-	-	-	-	-	-	-	-	R	1.00	-1.16	3.80	-0.84	46.52	-1.24
BW_01099	-	-	A	-	-	-	-	-	-	-	-	G	A	-	-	-	-	-	-	-	-	-	-	-	-	-	-	R	1.40	-0.87	4.50	-0.04	339.39	-0.01
BW_01100	-	-	-	-	-	-	-	-	-	-	-	G	-	-	-	-	-	-	-	-	-	-	-	-	-	-	-	R	1.67	-0.68			73.45	-1.12
BW_01106	-	-	-	-	-	-	-	-	-	-	-	-	-	-	-	-	-	-	-	-	-	-	-	-	-	-	-	R	1.00	-1.16	4.40	-0.15	452.43	0.47
BW_01107	-	-	-	-	-	-	-	-	-	-	-	G	-	-	-	-	T	-	-	-	-	-	G	-	-	-	-	R	1.00	-1.16	4.75	0.25	75.81	-1.11
BW_01108	-	-	-	-	-	-	-	-	-	-	-	-	-	-	-	-	-	-	-	-	-	-	-	-	-	-	-	R	1.25	-0.98	5.67	1.30	291.88	-0.21
BW_01111			A	-	-	-	-	-	-	-	-	G	A	-	-	-	-	-	-	-	-	-	-	-	-	-	-	R	1.00	-1.16	5.00	0.54	394.80	0.23
BW_01116	-	-	-	-	-	-	-	-	-	-	-	-	-	-	-	-	-	-	-	-	-	-	-	-	-	-	-	R	1.00	-1.16	3.00	-1.76	132.64	-0.88
BW_01128	-	-	-	-	-	-	-	-	-	-	-	G	-	-	-	-	-	-	-	-	-	-	-	-	-	-	-	R	1.00	-1.16	5.00	0.54	92.84	-1.04
BW_01132	-	-	A	-	-	-	-	-	-	-	-	G	A	-	-	-	-	-	-	-	-	-	-	-	-	-	-	R	1.40	-0.87	4.50	-0.04	203.18	-0.58
BW_01144	-	-	-	-	-	-	-	T	-	-	-	G	-	-	-	-	-	-	-	-	T	-	-	-	-	-	-	R	2.00	-0.43	5.60	1.22	63.84	-1.16
BW_01146	-	-	-	-	-	-	-	-	-	-	-	G	-	-	-	-	-	-	-	-	-	-	-	-	-	-	-	R	1.00	-1.16	5.00	0.54	251.47	-0.38
BW_01151	-	-	-	-	-	-	-	-	-	-	-	-	-	-	-	-	-	-	-	-	-	-	-	-	-	-	-	R	1.00	-1.16	4.20	-0.38	489.00	0.62
BW_01153	-	-	-	-	-	-	-	T	-	-	-	G	-	-	-	-	-	-	-	-	T	-	-	-	-	-	-	R	1.00	-1.16	5.40	0.99	50.67	-1.22
BW_01155	-	-	-	-	-	-	-	T	-	-	-	G	-	-	-	-	-	-	-	-	T	-	-	-	-	-	-	R	1.00	-1.16	5.25	0.82	130.48	-0.88
BW_01156	-	-	-	-	-	-	-	-	-	-	-	G	-	-	-	-	-	-	-	-	-	-	-	-	-	-	-	R	1.00	-1.16	3.60	-1.07	19.37	-1.35
BW_01177	-	-	-	-	-	-	-	T	-	-	-	G	-	-	-	-	-	-	-	-	T	-	-	-	-	-	-	R	1.20	-1.01	5.40	0.99	106.63	-0.99
BW_01179	-	-	-	-	-	-	-	-	-	-	-	-	-	-	-	-	-	-	-	-	-	-	-	-	-	-	-	R	0.80	-1.30	4.00	-0.61	232.44	-0.46
BW_01008	-	-	-	-	-	-	-	-	-	-	-	-	-	-	-	-	-	-	-	-	-	-	-	-	-	-	-	SWRH	2.80	0.14	3.80	-0.84		
BW_01011	-	-	A	-	-	G	-	-	-	-	-	G	A	-	-	-	-	-	-	-	-	-	-	-	-	-	-	SWRH	5.20	1.88	6.00	1.68		
BW_01015	-	-	-	-	-	-	-	-	-	-	-	G	-	-	-	-	-	-	-	-	-	-	-	-	-	-	-	SWRH	2.80	0.14	5.00	0.54		
BW_01020	-	-	A	-	-	-	-	-	-	-	-	G	A	-	-	-	-	-	-	-	-	-	-	-	-	-	-	SWRH	2.50	-0.07	4.75	0.25		
BW_01021	-	-	A	-	-	-	-	-	-	-	-	G	A	-	-	-	-	-	-	-	-	-	-	-	-	-	-	SWRH	2.20	-0.29	5.00	0.54		
BW_01027	-	-	A	-	-	-	-	-	-	-	-	G	A	-	-	-	-	-	-	-	-	-	-	-	-	-	-	SWRH	3.50	0.65	5.60	1.22		
BW_01066	-	-	A	-	-	-	-	-	-	-	-	G	A	-	-	-	-	-	-	-	-	-	-	-	-	G	-	SWRH	3.40	0.58	5.20	0.76	652.72	1.31
BW_01118	-	-	A	-	-	-	-	-	-	-	-	G	A	-	-	-	-	-	-	-	-	-	-	-	-	G	-	SWRH	2.40	-0.14	4.60	0.08	693.63	1.48
BW_01126	-	-	A	-	-	G	-	-	-	-	-	G	A	-	-	-	-	-	-	-	-	-	-	-	-	-	-	SWRH	2.80	0.14	4.25	-0.33	219.33	-0.51
BW_01129	-	-	A	-	-	-	-	-	-	-	-	G	A	-	-	-	-	-	-	-	-	-	-	-	-	-	-	SWRH	2.60	0.00	5.00	0.54	570.24	0.96
BW_01159	-	-	-	-	-	-	-	-	-	-	-	G	-	-	-	-	-	-	-	-	-	-	-	-	-	-	-	SWRH	3.00	0.29	5.60	1.22	19.67	-1.35
BW_01161	-	-	A	-	-	-	-	-	-	-	-	G	A	-	-	-	-	-	-	-	-	-	-	-	-	-	-	SWRH	3.20	0.43	4.33	-0.23	161.32	-0.76
BW_01162	-	-	A	-	-	-	-	-	-	-	-	G	A	-	-	-	-	-	-	-	-	-	-	-	-	-	-	SWRH	3.60	0.72	4.25	-0.33	544.25	0.85
BW_01163	-	-	A	-	-	G	-	-	-	-	-	G	A	-	-	-	-	-	-	-	-	-	-	-	-	-	-	SWRH	3.80	0.87	4.67	0.15	482.92	0.60
BW_01175	-	-	A	-	-	-	-	-	-	-	-	G	A	-	-	-	-	-	-	-	-	-	-	-	-	-	-	SWRH	4.00	1.01	4.00	-0.61	457.96	0.49
BW_01176	-	-	A	-	-	-	-	-	-	-	-	G	A	-	-	-	-	-	-	-	-	-	-	-	-	-	-	SWRH	3.20	0.43	5.20	0.76	296.19	-0.19
BW_01178	-	-	A	-	-	-	-	-	-	-	-	G	A	-	-	-	-	-	-	-	-	-	-	-	-	-	-	SWRH	2.60	0.00	5.00	0.54	487.11	0.61
BW_01102	-	-	-	-	-	-	-	-	-	-	-	-	-	-	-	-	-	-	-	-	-	-	-	-	-	-	-	??			5.20	0.76		
BW_01105	-	-	A	-	-	-	-	-	-	-	-	G	A	-	-	-	-	-	-	-	-	-	-	-	-	-	-	??			4.40	-0.15		
BW_01190	-	-	A	-	-	-	-	-	-	-	-	-	A	-	-	-	-	-	-	-	-	-	-	-	-	-	-	??			3.00	-1.76		

* R = Resistant, SWRH = Susceptible with resistant haplotype.

3.3.1.9 Melt curve marker analysis

The Kompetitive Amplified Sequence Polymorphism assay is the work-horse for high through-put marker analysis in wheat breeding programmes. KASP assays function through the use of primers designed to specific SNPs differentiating the desired and non-desired genotype. The *Avr-Rmg8* resistance identified on 7D of *Ae. tauschii* involves completely different haploytpes with distinct gene content. An alternative approach was taken to design a screen to establish whether plant material contains the resistant *Ae. tauschii* 7D haplotype or the susceptible *Ae. tauschii*/wheat haplotype. Real-time PCR primers were designed to amplify products with distinct curves, based on their melting temperatures. The resistant haplotype primers were designed between exons 4 and 5 of Kinase 1. The susceptible haplotype primers were located within Kinase 4 (unique to the susceptible haplotype) and designed to amplify the same product in accessions of wheat and *Ae. tauschii*. Both sets of primers are used together in the same reaction, as a non-competitive PCR, with the resistant and susceptible products giving melt peaks at 85°C and 81.6°C respectively (**Figure 26**). Additionally, if any secondary targets were to be amplified they would be easily identifiable as the products would have a different melting temperature peak. The primers were tested using DNA samples taken from the original *Ae. tauschii* accessions used in the NO6047+*Avr-Rmg8* detached leaf assay, and the melt-curve genotypes correlated perfectly with genotypes assigned by BLAST analysis.

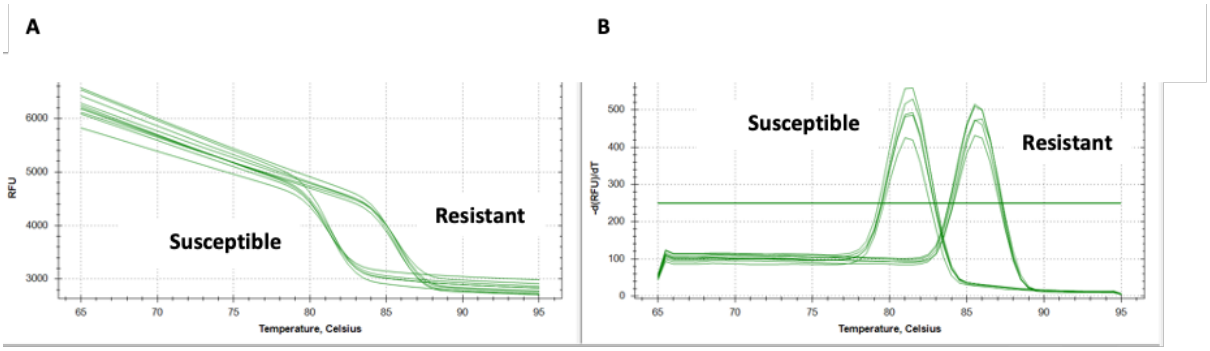

Figure 26: Representative melt curves (**A**) and melt peaks (**B**) for resistant *Ae. tauschii* and susceptible *Ae. tauschii*/wheat haplotype markers.

3.3.1.10 NIAB synthetic wheat

Having identified a resistance interval in *Ae. tauschii*, it was necessary to establish whether this resistance functions in a hexaploid background, and at both the seedling leaf and the spike stage. A number of synthetic hexaploid (SHW) lines have been generated by NIAB by crossing of accessions of *Ae. tauschii* to tetraploid wheats. Prior to testing the SHW lines it was necessary to ensure that the tetraploid donors to the synthetics were susceptible to NO6047+*Avr-Rmg8*, in order to be confident that any resistance observed in the SHW lines originated from the D genome. The durum wheat cultivars Hoh-501 and Hoh-506 (AABB) were highly susceptible and so 27 SHW lines using these tetraploid donors were selected, along with their DD donors. SHW lines NIAB-SHW018 and NIAB-SHW051 have the same DD donor, BW_26041. Synthetics NIAB-SHW042 and NIAB-SHW072 have the same DD donor, BW_26060 (**Table 16**).

The DD donors to 22 of the SHW lines had been sequenced to 7.5X genome coverage, so it was possible to perform a BLAST analysis and establish that 15 of the SHW lines contained the resistant haplotype (Gaurav et al. 2022). The melt-curve marker analysis was run on all 27 SHW lines and their donors. The melt-curve marker analysis completely agreed with the BLAST analysis and revealed that a further four DD donors contained the resistant haplotype, bringing the total to 19/27. There is strong agreement between the DD marker genotype and the SHW marker genotype with two exceptions. SHW088 and SHW091 have the susceptible marker genotype yet their DD donors (BW_25578 and BW_26055 respectively) contain the resistant haplotype according to both BLAST and melt curve marker analyses. The most likely explanation for this discrepancy is that these SHW lines do not derive from these two D genome donors.

NIAB synthetic wheat detached leaf assay

A detached leaf assay was carried out using the NO6047+*Avr-Rmg8* isolate as described in **Section 2.2**. The tetraploid donor Hoh-501 was used as a susceptible control. Leaves were scored at 5 dpi (**Table 5**). Accessions with a score of <4.8 were classed as resistant.

Seventeen of the 19 DD donors that contained the resistant 7D haplotype showed resistance, to varying degrees, at the leaf stage, however only six of the 27 SHW lines were resistant (SHW018, SHW070, SHW075, SHW076, SHW084 and SHW086) (**Table 16**). The melt-curve marker analysis confirmed that all six synthetics contained the resistant haplotype. Reassuringly there were no examples of SHW lines that had a DD donor lacking the resistant 7D haplotype exhibiting resistance to the NO6047+*Avr-Rmg8* isolate. Five of the DD donors from the 6 SHW lines that were resistant were also resistant at the leaf stage (BW_20622 was the exception, with a score of 5).

Boxplots of the leaf phenotype data show that the presence of the resistant 7D haplotype in the DD donor and in the SHW line results in greater resistance to the NO6047+*Avr-Rmg8* isolate. Plots were split into 'resistant' and 'susceptible' groups based on the melt curve analysis (**Figure 27**).

Table 16: Detached leaf and spike assay scores for NIAB synthetics and their D and tetraploid genome donors. SHW that showed resistance in the leaves highlighted in yellow. Sequenced D donors that have the resistant haplotype highlighted in green.

Tetraploid Donor		*DD Donor*					*Synthetic*			
Tetraploid Donor	**Tetraploid DLA***	**DD donors**	**DD donor sequenced?**	**DD phenotype DLA**	**DD phenotype DSA ****	**DD MCA*****	**SHW**	**SHW DLA**	**SHW DSA**	**Synthetic MCA**
Hoh-501-P14	6.00	BW_20607	*	3.00	3.67	86	NIAB-SHW071	6.00	5.33	86
Hoh-501-P14	6.00	BW_20608	YES	3.20	2.83	86	NIAB-SHW095	5.20	5.00	86
Hoh-501-P14	6.00	BW_20622	*	5.00	3.00	86	NIAB-SHW084	4.80	5.33	86
Hoh-501-P14-11	6.00	BW_20718	*	4.80	*	82	NIAB-SHW073	6.00	5.50	82
Hoh-501-P14	6.00	BW_20726	YES	6.00	*	82	NIAB-SHW092	5.40	*	82
Hoh-501-P14	6.00	BW_20745	YES	3.60	*	82	NIAB-SHW087	5.40	6.00	82
Hoh-501-P14	6.00	BW_20749	YES	3.60	*	82	NIAB-SHW094	5.60	6.00	82
Hoh-501-P14	6.00	BW_25578	YES	5.20	2.50	86	NIAB-SHW088	6.00	6.00	82
Hoh-501-P14-1	6.00	BW_26040	*	3.80	2.00	86	NIAB-SHW012	5.20	5.00	86
Hoh-506-P9-1	5.25	BW_26041	YES	4.60	4.00	86	NIAB-SHW018	2.60	5.83	86
Hoh-501-P14-23	6.00	BW_26041	YES	4.60	4.00	86	NIAB-SHW051	5.80	*	86
Hoh-501-P14	6.00	BW_26045	YES	2.20	3.16	86	NIAB-SHW089	5.60	5.83	86
Hoh-501-P14	6.00	BW_26046	YES	3.60	*	86	NIAB-SHW083	6.00	*	86
Hoh-501-P14-35	6.00	BW_26047	YES	2.60	3.67	86	NIAB-SHW043	5.00	5.16	86
Hoh-501-P14	6.00	BW_26048	YES	4.80	*	82	NIAB-SHW090	5.40	*	82
Hoh-501-P14	6.00	BW_26050	YES	2.80	3.55	86	NIAB-SHW086	4.20	5.00	86
Hoh-506-P6	5.25	BW_26051	YES	3.00	*	86	NIAB-SHW070	3.60	5.83	86
Hoh-501-P14	6.00	BW_26055	YES	2.40	*	86	NIAB-SHW091	5.60	6.00	82
Hoh-501-P14	6.00	BW_26057	YES	2.20	3.67	86	NIAB-SHW080	5.20	5.33	86
Hoh-501-P14	6.00	BW_26058	YES	2.40	4.67	86	NIAB-SHW093	5.20	5.33	86
Hoh-506-30	5.25	BW_26060	YES	4.80	5.66	82	NIAB-SHW042	5.80	6.00	82
Hoh-501-P14-11	6.00	BW_26060	YES	4.80	5.66	82	NIAB-SHW072	5.20	6.00	82
Hoh-501-P14	6.00	BW_26062	YES	5.80	4.33	82	NIAB-SHW085	6.00	5.00	82
Hoh-501-P14	6.00	BW_26065	YES	2.67	*	86	NIAB-SHW077	5.60	5.33	86
Hoh-501-P14	6.00	BW_26066	YES	2.60	*	86	NIAB-SHW075	4.80	5.00	86
Hoh-501-P14	6.00	BW_26067	*	2.60	3.00	86	NIAB-SHW076	3.80	5.00	86
Hoh-501-P14	6.00	BW_26069	YES	3.40	4.67	86	NIAB-SHW099	5.20	*	86

* = Detached Leaf Assay
** = Detached Spike Assay
*** = Melt-curve Analysis (resistant = 86/green, susceptible = 82/salmon).

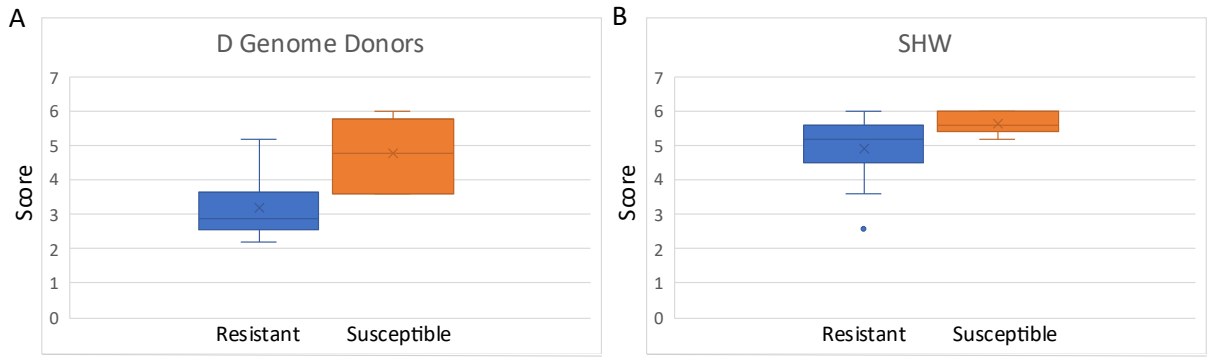

Figure 27: Boxplots of the leaf phenotype data split into 'resistant' and 'susceptible' groups based on the melt curve analysis. (**A**) D genome donors (**B**) SHW.

NIAB synthetic wheat detached spike assay

A detached spike assay was performed on 22 of the SHW lines, and 17 of their DD donors. Spikes were sampled twice, one week apart. The first and second samples were scored at 5 dpi and 7 dpi respectively (**Table 5**). Different scoring days were used for the two samplings to account for different rates of disease progress.

Fifteen of 17 of the DD donors contained the resistant 7D haplotype and all showed resistance. Note this included two of the accessions that showed susceptibility at the leaf stage (BW_25578 and BW_26055). Of the six SHW lines that showed resistance at the leaf stage only four of their DD were phenotyped at the spike stage, however these four were all classified as resistant to spike infection (**Table 16**).

None of the six SHW lines that exhibited resistance at the leaf stage showed high levels of resistance in the spike. Overall, however, accessions containing the resistant haplotype were more resistant in the spike than those that have the susceptible haplotype (**Figure 28**). This suggests the 7D resistance only results in a relatively weak resistance in the spikes in a hexaploid background.

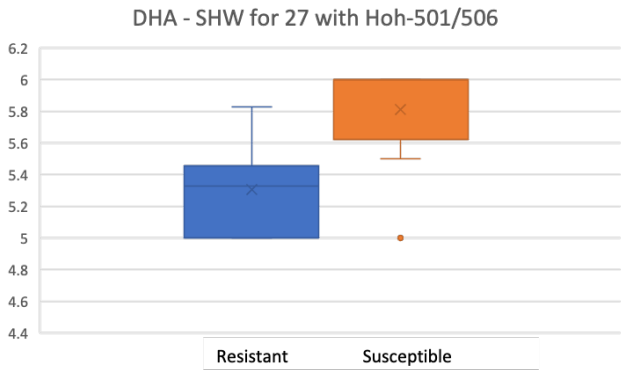

Figure 28: Boxplot of the SHW spike phenotype data split into 'resistant' and 'susceptible' groups based on the melt curve analysis.

3.3.1.11 NIAB RIL populations

As an additional approach to characterising the 7D resistance in a hexaploid background, the resistance was assessed in two backcross populations. Paragon is highly susceptible to NO6047+*Avr-Rmg8* so two populations generated by crossing Paragon with resistant synthetic wheat lines carrying the 7D resistant haplotype, SHW031 (Population A) and SHW029 (Population B) were selected for testing (**Tables 4 and 5**). Unfortunately, both SHW lines had tetraploid donors with unknown phenotypes for NO6047+Avr-*Rmg8.* Nonetheless, both populations were phenotyped at both the seedling and spike stages with NO6047+Avr-*Rmg8* with the expectation that a 1:1 segregation of resistance would indicate a single major gene effect attributable to the 7D resistance.

NIAB RILs detached leaf assay

A detached leaf assay was carried out using the NO6047+Avr-*Rmg8* isolate as described in **Section 2.2**. There was no germination for 16 accessions leaving 51/61 accessions for population A and 44/51 accessions of population B for phenotyping. There was little evidence of resistance in either population (**Sup. tables S4 and S5**). DNA was extracted for each accession. The melt-curve marker analysis was carried out on both populations. In both populations the markers are present in a 1:1 ratio for resistant:susceptible haplotype (population A = 26:26 and population B = 21:23). Boxplots of the leaf phenotype data split into two groups based on the melt curve analysis were generated and showed that for both populations the phenotypes overlap with similar/identical ranges. The lines carrying the susceptible marker have higher medians suggesting that the presence of the resistant haplotype may have a marginal effect in both populations (**Figure 29**). It is worth noting however that very limited seed was available for both populations so there were many lines where only one

replicate could be phenotyped; 27/61 lines in population A and 19/51 lines in population B. It would therefore be unwise to base any conclusions solely on the leaf phenotype data.

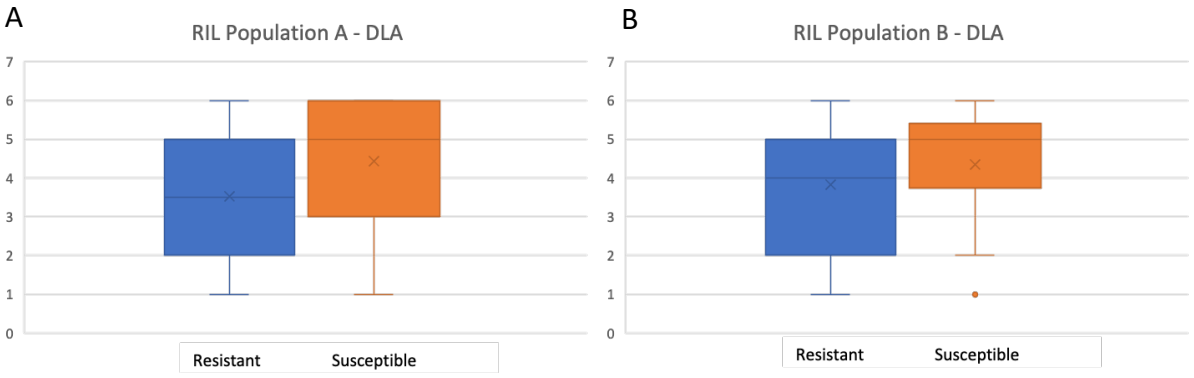

Figure 29: Boxplots of the RIL leaf phenotype data split into 'resistant' and 'susceptible' groups based on the melt curve analysis. (**A**) Population A (**B**) Population B.

NIAB RILs detached spike assay

To verify whether the 7D resistance functions in the spikes when the D genome undergoes recombination, a detached spike assay was carried out with NO6047+Avr-*Rmg8* isolate as described in **Section 2.4**. Spikes were sampled four times over four weeks (**Table 5**). Scoring was carried out at 6 or 7 dpi (**Sup. tables S4 and S5**).

Boxplots of the data split into two groups based on the melt curve analysis were generated (**Figure 30**). The range and spread of phenotypes within both populations for lines with/without the resistant haplotype was very similar, suggesting the presence/absence of the resistant haplotype does not result in a difference in blast susceptibility in the spikes.

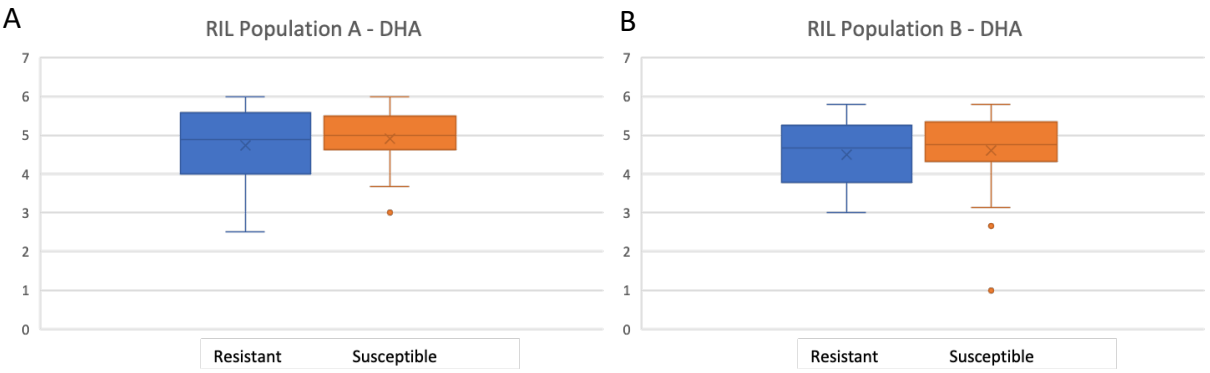

Figure 30: Boxplots of the RIL head phenotype data split into 'resistant' and 'susceptible' groups based on the melt curve analysis. (**A**) Population A (**B**) Population B.

3.4 Discussion

Wheat was first domesticated approximately 12,000 years ago in the fertile crescent. The sequential natural hybrid speciation events between the diploid A genome (*T. urartu*), B genome (an unknown wheat closely related to *Ae. speltoides*) and D genome (*Ae. tauschii)* that gave rise to hexaploid bread wheat (*T. aestivum*) each caused a loss of genetic variation in wheat compared to the wild progenitor spp (Salamini et al. 2002; Zhou et al. 2020). In addition to the bottle necks imposed during domestication, further variation was lost through the evolution of landraces and modern breeding (Zhou et al., 2020). Combined, the loss of variation between wild emmer wheat (*T. turgidum*; AABB), pasta (*T. turgidum L.* subsp*. durum*) and bread wheat alone has been estimated at 84% and 69% respectively (Haudry et al. 2007). Compared to landraces, modern wheat varieties show an average loss of nucleotide variation of 21.8% (Pont et al. 2019). Increasingly CWRs of domesticated species are being utilised to expand the gene pool available for crop improvement (Brozynska, Furtado, and Henry 2016; Hao et al. 2020). Introgressing genes from wild relatives into wheat was first demonstrated by introducing leaf-rust resistance from *Aegilops umbellulata* into hexaploid wheat Sears, 1956). There have since been numerous *R* genes for a variety of pathogens introgressed from CWRs into wheat. These include stem rust resistance genes *Sr47* from *Ae. speltoides* into durum wheat (Klindworth et al. 2012) and *Sr60* from *T. monococcum* into hexaploid wheat (Chen et al. 2020). Other examples include the *Ae. speltoides Su1-Ph1* suppressor and *Ae. tauschii* powdery mildew resistance gene *Pm34* which have both been introgressed into hexaploid wheat (Li, Deal, et al. 2017; Miranda et al. 2006).

Ae. tauschii has an estimated sequence diversity 30 times higher than the D genome of bread wheat and in recent years has received particular attention (Caldwell et al. 2004; Kishii 2019). This was recently exploited to generate an *Ae. tauschii*-wheat synthetic octoploid wheat (A-WSOW) pool (Zhou et al. 2021). Eighty-five SOWs ($AABBDDD^tD^t$) were produced by directly crossing *Ae. tauschii* accessions to elite hexaploid wheat cultivars. Unlike SHW, synthetic octoploid wheat only introduces variation from the D genome, removing the need to remove unwanted loci from the A and B genomes. *Ae. tauschii* genes introgressed into wheat include *Lr42* which confers broad resistance to leaf rust (Cox et al. 1994) and the stripe rust resistance gene *YrAS2388R* (Zhang et al. 2019).

This chapter focused on efforts to identify resistance in the D genome effective against *MoT* isolates carrying the eI allele of *Avr-Rmg8*, utilising the *Ae. tauschii* AgRenSeq and OWWC pipelines. Very little resistance was observed within the panel against NO6047, with only 20/148 accessions classed as resistant (scores ≤ 3). An additional 20 accessions showed weak resistance (scores >3, <4). AgRenSeq analysis using the NO6047 data did not produce any significant peaks, suggesting that the resistance

is polygenic or that different accessions have a different genetic basis for resistance. Based on the phenotyping performed by Jensen and Saunders (2019) it was thought that NO6047 did not contain an *Avr-Rmg8* effector that recognises *Rmg8* because this isolate is virulent on S-615, the accession in which *Rmg8* was first reported (Anh et al. 2015). Sequencing has since shown that NO6047 contains the *Avr-Rmg8* type eII effector (discussed further in **Section 4.3.2**).

It was hypothesised that by removing the 40 accessions that showed resistance to NO6047, any resistance identified with the transformed NO6047+*Avr-Rmg8* isolate would be in response to the type eI *Avr8* effector. The NO6047+*Avr-Rmg8* DLA revealed very little susceptibility, and produced a KDE plot with a bimodal distribution suggesting resistance is controlled by a single or few genes. There was a strong correlation between the iso008 spike data and the NO6047+*Avr-Rmg8* DLA data with a Pearson's correlation coefficient score of 0.71 (p-value of 1.4398E-11). The strength of the correlation between the NO6047+*Avr-Rmg8* leaf data and the iso008 spike data combined with AgRenSeq identifying an identical association in both datasets suggested that the 7D haplotype genuinely associates with resistance. An association on 7D was unexpected is it had been anticipated that any peak would be on 2D if the resistance was homoeologous to *Rmg7* (2A) and *Rmg8* (2B) (Tagle, Chuma, and Tosa 2015; Anh et al. 2018). The iso008 spike data also supported the DLA data as being a true representation of the phenotype and confirmed that the resistance functioned in both the leaves and the spikes in a diploid background. The iso008 phenotype again followed a bimodal distribution suggesting the involvement of a single gene.

Both Kinase 1 and Kinase 5 were unique to the resistant haplotype and showed moderate to high levels of expression with clear intron/exon boundaries. There were 17 accessions that were phenotyped as susceptible to NO6047+*Avr-Rmg8* but which contained the resistant haplotype (SWRH). Examining the polymorphisms within Kinase 1 for all accessions that carried the resistant haplotype identified three INDELs which all resulted in a sequence frameshift. As the INDELs were present in both resistant and susceptible accessions Kinase 1 could be excluded as an *R* gene candidate. There were nine polymorphisms within sequences for Kinase 5 however no INDELs or premature stop codons were identified. The presence of Kinase 5 alleles in susceptible accessions suggests that it may be required but not sufficient for resistance. The data from the SHW lines showed greater resistance in lines carrying the resistant haplotype, where the entire D genome complement of the donor is present but the effectiveness of the resistance is almost lost in spikes in recombinant materials. This finding supports the idea that Kinase 5, on its own, is insufficient to provide resistance. Based upon the presence/absence of the resistant haplotype in the RIL populations there is negligible difference in blast susceptibility. In the RIL material the D genome will be radically recombined.

Essential genetic components required for function may be lost, resulting in a loss of resistance. Similarly, it is possible that the lack of resistance in some SHW lines that carry the resistant marker could be due to the loss of genetic elements on the D genome that are required for the function or expression of the causal gene. It has been previously observed that resistances introgressed into a hexaploid background can lose their efficacy in certain genetic backgrounds (Dreisigacker et al. 2008). CWR genes experience different selection pressures compared to elite wheat cultivars and so maybe deleterious in their new background (Coombes et al. 2022). Gene expression can also be altered by the disruption of established wheat regulatory gene networks which can have an indirect effect on the introgressed gene. Studies exploring the expression of introgressed genes within wheat-barley and wheat-*Ae. longissima* introgression lines have shown that many introgressed genes are differentially expressed with a majority that are downregulated or silenced (Dong et al. 2020; Rey et al. 2018). However, where an introgressed gene replaces a direct orthologue most do not show differential expression compared to the native wheat gene. Coombes et al. reported that of 4989 introgressed genes within six wheat-*Ambylopyrum muticum* introgression lines, 35.1% were expressed (2022). Of the genes that were novel only 9.48% were expressed, compared to 44.1% of introgressed genes that had a wheat orthologue. Furthermore, in cases where the introgressed gene was not expressed despite the presence of wheat orthologues, silencing the wheat orthologues may restore the expression/phenotype of the introgressed gene.

In addition, the remaining candidates in the 7D interval need to be reconsidered as candidates. Aet7Gv21305800 did not follow the presence/absence pattern observed for either the resistant or susceptible haplotypes and so is not the causal gene. Whilst the 'NLR fragment' identified in BW_01111 did not show expression in either the RNAseq or cDNA RenSeq data, the BLAST analysis showed that the nucleotide sequence segregated with the resistant haplotype. NLR-Annotator did not predict any LRRs for this gene and the partial NLR was not detected in the resistant accessions BW_01190 and BW_01106. On the basis of these findings the partial NLR was considered unlikely to be the causal gene. However, there is evidence that a non-canonical partial NLR can function as an *R* gene. Rpw8 contains a NH_2-terminal transmembrane domain (TM) and coiled-coiled motif but lacks NB-ARC and LRR domains yet exhibits broad spectrum powdery mildew resistance in *Arabidopsis thaliana* (Xiao et al. 2001). Within the current study the possibility that the 7D effect could be controlled by a susceptibility (*S*) gene was not explored. *S* genes have been shown to play an important role in controlling resistance/susceptibility to many pathogens. In wheat resistance breeding, *S* genes have mainly been identified for yellow rust (*Puccinia striiformis* f. sp. *tritici* (*Pst*)) and powdery mildew (*Blumeria graminis* f. sp. *tritici* (*Bgt*)) (Li, Yang, and Chang 2022; Feng et al. 2014). For example, silencing TaWIN1, a gene involved in regulating the cuticle biosynthesis pathway in wheat, reduces

cuticle formation which inhibits conidial germination of *Bgt* (Kong and Chang 2018) and inactivation of wheat protein kinase *TaPsIPK1* gives broad spectrum resistance to *Pst* by upregulating expression of downstream defence pathways (Wang et al. 2022). To date no *S* genes have been identified for wheat blast, however several have been characterised for rice blast, including the transcription factor *Bsr-d1* and proline-rich protein *Pi21* (Li, Zhu, et al. 2017; Fukuoka et al. 2009; Tao et al. 2021). Aet7Gv21305100 (Kinase 4) and Aet7Gv21305200/5300 (NLR) are both only present in the susceptible 7D haplotype and could be *S* gene candidates. The remaining genes were present in both resistant and susceptible haplotypes but they were not expressed in either resistant or susceptible accessions. The RNAseq and cDNA RenSeq data used in this study was generated using material that was not exposed to *Mot*. A RNAseq experiment comparing samples inoculated with NO6047+*Avr-Rmg8* to uninoculated controls may identify a candidate with differential expression which would provide evidence that it was involved in the response to *Avr-Rmg8*. Additionally, the nucleotide sequences of the remaining candidates should be compared to try to identify polymorphisms that could explain the phenotype.

4. PHENOTYPING THE WATKINS PANEL

4.1 Introduction

The Watkins collection is a panel of 826 bread wheat landraces collected from 32 countries by A. E Watkins in the 1930's. It represents a snapshot of genetic diversity present before intensive modern breeding (Wingen 2014). When compared to the Gediflux collection, a panel of more than 500 modern elite cultivars from across Europe, the Watkins collection had a higher level of genetic diversity and may provide a source of novel of resistance genes lost through breeding (Winfield et al. 2018). A core set of 300 Watkins lines with spring growth habit capturing this diversity has been developed. The core set was combined with 20 non-Watkins lines to develop a Watkins RenSeq association genetics pipeline, hereafter termed WatRenSeq (Arora et al. 2022) (**Sup. table S6**).

Following the completion of the first fully sequenced hexaploid wheat assembly, Chinese Spring, in 2018, The 10+ Wheat Genomes Project published an additional 15 assemblies (Walkowiak et al., 2020). Combined they capture additional geographical and historical variation absent in the Chinese Spring assembly. Without access to the whole genome shotgun sequence data for the core Watkins panel, the 10+ Genomes assemblies would be relied upon to interrogate the gene content of any intervals associated with resistance. Ahead of any association genetics, the 10+ Genomes cultivars were phenotyped to determine which cultivars were suitable as resistant reference accessions.

Having identified an interval for *Avr-Rmg8* resistance on 7D in *Ae. tauschii,* the core Watkins set was phenotyped with NO6047+*Avr-Rmg8* isolate to establish whether the 2A (*Rmg7*) and 2B (*Rmg8*) genome resistances reported for *Avr-Rmg8* could be detected using the WatRenSeq pipeline. The panel was also phenotyped with a recent Brazilian isolate, Py15.1.018 (personal communication, João Nunes-Maciel, Embrapa). The isolate was collected in the Serra do Salitre, on the hexaploid wheat cultivar BRS264 in 2015. Py15.1.018 was designated as 'Super-race A' (SRA). SRA is virulent on cultivars that carry the *Ae. ventricosa* 2NS translocation, and has high virulence at the spike stage, so any resistance identified against this isolate could potentially be deployable in Brazil. Both the NO6047+*Avr-Rmg8* and SRA DLA data was run through the WatRenSeq pipeline, which identified the same interval of approximately 5.3Mb to positively associate with resistance. Additional phenotyping was performed to verify that the association was genuine, and to establish if the resistance functions at a higher temperature of 26^{o}C at the leaf stage.

4.2 Materials and Methods

4.2.1 Plant and pathogen material

4.2.1.1 10+ Genomes cultivars

Following the completion of the first fully sequenced hexaploid wheat assembly, Chinese Spring, in 2018, The 10+ Wheat Genomes Project published an additional 15 assemblies (**Table 17**) (Walkowiak et al., 2020). Ten cultivars have reference-quality pseudomolecule assemblies (RQAs) with another five sequenced to scaffold level. These lines were screened alongside Chinese Spring to use as additional reference assemblies for association genetics.

4.2.1.2 Watkins core collection

The Watkins collection is a panel of 826 bread wheat landraces collected from 32 countries by A. E Watkins in the 1930's and represents a snapshot of genetic diversity present before intensive modern breeding (Wingen 2014). A core set of 300 Watkins lines with spring growth habit capturing this diversity has been developed (Arora et al., 2023). The core set was combined with 20 non-Watkins lines to develop a Watkins RenSeq association genetics pipeline (Arora et al., 2022) and were used in this chapter (**Sup. table S6**).

4.2.1.2 Watkins validation set

To confirm that the 2A association was genuine, additional Watkins cultivars, not included in the Watkins core set, were selected for phenotyping based on the presence/absence of the 2A haplotype (**Table 18**).

Table 17: The 10+ Wheat Genomes Project cultivars, their pedigree, origins and assembly type. Adapted from Supplementary Table 1 of Walkowiak et al. (2020).

Line	Pedigree	Growth Habit	Origin	Assembly Type*
Mace	WYALKATCHEM/STYLET//WYALKATCHEM	Spring	Australia	RQA
LongReach Lancer	VI184/Chara//Chara/3/Lang	Spring	Australia	RQA
CDC Stanley	CDC Teal//EE8/Kenyon35//AC Barrie	Spring	Canada	RQA
CDC Landmark	Unity/Waskada//Alsen/Superb	Spring	Canada	RQA
Julius	Asketis/Drifter	Winter	Germany	RQA
Norin 61	Fukuoka Komugi 18/Shinchunaga	Facultative Spring	Japan	RQA
Arina*LrFor*	Arina*3/Forno	Winter	Switzerland	RQA
PI190962 (spelt wheat)	Unknown	Winter	Central Europe	RQA
Jagger	KS-82-W-418/STEPHENS	Winter	USA	RQA
SY Mattis	Apache/Intense	Winter	France	RQA
Cadenza	AXONA/TONIC	Spring	UK	Scaffold
Paragon	CSW-1724-19-5-69//Axona/Tonic	Spring	UK	Scaffold
Robigus	1366/Z-836	Winter	UK	Scaffold
Claire	WASP/FLAME	Winter	UK	Scaffold
Weebill 1	BABAX/AMADINA//BABAX	Spring	CIMMYT	Scaffold

*RQA = Reference Quality Pseudomolecule Assembly

Table 18: Watkins validation set. Additional Watkins cultivars used to verify the 2A resistance, their origins and growth habit.

GRU Store Code	Collection ID	Origin Country	Growth Habit
WATDE0056	Wat1190433-1	India	Spring
WATDE0122	Wat1190003-4	Iran	Spring
WATDE0141	Wat1190017-2	Spain	Winter
WATDE0152	Wat1190027-1	Australia	Spring
WATDE0162	Wat1190037-1	Poland	Winter
WATDE0175	Wat1190049-1	Spain	Spring
WATDE0185	Wat1190058-1	Portugal	Spring
WATDE0199	Wat1190068-1	Spain	Spring
WATDE0207	Wat1190075-1	Yugoslavia	Winter
WATDE0220	Wat1190086-2	India	Spring
WATDE0232	Wat1190097-1	Poland	Winter
WATDE0426	Wat1190267-1	Spain	Spring
WATDE0428	Wat1190269-1	Spain	Spring
WATDE0465	Wat1190309-1	Iran	Winter
WATDE0484	Wat1190320-3	China	Winter
WATDE0505	Wat1190337-1	Hungary	Spring
WATDE0527	Wat1190357-2	Yugoslavia	Spring
WATDE0541	Wat1190369-2	Yugoslavia	Spring
WATDE0546	Wat1190373-1	Iran	Spring
WATDE0566	Wat1190389-1	Portugal	Spring
WATDE0567	Wat1190390-1	Portugal	Spring
WATDE0568	Wat1190391-1	Portugal	Spring
WATDE0592	Wat1190412-1	India	Spring
WATDE0672	Wat1190488-1	USSR	Winter
WATDE0687	Wat1190500-1	Iraq	Winter
WATDE0720	Wat1190525-1	India	Spring
WATDE0786	Wat1190586-2	China	Winter
WATDE0804	Wat1190601-1	Spain	Spring
WATDE0970	Wat1190758-2	Italy	Spring
WATDE0974	Wat1190761-1	USSR	Spring
WATDE1062	Wat1190911-1	Hungary	Spring

4.2.1.4 Isolates

Three isolates were used for phenotyping in this chapter. Brazilian isolates NO6047 and SRA, in addition to the transformed NO6047+*Avr-Rmg8* isolate (**Sup. table S2**). NO6047 and NO6047+*Avr-Rmg8* were cultured on oatmeal media plates and SRA was cultured on CMA media plates as described in **Section 2.1**.

4.2.2 Detached leaf and spike assays

Detached leaf and spike assays were performed as described in **Sections 2.2 and 2.4**. The inoculum concentrations, scoring day(s) and relevant section describing the results of each DLA and DSA in this chapter are listed in **Table 19.**

Table 19: Detached leaf and spike assays described in this chapter.

Isolate	Test*	Inoculum [x 10^6/ml]	Scoring day (dpi)	Section
NO6047	10+ Genomes DLA	0.31	5	4.3.2.1
NO6047+*Avr-Rmg8*	10+ Genomes DLA	0.17	5	4.3.2.2
SRA	10+ Genomes DLA	0.25	5	4.3.2.3
NO6047+*Avr-Rmg8* & SRA	Comparison between NO6047+*Avr-Rmg8* and SRA DLA	0.25	5	4.3.2.4
NO6047	10+ Genomes DSA	0.07 - 0.31	5 - 7	4.3.2.5
NO6047+*Avr-Rmg8*	10+ Genomes DSA	0.12 - 0.16	5 - 7	4.3.2.5
SRA	10+ Genomes DSA	0.18 - 0.3	5 - 7	4.3.2.5
NO6047+*Avr-Rmg8*	Core Watkins DLA	0.30	5	4.3.3.1
SRA**	Core Watkins DLA	0.36	5	4.3.3.2
SRA	Watkins validation set DLA	0.25	5	4.3.3.3
SRA	Watkins validation set DSA	0.22 - 0.30	5	4.3.3.3
NO6047+*Avr-Rmg8*	Differential temperature experiment	0.17	5 - 6	4.3.3.4
SRA	Differential temperature experiment	0.25	5 - 6	4.3.3.4

* DLA = detached leaf assay. DSA = detached spike assay.

** Scored by Andrew Steed

4.2.3 CTAB DNA extraction of *M. oryzae* isolates

Isolates were cultured from filter paper in 9cm Petri dishes on CMA media and incubated for two weeks at 22°C under a 16 h/8 h light-dark photoperiod. Mycelium was gently scraped from the surface of the medium using a thin spatula and transferred into 2ml Eppendorf tubes. Tubes were stored on dry ice until needed. The mycelium was ground into a fine powder in a mortar and pestle under liquid nitrogen and decanted into 15ml centrifuge tubes. 5ml of room temperature CTAB buffer was added to each tube before vortexing and incubating in a 65^{o}C water bath for 90 minutes. Tubes were shaken every 30 minutes. Potassium acetate (1.7ml of 5M solution) and 1.25ml chloroform + isoamyl alcohol (IAA) (100ml IAA in 2.5L chloroform) were added to each tube in a fume hood. Tubes were shaken well and held in a freezer at -20^{o}C for 20 minutes. Samples were removed from the freezer and each divided into four Eppendorfs, then centrifuged at 13,400 relative centrifugal force (rcf) for 15 minutes. A new set of 15ml tubes were labelled, 5ml of isopropanol added and kept at 4^{o}C. 1.25ml of supernatant from each Eppendorf was pipetted into the relevant 15ml centrifuge tube with isopropanol and inverted to mix. Samples were left to stand for 15 minutes at 4^{o}C, then centrifuged at 3200 rcf for 30 minutes. Most of the isopropanol was carefully tipped away, leaving 2ml behind containing the sample. The remaining 2ml was transferred to a 2ml Eppendorf and centrifuged at 13,400 rcf for 15 minutes. The residual isopropanol was pipetted off, taking care not to dislodge the pellet. The pellet was washed with 1ml of ice cold 70% ethanol (kept at -20^{o}C overnight), and spun at 13,400 rcf for five minutes. The ethanol was removed and the tubes upturned to evaporate any free liquid. The pellets were resuspended in 50µl dH_2O. Samples were quantified using a NanoDrop™ spectrophotometer (Thermo Scientific™).

4.2.4 *Avr-Rmg8* sequencing

To establish which *Avr-Rmg8* alleles were present in the blast isolates used in this study, a 550bp DNA fragment was amplified and gel extracted using primers designed to the ORF of *Avr-Rmg8* (primers published by Horo et al, 2020). Gel extraction was performed using the QIAquick® Extraction Kit (Qiagen) following manufacturer's instructions.

Table 20: Primers used to amplify *Avr-Rmg8*.

Name	**Sequence (5' to 3')**
A8_ORF_Seq-F	TCTAGTTGCATTTTCTCACTCCA
A8_ORF_Seq-R	GGCCGTTTAACGTTTTTGG

4.3 Results

4.3.1 *Avr-Rmg8* sequencing

Sequencing showed that the SRA isolate contains the eI *Avr-Rmg8* allele. The same approach was used to confirm that the NO6047 and NO6047+*Avr-Rmg8* isolates had the eII allele. The eI allele used to transform NO6047 was inserted randomly within the genome and so the primers used in this study were not expected to amplify eI in NO6047+*Avr-Rmg8*.

4.3.2 Phenotyping the 10+ Genomes cultivars

4.3.2.1 NO6047 detached leaf assay

To determine if any of the 10+ Genomes cultivars had background resistance to the wildtype NO6047 isolate, which could mask resistance to NO6047+*Avr-Rmg8*, a DLA was performed. Kronos was included in the assay as a susceptible control. All 14 cultivars were susceptible at 5 dpi with negligible or no necrosis present (**Figures 30 and 33**).

Figure 30: Representative leaves from the 10+ Genomes DLA with the NO6047 isolate. Kronos was included as a susceptible control. All cultivars have a susceptible phenotype. Images were taken at 5 dpi.

4.3.2.2 NO6047+Avr-Rmg8 detached leaf assay

To identify if any of the 10+ Genomes cultivars have resistance to NO6047+*Avr-Rmg8*, a DLA was performed. Chinese Spring was identified as susceptible in a previous assay and so was omitted. Claire, Mattis and Stanley were all highly resistant, with just a few small necrotic lesions present in some replicates (**Figure 31**). Arina had a weaker resistance with larger and more numerous necrotic lesions and some chlorotic tissue. Cadenza, Julius, Norin and Paragon were highly susceptible, showing complete collapse of the leaf tissue and water soaking. The remaining cultivars (Jagger, Lancer, Landmark, Mace and Robigus) had an intermediate phenotype, with partial tissue collapse as well as areas of green tissue and some necrotic flecking.

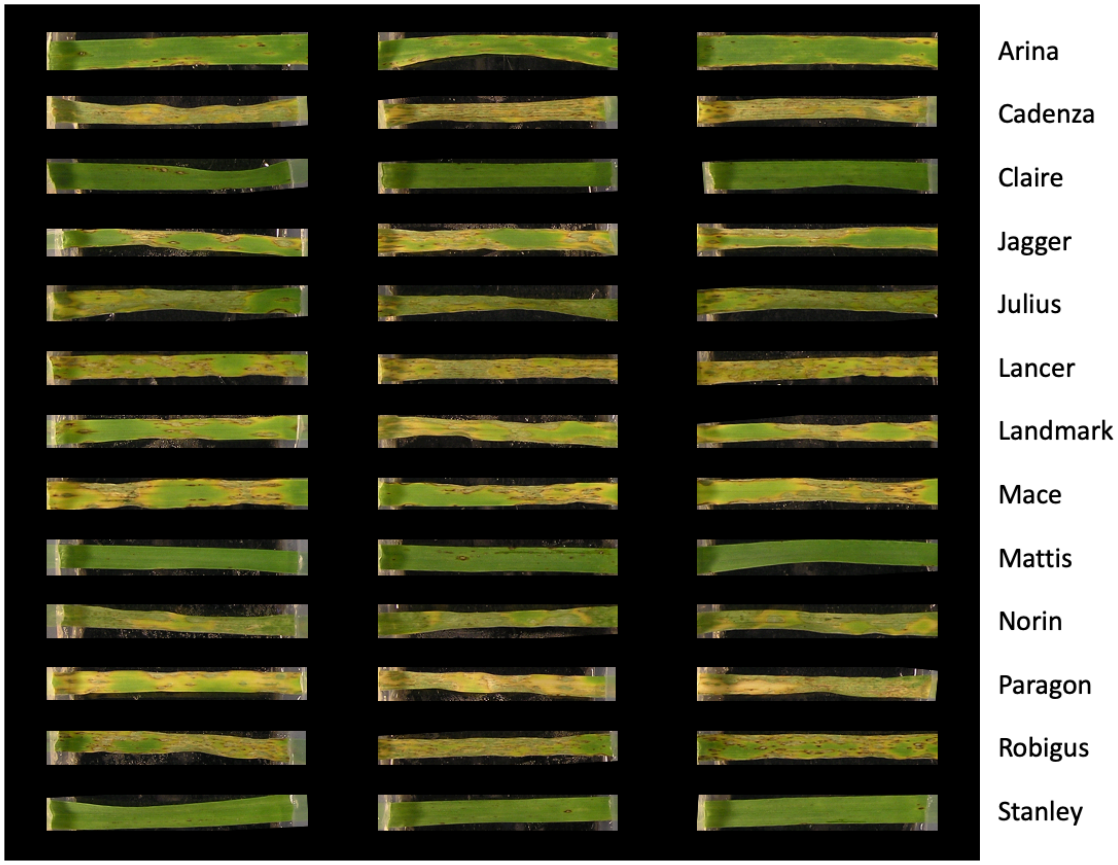

Figure 31: Representative leaves from the 10+ Genomes detached leaf assay with NO6047+*Avr-Rmg8.* Images were taken at 5 dpi.

4.3.2.3 SRA detached leaf assay

To identify if any of the 10+ Genomes cultivars show the same resistance pattern to the SRA isolate as they do to NO6047+*Avr-Rmg8*, a DLA was performed. This assay gave a very clear differential between most of cultivars. Claire, Mattis and Stanley were again all highly resistant, even more so than with NO6047+*Avr-Rmg8*, with almost completely unblemished leaves (**Figure 32**). Arina showed a much weaker resistance response compared to the NO6047+*Avr-Rmg8* assay, with large grey lesions and very little necrotic flecking. With the exception of Lancer, which had an intermediate phenotype, the remaining cultivars were highly susceptible, showing complete collapse of the leaf tissue and water soaking. Comparing the phenotypes from the NO6047+*Avr-Rmg8* and SRA assays; Jagger, Landmark, Mace and Robigus all showed a loss of resistance, going from intermediate to fully susceptible. Arina also showed a loss of resistance from a moderate to very weak resistance response. Of all the cultivars, Arina had the least consistency between replicates so more phenotyping was necessary to confirm the phenotype.

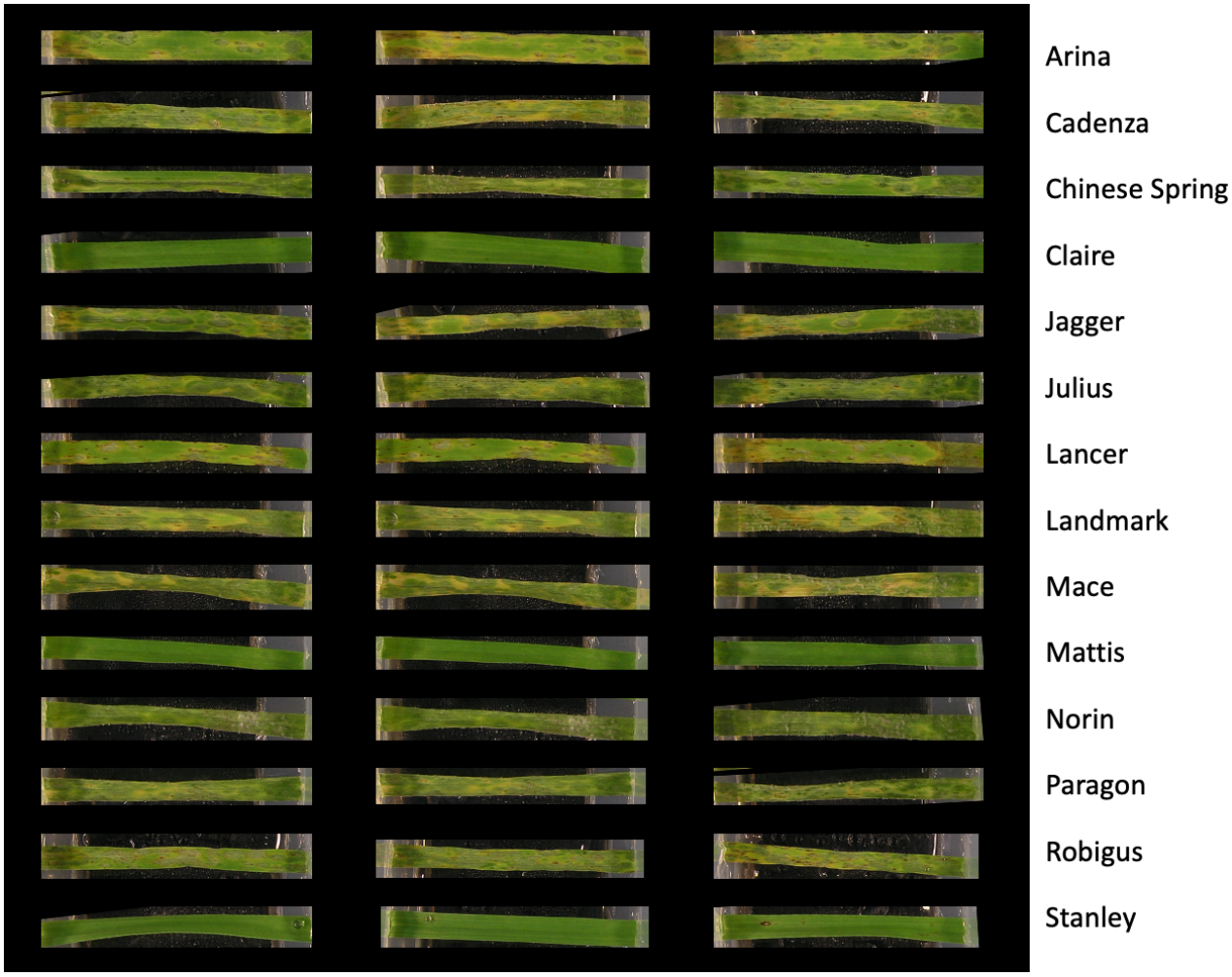

Figure 32: Representative leaves from the 10+ Genomes detached leaf assay with the SRA isolate. Images were taken at 5 dpi.

4.3.2.4 Comparison between isolates

To confirm the phenotype of Arina, repeat DLAs were performed using NO6047+*Avr-Rmg8* and SRA. The cultivars Claire, Stanley and Mattis were included, with Kronos as a susceptible control. The plant material for the two assays was grown together to minimise between experiment variation. The NO6047 DLA data from **Section 4.3.2.1** was used to make comparisons. Claire, Stanley and Mattis were again highly resistant to both NO6047+*Avr-Rmg8* and SRA, with some small necrotic lesions present in all three cultivars with NO6047+*Avr-Rmg8* (**Figure 33**). Arina exhibited more susceptibility to NO6047+*Avr-Rmg8* than in the previous leaf assay, with a higher proportion of leaf collapse and chlorosis along with some necrotic flecking. When inoculated with SRA, large grey lesions developed clearly indicating that Arina demonstrated susceptibility to SRA in this assay.

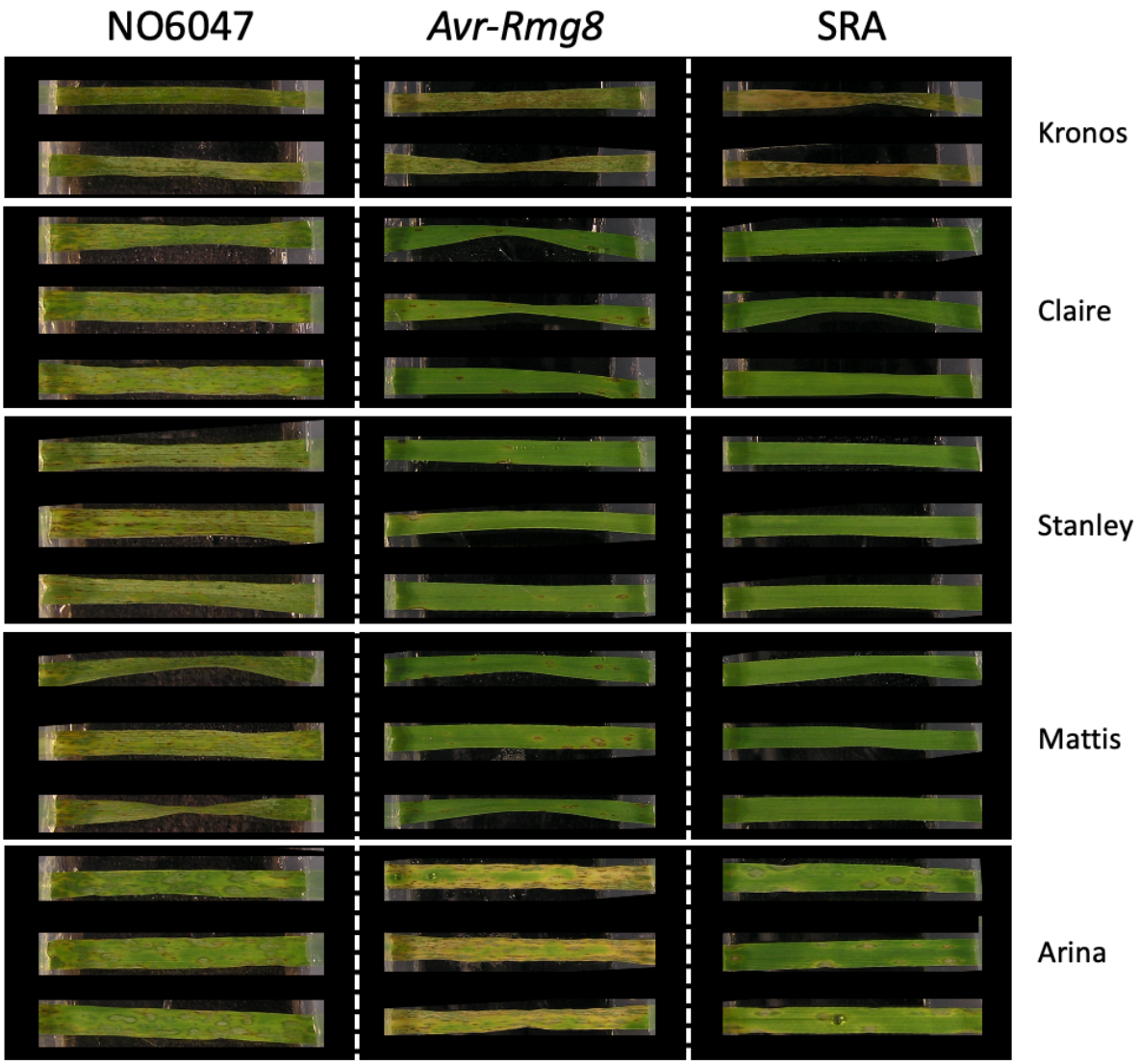

Figure 33: Comparison of leaf phenotypes for NO6047, NO6047+*Avr-Rmg8* and SRA detached leaf assays. Images were taken at 5 dpi.

4.3.2.5 10+ Genomes detached spike assays

To establish whether the resistance observed in the leaves is maintained at the spike stage, detached spikes were phenotyped using the three isolates. Spikes were sampled over multiple days and scored at 5 to 7 dpi. Chinese Spring was included as a susceptible control (**Figure 34**). Arina showed complete susceptibility to both NO6047 and SRA. Arina did develop some initial necrotic flecking with NO6046+*Avr-Rmg8* but to a lesser extent than at the leaf stage. Claire, Mattis and Stanley all showed resistance to both NO6046+*Avr-Rmg8* and SRA, with a necrotic response that was not overcome by the pathogen. Stanley was particularly resistant to both NO6047+*Avr-Rmg8* and SRA. Mattis and Stanley had exhibited initial necrosis in response to NO6047 before being overcome by the fungus but both were clearly resistant to NO6047+*Avr-Rmg8* (**Figure 34**). Overall, the resistance/susceptibility expressed in spikes agreed with the phenotypes observed in the leaves.

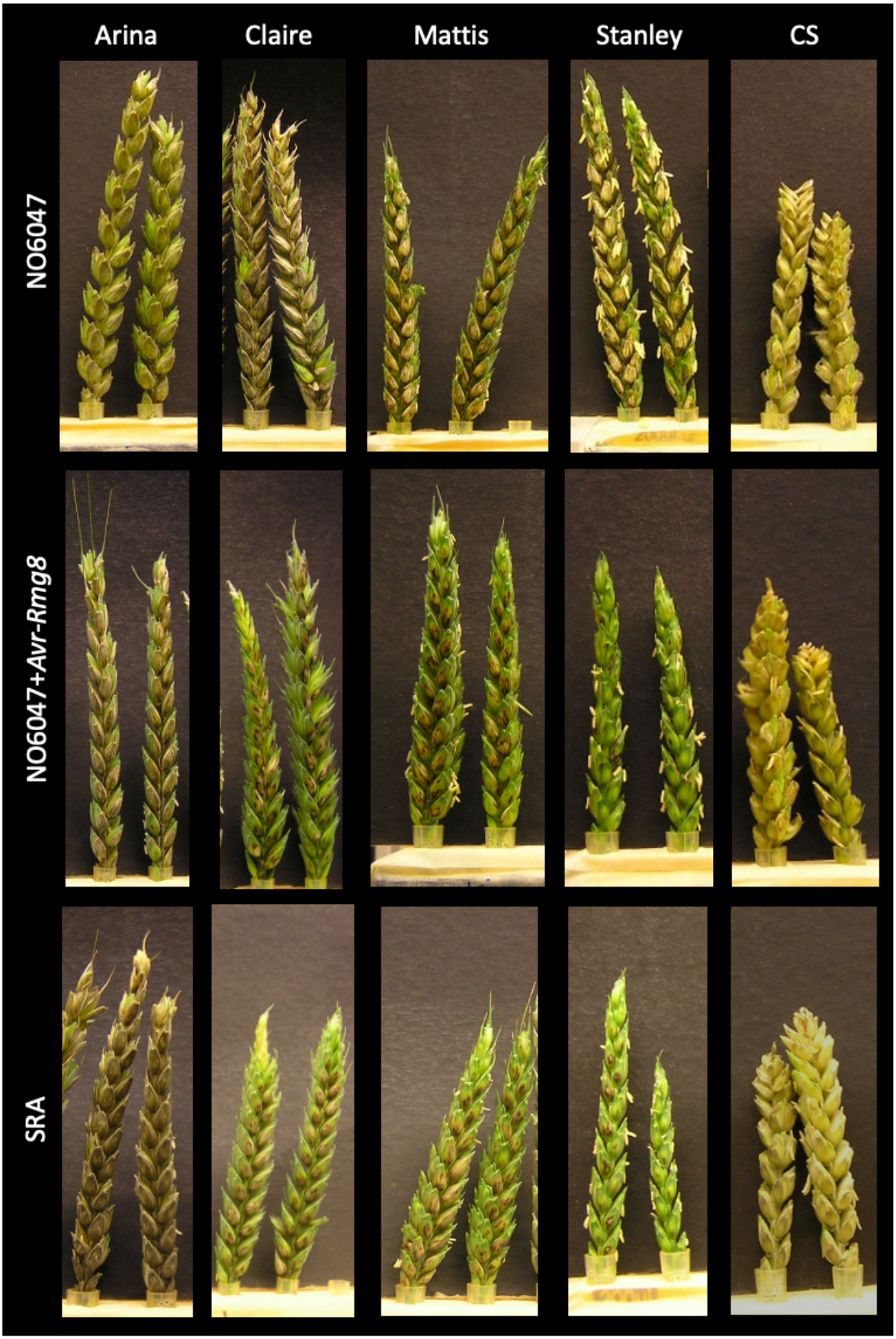

Figure 34: Comparison of spike phenotypes for NO6047, NO6047+*Avr-Rmg8* and SRA detached spike assays. Images were taken at 5 to 7 dpi.

4.3.3 Phenotyping the core Watkins panel

4.3.3.1 Detached leaf assay with NO6047+Avr-Rmg8

A DLA was carried out on the core Watkins set using the NO6047+*Avr-Rmg8* isolate as described in **Section 2.2**. Accessions WATDE0062, Sears Synth Type and Wyalkatchem were excluded from the test due to low seed numbers or poor germination (**Sup. table S7**). The average score was 4.27. A high proportion of the accessions exhibited resistance with 58 highly resistant accessions (score of 3 or less) and 114 highly susceptible accessions (score of 5 or more). Thirty-one accessions showed complete susceptibility (score of 6). To visualise the distribution of observations a KDE plot was generated (**Figure 35**). Mapping the NLR compliment of resistant accession WATDE0973 to the reference accession Mattis produced a clear association peak on 2AL, spanning 788.8 to 794.1 Mb (**Figure 36**).

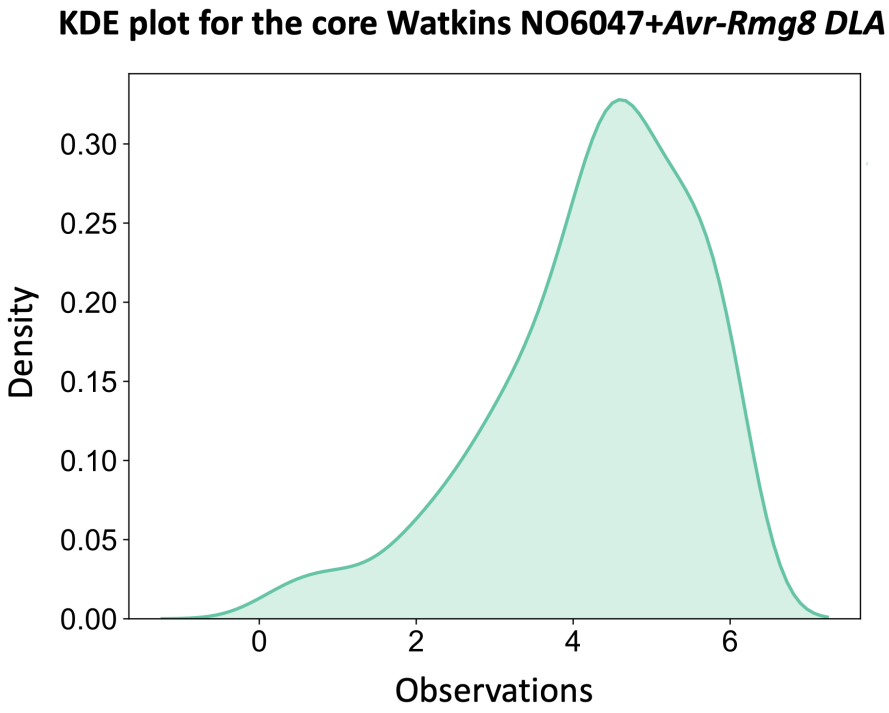

Figure 35: Kernel Density Estimation (KDE) plots for the NO6047+*Avr-Rmg8* core Watkins DLA. Scores were taken at five days post inoculation.

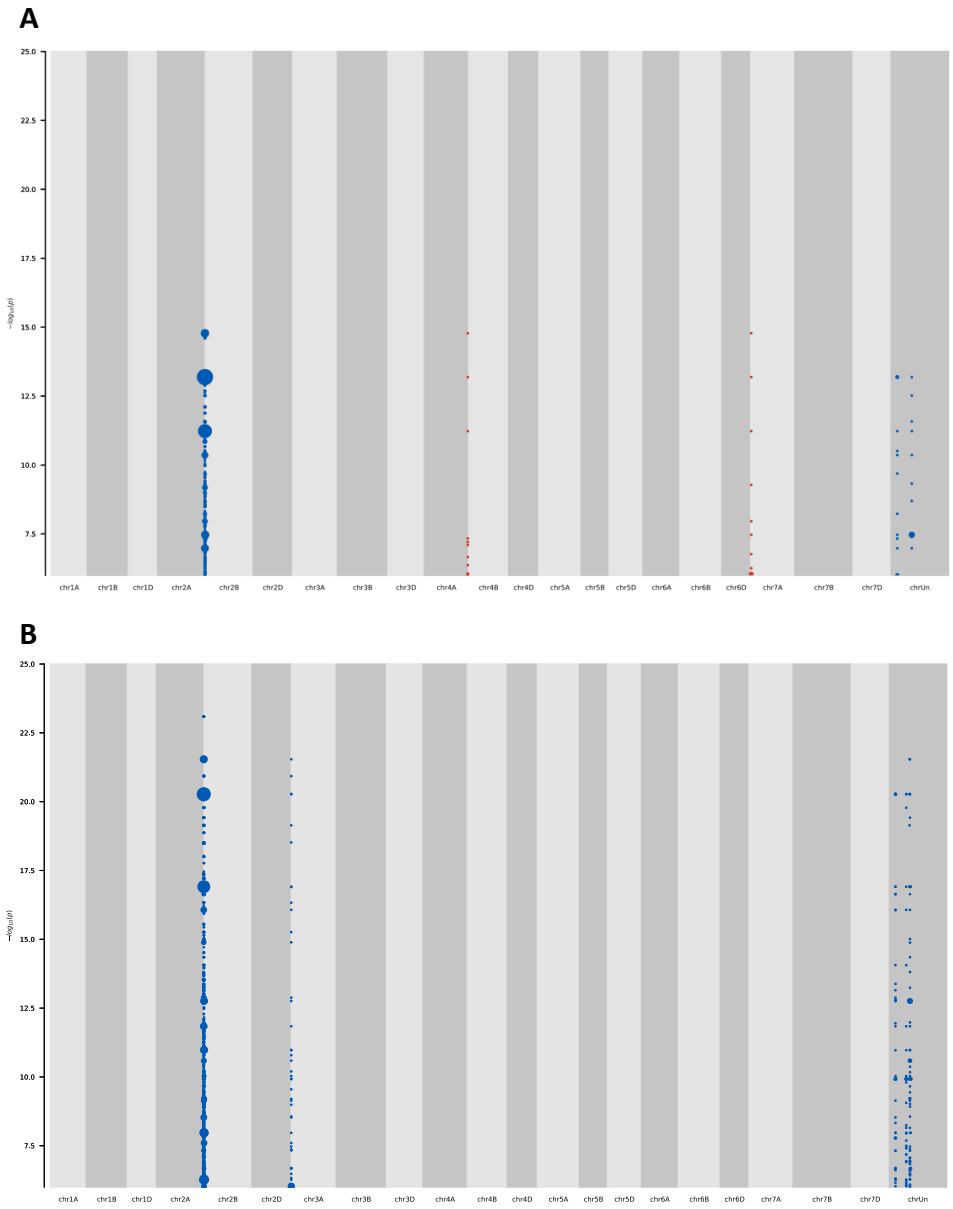

Figure 36: WatRenSeq Manhattan plots for Watkins detached leaf assay phenotypes with (**A**) NO6047+*Avr-Rmg8* (**B**) SRA. The positively associated k-mers for the NLR compliment of resistant accession WATDE0973 were mapped to the reference accession Mattis. Clear association peaks are present on chromosome 2A, spanning 788.8 to 794.1 Mb.

4.3.3.2 Detached leaf assay with SRA

The core Watkins panel was also phenotyped with SRA, as described in **Section 2.2**. Accessions WATDE0063, WATDE0064, WATDE0727, Pfau and Reedling were excluded from the test due to low seed numbers or poor germination (**Sup. table S7**). There was a much lower proportion of resistance compared to the NO6047+*Avr-Rmg8* assay, with an average score of 4.70 and only 34 accessions scored 3 or less. Only a subset of accessions classed as highly resistant to NO6047+*Avr-Rmg8* (24/58) maintained their resistance with SRA. The majority of accessions (169) were classed as highly susceptible (score of 5 or more), compared to 114 accessions in the NO6047+*Avr-Rmg8* assay, with 75 accessions scoring 6. None the less, the Pearson's correlation of the mean scores at 5 dpi produced a coefficient score of 0.66, indicating a moderate positive correlation between the two datasets. To visualise the distribution of observations for the SRA DLA a KDE plot was generated (**Figure 37**). To visualise the scores between the NO6047+*Avr-Rmg8* and SRA DLAs, line graphs comparing the phenotype scores for NO6047+*Avr-Rmg8* and SRA detached leaf assays were plotted (**Figure 38**). The line graphs were used solely to visualise the data and so the lines do not infer a relationship between datapoints.

The NLR compliment of resistant accession WATDE0973 was again mapped to Mattis and produced the same association peak on 2AL, spanning 788.8 to 794.1 Mb (**Figure 36**). An additional 10 accessions of the Watkins collection were identified as carrying this 5.3 Mb interval, or the 'functional 2A haplotype'; WATDE0120, WATDE0171, WATDE0310, WATDE0369, WATDE0427, WATDE0477, WATDE0526, WATDE0571, WATDE0770, WATDE0971 (Kumar Gaurav, personal communication) (**Table 21**).

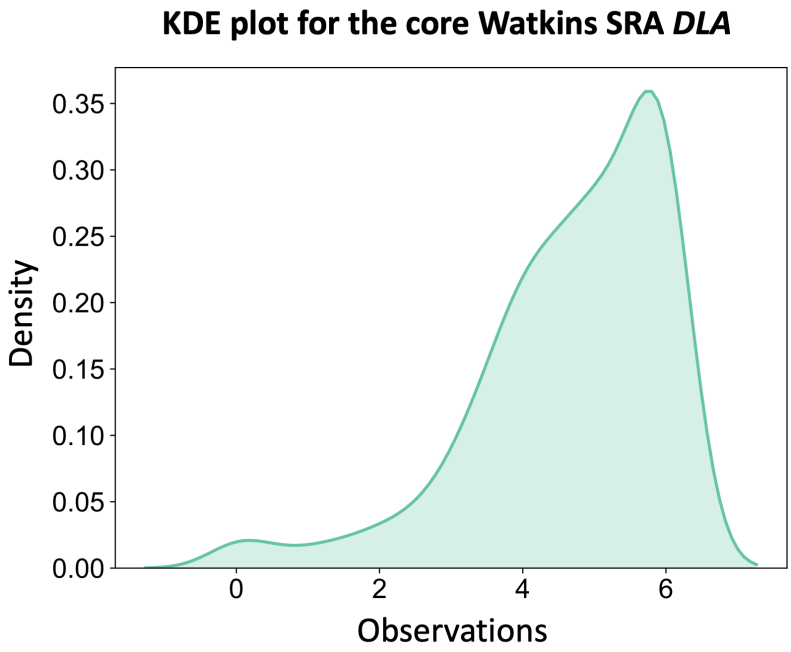

Figure 37: Kernel Density Estimation (KDE) plots for the SRA core Watkins DLA. Scores were taken at five dpi.

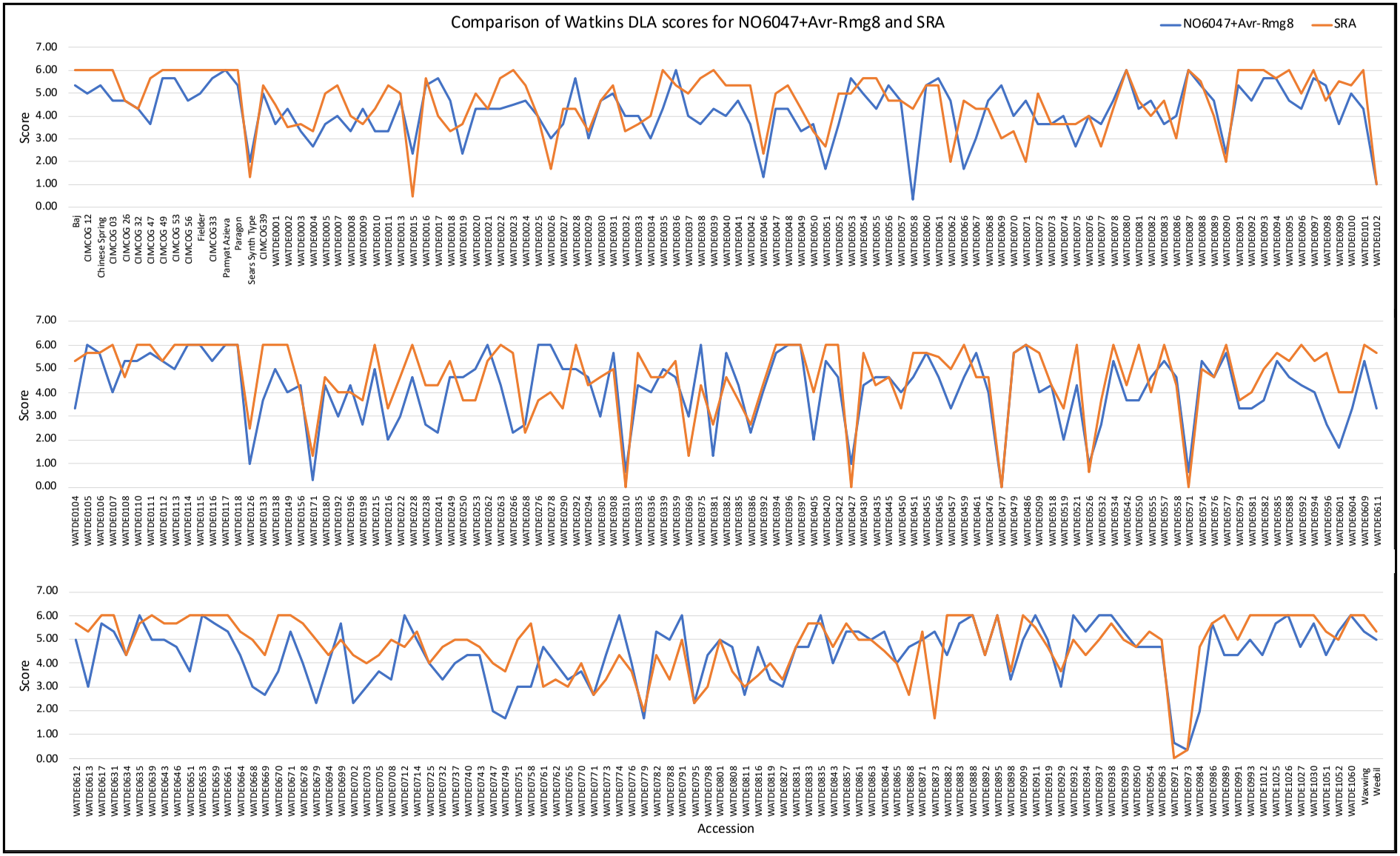

Figure 38: Line graphs comparing the phenotype scores for NO6047+*Avr-Rmg8* and SRA detached leaf assays. Lines do not infer a relationship between datapoints.

Table 21: Accessions from the core Watkins collection that have the functional 2A haplotype, and their detached leaf assay scores for NO6047+*Avr-Rmg8* and SRA isolates, both at 5 dpi.

	NO6047+*Avr-Rmg8*	**SRA**
WATDE0102	1.00	1.0
WATDE0171	0.33	1.3
WATDE0310	0.67	0.0
WATDE0369	3.00	1.3
WATDE0427	1.00	0.0
WATDE0477	0.00	0.0
WATDE0526	1.00	0.7
WATDE0571	0.67	0.0
WATDE0770	3.67	4.0
WATDE0971	0.67	0.0
WATDE0973	0.33	0.3

4.3.3.3 Watkins validation set

To verify that the 2A haplotype was associated with resistance, 31 additional Watkins lines (coined the 'validation set'), outside of the core set, were selected and their expected phenotype based on the presence/absence of the 2A haplotype was determined (Curtesy of Kumar Gaurav). Detached leaf and spike assays were performed using the same plant material, as described in **Sections 2.2 and 2.4**. Encouragingly, 24/31 accessions had the expected phenotype. Six of the remaining accessions were predicted to be resistant but phenotyped as susceptible at both the leaf and spike stages; WATDE0056, WATDE0527, WATDE0568, WATDE0593, WATDE0720 and WATDE0786 (**Tables 19 and 22**). Five accessions weren't sampled at the spike stage, but their leaf phenotypes matched the predictions. Interestingly, the two accessions used as resistant controls, WATDE0102 and WATDE0310, phenotyped as highly resistant in the leaves but were susceptible in the spikes, as did WATDE0505.

Table 22: Predicted phenotypes for the Watkins validation set, with their SRA detached leaf and spike scores at 5 dpi.

GRU code	Haplotype	DLA 5 dpi (1dp)	DSA 5 dpi (1dp)
WATDE0102	R CONTROL	1.0	6.0
WATDE0310	R CONTROL	1.0	4.8
WATDE0056	R	5.2	4.9
WATDE0122	S	5.6	5.3
WATDE0141	S	5.4	6.0
WATDE0152	S	5.6	-
WATDE0162	S	6.0	6.0
WATDE0175	S	6.0	6.0
WATDE0185	S	5.6	-
WATDE0199	S	5.8	-
WATDE0207	S	6.0	5.7
WATDE0220	S	4.6	-
WATDE0232	S	6.0	4.8
WATDE0426	R	1.0	0.7
WATDE0428	R	1.0	2.7
WATDE0465	R	1.2	-
WATDE0484	R	1.6	3.0
WATDE0505	R	1.2	5.0
WATDE0527	R	5.0	5.7
WATDE0541	R	0.8	2.7
WATDE0546	R	0.6	2.3
WATDE0566	R	1.2	2.0
WATDE0567	R	1.2	4.0
WATDE0568	R	5.4	6.0
WATDE0592	R	6.0	6.0
WATDE0672	R	1.2	2.5
WATDE0687	R	0.8	3.0
WATDE0720	R	5.4	6.0
WATDE0786	R	6.0	4.5
WATDE0804	R	1.6	4.0
WATDE0970	R	1.0	2.7
WATDE0974	R	1.0	3.7
WATDE1062	R	1.2	2.7

4.3.3.4 Phenotyping at 26°C

The *Rmg7* resistance is reported to be temperature sensitive (Anh et al. 2018). To verify whether the resistance identified in the 10+ Genomes is maintained at a higher temperature the resistant cultivars were phenotyped at 26°C at the leaf stage (**Table 19**). Six resistant Watkins accessions with the 2A haplotype were also included (WATDE0102, WATDE0171, WATDE0310, WATDE0477, WATDE0571 and WATDE0973). The same lines were also phenotyped at 20°C (2°C lower than normal) to establish whether the phenotype differential for resistance and susceptibility increased at a lower temperature (**Table 19**). The six Watkins lines, Mattis and Claire all maintained their resistance at 26°C at 6 dpi (**Figure 39**). Arina had previously shown an inconsistent phenotype with SRA however this assay clearly shows a moderate resistance to both NO6047+*Avr-Rmg8* and SRA at 20°C, which is absent at 26°C. Whilst Stanley exhibited a high level of resistance to SRA at 26°C at 5 dpi, by 6 dpi the resistance appeared to be less effective when compared to Mattis and Claire.

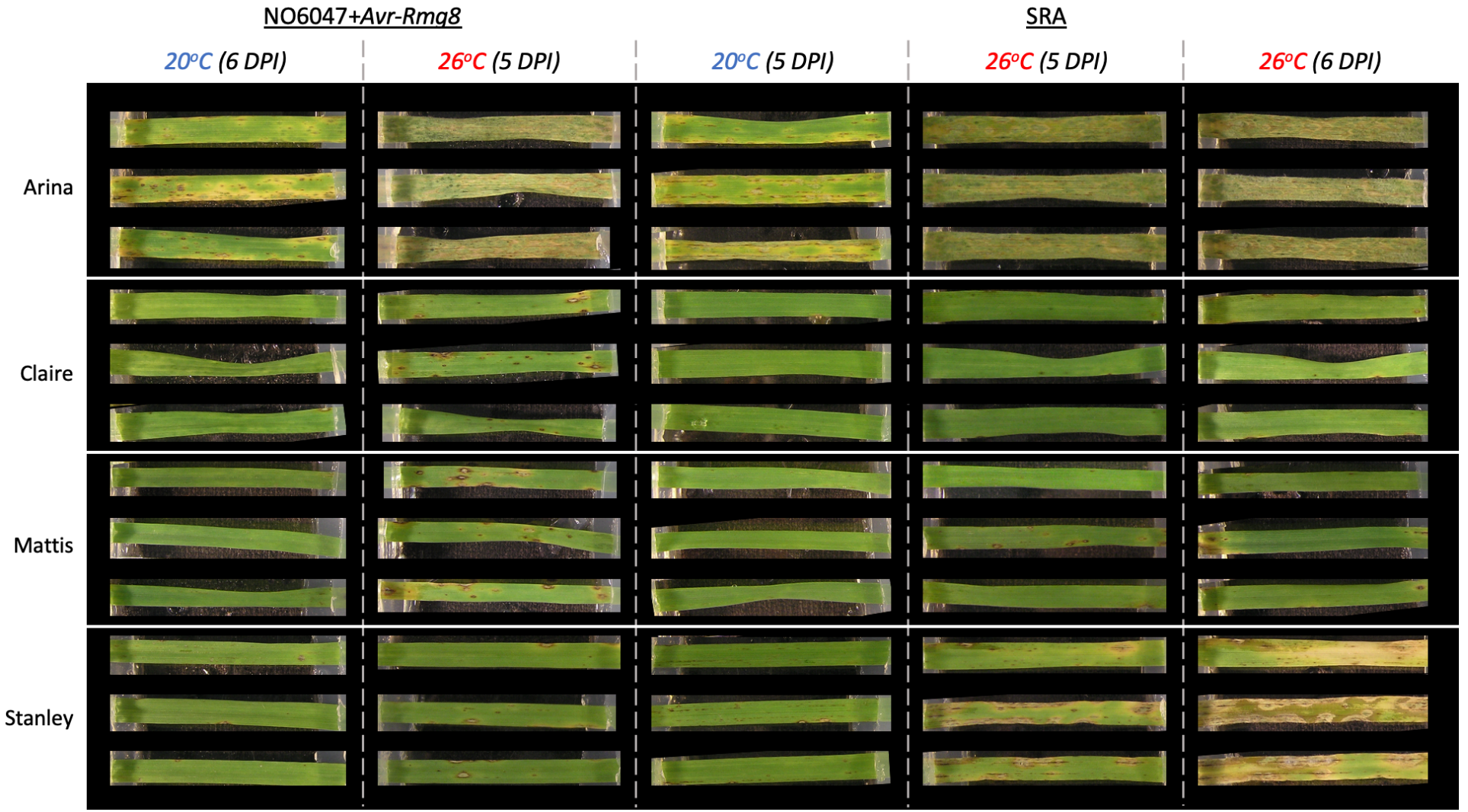

Figure 39: Representative leaves from the differential temperature leaf assay with NO6047+*Avr-Rmg8* and SRA, for Arina, Mattis, Claire and Stanley at 20 and 26°C. Pictures were taken at 5 and 6 dpi.

4.4 Discussion

In this chapter, the wheat blast resistance response of the 10+ Genomes cultivars and the Watkins core set was explored using isolates NO6047, NO6047+*Avr-Rmg8* and SRA. In the NO6047 10+ Genomes DLA, all of the cultivars were susceptible which suggested that there was no resistance to the type eII *Avr-Rmg8* effector within the 10+ Genomes (**Figure 30**). Consequently, any resistance identified with the transformed NO6047+*Avr-Rmg8* isolate would be in response to the type eI *Avr-Rmg8* effector. Comparing detached leaf phenotypes for the three isolates at 22°C suggested that there were two genes responsible for the resistance observed in Arina, Claire, Mattis and Stanley; a weak/moderate resistance effective against NO6047+*Avr-Rmg8* present in Arina, and a second more potent resistance that functions against both NO6047+*Avr-Rmg8* and SRA present in Claire, Mattis and Stanley (**Figure 33**). Phenotyping at 20°C confirmed that Arina exhibits a moderate level of resistance to both NO6047+*Avr-Rmg8* and SRA. This resistance was temperature sensitive, collapsing at 26°C and distinct from the 2A resistance identified in the Wakins core set (**Figure 39**). The variable responses of Arina at 22°C suggests that this is the upper temperature limit that the moderate Arina resistance functions and fluctuations in temperature during previous assays could have prevented the resistance from manifesting itself. In an attempt to identify the moderate temperature sensitive resistance, accessions with the 'functional 2A haplotype' were removed from the NO6047+*Avr-Rmg8* DLA dataset. The WatRenSeq analysis was rerun with the amended scores, using the NLR complement of accession WATDE0973 however there was no association observed. The gene responsible for the temperature sensitive resistance in Arina may be absent in the Watkins core set, or too rare to be detected. Alternatively, the causal gene may not be in LD with an NLR and so could not be detected using a RenSeq GWAS approach.

With global temperatures continuing to rise due to climate change, there is an increasing awareness of the need to identify resistances that will withstand higher temperatures (Chakraborty et al. 2011). Changes in ambient temperature can have a significant effect on plant ETI and PTI (Li, Liu, et al. 2020). A increase in temperature has been shown to increase expression of PTI-induced genes, shifting resistance from ETI to PTI (Cheng et al. 2013). Salicylic acid (SA) is an important regulator of both ETI and PTI responses and is synthesised predominantly via the isochorismate pathway (Vlot, Dempsey, and Klessig 2009). Isochorismate Synthase 1 is the critical enzyme within the pathway and is considered vital for pathogen induced SA production (Wildermuth et al. 2001). Compared to a normal growth temperature of 22°C, at 30°C SA biosynthesis is inhibited, however when the SA analog benzothiadiazole is applied potentiates resistance to pathogens virulent at 30°C is restored (Huot et al. 2017). This suggests that SA inhibition is crucial for the inhibition of resistance at high

temperatures. Alteration of NLR activity at high temperatures can also inhibit disease resistance, notably by altering the subcellular localisation of NLR proteins (Zhu, Qian, and Hua 2010).

Several temperature sensitive resistances haves been identified in cereals, particularly within the rust/wheat pathosystem. Usually the resistance is weakened at higher temperatures; for example the leaf rust resistances *Lr11, Lr14a, Lr14b, Lr18, Lr20* and Lr37 are more effective at lower temperatures (Kolodziej et al. 2021; Dyck and Johnson 1983; McIntosh, Wellings, and Park 1995). The same is true for temperature sensitive stem rust resistances including *Sr6* (Leonard and Szabo 2005). There are exceptions, such as the stripe rust genes *Yr17* and *Yr18* in addition to *LrZH22* provide enhanced resistance at higher temperatures (Li et al. 2023; Park, Ash, and Rees 1992; Wang et al. 2016).

WatRenSeq analysis using the scores from both the NO6047+*Avr-Rmg8* and SRA assays identified the same association on 2AL, corresponding to an interval of approximately 5.3 Mb (788.8 to 794.1 Mb). Encouragingly, 24/31 accessions from the 'validation set' produced the expected resistant/susceptible phenotype based on the presence/absence of the 2A haplotype. This suggested that the 2A haplotype genuinely associates with resistance. This is very encouraging as *Rmg7* maps to 2A (Anh et al. 2015). Six of the remaining accessions were predicted to be resistant but phenotyped as susceptible at both the leaf and spike stages. It was hypothesised that these accessions may have polymorphisms in the causal gene leading to loss of function. If this is correct then this could be invaluable in determining the identity of the causal gene among the various candidates within the defined interval. Data from both the NO6047+*Avr*-Rmg8 and SRA datasets produced KDE plots with a unimodal distribution which highlighted the small number of resistant lines. A large proportion of lines in both datasets were susceptible, with some initial resistance to the development of disease symptoms which is likely quantitative. Indeed the 2AL haplotype was rare in the Watkins core panel. This demonstrates the power of GWAS based cloning approaches as despite being present in only 11 accessions (approximately 3% of the Watkins core panel), a clear and significant association was detected. Over the past decade numerous GWAS have been performed using various wheat and CWR germplasm resources to elucidate the genetic basis of many agronomically important traits. For example: GWAS in *T. turgidum* subsp. *durum* have identified QTLs for stripe rust resistance and erect growth habit (Aoun et al. 2021; Marone et al. 2020), whilst studies in *Ae. tauschii* have identified SNPs associated with grain size, drought tolerance and micro-nutrient content (Arora et al. 2017; Qin et al. 2016; Arora et al. 2019).

Surprisingly whilst Stanley had a moderately high level of resistance to SRA at 26^{o}C at 5 dpi, by 6 dpi there was a striking loss in resistance compared to Mattis and Claire. This suggested that Mattis and

Claire may have an additional resistance that is absent in Stanley. One explanation could be that the moderate Arina resistance, which on its own collapses at 26°C, combined with the 2A resistance helps maintain resistance at higher temperatures. Alternatively, a third gene could be involved. *RmgGR119* is reported to give additive resistance to *Rmg8* in both leaf and spikes, however the effect of *RmgGR119* with *Rmg7* is unknown (Wang et al. 2018; Horo et al. 2020). The 2A resistance was maintained at 26°C in the leaves. This was unexpected as Anh et al., reported that *Rmg7* was temperature sensitive and lost efficacy at 25°C (2018). Nonetheless the 2A resistance was maintained at the spike stage at 22°C to both NO6047+*Avr-Rmg8* and SRA (**Figure 34**) but has not been investigated at 26°C. Given that the vast majority of the cloned *R* genes, including those against rice blast and the *MoT* host specificity gene *Rwt3,* encode NLRs, it was hypothesised that the 2A resistance was likely NLR based. Alternatively, as RLKs are the second most common class of *R* gene, and *Rwt4* encodes a wheat tandem kinase (WTK) a kinase may be involved.

5. INTERROGATING THE 2A INTERVAL

5.1 Introduction

Having identified a 5.3Mb interval on chromosome 2A in Mattis and verified that that it genuinely associated with resistance to both NO6047+*Avr-Rmg8* and SRA, the next task was to try to discover the causal gene. Traditionally, map based (positional) cloning approaches would be used to refine the interval to a smaller fragment that was suitable for sequencing. The first step would be to cross two parents differing in the trait of interest, say disease resistance, to generate a large segregating F_2 bi-parental mapping population. Several generations are required to generate a segregating population potentially making this a time consuming process (Bettgenhaeuser and Krattinger 2019). The larger the population the higher the chance of a recombination point close to the causal gene. Next, the parents and the mapping population are screened with previously generated polymorphic genetic markers that have a known physical position within the genome, to identify markers that segregate with the phenotype, thus identifying recombinants. Saturating the interval with markers increases the amount of refinement that can be achieved. The closer two markers are to each other, the more likely they will be co-inherited. Linkage analysis is used to establish the recombination frequencies between markers. The genotype and phenotype data is then integrated to reveal associations between traits scores and parental alleles at each position. This results in the location of the causal gene relative to the genetic markers. Once an interval has been found, additional markers may be used to narrow down the region. The genetic map is then converted to a physical map to identify the region between the closest flanking markers. This and related approaches have been used to clone numerous *R* genes, for example, Chen et al. used a map-based approach to clone the dominant rice bacterial leaf streak *R* gene *Xo2* (2022). Two F_2 mapping populations were generated using the resistant cultivar X455 and susceptible cultivars Jingang 30 (JG30) and Wushansimiao (WSSM) (1882 and 3144 F_2 lines respectively). After phenotyping, DNA was extracted from the three parent cultivars and the mapping populations and used for bulked segregant analysis, generating resistant and susceptible pools of DNA, designated RP and SP respectively. The parental DNA and resistant/susceptible pools were then analysed using the rice GSR40K chip, containing 44263 markers, which identified a 10 - 12.5 Mb interval on chromosome 2 as most highly associated with resistance. To refine the interval, 103 SSR spanning 8.6 - 13 Mb on chromosome 2 were used to screen the parent cultivars. PCR products from the parent cultivars were separated using either polyacrylamide or agarose gels and analysed for presence/absence polymorphisms. Two polymorphic markers were identified, RM12865 and RM13093. Linkage analysis using the RP, SP, X455 and JG30 DNA, followed by screening with additional markers that were polymorphic between X455 and JG30 indicated that the gene was located in a 1.0

cM region. Fine mapping the region using an addition 77 markers against the X455/WSSM population positioned the gene between markers RM12941 and M6-1. A physical map spanning 2.9Mb was generated using 27 bacterial artificial clones (BACs), within which an 110kb interval was found to co-segregate with *Xo2. De novo* sequencing of the 110kb interval within X455 and JG30 revealed 12 and 13 genes respectively. An 85 bp indel and 23 SNPs were found within the CDS of the JG30 allele of an NLR gene, *Osaoo2T0115800,* designated as *Xo2* (Chen et al. 2022).

Additional examples of *R* genes cloned before high-quality RefSeqs for crops were available include *Xa21* which confers resistance to bacterial blight (*Xanthomonas oryzae*) in rice (Song et al. 1995), *Mlo* in barley which confers resistance to *Bgt* (Büschges et al. 1997) and *Rpg1* and *Rpg5* which both provide resistance to stem rust in barley (Brueggeman et al. 2008; Brueggeman et al. 2002). The advancement of sequencing technologies facilitated the generation of RefSeqs for more than 200 plant genomes, drastically decreasing the time and resources required to identify a mapping interval (Dinh et al. 2020). However map-based cloning relies on meiotic recombination and in regions with low rates of recombination where there is a large ratio between physical and genetic distance, such as near the centromere, a larger mapping population may be required (Li, Chen, et al. 2017). If the causal gene is in an area of particularly strong LD, potentially due to a hidden introgression, cloning may not be feasible using this approach.

In the current study, a direct cloning approach was used, exploiting historical recombination within a diversity panel thus negating the need to develop mapping populations. Irrespective of the chosen cloning strategy, a number of different techniques can be adopted to interrogate an interval to identify the gene associated with the trait of interest. In this chapter several approaches were used to identify the gene content of the 2A interval and then refine the list of candidates down to a signal gene. Gene annotation models for the Mattis RefSeq were used, in addition to the NLR-Parser tool to establish a comprehensive list of the gene content within the 2A interval. To further refine the interval, a haplotype based approach, Identity By State in python (IBSpy), was then used to identify smaller haplotype blocks within the interval that were highly associated with resistance. RNAseq data, combined with WGS data was used to interrogate the remaining candidate genes to identify those expressed in relevant tissues and to identify critical polymorphisms or INDELs that explain the loss of resistance in susceptible accessions that contain the resistant haplotype.

5.2 Materials and methods

5.2.1 Identity by State in python analysis

IBSpy is a *k*-mer based GWAS haplotype analysis tool developed by Ricardo Ramirez-Gonzalez and Jesus Quiroz-Chavez, JIC. Using the WGS data generated as part of the 'WatSeq' project (unpublished), *k*-mer databases (*k*-mer length = 31bp) were produced for each accession (Quiroz-Chavez, unpublished). Unique *k*-mers, present in only one contig were removed unless the read coverage was low (less than 10-fold with a read length of 150bp). IBSpy is then run, querying each of the *k*-mer databases against a genome reference. The presence/absence of *k*-mers is measured within 50kb windows, giving three scores; '*observed k-mers*', '*variations*', and '*k-mer distance*'. The '*observed k-mers*' score is generated by counting the number of *k*-mers from the reference genome that are also present in the *k*-mer data base for a given sample, within each 50kb window. Each *k*-mer from the reference is also read from the beginning of the 50kb window, one by one, comparing to the *k*-mer data base. If one, or a series of overlapping *k*-mers are absent in the *k*-mer data base, a single '*variation*' is recorded. IBSpy can detect single SNPs, deletions and multiple SNPs with 31bp (or the *k*-mer size used), which are given different '*variations*' scores. '*k-mer distance*' is the length between the first and last SNP within a series of overlapping *k*-mers plus one, in bp. The chromosome location and number of '*variations*' within each 50kb window are recorded.

The 'variation' scores are then used to call haplotypes, using the clustering algorithm Affinity Propagation (AP). To allow multiple-genome IBSpy, the genome annotations are projected into a block of the chosen reference. Predicted gene regions are used to build blocks of syntenic windows. In this study Mattis (resistant to NO6047+*AVR-Rmg8* and SRA isolates) was used as the reference genome, with 1Mb blocks used for clustering and calling haplotypes, comprising 20 of the 50kb IBSpy windows per 1Mb. Haplotypes are visualised in a cluster heat map. The syntenic blocks can also be used to run a presence/absence haplotype GWAS (hapGWAS). For example, if there are 10 haplotypes within the first 1Mb window, each haplotype call is altered to the presence/absence (1/0) for all the genotypes in the WatSeq database. The haplotypes will be assigned a unique name but have the same chromosome position (0 to 1Mb). The hapGWAS generates the associations of the 1Mb windows with the phenotype.

5.2.2 Plant and pathogen material

5.2.2.1 Adapted wheat lines

Haplotype blocks from the IBSpy analysis that most likely associated with resistance were found in 20 modern adapted wheat varieties. These varieties were phenotyped for resistance to NO6047+*Avr-Rmg8* and SRA isolates in DLAs. (**Table 23**).

5.2.2.2 Pm4 overexpression lines, EMS mutants and near-isogenic lines

Pm4a and *Pm4b* NILs in a background of the spring wheat variety Federation, eight ethyl methanesulfonate (EMS) mutants in *Fed-Pm4b* NIL background and two *Pm4b* overexpression transgenic lines in the susceptible Bobwhite S26 background (plus susceptible sister lines that had lost the transgene via segregation) were used to validate the recognition of *Avr-Rmg8* by *Pm4* (**Table 24**). All EMS mutations were within the S_TKc domain of transcript one. Seed was provided by Beat Keller (Zurich University).

Table 23: Adapted wheat varieties used in this study.

Accession	JIC GRU store code
Sy-Epson	W10079
Revelation	W10190
Riband	WGED0128
Flame	WGED0155
Spark	WGED0159
Torfrida	WGED0161
Stava	WGED0211
Savannah	WGED0280
Boxer	WGED0540
Legend	WGED0561
Ability	WGED0562
Turpin	WGED0629
Wasp	WGED0630
Malacca	WGED0639
Holster	WGED0663
Crest	WGED0666
Consort	WGED0670
Encore	WGED0671
Spitfire	WGED0712
Shango	WGED0713

Table 24: NIL, EMS mutant and overexpression lines used to validate the recognition of *Avr-Rmg8* by *Pm4.*

Line	Description
Bobwhite S26	Susceptible background for overexpression transformants
Federation	Susceptible background for NILs
***Fed-Pm4a* NIL**	*Pm4a* from Khapli introgressed into Chancellor, then Federation
***Fed-Pm4b* NIL**	*Pm4b* from *T. carthlicum* introgressed into W804, then Federation
***Pm4b*_mutant_123**	EMS mutant (G132D) in *Fed-Pm4b* NIL background
***Pm4b*_mutant_151**	EMS mutant (P184L) in *Fed-Pm4b* NIL background
***Pm4b*_mutant_207**	EMS mutant (D170N) in *Fed-Pm4b* NIL background
***Pm4b*_mutant_495_1**	EMS mutant (Q274X) in *Fed-Pm4b* NIL background
***Pm4b*_mutant_495_3**	EMS mutant (Q274X) in *Fed-Pm4b* NIL background
***Pm4b*_mutant_526**	EMS mutant (R291K) in *Fed-Pm4b* NIL background
***Pm4b*_mutant_532**	EMS mutant (G104E) in *Fed-Pm4b* NIL background
***Pm4b*_mutant_641**	EMS mutant (G45E) in *Fed-Pm4b* NIL background
***Pm4b*_Nr#3**	*Pm4b* overexpression line
***Pm4b*_S#3**	Susceptible sister line to P*m4b*_Nr#3
***Pm4b*_Nr#52**	*Pm4b* overexpression line
***Pm4b*_S#52**	Susceptible sister line to *Pm4b*_Nr#52

5.2.2.3 Isolates

Four isolates were used for phenotyping in this chapter: Brazilian isolates NO6047, NO6047+*Avr-Rmg8* and SRA, in addition to an isolate BTJ4P-1 from Bangladesh (designated in this study as BTJ4P), that is representative of the clonal lineage from Bangladesh (**Sup. table S2**). NO6047, NO6047+*Avr-Rmg8* were cultured on oatmeal media plates and SRA and BTJ4P were cultured on CMA media plates as described in (**Section 2.1**).

5.2.3 Detached leaf and spike assays

Detached leaf and spike assays were performed as described in **Sections 2.2 and 2.4**. The inoculum concentrations, scoring day(s) and relevant section describing the results of each DLA and DSA in this chapter are listed in **Table 25.**

Table 25: Detached leaf and spike assays described in this chapter.

Isolate	Test*	Inoculum [x 10^6/ml]	Scoring day (dpi)	Section
NO6047+*Avr-Rmg8*	Adapted wheat DLA	0.18	6	5.3.2/7
SRA	Adapted wheat DLA	0.26	6	5.3.2/7
NO6047+*Avr-Rmg8*	*Pm4b* overexpression and EMS mutants, *Pm4a* and *Pm4b* NILs	0.20	5	5.3.6
SRA	*Pm4b* overexpression and EMS mutants, *Pm4a* and *Pm4b* NILs	0.22	5	5.3.6
SRA	*Pm4* alleles DLA	0.25	5	5.3.7
SRA	*Pm4* alleles DSA	0.22 - 0.30	5	5.3.7
SRA (26°C)	*Pm4* alleles DSA	0.16 - 0.24	4	5.3.8
NO6047	*Pm4* alleles DLA	0.2	5	5.3.9
NO6047	*Pm4* alleles DSA	0.07	9	5.3.9
BTJ4P	*Pm4* alleles DSA	0.08 - 0.15	6	5.3.10

* DLA = detached leaf assay. DSA = detached spike assay.

5.2.4 KASP assays

KASP markers were designed to genotype plant material for the presence/absence of *Pm4,* as well as to identify lines carrying alleles *Pm4f, Pm4f+SNP1* and *Pm4f+SNP9* (**Table 26**).

Table 26: KASP primers for genotyping material for *Pm4.*

Genotypes	Primer	Sequence*
Presence/absence of *Pm4*	Primer1_For_HEX	gaaggtcggagtcaacggatCAAGGCCAACTTCTACCGCT
	Primer1_For_FAM	gaaggtgaccaagttcatgctAAGGCCAACTTCTACCGCA
	Primer1_COM	ACTTGCAGATGCCGTCGA
Pm4f/ Pm4f+SNP1	SNP1_Rev_HEX	gaaggtcggagtcaacggatAGAGGGAATACCTTATAAACCACTG
	SNP1_Rev_FAM	gaaggtgaccaagttcatgctAGAGGGAATACCTTATAAACCACTT
	SNP1_COM	GCCCTGCCACTATCACTTTT
Pm4f/ Pm4f+SNP9	SNP9_For_HEX	gaaggtcggagtcaacggatCTTCATGTGCACGTCGTG
	SNP9_For_FAM	gaaggtgaccaagttcatgctGCTTCATGTGCACGTCGTA
	SNP9_COM1	GGAGGTGGTCCTGCTGAAG

* Lowercase sequence = HEX™/FAM™ tag

5.3 Results

5.3.1 Gene content of Mattis 2A interval

Several different methods were used to determine the gene content of the 5.3 Mb interval of 2A in the resistant variety Mattis. Given the high proportion of cloned *R* genes that are NLRs, the software tools NLR-Parser and NLR-Annotator were run on the Mattis 2A interval to predict putative NLR loci (Kourelis and Van Der Hoorn 2018; Steuernagel 2020; Steuernagel et al. 2015). The Mattis sequence was extended by approximately 250kb upstream, and to the end of the chromosome arm (7kb) to ensure all NLRs associated with resistance were captured (2A:788600000 – 794150360).

28 NLR loci were predicted, comprising 15 complete NLRs, two partial NLRs and 11 pseudogenes (three of which were predicted to be partial NLRs) (**Table 27**). Pseudogenes are likely non-functional in the reference they were annotated in, but there may be functional alleles in other accessions (Steuernagel 2020; Cheetham, Faulkner, and Dinger 2020). As Mattis is resistant, the NLRs predicted as pseudogenes by NLR-Annotator were considered unlikely to be the causal *R* gene. No NLRs were predicted within the extended parts of the Mattis sequence.

Table 27: NLR loci predictions within the Mattis 2A interval using the NLR-Annotator pipeline.

Code	Coordinates	Prediction
NLR1	788846217 - 788849367	complete
NLR2	788886926 - 788890065	complete
NLR3	789130131 - 789131985	partial (pseudogene)
NLR4	789185129 - 789186100	complete
NLR5	789189787 - 789192901	complete
NLR6	789229395 - 789232272	complete
NLR7	789251209 - 789254306	complete (pseudogene)
NLR8	789285616 - 789288484	complete
NLR9	789356140 - 789358877	complete
NLR10	789375648 - 789376022	partial (pseudogene)
NLR11	789381944 - 789384821	complete
NLR12	789393344 - 789395390	complete
NLR13	789404272 - 789408714	complete (pseudogene)
NLR14	789425494 - 789428605	complete
NLR15	792684208 - 792688408	complete (pseudogene)
NLR16	792691852 - 792693630	partial
NLR17	792782163 - 792786044	complete (pseudogene)
NLR18	794139786 - 794142198	complete
NLR19	794127626 - 794132648	complete (pseudogene)
NLR20	794037279 - 794040360	complete
NLR21	794009544 - 794013626	complete (pseudogene)
NLR22	793890442 - 793892596	complete (pseudogene)
NLR23	793785606 - 793790096	complete (pseudogene)
NLR24	793743886 - 793744647	partial
NLR25	793703986 - 793707081	complete
NLR26	793669279 - 793670511	complete
NLR27	793628381 - 793628678	partial (pseudogene)
NLR28	788965435 - 788968572	complete

The non-NLR gene content of the expanded Mattis interval was also determined. At the time of this study, publicly available genome annotations for the 10+ Genomes cultivars were based on projections of the gene models from the Chinese Spring RefSeq (IWGSC et al. 2018). As Chinese Spring lacked the 2A interval associated with resistance, *de novo* gene annotations for Mattis were investigated, provided by Ricardo Ramirez-Gonzalez (JIC). Two hundred and twenty-eight genes were predicted, including 73 high confidence genes (**Table 28**). Twelve of the 28 putative NLR loci predicted by NLR-Annotator were not present in the *de novo* gene models (NLRs 3, 4, 7, 9, 10, 11, 18, 19, 21, 22, 23 and 24). An additional seven of the putative NLR loci were low confidence (NLRs 14, 15, 16, 25, 26, 27 and 28, corresponding to TraesSYM2A03G00828860, TraesSYM2A03G00829680, TraesSYM2A03G00829690, TraesSYM2A03G00830330, TraesSYM2A03G00830320, TraesSYM2A03G00830310 and TraesSYM2A03G00828510 respectively). As well as being low confidence or absent from the gene annotation, NLRs 3, 7, 10, 15, 17, 19 and 21 were predicted by NLR-Annotator as pseudogenes so were considered unlikely to be resistance gene candidates (**Table 28**). Genes of note included one additional NLR (TraesSYM2A03G00829660) that wasn't included in the NLR-Annotator output, along with three RLKs (TraesSYM2A03G00828360, TraesSYM2A03G00829670 and TraesSYM2A03G00830320). TraesSYM2A03G00830320 was denoted as low confidence but was immediately adjacent to NLR26 so was kept in consideration as a candidate. All remaining low confidence genes were considered unlikely to be resistance gene candidates, along with five high confidence genes linked to retrotransposons (TraesSYM2A03G00828410, TraesSYM2A03G00829520, TraesSYM2A03G00829710, TraesSYM2A03G00829850 and TraesSYM2A03G00830590) and 29 high confidence genes that had an unknown function. **Table 28** lists the high confidence gene content of the Mattis 2A interval, NLR loci predicted by NLR annotator that are absent in the Mattis annotations and low confidence NLRs.

Table 28: High confidence gene content of the Mattis 2A interval, their location and function from the de novo genome annotation. Putative NLR loci predicted by NLR annotator but absent in the Mattis annotations are included, along with low confidence NLRs.

Gene code*	Coordinates (orientation)	Function	NLR-Annotator prediction
TraesSYM2A03G00828360	788728552 - 788738447(+)	Receptor-like kinase	
TraesSYM2A03G00828370	788768076 - 788769438(+)	*unknown*	
TraesSYM2A03G00828380	788811120 - 788813175(+)	*unknown*	
TraesSYM2A03G00828390	788825472 - 788828016(+)	*unknown*	
TraesSYM2A03G00828400	788828264 - 788832085(+)	methyltransferases superfamily protein	
TraesSYM2A03G00828410	788833791 - 788837343(+)	RNase P 1	
TraesSYM2A03G00828420	788837936 - 788839387(+)	STAY-GREEN LIKE, chloroplastic	
TraesSYM2A03G00828440	788841216 - 788842285(+)	*unknown*	
TraesSYM2A03G00828450	788845950 - 788849102(+)	resistance protein RGA2	NLR1 - complete
TraesSYM2A03G00828460	788885045 - 788890732(+)	resistance protein RGA2	NLR2 - complete
TraesSYM2A03G00828500	788960342 - 788962593(+)	*unknown*	
TraesSYM2A03G00828510*	788964833 - 788969435(-)	resistance protein RGA2	NLR28 - complete
TraesSYM2A03G00828540	789110507 - 789111037(+)	*unknown*	
-	789130131 - 789131985(+)	-	NLR3 - partial (pseudogene)
TraesSYM2A03G00828580	789151116 - 789153155(+)	*unknown*	
TraesSYM2A03G00828590	789161156 - 789162436(+)	F-box/kelch-repeat protein	
-	789185129 - 789186100(+)	-	NLR4 - complete
TraesSYM2A03G00828600	789188895 - 789193763(+)	resistance protein RGA2/ transposon TNT	NLR5 - complete
TraesSYM2A03G00828640	789217066 - 789233090(+)	F-box/kelch-repeat protein	NLR6 - complete
-	789251209 - 789254306(+)	-	NLR7 - complete (pseudogene)
TraesSYM2A03G00828700	789264657 - 789265305(-)	protein 5NG4	
TraesSYM2A03G00828720	789284536 - 789289459(+)	resistance protein RGA2	NLR8 - complete
-	789356140 - 789358877(+)	-	NLR9 - complete
-	789375648 - 789376022(+)	-	NLR10 - partial (pseudogene)
-	789381944 - 789384821(+)	-	NLR11 - complete
TraesSYM2A03G00828810	789390224 - 789396435(+)	resistance protein RGA2	NLR12 - complete
TraesSYM2A03G00828830	789403251 - 789408104(+)	resistance protein RGA2	NLR13 - complete (pseudogene)
TraesSYM2A03G00828840	789408643 - 789409011(-)	peptidase subunit alpha	
TraesSYM2A03G00828850	789416992 - 789419026(+)	phosphodiesterases superfamily protein	
TraesSYM2A03G00828860*	789425236 - 789427216(+)	resistance protein RGA2	NLR14 - complete
TraesSYM2A03G00828930	789745589 - 789748504(-)	4-like protein	
TraesSYM2A03G00829020	790122656 - 790126161(-)	*unknown*	
TraesSYM2A03G00829080	790381831 - 790387386(+)	*unknown*	
TraesSYM2A03G00829120	790568231 - 790571224(-)	*unknown*	
TraesSYM2A03G00829200	790955915 - 790959358(-)	*unknown*	
TraesSYM2A03G00829250	791221535 - 791225005(+)	*unknown*	
TraesSYM2A03G00829350	791855004 - 791858879(-)	*unknown*	
TraesSYM2A03G00829450	792130947 - 792134542(+)	*unknown*	
TraesSYM2A03G00829510	792400216 - 792404527(-)	N-methyltransferase SUVR4	

TraesSYM2A03G00829520	792405026 - 792406692(+)	non-LTR retrotransposon	
TraesSYM2A03G00829540	792410750 - 792414847(-)	glycosyltransferase subunit 1	
TraesSYM2A03G00829560	792465474 - 792467366(-)	beta-1,6-N-acetylglucosaminyltransferase family protein	
TraesSYM2A03G00829570	792472433 - 792473359(+)	*unknown*	
TraesSYM2A03G00829580	792519361 - 792525805(-)	toxin-like protein Hfr-2	
TraesSYM2A03G00829600	792527494 - 792528414(-)	*unknown*	
TraesSYM2A03G00829610	792534358 - 792535178(+)	*unknown*	
TraesSYM2A03G00829620	792554319 - 792557912(+)	domain-containing protein 78	
TraesSYM2A03G00829630	792559869 - 792562916(+)	protein Rab-18	
TraesSYM2A03G00829640	792660864 - 792662136(+)	*unknown*	
TraesSYM2A03G00829650	792660869 - 792662507(-)	*unknown*	
TraesSYM2A03G00829660	792670265 - 792673854(+)	resistance protein RGA2	
TraesSYM2A03G00829670	792679164 - 792680963(+)	Receptor-like kinase family	
TraesSYM2A03G00829680*	792684200 - 792684502(+)	resistance protein CC-NBS-LRR	NLR15 - complete (pseudogene)
TraesSYM2A03G00829690*	792692846 - 792693976(+)	resistance protein RGA2	NLR16 - partial
TraesSYM2A03G00829710	792724770 - 792728735(-)	protein, putative, Ty1-copia	
TraesSYM2A03G00829740	792765879 - 792768798(+)	*unknown*	
TraesSYM2A03G00829750	792781806 - 792786738(+)	resistance protein RGA2	NLR17 - complete (pseudogene)
TraesSYM2A03G00829800	792879278 - 792881875(-)	Protease	
TraesSYM2A03G00829810	792928596 - 792934980(+)	Peptidase	
TraesSYM2A03G00829820	792935138 - 792938913(-)	transporter NIPA (DUF803)	
TraesSYM2A03G00829830	792983207 - 792991299(+)	*unknown*	
TraesSYM2A03G00829850	793062876 - 793066852(+)	Putative protein, Ty1-copia	
TraesSYM2A03G00830090	793345006 - 793347118(+)	*unknown*	
TraesSYM2A03G00830110	793359286 - 793361111(+)	domain-containing protein 78	
TraesSYM2A03G00830160	793436071 - 793438232(-)	*unknown*	
TraesSYM2A03G00830190	793470556 - 793474718(+)	ATP-dependent RNA helicase	
TraesSYM2A03G00830210	793492346 - 793493598(+)	*unknown*	
TraesSYM2A03G00830260	793585072 - 793585649(-)	*unknown*	
TraesSYM2A03G00830280	793602733 - 793603198(-)	ATPase sarcoplasmic/ERCC-6-like protein	
TraesSYM2A03G00830300	793618964 - 793626781(+)	excision repair protein	
TraesSYM2A03G00830310*	793627490 - 793629635(-)	-	NLR27 - partial (pseudogene)
TraesSYM2A03G00830320*	793666286 – 793669583(-)	Receptor-like kinase	NLR26 - complete
TraesSYM2A03G00830330*	793670182 – 793708537(-)	resistance protein RGA2	NLR25 - complete
-	793743886 – 793744647(-)	-	NLR24 - partial
-	793785606 - 793790096(-)	-	NLR23 - complete (pseudogene)
TraesSYM2A03G00830400	793840966 - 793844595(-)	*unknown*	
TraesSYM2A03G00830410	793848007 - 793848435(+)	*unknown*	
TraesSYM2A03G00830420	793853596 - 793855385(+)	*unknown*	
TraesSYM2A03G00830430	793857902 - 793860706(-)	transcription factor 28	
TraesSYM2A03G00830440	793864325 - 793867928(-)	transcription factor 28	
TraesSYM2A03G00830450	793882890 - 793884880(+)	transcription factor 28	
-	793890442 - 793892596(-)	-	NLR22 - complete (pseudogene)

TraesSYM2A03G00830490	793986412 - 793987375(-)	*unknown*	
-	794009544 - 794013626(-)	-	NLR21 - complete (pseudogene)
TraesSYM2A03G00830530	794021318 - 794024342(-)	phosphodiesterases superfamily protein	
TraesSYM2A03G00830550	794036223 - 794041272(-)	resistance protein RGA2 - related family	NLR20 - complete
TraesSYM2A03G00830580	794071710 - 794073655(-)	putative protein, Mutator subclass	
TraesSYM2A03G00830590	794082632 - 794085547(+)	protein putative, Ty1-copia	
-	794127626 - 794132648(-)	-	NLR19 - complete (pseudogene)
TraesSYM2A03G00830600	794135460 - 794136365(-)	SKIP23-like protein	
-	794139786 - 794142198(-)	-	NLR18 - complete
TraesSYM2A03G00830620	794148636 - 794150360(+)	glucosyltransferase 1	

* Indicates low confidence genes

5.3.2 Identity by state in python haplotype analysis

IBSpy haplotype analysis was run on the 5.3Mb 2A interval, by Jesus Quiroz-Chavez (JIC). Mattis was used as the reference genome and a cluster heat map was generated to visualise the haplotypes present within this interval (**Figure 40**). The cluster heat map shows each 50kb window within a genotype as a coloured square; the darker the colour the closer that region is to being identical by state (IBS) to Mattis. As a guide, Mattis was included in the cluster heat map and appears as a black line throughout the interval, ie IBS. Two main blocks of similarity were observed, ***Region 1*** (788550000 to 789550000 = 1Mb) and ***Region 2*** (793250000 - 794250000 = 1Mb). The blocks were physically separate but were present together in some genotypes while other genotypes contained only *Region 1*. No variety contained only *Region 2* (**Figure 40**) *T. timopheevii* accession 33255 had high sequence similarity to *Region 1* and 600kb of high similarity to *Region 2* so it was hypothesised that the interval originated as an introgression from a wheat relative similar to *T. timopheevii*. Five Watkins lines (WATDE0102, WATDE0171, WATDE0310, WATDE0566 and WATDE0804) lacked *Region 2* but were resistant, suggesting that *Region 2* did not contain the candidate gene.

To establish the phenotype of the adapted wheat lines carrying *Region 1*, a DLA was performed, using both the NO6047+*Avr-Rmg8* and SRA isolates (**Tables 25 and 31**). Susceptible and resistant '10 plus Genomes' varieties were included as controls (susceptible = Arina, Jagger and Mace; resistant = Claire, Mattis and Stanley). A selection of Watkins accessions with the different haplotypes were also included. All of the 20 adapted varieties were resistant in the DLA to both NO6047+*Avr-Rmg8* and SRA at six dpi. 16/22 adapted varieties lacked *Region 2*, confirming that *Region 2* could be removed from further analysis. WATDE0571 was resistant but lacked the last 200kb of the *Region 1* (highlighted in blue in **Figure 40**), and WATDE048 and WATDE0720 were susceptible but lacked the first 400kb of *Region 2* (highlighted in yellow in **Figure 40**). Combined, these two observations suggested that the first 400kb of *Region 1* contained the causal gene, designated the '2A IBSpy haplotype'. According to the *de novo* Mattis gene models, the 2A IBSpy haplotype contained five genes. To avoid confusion and simplify differentiation between them these genes were recoded and will be referred to using the following new codes hereafter: TraesSYM2A03G00828360 = *MA4*, TraesSYM2A03G00828400 = *MA5*, TraesSYM2A03G00828410 = *MA6*, TraesSYM2A03G00828420 = *MA7* and TraesSYM2A03G00828460 = *NLR2* (**Table 29**). Four Watkins lines contained *Region 1* but were susceptible (WATDE0048, WATDE0527, WATDE0568 and WATDE0592). These lines may contain deleterious mutations in the causal gene however the IBSpy pipeline cannot distinguish lines based on small numbers of polymorphisms between sequences.

To determine if there were potential homologs for the gene content of the IBSpy haplotype, the CDS sequence for each gene was BLASTed back into Mattis. The best off-target BLAST hits were selected based on BLAST score, sequence length and percent identity. For genes MA4, MA5, MA6, MA7 and NLR1, the best off-target BLAST hit for the B and D genomes were on the distal ends of chromosomes 2BL and 2DL respectively and followed the same gene order as on chromosome 2A (**Table 30**). However, the best off-target BLAST hits for MA8 and NLR2 were outside of the group two chromosomes and had low scores/percent identities making it unclear if homologs were present.

Table 29: Gene content of the 2A IBSpy haplotype.

Gene code	Coordinates (orientation)	Function (NLR-Annotator prediction)	TOH code
TraesSYM2A03G00828360	788728552 - 788738447(+)	Receptor-like kinase	MA4
TraesSYM2A03G00828400	788828264 - 788832085(+)	methyltransferases superfamily protein	MA5
TraesSYM2A03G00828410	788833791 - 788837343(+)	RNase P 1	MA6
TraesSYM2A03G00828420	788837936 - 788839387(+)	STAY-GREEN LIKE, chloroplastic	MA7
TraesSYM2A03G00828460	788885045 - 788890732(+)	resistance protein RGA2 (complete NLR)	NLR2

Table 30: Gene content of the IBSpy haplotype and their potential homologs.

TOH Code	2A Gene Code	Potential homologs	
		Chromosome 2B	Chromosome 2D
MA4	TraesSYM2A03G00828360	TraesSYM2B03G01094850	TraesSYM2D03G01324910
MA5	TraesSYM2A03G00828400	TraesSYM2B03G01095820	TraesSYM2D03G01325190
MA6	TraesSYM2A03G00828410	TraesSYM2B03G01095830	TraesSYM2D03G01325200
MA7	TraesSYM2A03G00828420	TraesSYM2B03G01095850	TraesSYM2D03G01325210
MA8	-	-	-
NLR1	TraesSYM2A03G00828450	TraesSYM2B03G01095950	TraesSYM2D03G01325240
NLR2	TraesSYM2A03G00828460	-	-

Table 31: Scores from the adapted wheat varieties plus Watkins DLAs with NO6047+*Avr-Rmg8* and SRA. Haplotypes based on the presence/absence of the 50kb windows within *Region 1* and *Region 2* were determined. Scores were taken at 6 dpi.

Accession	NO6047+*Avr-Rmg8*	SRA	IBSpy Haplotype*
WATDE0571	1.80	1.00	3' of R1 absent
WATDE0056	5.80	5.80	5' of R1 absent
WATDE0720	5.00	5.80	
WATDE0477	1.40	0.80	5' of R2 absent
Arina	5.00	5.20	Lacks 2A
Mace	4.60	5.00	
Jagger	3.80	5.20	
WATDE0015	4.40	5.20	R1 and R2 absent
WATDE0484	4.60	6.00	
WATDE0795	5.20	5.20	
WATDE0048	4.60	5.60	R1 and R2 present
WATDE0527	4.60	5.80	
WATDE0568	5.60	5.80	
WATDE0592	4.60	5.60	
Mattis	1.80	1.20	
Stanley	2.60	1.20	
Sy-Epson	1.20	0.00	
Renan	2.00	0.80	
Rendevous	2.60	1.80	
Holster	3.00	3.00	
Torfrida	3.00	1.33	
Turpin	3.67	1.67	
WATDE0310	1.20	0.80	R2 absent
WATDE0804	0.80	1.80	
Claire	1.20	1.20	
Revelation	1.40	1.20	
Ability	2.33	1.00	
Boxer	1.67	1.00	
Consort	3.00	3.00	
Crest	3.00	2.00	
Encore	2.33	2.00	
Flame	2.33	1.00	
Legend	1.33	1.33	
Malacca	3.33	2.00	
Riband	3.00	1.67	
Savannah	2.67	1.67	
Shango	2.33	1.67	
Spark	0.67	1.33	
Spitfire	2.00	1.67	
Stava	1.67	1.00	
Wasp	2.00	1.00	
WATDE0102	2.60	2.20	
WATDE0171	1.80	0.80	
WATDE0566	1.60	2.20	
WATDE0786	3.60	6.00	

* R1 = *Region 1*, R2 = *Region 2*. 5' = first 400kb. 3' = last 200kb.

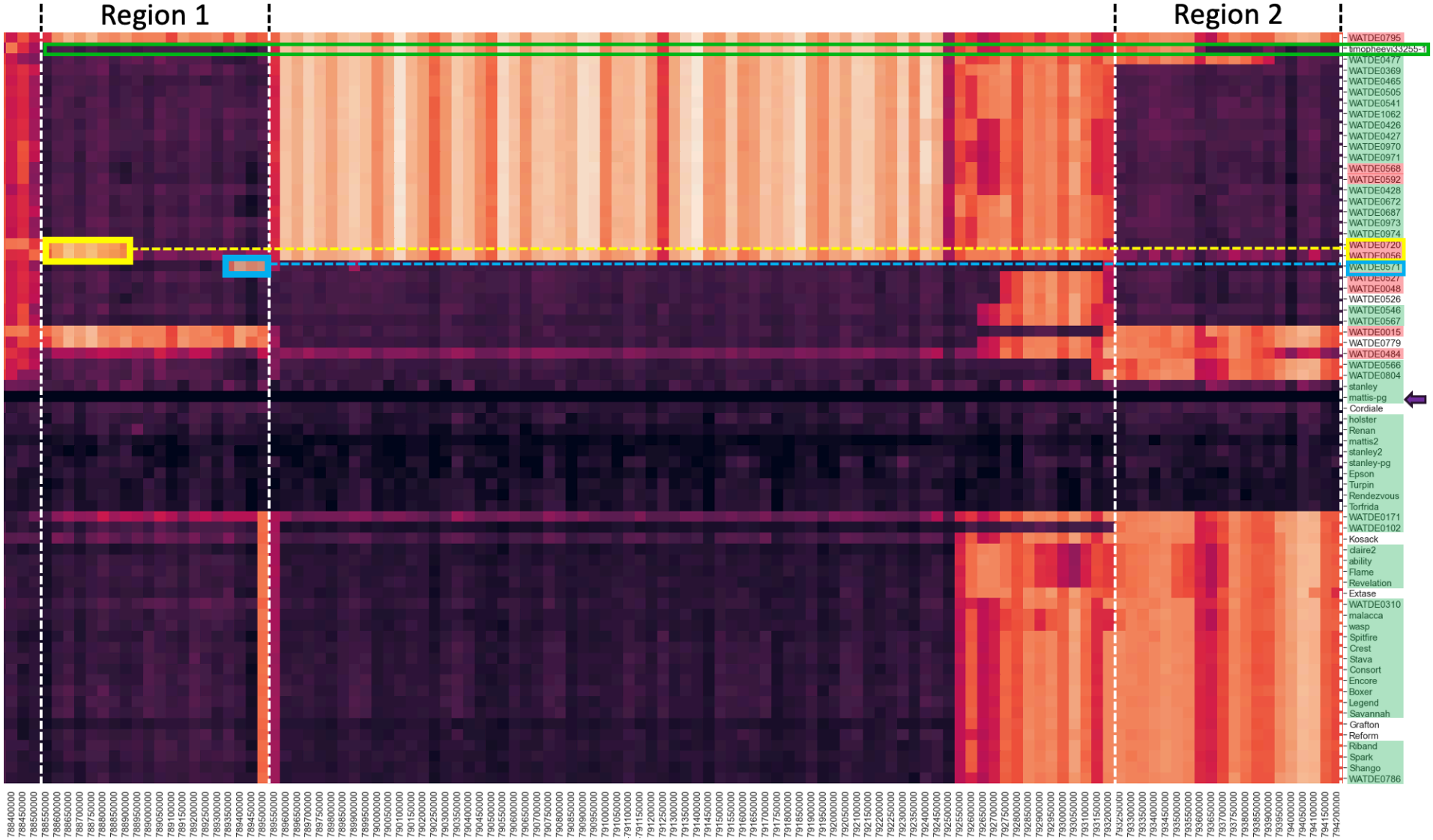

Figure 40: Cluster heat map for the IBSpy haplotype analysis of the 5.2Mb interval, using Mattis as the reference. Each 50kb window within a genotype is represented as a coloured square; the darker the colour the closer that region is to being identical by state to Mattis (purple arrow). WATDE0571 is resistant but lacks the last 200kb of the Region 1 (blue box), and WATDE048 and WATDE0720 are susceptible but lack the first 400kb of Region 2 (yellow box). *T. timopheevii* is shown in the green. Resistant/susceptible accessions are highlighted in green/red respectively.

5.3.3 RNAseq analysis

One approach to try to reduce the number of candidate genes within the region highlighted by the IBSpy analysis was to determine which genes were expressed. Pre-existing RNAseq data available from the Uauy group (JIC) were analysed. Two replicates of data from whole aerial organ samples of Mattis were investigated, V1 and V2. Samples were harvested at the three leaf stage and were collected four hours after dawn to reduce the amount of metabolites within samples that could interfere with downstream molecular genetic processes. Note that the seedling leaf tissue used was not exposed to wheat blast when the data was captured. Both datasets were mapped to Mattis before being visualised using the Integrative Genomics Viewer (IGV) tool (Robinson et al. 2011). A full list of all the genes in the 2A interval with read coverage is in **Sup. table S8**.

Within the '2A IBSpy' interval six regions showed read coverage, including the five annotated within the de novo Mattis gene models (**Table 32**). There was also an additional region that was not annotated within the *de novo* Mattis gene annotations, designated *MA8*. *MA4* had good read coverage in both datasets, with consistent intron/exon boundaries. *MA4* showed alternate splicing resulting in two potential transcripts. Both transcripts had six exons. The intron/exon structure for the first five exons was the same in both transcripts, however the last exons were completely distinct from one another (**Figure 41**). The first transcript produced a protein of 560 amino acids in length. In the second transcript the fifth intron extended an additional 1082 bp (encapsulating the sixth exon from transcript one) and produced a protein of 747 amino acids in length. Exon 6 within the second transcript was denoted 'exon 6A'.

Table 32: Regions of expression within the 2A IBSpy haplotype.

Gene code	Coordinates (orientation)	Function (NLR-Annotator prediction)	RNAseq read coverage	TOH code
TraesSYM2A03G00828360	788728552 - 788738447(+)	Receptor-like kinase	good coverage, 7 exons	MA4
TraesSYM2A03G00828400	788828264 - 788832085(+)	methyltransferases superfamily protein	good coverage, 8 exons	MA5
TraesSYM2A03G00828410	788833791 - 788837343(+)	RNase P 1	good coverage, 6 exons	MA6
TraesSYM2A03G00828420	788837936 - 788839387(+)	STAY-GREEN LIKE, chloroplastic	very high coverage, 3 exons	MA7
-	788878849 - 788879888(-)	-	very high coverage, 2 exons	MA8
TraesSYM2A03G00828460	788885045 - 788890732(+)	resistance protein RGA2 (complete NLR)	very poor coverage	NLR2

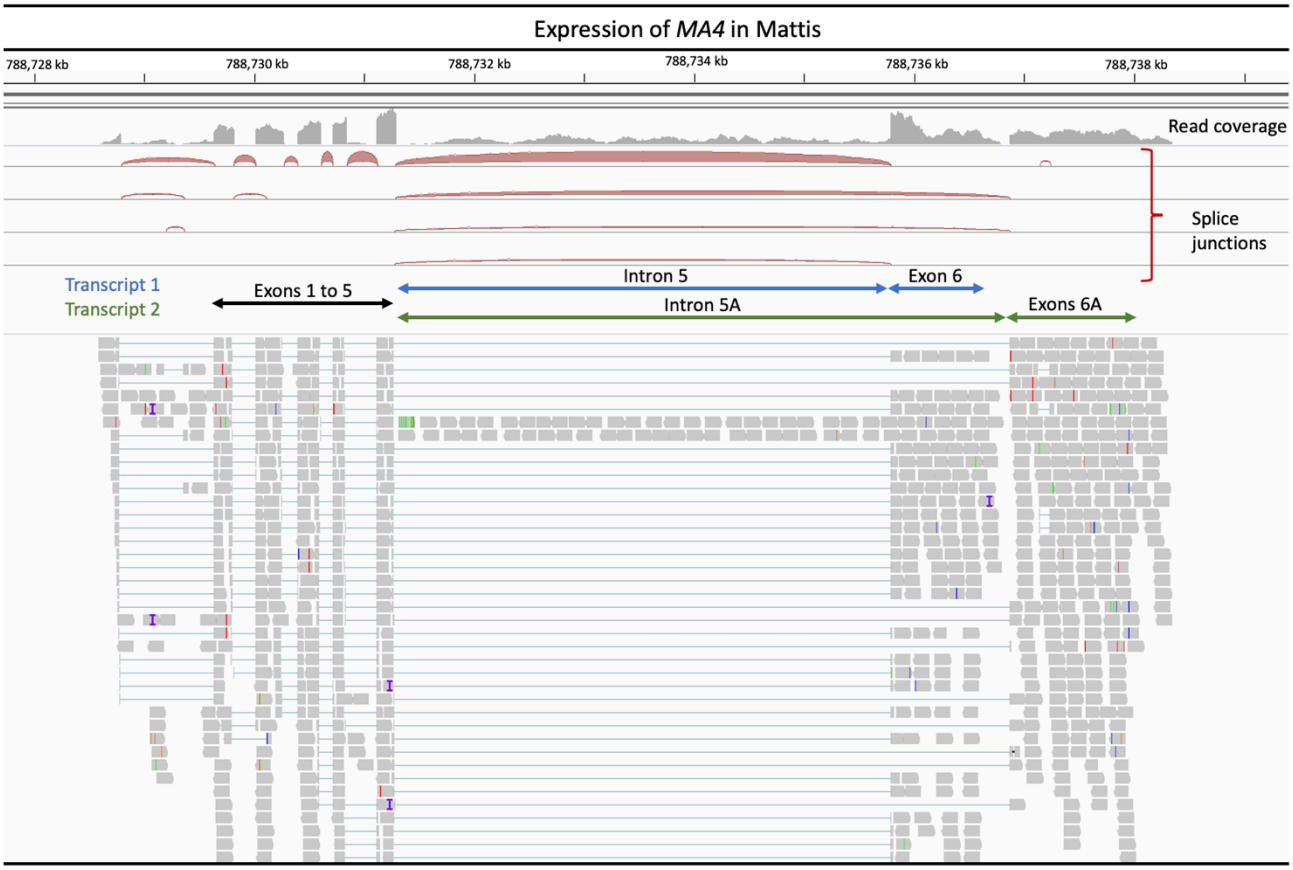

Figure 41: Representative expression profile of *MA4* for the Mattis RNAseq data mapped to Mattis. Red arches within the 'Splice junctions' tracks show predicted intron/exon boundaries on the forward strand.

MA5 showed good coverage but only in one of the datasets, V2, with eight clearly defined exons (**Figure 42**). Note several 'white' reads were present indicating they mapped to another location with equally good placement. There were also several instances of multiple reads with the same SNP(s), displayed as coloured lines. Combined, the white reads and SNPs suggested that a proportion of the reads had been mis-mapped.

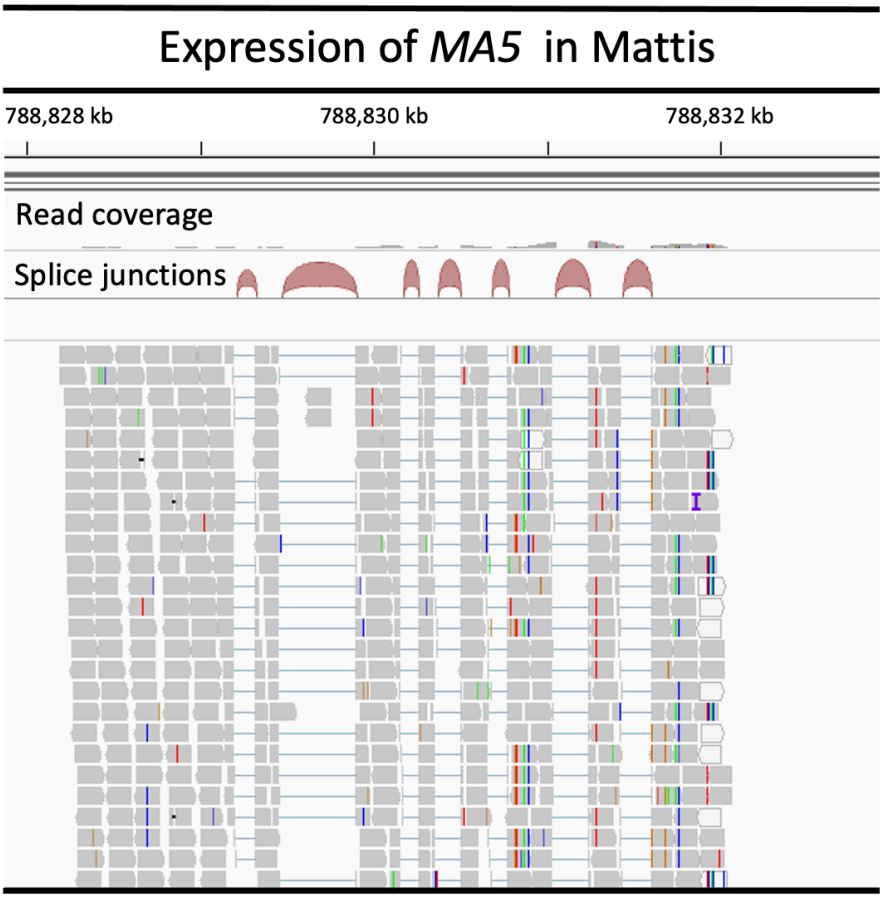

Figure 42: Expression profile of *MA5* for the Mattis RNAseq data mapped to Mattis. Red arches within the 'Splice junctions' track show predicted intron/exon boundaries on the forward strand.

MA6 had good read coverage in both datasets, consisting of six exons with consistent intron/exon boundaries (**Figure 43A**). MA7 showed very high coverage in both datasets with three clearly defined exons. Coverage exceeded the default maximum coverage of 100 reads so was down-sampled, illustrated with black rectangles below the 'Splice junctions' track (**Figure 43B**).

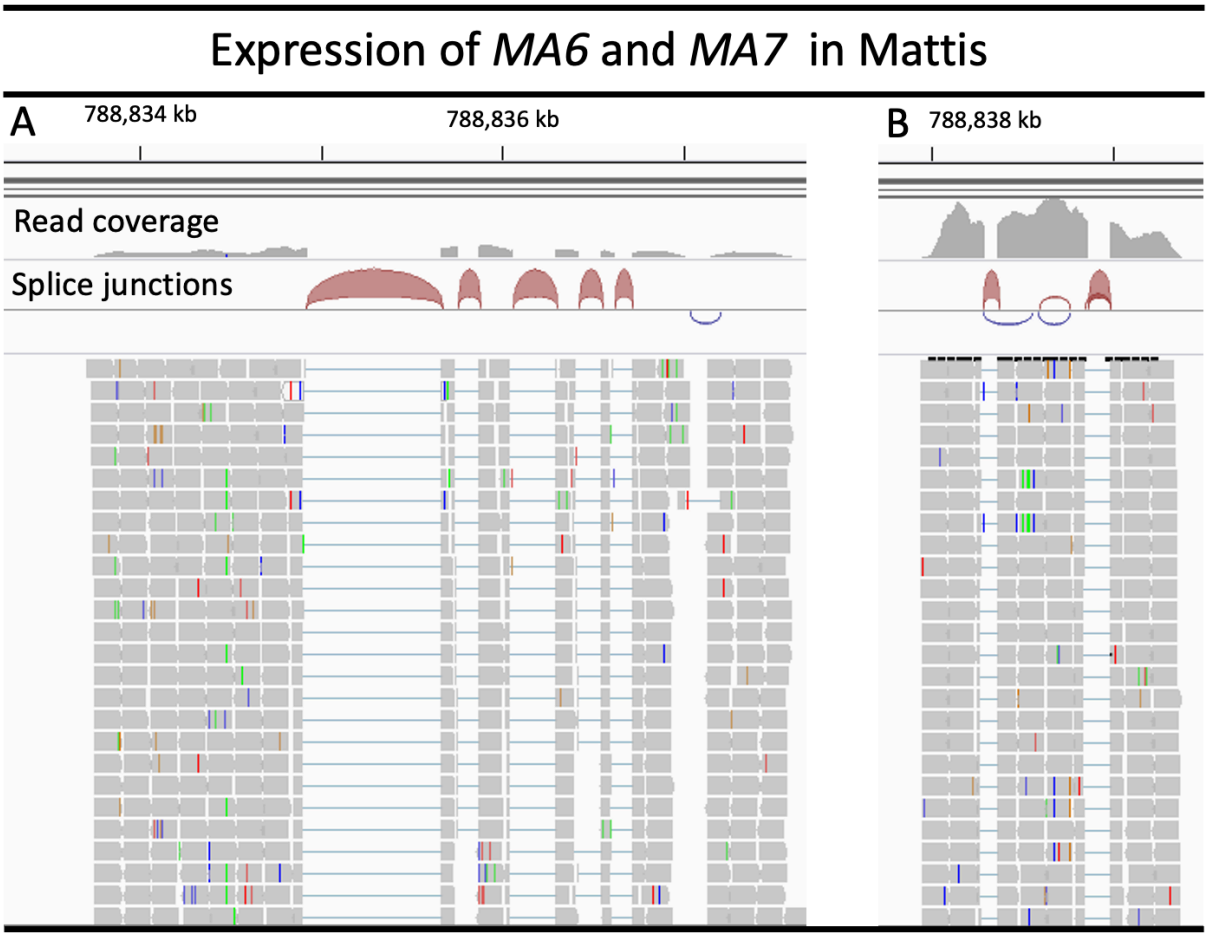

Figure 43: Representative expression profiles of (**A**) *MA6* (**B**) *MA7* for the Mattis RNAseq data mapped to Mattis. Red and blue arches within the 'Splice junctions' track show predicted intron/exon boundaries on the forward and reverse strand respectively. Black rectangles below the 'Splice junctions' track indicate regions where read covered exceeded 100 reads and so was down-sampled.

MA8 also showed very high coverage that was down-sampled in both datasets, with two Exons (**Figure 44A**). The nucleotide sequence for *MA8* was assessed using the NCBI Conserved Domain predictor to determine whether the expression was genuine however no domains were identified (Marchler-Bauer and Bryant 2004; Marchler-Bauer et al. 2010)**.**

NLR2 showed very poor coverage, potentially with three exons (**Figure 44B**). As NLRs are often poorly or transiently expressed (Steuernagel 2020), poor expression wasn't sufficient to discount *NLR2* as a *R* gene candidate.

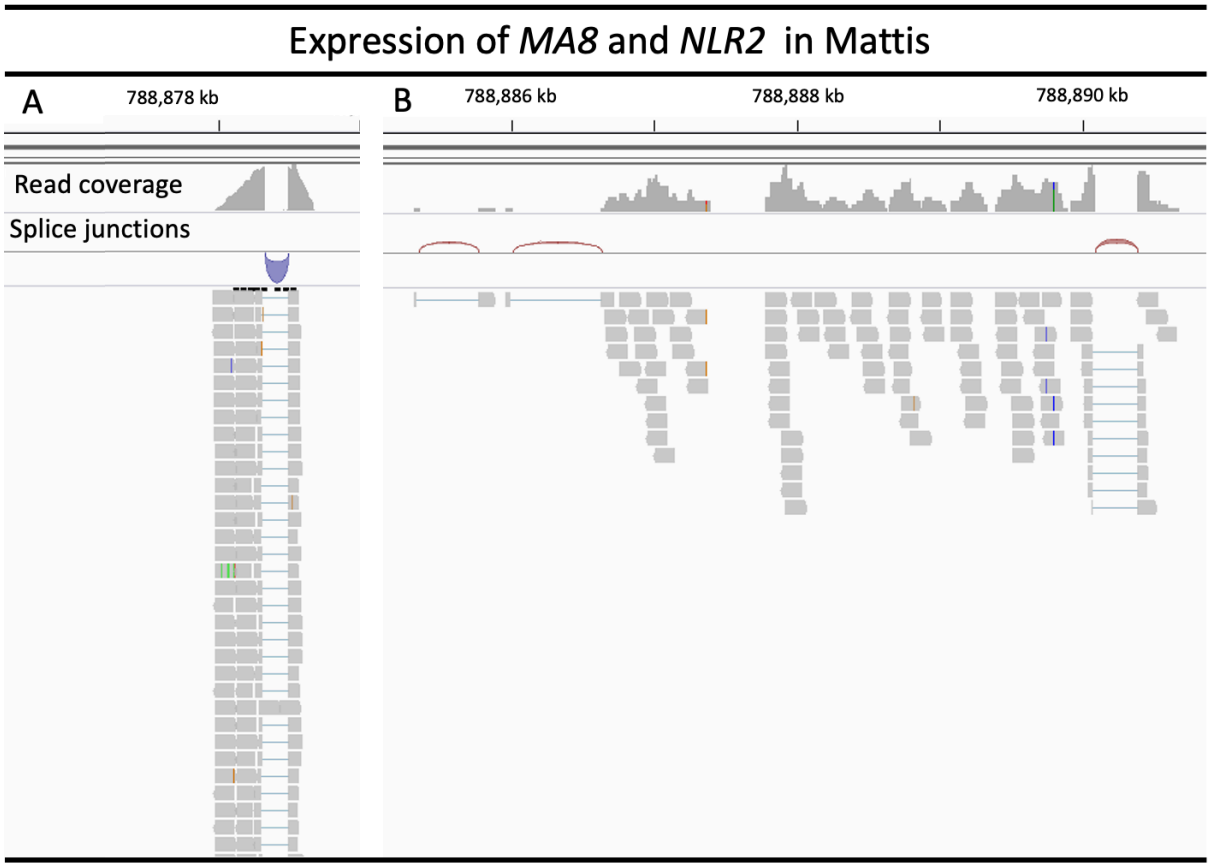

Figure 44: Representative expression profiles of (**A**) *MA8* (**B**) *NLR2* for the Mattis RNAseq data mapped to Mattis. Red and blue arches within the 'Splice junctions' track show predicted intron/exon boundaries on the forward and reverse strand respectively. Black rectangles below the 'Splice junctions' track indicate regions where read covered exceeded 100 reads and so was down-sampled.

To determine if the alternate splicing of *MA4* resulted in kinases with a different domain structure, the ORF of both transcripts was run through the NCBI domain predicter using default parameters for a standard output (Marchler-Bauer and Bryant 2004; Marchler-Bauer et al. 2010). A specific hit is the highest scoring hit for a given domain and infers that the query sequence has been assigned to the same protein family as the sequences used to create the domain model, with very high confidence. Non-specific hits are additional hits that are equal to or exceed the default threshold for statistical significance, 0.01. A superfamily is a cluster of conserved domain models that generate overlapping annotations on the same protein sequence to which specific and/or non-specific hits belong. Members of the same superfamily are assumed to represent evolutionarily related domains. Indeed, the two transcripts differed at the C-terminus. The 5' shared portion of the transcripts contained hits from three superfamiles; Protein Kinases catalytic_like (PKc_like) family, serine/threonine kinase with penicillin-binding protein and serine/threonine kinase associated domain (PknB_PASTA_kin) family and a provisional mitogen-activated protein kinase kinase (PLN00034) family (**Figure 45**). There were two specific hits: Serine/Threonine protein kinase catalytic domain (S_TKc) and Serine/threonine protein kinase domain (SPS1), both within the PKc_like superfamily. There were also two nonspecific domains hits within the PKc_like superfamily: Catalytic domain of the Serine/Threonine kinases, Interleukin-1 Receptor Associated Kinases (STKc_IRAK) and Protein tyrosine kinase (Pkinase_Tyr) domains. PknB_PASTA_kin and PLN00034 superfamilies both had a single non-specific hit. Transcript 'one' had a protein kinase C conserved region (C2) at the C terminus, with a non-specific hit for a 'C2 domain third repeat found in multiple C2 domain and transmembrane region proteins' (C2C_MCTP_PRT_plant) domain. Transcript 'two' had a similar C2 domain downstream of the STK domain, with a non-specific hit for a 'C2 domain fourth repeat found in multiple C2 domain and transmembrane region proteins' (C2D_MCTP_PRT_plant) domain. Interestingly transcript 'two' had an additional domain at the C terminus for a 'plant phosphoribosyltransferase C-terminal' domain (PRT_C).

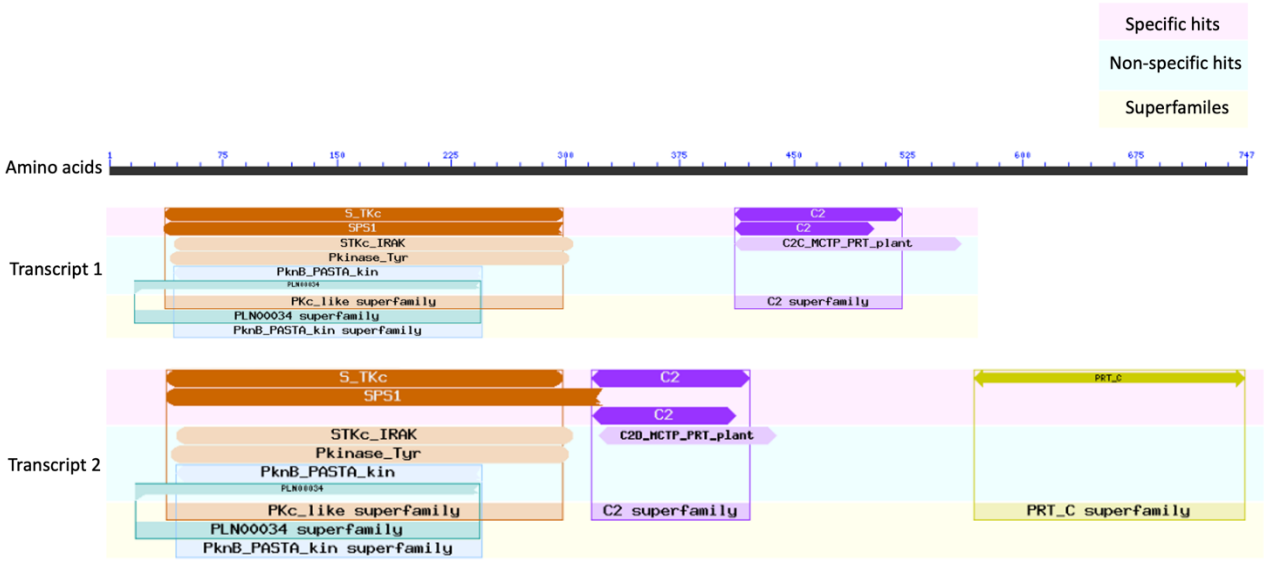

Figure 45: Domain structure of the two transcripts of MA4. Both transcripts have identical predicted domains at the N terminus: PKc_like = Protein Kinases catalytic_like family, PknB_PASTA_kin = serine/threonine kinase with penicillin-binding protein and serine/threonine kinase associated domain family, PLN00034 = provisional mitogen-activated protein kinase kinase family. S_TKc = Serine/Threonine protein kinase catalytic domain, SPS1 = Serine/threonine protein kinase domain, STKc_IRAK = Catalytic domain of the Serine/Threonine kinases, Interleukin-1 Receptor Associated Kinases and Pkinase_Tyr = Protein tyrosine kinase domain. Transcript one has a protein kinase C conserved region (C2) at the C terminus, with a non-specific hit for a 'C2 domain third repeat found in multiple C2 domain and transmembrane region proteins' (C2C_MCTP_PRT_plant) domain. Transcript two has a similar C2 domain downstream of the STK domain, with a non-specific hit for a 'C2 domain fourth repeat found in multiple C2 domain and transmembrane region proteins' (C2D_MCTP_PRT_plant) domain. Transcript two had an additional domain at the C terminus: PRT_C = plant phosphoribosyltransferase C-terminal domain.

5.3.4 Polymorphism analysis

Within the accessions included in the IBSpy haplotype analysis, there were five accessions that contained the 2A IBSpy haplotype but that were susceptible to both NO6047+*Avr-Rmg8* and SRA at 6 dpi (WATDE0048, WATDE0527, WATDE0568, WATDE0592 and WATDE0786). The nucleotide and aa sequences of the candidate genes were examined to identify polymorphisms that could explain the phenotype of the five susceptible accessions that contained the 2A IBSpy haplotype. Alignments from 10 of the adapted wheat varieties and 29 Watkins accessions were generated using the whole genome sequencing data generated as part of the 'WatSeq' project (unpublished), using Mattis as the reference assembly (courtesy of Jesus Quiroz Chavez, JIC). Accessions were sequenced to an average depth of 13X coverage. The alignment files were viewed using IGV (Robinson et al. 2011) (**Tables 33 and 34**).

The Mattis RNAseq data was re-examined to find the ORF of *MA4* (**Table 32**). Five polymorphisms were identified. Exons 1 and 3 both contained a single non-synonymous polymorphism, at aa residue 50 (alanine to glutamine (A50E)) and 205 (glutamine to lysine (E205K)) respectively. Exon 6A contained two non-synonymous polymorphisms at residues 446 (tryptophan to a stop codon (W446X)) and (alanine to glycine (A713G)) respectively. Exon 6A also contained a single synonymous polymorphism at aa residue 697 (valine to valine (V697V)). The A50E polymorphism was present in WATDE0048 and WATDE0527 whilst the W446X polymorphism was present in WATDE0568 and WATDE0592. If these polymorphisms resulted in altered protein function then they could explain the susceptibility in four of the five accessions that have the IBSpy 2A haplotype but are susceptible to both isolates. The A50E and W446X polymorphisms were designated as critical 'SNP 1' and 'SNP 9' respectively. There was no coverage for the last 11 aa residues for the WATDE0786 allele of *MA4*. Additional sequencing confirmed that WATDE0786 contained the A713G SNP.

Very little polymorphism was identified for the remaining genes in the interval and a number were monomorphic between resistant and susceptible accessions. The intron/exon structure for the remaining genes was determined from the gene annotation predictions. *NLR2* had poor read coverage so the intron/exon boundaries were unclear. Alignments for *MA6*, *NLR1 and MA8* showed no polymorphisms. There was no sequence coverage for approximately the last 300 nucleotides of *MA8* for WATDE0477, WATDE0566 and WATDE0804. *MA5*, *MA7* and *NLR2* had only two, one and three polymorphisms respectively, none of which related the differences in phenotype (**Table 34**). Of the five susceptible accessions with the resistant 2A haplotype, there was only one polymorphism outside of those found in *MA4*, (in WATDE0786 for *NLR2*). Combined, the observations from the polymorphism analysis made *MA4* the best candidate gene for the 2A resistance. The presence of a

potentially ‘critical’ SNP in each transcript indicated that both transcripts were required for resistance and that there was an allelic series for *MA4*.

Table 33: Polymorphisms present in the ORF of *MA4* for all adapted wheat varieties and Watkins accessions with sequence alignments. Claire and Mattis were also included. Sequences were mapped to Mattis. Scores were taken at 6 dpi unless stated otherwise.

			EXON 1			EXON 3			EXON 6A								
	Phenotype		A50E			E205K			W446X			V697V			A713G		
Cultivar	NO6047+ *Avr-Rmg8*	SRA	ala - glu			glu - lys			trp - STOP			val - val			ala - gly		
			G	C	A	G	A	A	T	G	G	G	T	C	G	C	C
Ability	2.33	1.00	-	-	-	-	-	-	-	-	-	-	-	G	-	G	-
Claire	1.20	1.20	-	-	-	-	-	-	-	-	-	-	-	G	-	G	-
Epson	1.20	0.00	-	-	-	-	-	-	-	-	-	-	-		-		-
Flame	2.33	1.00	-	-	-	-	-	-	-	-	-	-	-	G	-	G	-
Malacca	3.33	2.00	-	-	-	-	-	-	-	-	-	-	-	G	-	G	-
Renan	2.00	0.80	-	-	-	-	-	-	-	-	-	-	-		-		-
Revelation	1.40	1.20	-	-	-	-	-	-	-	-	-	-	-	G	-	G	-
Riband	3.00	1.67	-	-	-	-	-	-	-	-	-	-	-	G	-	G	-
Shango	2.33	1.67	-	-	-	-	-	-	-	-	-	-	-	G	-	G	-
Spark	0.67	1.33	-	-	-	-	-	-	-	-	-	-	-	G	-	G	-
Mattis	1.80	1.20	-	-	-	-	-	-	-	-	-	-	-	-	-	-	-
Wasp	2.00	1.00	-	-	-	-	-	-	-	-	-	-	-	G	-	G	-
WATDE0048	4.60	5.60	-	A	-	A	-	-	-	-	-	-	-	-	-	-	-
WATDE0102	2.60	2.20	-	-	-	-	-	-	-	-	-	-	-	G	-	G	-
WATDE0171	1.80	0.80	-	-	-	-	-	-	-	-	-	-	-	G	-	G	-
WATDE0310	1.20	0.80	-	-	-	-	-	-	-	-	-	-	-	G	-	G	-
WATDE0369*	3.00	1.30	-	-	-	A	-	-	-	-	-	-	-	-	-	-	-
WATDE0426**		1.00	-	-	-	A	-	-	-	-	-	-	-	-	-	-	-
WATDE0427*	1.00	0.00	-	-	-	A	-	-	-	-	-	-	-	-	-	-	-
WATDE0428**		1.00	-	-	-	A	-	-	-	-	-	-	-	-	-	-	-
WATDE0465**		1.20	-	-	-	A	-	-	-	-	-	-	-	-	-	-	-
WATDE0477*	0.00	0.00	-	-	-	A	-	-	-	-	-	-	-	-	-	-	-
WATDE0505**		1.20	-	-	-	A	-	-	-	-	-	-	-	-	-	-	-
WATDE0527	4.60	5.80	-	A	-	-	-	-	-	-	-	-	-	-	-	-	-
WATDE0541**		0.80	-	-	-	A	-	-	-	-	-	-	-	-	-	-	-
WATDE0546**		1.20	-	-	-	A	-	-	-	-	-	-	-	-	-	-	-
WATDE0566	1.60	2.20	-	-	-	A	-	-	-	-	-	-	-	-	-	-	-
WATDE0567**		1.20	-	-	-	A	-	-	-	-	-	-	-	-	-	-	-
WATDE0568	5.60	5.80	-	-	-	A	-	-	-	A	-	-	-	-	-	-	-
WATDE0571	1.80	1.00	-	-	-	A	-	-	-	-	-	-	-	-	-	-	-
WATDE0592	4.60	5.60	-	-	-	A	-	-	-	A	-	-	-	-	-	-	-
WATDE0672**		1.20	-	-	-	A	-	-	-	-	-	-	-	-	-	-	-
WATDE0687**		0.80	-	-	-	A	-	-	-	-	-	-	-	-	-	-	-
WATDE0786	3.60	6.00	-	-	-	-	-	-	-	-	-	-	-	G	-	G	-
WATDE0804	0.80	1.80	-	-	-	A	-	-	-	-	-	-	-	-	-	-	-
WATDE0970**		1.00	-	-	-	A	-	-	-	-	-	-	-	-	-	-	-
WATDE0971*	0.67	0.00	-	-	-	A	-	-	-	-	-	-	-	-	-	-	-
WATDE0973*	0.33	0.30	-	-	-	A	-	-	-	-	-	-	-	-	-	-	-
WATDE0974**		1.00	-	-	-	A	-	-	-	-	-	-	-	-	-	-	-
WATDE1062**		1.20	-	-	-	A	-	-	-	-	-	-	-	-	-	-	-

* = scores taken from original Watkins core DLAs (5 dpi)

** = scores taken from Watkins validation DLA (5 dpi, **Section 4.3.3.3**)

Table 34: Polymorphisms present in all adapted wheat varieties and Watkins accessions with sequence alignments for *MA5*, *MA6*, *MA7*, *NLR1, MA8* and *NLR2*. Claire and Mattis were also included. Sequences were mapped to Mattis. Scores were taken at 6 dpi unless stated otherwise.

			MA5			*MA_7*			*NLR2*		
Cultivar	***NO6047+ Avr-Rmg8***	**SRA**	**Exon 1 788,828,724**	**Exon 5 788,830,642**	***MA6***	**Exon 1 788,838,013**	***NLR1***	***MA8***	**788,888,585**	**788,889,012**	**788,890,436**
Ability	2.33	1.00								T	
Claire	1.20	1.20								T	
Epson	1.20	0.00									
Extase										T	
Cordiale											
Grafton										T	
Flame	2.33	1.00								T	
Malacca	3.33	2.00								T	
Renan	2.00	0.80									
Revelation	1.40	1.20								T	
Riband	3.00	1.67								T	
Shango	2.33	1.67								T	
Spark	0.67	1.33								T	
Mattis	1.80	1.20									
timopheevii33255											
Wasp	2.00	1.00								T	
WATDE0048	4.60	5.60									
WATDE0102	2.60	2.20								T	
WATDE0171	1.80	0.80								T	
WATDE0310	1.20	0.80								T	
WATDE0369	3.00	1.30									
WATDE0426		1.00							T		
WATDE0427	1.00	0.00							T		
WATDE0428		1.00							T		
WATDE0465		1.20									
WATDE0477	0.00	0.00		A		G					
WATDE0505		1.20									
WATDE0527	4.60	5.80									
WATDE0541		0.80									
WATDE0546		1.20									
WATDE0566	1.60	2.20				G					
WATDE0567		1.20									
WATDE0568	5.60	5.80									
WATDE0571	1.80	1.00									
WATDE0592	4.60	5.60									
WATDE0672		1.20	T								
WATDE0687		0.80	T								
WATDE0786	3.60	6.00								T	
WATDE0804	0.80	1.80				G					
WATDE0970		1.00									
WATDE0971	0.67	0.00									
WATDE0973	0.33	0.30									A
WATDE0974		1.00									A
WATDE1062		1.20									

* = scores taken from original Watkins core DLAs (5 dpi)

** = scores taken from Watkins validation DLA (5 dpi **Section 4.3.3.3**)

5.3.5 *MA4* is equivalent to the powdery mildew gene *Pm4*

BLAST analysis of the *MA4* protein sequence revealed that *MA4* is identical to the previously isolated race specific *Bgt* resistance gene *Pm4* (Sánchez-Martín et al. 2021). *Pm4* was introgressed from the tetraploid Persian wheat *T. carthlicum* (McIntosh and Bennett 1979), which originated from a cross between emmer and hexaploid wheat (Matsuoka 2011; De Oliveira et al. 2020). Sánchez-Martín et al. also established that *Pm4* has alternate splicing, producing 'isoforms' *Pm4b*-V1 and *Pm4b*-V2 (2021). *Pm4b*-V1 and *Pm4b*-V2 produce proteins of 560 and 747 aa respectively and correspond to *MA4* transcripts 'one' and 'two'. Given this finding, *MA4* will be referred to as *Pm4* from this point onwards. Eight different alleles for *Pm4* have been reported: *Pm4a* (Briggle 1966), *Pm4b* (McIntosh and Bennett 1979), *Pm4c* (Hao et al. 2008), *Pm4d* (introgressed from *T. monococum* (Schmolke et al. 2012), *Pm4e* (Li, Jia, et al. 2017), *Pm4f, Pm4g and Pm4h* (Sánchez-Martín et al. 2021), forming an allelic series (**Table 35**). The two alleles containing the critical SNPs (SNP1 and SNP9) within *Pm4* identified within this study have not been reported previously. Both occur within the *Pm4f* background and so were designated *Pm4f+SNP1* and *Pm4f+SNP9*. Only a handful of SNPs distinguish the different alleles (**Table 36**) (Sánchez-Martín et al. 2021; Yao et al. 2022)(O'Hara et al. unpublished).

The *Pm4a* and *Pm4b* alleles have been introgressed into the susceptible Australian spring wheat cultivar Federation to produce near-isogenic lines, *Fed-Pm4a* and *Fed-Pm4b*. To generate the *Pm4a*-NIL, *Pm4a* was transferred from the emmer wheat variety Khapi into the hexaploid wheat Chancellor, and then into Federation (Briggle 1966) (**Table 24**). The *Pm4b*-NIL was created by transferring *Pm4b* from *T. carthlicum* into the *T. turgidum* accession W804, and then into Federation (McIntosh and Bennett 1979).

Eighteen *pm4b* loss of function mutants were generated through EMS mutagenesis in the *Fed-Pm4b* NIL background (Sánchez-Martín et al. 2021). Mutations in either of the mutually exclusive last exons of *Pm4b*-V1 and *Pm4b*-V2 resulted in a loss of resistance suggesting that both transcripts were required for function. Overexpression transgenic lines were produced in the susceptible Bobwhite S26 background to functionally validate that *Pm4b* was sufficient to provide *Bgt* resistance (Sánchez-Martín et al. 2021). Full cDNA sequences for either one, or both transcripts were transformed into Bobwhite S26 via a particle bombardment approach. Lines with both transcripts gained *Bgt* resistance and maintained the race specificity observed in *Fed-Pm4b* (Sánchez-Martín et al. 2021).

Table 35: Published alleles for *Pm4.*

***Pm4* allele**	**Origins**	
	Introgression	**Reference**
a	*T. dicoccum*	(Briggle 1966)
b	*T. carthlicum*	(McIntosh and Bennett 1979)
c	-	(Hao et al. 2008)
d	*T. monococum*	(Schmolke et al. 2012)
e	-	(Li, Jia, et al. 2017)
f	-	(Sánchez-Martín et al. 2021)
g	-	
h	-	

Table 36: Amino acid changes determining the *Pm4* allelic series. '?' indicates amino acids that have not been determined.

Allele	Pm4 Protein								
	Pm4_V1					Pm4_V2			
	S_TKc-domain				Spacer	Spacer			TMD2
	50	126	205	208	395	446	529	686	713
*Pm4a**	A	E	K	W	T	W	L	V	A
Pm4b	A	E	E	L	T	W	L	V	G
*Pm4c**	A	?	E	L	T	?	?	?	G
Pm4d	A	E	E	L	T	W	L	V	A
*Pm4e**	A	?	E	L	T	?	?	?	A
*Pm4f***	A	E	K	L	T	W	L	V	A
*Pm4g***	A	K	K	L	T	W	V	A	A
*Pm4h***	A	E	K	L	A	W	A	V	A
Pm4f+SNP1	E	E	K	L	T	W	L	V	A
Pm4f+SNP9	A	E	K	L	T	X	L	V	A

* genotype determined by (Sánchez-Martín et al. 2021)

** genotype determined by (Yoa et al. 2022)

5.3.6 Confirming recognition of *Avr-Rmg8* by *Pm4*

To validate the recognition of *Avr-Rmg8* by *Pm4,* a DLA was performed using a selection of the materials generated by the Keller group using both NO6047+*Avr-Rmg8* and SRA isolates (**Table 25 and Figure 46**). Eight EMS mutants in *Fed-Pm4b* NIL background were tested to confirm loss of resistance and two independently generated *Pm4b* transgenic lines (T3 generation) in the susceptible Bobwhite S26 background, NR#3 and NR#52, were tested to confirm gain of resistance by overexpression of *Pm4b*. Sister lines originating from the same T0 as the transgenics but that had lost the transgene through segregation were included, S#3 and S#52, along with Bobwhite S26 as susceptible controls. EMS mutations were all within the S_TKc domain of *Pm4b*-V1. *Fed-Pm4a* and *Fed-Pm4b* NILs were also tested alongside the Federation background. All lines phenotyped as expected were *Pm4* to be recognising *Avr-Rmg8*. *Fed-Pm4a* and *Fed-Pm4b* NILs were both resistant to both isolates confirming that *Pm4a* and *Pm4b* both recognise *Avr-Rmg8* (**Figure 46B**). The eight EMS mutants were all susceptible to both isolates, confirming that *Pm4* is required for resistance **Figure 46C**). NR#3 and NR#52 overexpression lines were both resistant and the sister lines S#3 and S#52 were both susceptible to both isolates, validating that *Pm4* is required for function **Figure 46A**). These results confirm that *Pm4* recognises *Avr-Rmg8* and that the causal gene within the 2A resistant interval is *Pm4*.

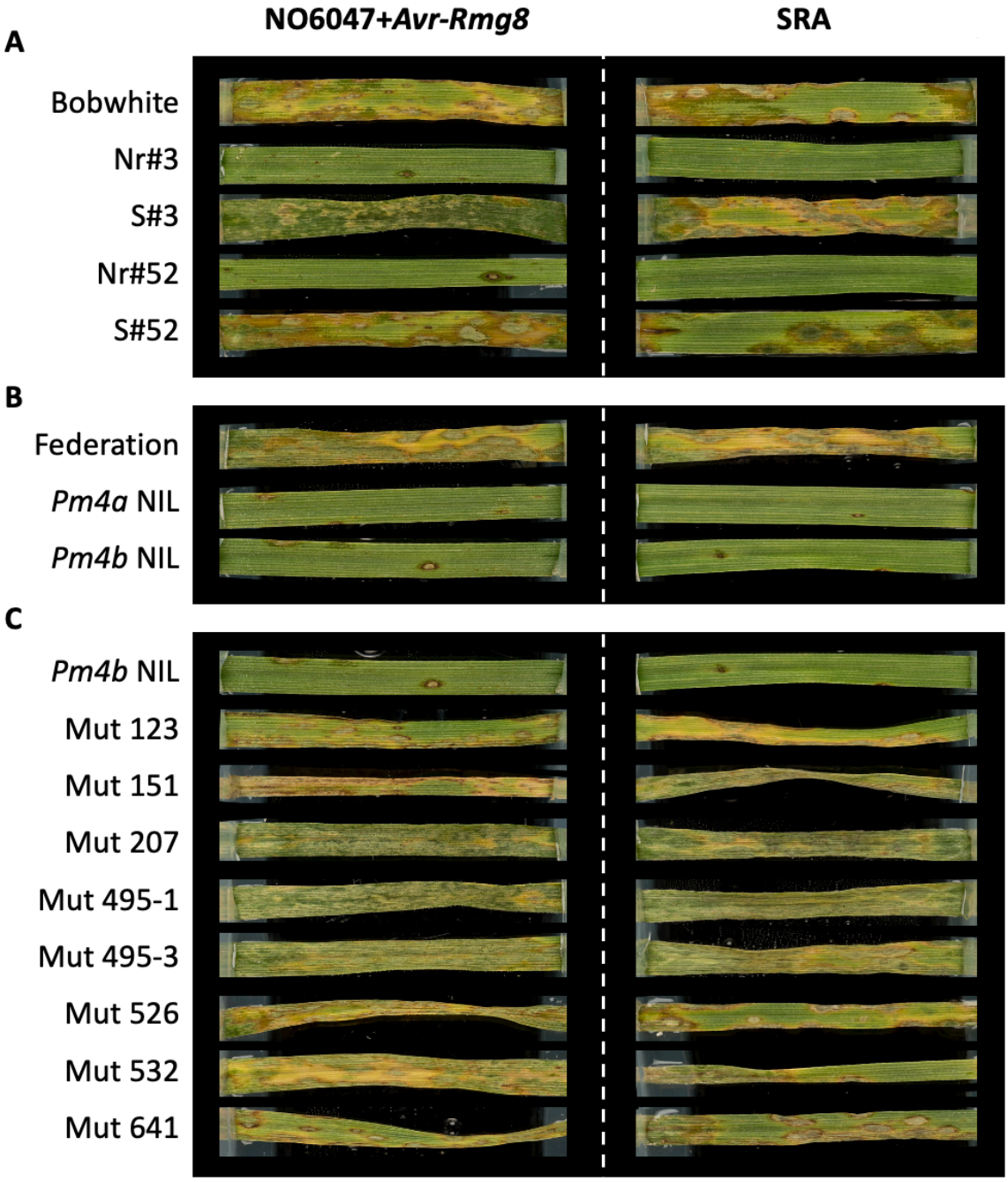

Figure 46: Detached leaf assay to validate the recognition of *Avr-Rmg8* by *Pm4*, using NO6047+*Avr-Rmg8* and SRA. (**A**) *Pm4b* overexpression lines in the susceptible Bobwhite background. 'Nr#' = transgenics, 'S#' = sister lines originating from the same T0 as the transgenics but that had lost the transgene through segregation. (**B**) *Fed-Pm4a* and *Fed-Pm4b* NILs, in the Federation background. (**C**) *Pm4b* EMS mutants in the *Fed-Pm4b* NIL background. All mutations were within the S_TKc domain of *Pm4b*-V1. Images were taken at six dpi.

5.3.7 Do different *Pm4* alleles result in different responses to *Avr-Rmg8 eI*?

The published *Pm4* alleles provide race-specific resistance to *Bgt* isolates (Sánchez-Martín et al. 2021; Yao et al. 2022). Plant material tested within this study contained alleles *Pm4b, Pm4d* and *Pm4f*, in addition to the novel alleles *Pm4f+SNP1* and *Pm4f+SNP1* (**Table 36**). The adapted wheat varieties carried either *Pm4b* or *Pm4d*. The Watkins lines predominantly carried *Pm4f* with no instances of *Pm4d*.

To establish if *Pm4b, Pm4d, Pm4f, Pm4f+SNP1* and *Pm4f+SNP1* give different responses to the *Avr-Rmg8* eI allele a DSA was performed with SRA on a selection of representative lines, as described in **Section 2.4** (**Table 25**). NO6047 carries the eII allele therefore the NO6047+*Avr-Rmg8* isolate produces both eI and eII effectors and was not used for this part of the study. Spikes were scored at 5 dpi and compared to detached leaf images from a previous SRA assay, also taken at 5 dpi (**Section 4.3.3.3**) (**Figure 47**). *Pm4b, Pm4d, Pm4f* carriers were all highly resistant at the leaf stage, however *Pm4b* carriers WATDE0102 and WATDE0310 were susceptible at the spike stage which suggested that *Pm4b* provides leaf specific resistance. *Pm4d* carriers Mattis and Stanley, and *Pm4f* carriers WATDE0426 and WATDE0541 were all resistant in the spikes. Mattis and Stanley both carry the 2NS translocation which gives head specific resistance to *MoT* so it is unclear whether the resistance observed is due to *Pm4d* (Cruz et al. 2016; Walkowiak et al. 2020). WATDE0527 (*Pm4f+SNP1*) and WATDE0568/WATDE0592 (*Pm4f+SNP9*) were all susceptible in both tissues.

Table 37: *Pm4* alleles present in the materials phenotyped within this study and their scores from DLAs with isolates NO6047, NO6047+*Avr-Rmg8* and SRA.

Line	*Pm4* allele	DLA		
		NO6047 (4 dpi)	NO6047+*Avr-Rmg8* (6 dpi)	SRA (6 dpi)
Ability	B		2.33	1.00
Claire		1.80	1.20	1.20
Flame			2.33	1.00
Malacca			3.33	2.00
Revelation			1.40	1.20
Riband			3.00	1.67
Shango			2.33	1.67
Spark			0.67	1.33
Wasp			2.00	1.00
WATDE0102		4.00	2.60	2.20
WATDE0171		3.00	1.80	0.80
WATDE0310		3.20	1.20	0.80
WATDE0786			3.60	6.00
Epson	D		1.20	0.00
Renan		3.40	2.00	0.80
Mattis		3.80	1.80	1.20
WATDE0369*	F	2.80	3.00	1.30
WATDE0426**				1.00
WATDE0427*		1.80	1.00	0.00
WATDE0477*		2.00	0.00	0.00
WATDE0566			1.60	2.20
WATDE0571**		2.00	1.80	1.00
WATDE0804			0.80	1.80
WATDE0971*			0.67	0.00
WATDE0973**			0.33	0.30
WATDE0048	F + SNP1	4.20	4.60	5.60
WATDE0527		4.60	4.60	5.80
WATDE0568	F + SNP9	2.20	5.60	5.80
WATDE0592		4.20	4.60	5.60
WATDE0015	X		4.40	5.20
WATDE0056			5.80	5.80
WATDE0720			5.00	5.80

* = NO6047+*Avr-Rmg8* and SRA scores taken from original Watkins core DLAs (5 dpi)

** = NO6047+*Avr-Rmg8* and SRA scores taken from Watkins validation DLA (5 dpi, **Section 4.3.3.3**)

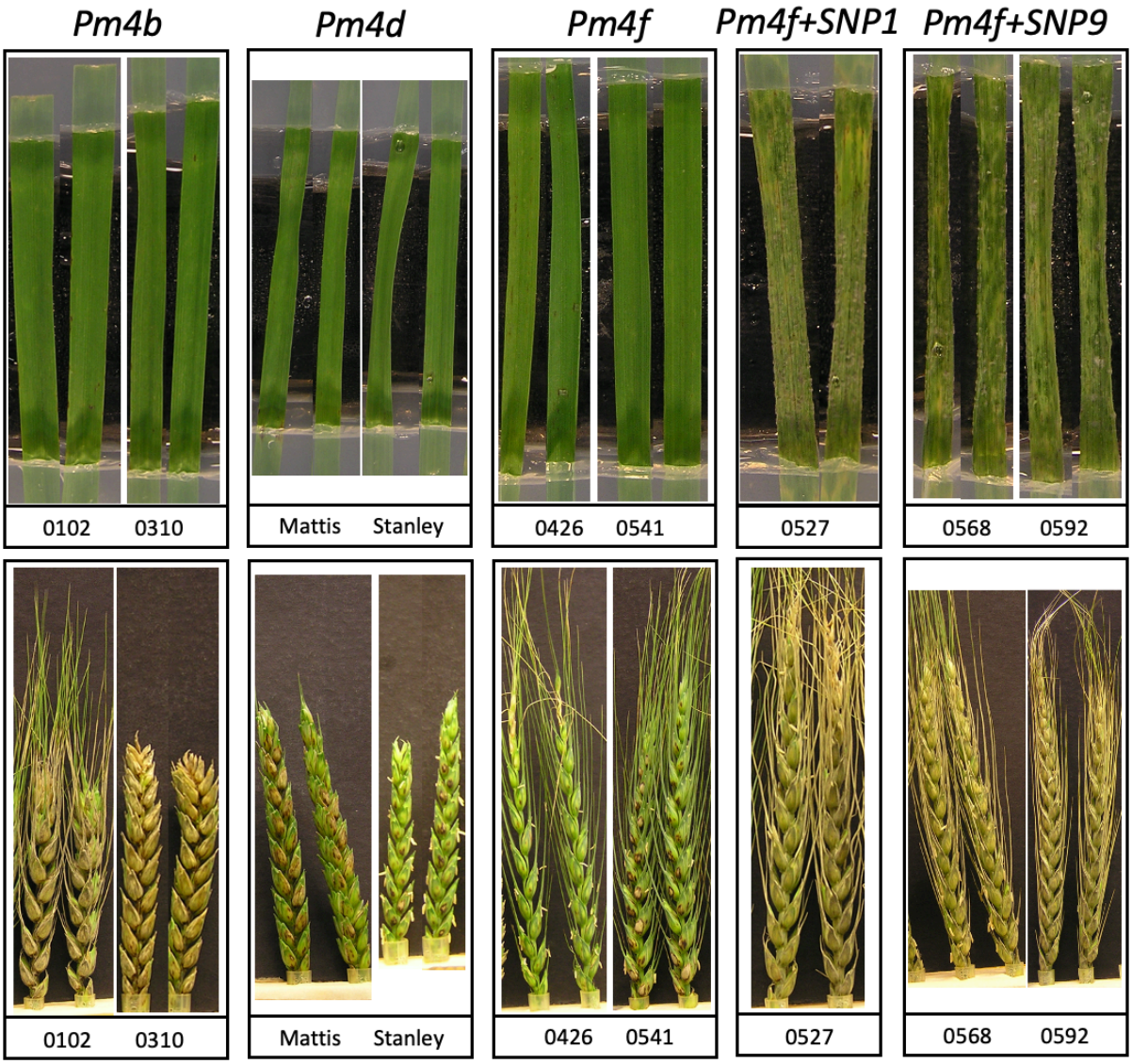

Figure 47: Representative leaves and spikes for the different *Pm4* alleles tested within this study, inoculated with SRA at 22°C. All accessions with numerical codes are Watkins lines that start 'WATDE'. Images were taken at 5 dpi.

5.3.8 Do different *Pm4* alleles result in *Avr-Rmg8* eI resistance at high temperatures?

To establish whether *Pm4b, Pm4d, Pm4f, Pm4f+SNP1* and *Pm4f+SNP1* are effective against *Avr-Rmg8* eI at high temperatures (more comparable to field conditions) a DSA was performed with SRA on a selection of representative lines and incubated at 26°C (**Table 25**).

Spikes were scored at 5 dpi and compared to detached leaf images from a previous SRA assay incubated at 26°C, also taken at 5 dpi (**Section 4.3.3.4**) (**Figure 48**). The DLA was performed before *Pm4* was identified as the causal gene and so there were no *Pm4f+SNP9* carriers included. Additionally different *Pm4f* carriers were included in the DLA compared to the DSA (**Figure 48**).

Pm4b, Pm4d, Pm4f carriers were all resistant at the seedling stage at 26°C. *Pm4b* carriers (WATDE0102 and WATDE0310) and *Pm4f* carriers (WATDE0477 and WATDE0571) were susceptible at the spike stage at 26°C. *Pm4f* carriers were resistant at the spike stage at 22°C suggesting that this allele is tissue specific at 26°C. *Pm4d* carriers Mattis and Stanley were moderately resistant in the spikes. The *Pm4f+SNP1* carrier WATDE0048 was susceptible in both tissues. WATDE0568/WATDE0592 (*Pm4f+SNP9*) were both susceptible at the spike stage.

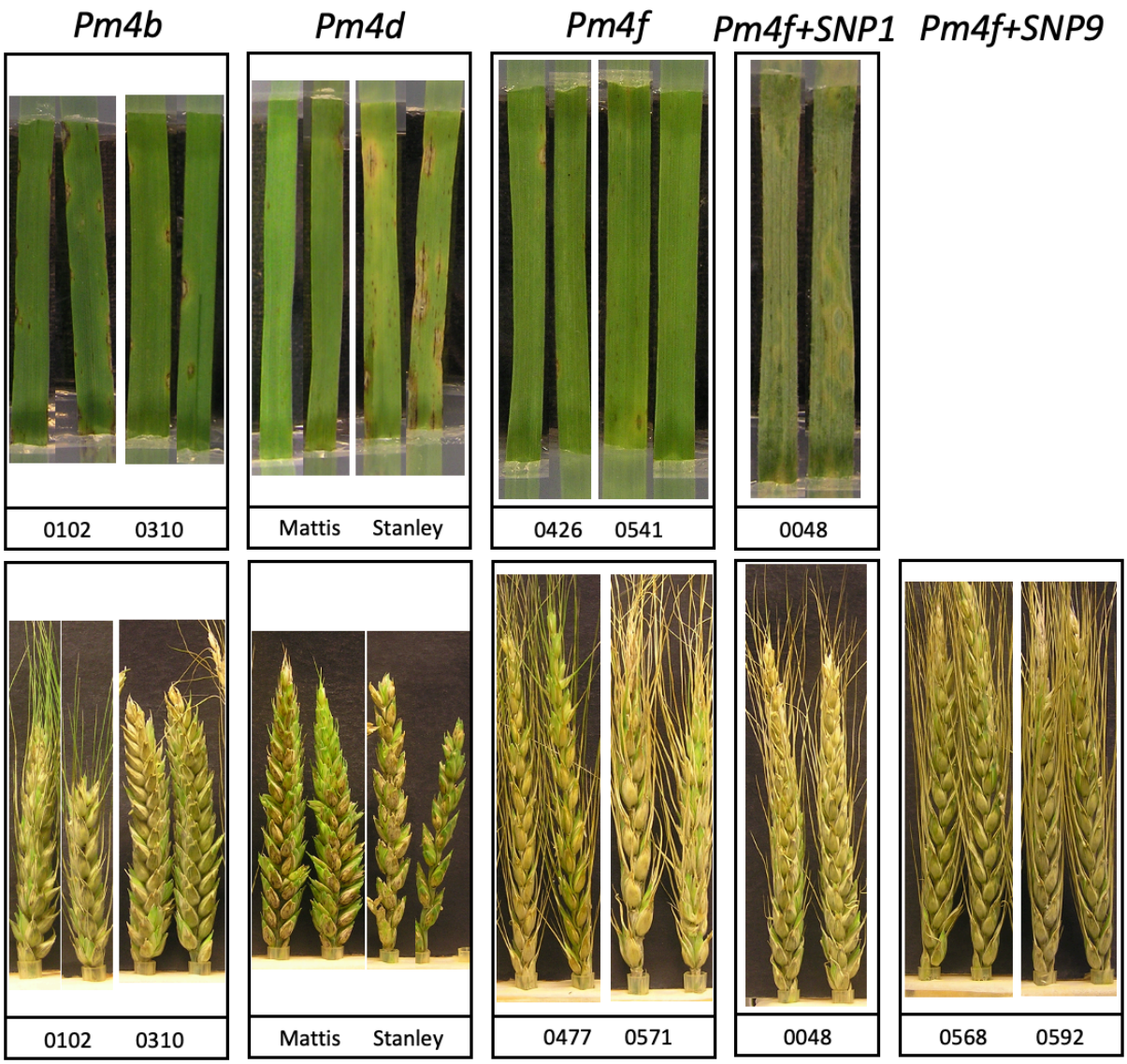

Figure 48: Representative leaves and spikes for the different *Pm4* alleles tested within this study, inoculated with SRA at 26°C. All accessions with numerical codes are Watkins lines that start 'WATDE'. Images were taken at 5 dpi.

5.3.9 Does *Pm4* recognise *Avr-Rmg8* eII?

To establish if any of the *Pm4* alleles recognise the *Avr-Rmg8* type eII effector, a selection of representative lines were phenotyped with NO6047 at the seedling leaf and spike stages (**Table 25**, **Figure 49**). Note the inoculum for the DSA had a low concentration of conidia at 0.07 x 10^6 conidia/ml. Different *Pm4f* carriers were included in the DLA compared to the DSA (**Figure 49**). *Pm4b* carriers Claire and WATDE0171 were resistant at the seedling stage however Claire was susceptible in a previous DLA (**Section 4.3.2.1** (**Figure 30**)). Claire showed some necrotic flecking in the spike but WATDE0171 was susceptible. *Pm4d* carriers Mattis and Renan had intermediate phenotypes at the seedling leaf stage. Mattis was highly resistant in the spikes however Renan had an intermediate phenotype with some necrotic flecking. Renan also has the 2NS translocation. *Pm4f* carriers were resistant at the seedling leaf stage (WATDE0427 and WATDE0571) and susceptible at the spike stage (WATDE0566 and WATDE0571). Both *Pm4f+SNP1* lines (WATDE0048 and WATDE0527) were susceptible at both tissue stages. The two *Pm4f+SNP9* carriers showed different phenotypes at the leaf stage (WATDE0568 = resistant, WATDE0592 = susceptible) but were both susceptible in the spikes. Images for all the detached spikes inoculated with NO6047 are shown in **Supplementary Fig. S4**.

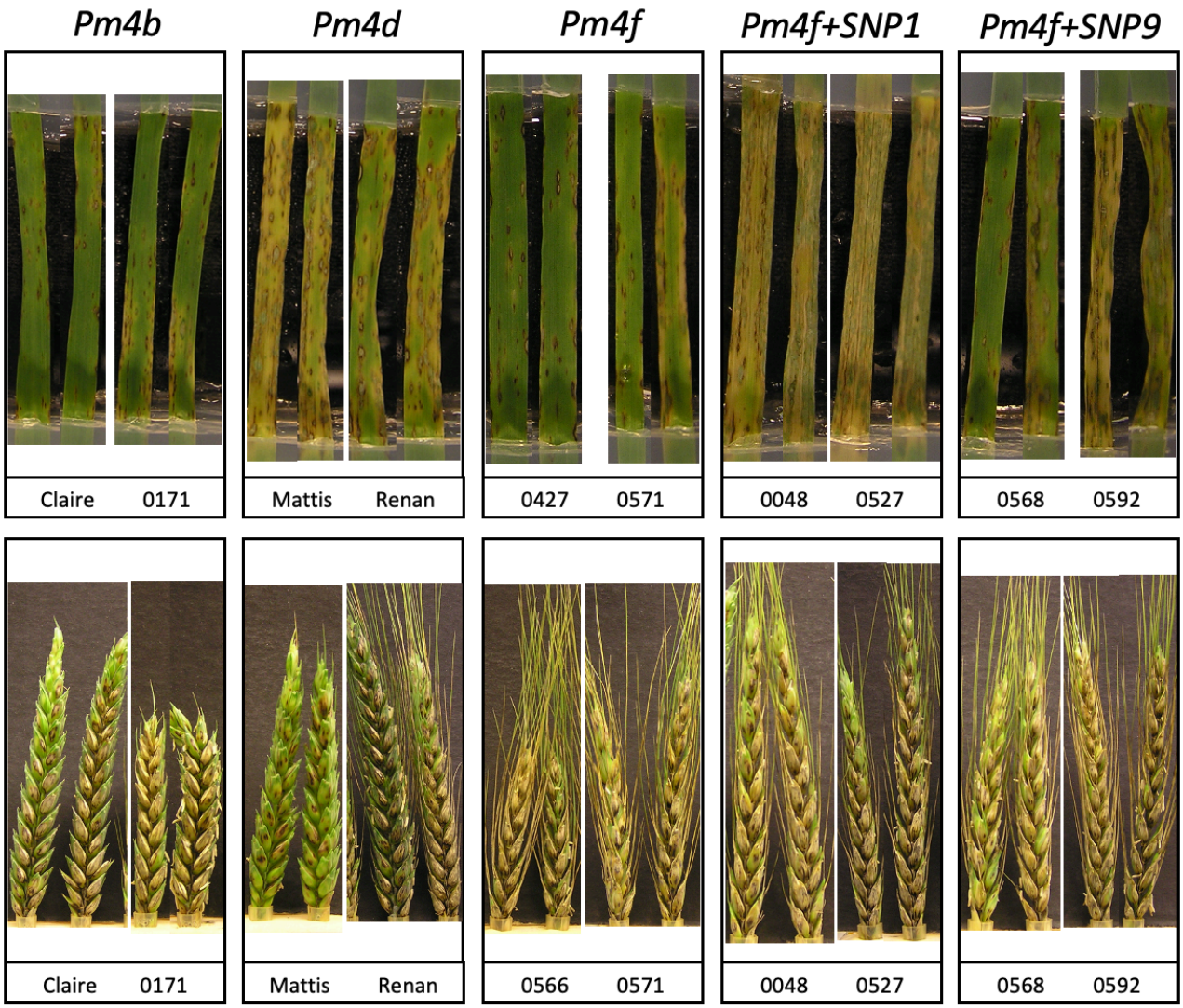

Figure 49: Representative leaves and spikes for the different *Pm4* alleles tested within this study, inoculated with NO6047. All accessions with numerical codes are Watkins lines that start 'WATDE'. Leaf and spike images were taken at 5 and 9 dpi respectively.

5.3.10 Does Pm4 provide resistance against the Bangladeshi isolate BTJ4P?

To establish if any of the *Pm4* alleles were effective against the Bangladeshi isolate BTJ4P, a DSA was performed (**Table 25**, **Figure 50**). *Pm4b* carriers WATDE0102 and WATDE0171 were susceptible. WATDE0310 carries the *Pm4b* allele and showed moderate resistance to BTJ4P, however this accession was susceptible to SRA at 22 °C in the spike, suggesting that there is additional resistance to BTJ4P present within WATDE0310 (**Supplementary Fig. S1**). *Pm4d* carriers Mattis and Stanley were both resistant to BJT4P. The *Pm4f* carriers WATDE0566 and WATDE0571 were both highly resistant to BTJ4P. WATDE0048/WATDE0527 (*Pm4f+SNP1*), WATDE0568/WATDE0592 (*Pm4f+SNP9*) were all susceptible. Images for all the detached spikes inoculated with BTJ4P are shown in **Supplementary Figs. S1-3**.

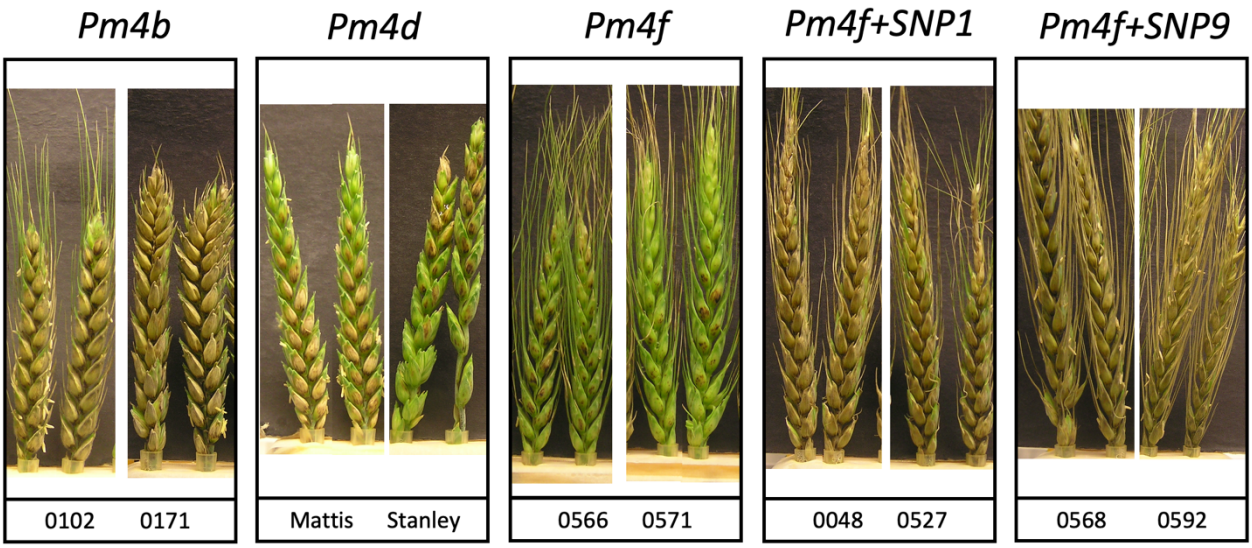

Figure 50: Representative spikes for the different *Pm4* alleles tested within this study, inoculated with the Bangladeshi isolate BTJ4P. All accessions with numerical codes are Watkins lines that start 'WATDE'. Images were taken at 6 dpi.

5.3.11 *Pm4* KASP assays

Three KASP primer sets were designed to enable discrimination of four *Pm4* haplotypes: *Pm4, pm4, Pm4f+SNP1* and *Pm4f+SNP9* (**Table 26**). The first primer set detects the presence/absence of *Pm4* (**Figure 51A**). Primers with the HEX™/FAM™ tag will bind to *Pm4/pm4* accessions respectively. The two remaining primer sets genotype for the two critical SNPs within the *Pm4f* allele, SNP 1 (**Figure 51B**) and SNP 9 (**Figure 51C**), that make the gene non-functional. *pm4* accessions should cluster with the 'no template controls' (NTCs) and correlate with the results from primer set 1. Primers with the HEX™/FAM™ tag will bind to *Pm4/Pm4f+SNP1 or SNP9* accessions respectively.

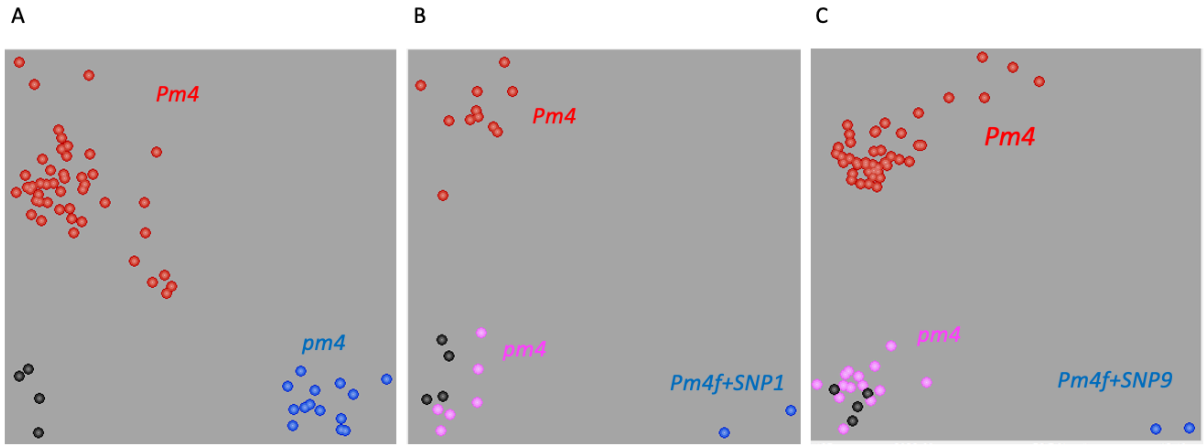

Figure 51: KlusterCaller cluster plot for *Pm4* KASP assays. (**A**) selects for the presence/absence of *Pm4*. Blue data points are homozygous for *pm4* associated with FAM™, red data points are homozygous for *Pm4* associated with HEX™. (**B**) selects for critical SNP 1. Blue data points are homozygous for *Pm4f+SNP1* associated with FAM™, red data points are homozygous for *Pm4* associated with HEX™. (**C**) selects for critical SNP 9. Blue data points are homozygous for *Pm4f+SNP9* associated with FAM™, red data points are homozygous for *Pm4* associated with HEX™. The black data points represent the no template controls (NTCs). Pink data points represent *pm4* genotypes and so segregate with the NTCs.

5.4 Discussion

In rice, *R* genes against *MoO* are predominantly NLRs, with just 3/38 of the cloned genes encoding non-NLR genes (Ngou, Ding, and Jones 2022). In the wheat/*MoT* pathosystem Arora et al. recently cloned the two wheat blast host specificity genes, *Rwt3* and *Rwt4*, which encode an NLR and a WTK respectively (Arora et al. 2023). As RLKs are the second largest class of plant *R* genes, it was hypothesised that the gene underlying the 2A resistance would be either an NLR or a kinase. Indeed in this chapter the 2A causal gene was identified as a kinase belonging to STK superfamily, previously designated as the *Bgt R* gene *Pm4* (Sánchez-Martín et al. 2021).

Pm4 was validated as the true candidate using both EMS derived loss of function mutants and overexpression transgenic material. *Pm4* undergoes alternate splicing to produce two isoforms (**Figure 52A**). Almost identical expression levels are observed for both transcripts, suggesting an equal contribution to the resistance (Sánchez-Martín et al., 2021). Transformation of the individual transcripts confirmed that both transcripts are required for function. Green and red fluorescent proteins (GFP and RFP) were used to tag the isoforms to identify co-expression with characterised markers. *Pm4b*-V1 and *Pm4b*-V2 isoforms colocalised with the endoplasmic reticulum (ER) and cytosol markers respectively. Transmembrane domains within the PRT_C domain have been shown to mediate ER localisation in *Arabidopsis* (Brault et al. 2019). The *Pm4b*-V2 PRT_C has two predicted transmembrane domains so it was hypothesised that *Pm4b*-V1 is recruited from the cytosol by *Pm4b*-V2 to the ER, potentially by forming an ER-associated chimera (**Figure 52B**) (Sánchez-Martín et al. 2021).

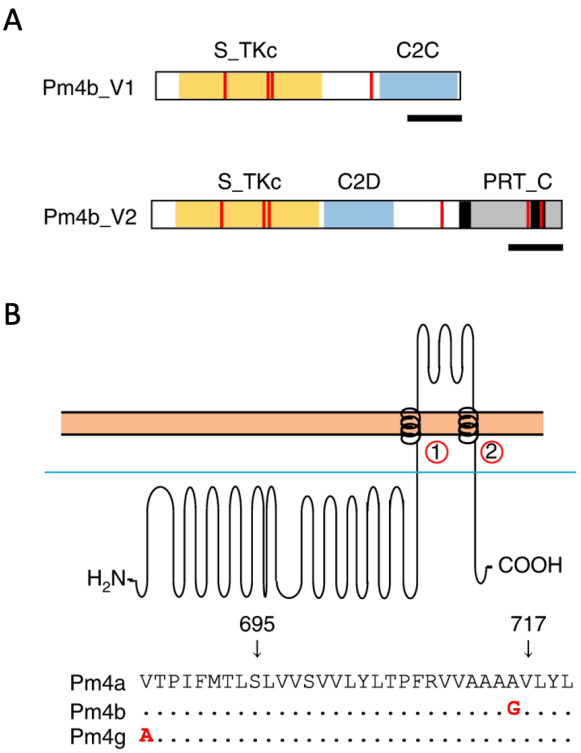

Figure 52: (**A**) *Pm4* protein isoforms: *Pm4*_V1 and *Pm4*_V2. The isoforms differ in only a few amino acid changes. Red bars indicate differences among *Pm4a, Pm4b, Pm4d, Pm4f, Pm4g and Pm4h.* Protein domains are indicated by colours: yellow, serine/threonine kinase; light blue, C2; grey, phosphoribosyl transferase C-terminal. Scale bars = 100 amino acids. (**B**) Topological model of *Pm4b*_V2 modified from Protter displaying the two transmembrane domains (circled numbers). Below, sequence alignment of the second transmembrane domain of the *Pm4a*, *Pm4b* and *Pm4g* protein variants, indicating their start and the endpoints at protein level. Dots represent identical amino acids compared to *Pm4a*. Adapted from Figure 3 from Sánchez-Martín et al. (2021).

Rwt4 is an allele of *Pm24,* making *Pm4* the second example of a gene involved in both *MoT* and *Bgt* resistance identified within the Nicholson group (Arora et al., 2023). Cadenza mutants (one homozygous, M0159; two heterozygous M0971 and M1103), developed through TILLING were tested in both the leaf and spike assays with a Brazilian isolate, BR48, transformed with the *Pwt4* effector (BR48+*Pwt4*). M0159 and all progeny of the heterozygous mutants that were homozygous for the SNPs were susceptible compared to the wildtype control. Virus induced gene silencing (VIGS) using a 400bp fragment of the kinase was performed in the cultivar Jagger and confirmed that the WTK was required for resistance against isolates carrying *Pwt4*. Furthermore, Brabham et al. recently showed that an NLR within the barley mildew resistance locus (*MLA*), confers resistance to both barley powdery mildew *(Blumeria graminis* f. sp. *hordei,* (*Bgh*)) and *M. oryzae. Mla3* in the barley cultivar Baronesse is infact *Resistance to M. oryzae 1* (*Rmo1*) which recognises *Avr-Rmo1 (PWL2)* in a dosage-dependent manner. Resistance was only observed in lines carrying three or more copies of *Mla3. PWL2* is a host specificity determinant and conditions virulence of rice infecting *M. oryzae* on weeping lovegrass (*Eragrostis curvula*) (Kang, Sweigard, and Valent 1995; Sweigard et al. 1995).

Whilst relatively rare, there are several other examples of resistance genes that recognise effectors from multiple taxonomically diverse pathogens (Wiesner-Hanks and Nelson 2016). Recognition of multiple effectors by the same NLR is thought to have evolved through convergent evolution, with most examples involving recognition through an integrated domain, or indirectly via modifications of a guarded host protein (Brabham et al. 2022). The NLR pair RPS4/RRS1 confer resistance to multiple bacterial pathogens (*Pseudomonas syringae*, *Ralstonia solanacearum* and *Xanthomonas campestris*) and the fungal pathogen *Colletotrichum higginsianum.* The integrated WRKY domain at the C-terminus of RRS1 recognises effectors *AvrRps4* and *PopP2* from *P. syringae* and *R. solanacearum* respectively (Deslandes et al. 2003; Gassmann, Hinsch, and Staskawicz 1999; Ma et al. 2018; Narusaka et al. 2009; Narusaka et al. 2013; Narusaka, Iuchi, and Narusaka 2017). The WRKY domain physically interacts with *AvrRps4* but requires acetyl-transferase activity from within the WRKY domain to recognise *PopP2* (Le Roux et al. 2015; Ma et al. 2018; Mukhi et al. 2021; Williams et al. 2014; Saucet et al. 2015; Sarris et al. 2015). The NLR ZAR1 from *A. thaliana* interacts with multiple guardees (closely related pseudokinases PBL2, RKS1, ZED1, and ZRK3) to recognise different bacterial effectors from *X. campestris* and *P. syringae* (Lewis et al. 2013; Seto et al. 2017; Wang et al. 2015).

The link between rust resistance and *Bgt* resistance is well known however the best studied examples are controlled by non-conventional major *R* genes. Stripe (or yellow) rust, leaf (or brown) and stem are caused by *Puccinia triticina*, *P. graminis* and *P. striiformis* respectively. A single gene on 7DS confers moderate slow-rusting adult plant resistance (APR) resistance to leaf, yellow and stem rusts, as well as adult powdery mildew resistance, designated *Lr34*, *Yr18*, *Sr57* and *Pm38* respectively (Liu and Kolmer 1998; Krattinger et al. 2009; Spielmeyer et al. 2005). An allelic series has been identified for *Lr34* with three alleles, distinguished by three SNPs and a 3bp indel (Krattinger et al. 2009) (Lagudah et al. 2009). *Lr34* is believed to encode an ABC transporter which transports phospholipids from the cytoplasmic to the exoplasmic membrane, altering the cellular lipid metabolism (Deppe et al. 2018). Similarly, parallel mapping studies using *T. aestivum* accession RL6007 identified that locus *Lr67*/*Yr46* on 4DL gives slow-rusting APR to leaf and yellow rusts (Herrera-Foessel et al. 2011; Hiebert et al. 2010). Herrera-Foessel et al. later discovered that *Lr67*/*Yr46* also confers adult stem rust and *Bgt* resistance, designated *Sr55* and *Pm46* respectively (Herrera-Foessel et al. 2014). *Lr67* has been isolated and encodes a predicted hexose sugar transporter (Moore et al. 2015). Moore et al. showed that *Lr67* provided resistance to the three rust species and *Bgt,* in addition to possibly limiting biotrophic fungal pathogen colonisation (2015). The *Lr46*/*Yr29*/Sr58/*Pm39* is another example of a single locus conferring partial APR to all four pathogens but this gene has yet to be identified (Lillemo et al. 2008; Kolmer et al. 2015).

Sanchez-Martin et al. reported that different *Pm4* alleles conferring race specific resistance to different isolates of *Bgt*, with *Pm4b* being the most widespread in hexaploid wheat (2021). The *Pm4a* and *Pm4b* NILs were used to compare the virulence spectra of *Pm4a* and *Pm4b* against 108 genetically diverse recent *Bgt* isolates (Sánchez-Martín et al. 2021). Thirty-seven and 28 of the isolates were avirulent and virulent respectively to both alleles. *Pm4a* and *Pm4b* gave different responses to the remaining 42 isolates, confirming these alleles were race specific. Screening 512 wheat lines from diverse origins revealed three novel alleles, *Pm4f, Pm4g and Pm4h*. *Pm4f* and *Pm4g* carrying lines were mostly susceptible to the *Bgt* isolates tested while *Pm4h* showed a similar resistance spectrum to *Pm4b* and *Pm4d.* Yao et al. also observed different resistance spectra against *Bgt* for alleles *Pm4a*, *Pm4b*, and *Pm4c* (2022). This suggested that *Pm4* allelic series may give different levels of resistance to *MoT*.

Plant material tested within this study contains the alleles *Pm4a, Pm4b, Pm4d* and *Pm4f*, all of which give seedling leaf resistance to NO6047+*Avr-Rmg8* and SRA. The SRA isolate was used to establish the response of *Pm4* to the eI allele of the *Avr-Rmg8* effector at the spike stage at 22^{o}C. Surprisingly, *Pm4b* carriers were susceptible to SRA at the spike stage, showing that the pattern of *Bgt* resistance conferred by *Pm4* cannot be used to infer resistance to *MoT. Pm4d* carriers were resistant at the spike stage however crucially they also carried the 2NS translocation so it is unclear which resistance is responsible for the phenotype. This emphasises the importance of identifying *Pm4d* varieties that do not carry 2NS to be able to make a proper comparison. Additional cultivars like Jagger which carry 2NS but do not contain *Pm4* should also be included. The Watkins collection was gathered before the 2NS translocation was introduced into wheat so the Watkins accessions will not contain the 2NS resistance, however there were no *Pm4d* carriers within the Watkins accessions tested within this study. *Pm4f* carriers gave strong resistance whilst *Pm4f+SNP1* and *Pm4f+SNP9* were susceptible, confirming that the critical SNPs result in a loss of recognition. These results also show that *Pm4b* is tissue specific and only provides leaf resistance against the eI effector.

A different pattern of resistance was observed with SRA at 26^{o}C. *Pm4b* carriers Claire, WATDE0102, WATDE0171 and WATDE0310 were all resistant at the leaf stage to SRA at 26^{o}C however WATDE0102 and WATDE0310 were susceptible at the spike stage at 26^{o}C. Only Claire maintained resistance in the spike stage (**Supplementary Fig. S1**). This supported previous phenotyping within this study which suggested that Claire and Mattis have an additional resistance that, when combined with *Pm4*, helps maintain resistance at higher temperatures (**Section 4.3.3.4**). *RmgGR119* is reported to give additive resistance to *Rmg8* in both leaf and spikes (Wang et al. 2018; Horo et al. 2020). The resistance was

still effective against isolates carrying *Avr-Rmg8* eI in the spike at 28°C but was reduced against the eII and eII' alleles (Horo et al. 2020). Whether *RmgGR119* also provides additive resistance in lines carrying *Rmg7* is unknown. *Pm4d* carriers maintained resistance at 26°C in the spike to SRA but again conclusions could not be made due to the presence of the 2NS translocation. The pedigree of Claire does not indicate that it involved any parent line carrying 2NS and so Claire may carry an additional resistance (http://wheatpedigree.net/). The resistance conferred by the *Pm4f* allele maintains effectiveness against SRA in leaves at 26°C however the resistance collapses in the spike stage. This suggests that *Pm4f* is leaf tissue specific at higher temperatures. This is consistent with findings of Anh et al. who demonstrated that *Rmg7* resistance against Brazilian isolates collapsed in the spike at 26°C (2018). *MoT* resistances *Rmg2* and *Rmg3* are also leaf specific and temperature sensitive (Zhan, Mayama, and Tosa 2008).

Tissue specific resistance has been reported against a variety of pathogens. Wheat blast resistances *Rmg2* and *Rmg3* are leaf specific and temperature sensitive (Zhan, Mayama, and Tosa 2008). QTL analysis to determine the genetic basis of resistace to *MoT* in the Brazilian cultivar BR 18-Terena identified 5 QTL associated with seedling resistance, and four QTL associated with spike resistance (Goddard et al. 2020). Seedling and spike QTLs did not co-locate suggesting that resistance was conferred by different genes in these tissues. Resistance to leaf rusts in cereals can be divided into seeding resistance or APR (Dinh et al. 2020). Seedling resistance is effective during all growth stages of the host and is also known as all stage resistance (ASR). ASR genes rarely provide complete resistance/immunity, where there are no macroscopically visible symptoms. Exceptions include barley *Rph18* and wheat *Lr1* (Park et al. 2015; Dyck and Kerber 1985). APR only provides resistance in adult plant growth stages and is often reported to be incompletely dominant, race non-specific and durable (Dinh et al. 2020; Gupta et al. 2018; Singh, Huerta-Espino, and WILLIAM 2005). For example *Rph20* in barley gives moderate to high levels of APR and has been durable for over 60 years (Hickey et al. 2012). Non-durable, race specific APR genes have also been reported (Dinh et al. 2020). The necrotic fungus *Stagonospora nodorum* is the casual agent of Septoria nodorum blotch (SNB). Resistance to SNB in leaves and glumes is reported to be genetically distinct (Lin et al. 2020; Aguilar et al. 2005). For example, Aguilar et al. reported 21 QTLs for SNB resistance however only one QTL was associated with both leaf and spike blotch (2005).

This study has identified the first example within the *MoT*/wheat pathosytem where both the *R* gene and effector are part of an allelic series. This is not a unique phenomenon however. Resistance to potato late blight, caused by *Phytophthora infestans,* is controlled in a gene-for gene manner. The *R* gene *Rpi-chc1* encodes a CC-NLR with an Arginine-(any aa)-Leucine-Arginine (RXLR) peptide motif.

Monino-lopez et al cloned 16 alleles of *Rpi-chc1* from four *Solanum spp* (2021). The alleles contained between 1296 to 1303 aa and had strong sequence similarity with 94.6 to 100% identity. The alleles had distinct patterns of effector recognition, recognising different members of the *P. infestans* extracellular (PEX) RXLR-DEER (PexRD) superfamily, PexRD12/31. The *Rpi-chc1.1* and *Rpi-chc1.2* alleles recognised PexRD12 and PexRD31 effectors respectively, however only *Rpi-chc1.1* resulted in resistance. Furthermore, the authors demonstrated that variations in the LRR domains were responsible for the different effector recognition specificities (Monino-Lopez et al. 2021). In rice, the NLR pair *Pik-1*/*Pik-2* and *MoO AvrPik* effectors both exist in allelic series and have been studied extensively (Xiao et al. 2022). Both NLRs are required and sufficient for function. *Pik* interacts directly with *AvrPik* via the heavy metal-associated (HMA) domain. To date six *AvrPik* alleles have been identified. As with *Pm4*, just a few aa changes distinguish the different *Pik* alleles. For example, alleles *Piks-1* and *Pikm-1* differ by just two aa changes; glutamate to glutamine at residue 229 (E229Q) and alanine to valine at residue 261 (A261V), both within the HMA domain. *Pikm-1* recognises *AvrPik* alleles *A*, *D*, and *E* whereas *Piks-1* does not bind to any of the known *AvrPik* effectors. Transgenic lines were generated to establish the effect of each aa change. *Piks-2* and *Pikm-2* are identical so were not expected to determine the recognition specificities. The *Piks-1*^{E229Q}/*Piks-2* transgenics gained recognition of the *AvrPik-D* allele, demonstrating that a single polymorphism can condition recognition. The *Piks-1*^{A261V}/*Piks-2* mutant however did not gain recognition of any of the *AvrPik- A*/*-D*/*-E* alleles. As *Piks-1*^{A261V} is equivalent to *Pikm-1*^{Q229E} the authors hypothesised that the change glutamine to glutamate in *Pikm-1* results in the loss of recognition of *AvrPik* alleles *A*, *D*, and *E.*

Within the present study the response of *Pm4* to the eII *Avr-Rmg8* effector by phenotyping with NO6047 was unclear. The DLA suggested that *Pm4b* and *Pm4f* carriers recognise eII, however background resistances in the host that potentially recognise additional effectors make drawing comparisons from NO6047 to the SRA and BTJ4P assays compromised. Additionally, only two lines carrying either *Pm4d* or *Pm4f* were phenotyped with NO6047 at the spike so these results may not be representative. Collaborators at Kobe University have generated a deletion/replacement isogenic series for *Avr-Rmg8* alleles within the Brazilian isolate Br48 (which carries the eI allele). A Br48 deletion isolate from which its native eI allele had been removed was transformed separately with the eI, eII and eII' alleles (Wang et al., 2018; Horo et al., 2020). These isolates will be used in future experiments to identify and quantify potential differential efficacies of the *Pm4* resistance alleles in the host against the allelic series of the *Avr-Rmg8* effector in the pathogen.

Pm4c, Pm4e, Pm4g and Pm4h have to date not been screened for blast resistance. *Pm4a* was only tested in the *Fed-Pm4a* NIL at the leaf stage so the response of *Pm4a* at the spike to *MoT* is also yet

to be established. Within this study the effects of the *Pm4d* allele could not be robustly determined due to potentially being masked by the 2NS translocation. The Watkins collection may include accessions carrying some of the other *Pm4* alleles described but this study was limited to analysing those Watkins lines with sequence alignments. Genotyping with markers would be a time efficient and high throughput approach to establish if any additional *Pm4* alleles are present within the Watkins panel. Yoa et al. have already developed SNP markers for *Pm4a*, *Pm4b*, *Pm4c* and *Pm4e* (2022). Conversely, the response of the two novel susceptible alleles identified within this study (*Pm4f+SNP1* and *Pm4f+SNP*) to mildew is unknown. The *Bgt* effector recognised by *Pm4* is currently unknown so it has not been established if it also forms part of an allelic series. Through continued collaboration with the Keller group, the effects of all known *Pm4* alleles against both pathogens will be elucidated. This will inform breeders which alleles offer the best protection against both *Bgt* and *MoT*. The BTJ4P spike test indicated that *Pm4f* has the most potent effect against the Bangladesh isolates. Additional phenotyping is required to establish whether the resistance against BTJ4P is maintained at 26^{o}C, which would be highly significant for breeding efforts in Bangladesh.

6. GENERAL DISCUSSION

Since the emergence in Brazil in 1985, wheat blast has spread throughout South America, and into Bangladesh, India and Africa, posing a serious threat to global wheat production (Igarashi et al. 1986; Igarashi 1990; Calloway 2016; Tembo et al. 2020). In South America several moderately resistant varieties were identified within existing cultivars, such as BRS49 and BRS120 in Brazil (Prestes et al. 2007), Motacu CIAT and Patuju CIAT in Bolivia and Caninde 1 and Itapua 75 in Paraguay (Buerstmayr et al. 2017, as referenced in Singh et al. 2021). It was later found that many of these varieties had the CIMMYT cultivar Milan in their pedigree and that the resistance was due to the 2NS translocation (Cruz et al. 2016). The 2NS translocation is present within a large proportion of the advanced lines within CIMMYTs international bread wheat breeding programme as it provides resistance to a wide range of pathogens, and it continues to be used in breeding programmes for blast resistance (Juliana et al. 2017). For example two years after the Bangladesh wheat blast outbreak a new biofortified variety carrying 2NS, BARI Gom 33, was deployed in Bangladesh (Velu et al. 2019; Hossain et al. 2019). However, due to the lack of novel sources of blast resistance, 2NS based resistance has been heavily relied upon and has been deployed across large areas in both South America and South Asia (Singh et al. 2021). This has created a strong selection pressure for new *MoT* isolates to overcome the 2NS resistance and virulent strains have already been reported across South America (Cruz et al. 2016; Cruppe et al. 2019). Non-2NS varieties such as BR 18-Terena and BRS229 give spike blast resistance and have also been widely used as parents in Brazil, however these also show susceptibility in some areas of Brazil (Ferreira et al. 2020; Ceresini, Castroagudin, Rodrigues, Rios, Aucique-Perez, Moreira, Croll, et al. 2018; Goddard et al. 2020; Urashima, Bruno, and Lavorenti 2001; Urashima, Galbieri, and Stabili 2005). It is therefore vital to identify novel, non-2NS resistance against *MoT*. Isolates in Bangladesh are believed to be clonally derived from a single South American strain and have been found to contain the eI allele of the *Avr-Rmg8* effector, suggesting that resistance based on recognition of *Avr-Rmg8* could be of use in Bangladesh (Malaker et al. 2016; Cruz and Valent 2017; Horo et al. 2020). This study has focused on attempting to identify resistance to Avr-Rmg8 using various GWAS based approaches.

CWR have previously been exploited to introduce biotic and abiotic resistance into crops, most notably with respect to pest and disease resistance (Maxted et al. 2012; Maxted et al. 2006). *MoT* resistance genes *Rmg7* and *Rmg8* both recognise the *Avr-Rmg8* effector and are thought to be homoeologous (Tagle, Chuma and Tosa 2015; Anh et al. 2015; Anh et al. 2018). *Rmg7* and *Rmg8* map to 2AL and 2BL in wheat respectively so it was hypothesised that a homeolog might also exist on the D genome and be present on 2D (Anh et al. 2015; Anh et al. 2018). This was investigated in **Chapter 3** using the *Ae.*

tauschii diversity panel. Only 20 accessions within the *Ae. tauschii* panel showed moderate levels of resistance against the Brazilian isolate NO6047 suggesting that high levels of resistance against this isolate are rare in *Ae. tauschii*. AgRenSeq analysis using the NO6047 data did not produce any significant peaks, suggesting that the resistance is polygenic or that different accessions have a different genetic basis for resistance. These accessions may have created noise during the analysis, masking any associations. Removing resistant accessions from the dataset and rerunning AgRenSeq may reveal an association that explains the remaining resistance within the panel. The isolate NO6047 was transformed with the *Avr-Rmg8* type eI allele (Jensen and Saunders 2023). Using phenotype data from the NO6047+*Avr-Rmg8 Ae. tauschii* DLA, both the AgRenSeq and OWWC pipelines identified an association on 7DL, corresponding to an interval of approximately 161kb in the resistant accession BW_01105, and 210kb in the *Ae. tauschii* RefSeq accession AL8/78, which was susceptible (**Section 3.3.1.2**). Resistant and susceptible haplotypes were identified, with five genes showing a presence/absence across the haplotypes. *Kinase 1* and *Kinase 5* were unique to the resistant haplotype and both showed moderate/good levels of expression. Analysis of the ORF of all accessions containing *Kinase 1* revealed three INDELs that all resulted in a frameshift. The INDELs were present in both resistant and susceptible accessions so *Kinase 1* was eliminated as a candidate. Nine polymorphisms were present within sequences for *Kinase 5* however no INDELs or premature stop codons were identified. The presence of *Kinase 5* alleles in susceptible accessions suggested that it may be required but not sufficient for resistance. The data from the SHW lines showed greater resistance in lines carrying the resistant haplotype, where the entire D genome of the donor is present, however the resistance is almost lost in spikes from recombinant materials which supports the hypothesis that *Kinase 5* is insufficient to provide resistance. Based upon the presence/absence of the resistant haplotype in the RIL populations there is negligible difference in blast susceptibility, suggesting that essential genetic components required for function may have been lost. This corroborates previous work within the literature which demonstrated that resistances introgressed into a hexaploid background can lose their efficacy in certain genetic backgrounds (Dreisigacker et al. 2008; Coombes et al. 2022). Interestingly, both *Kinase 1* and *Kinase 5* within the resistant 7D haplotype do not have homeologues on the D genome in Chinese Spring, which may be evidence that they originated from an introgression into *Ae. tauschii* as a result of a cross to a related species.

Within **Chapter 4** the 10+ Genomes cultivars were phenotyped to establish which cultivars were suitable to use as resistant reference accessions ahead of any association genetic analysis. Comparing detached leaf phenotypes for NO6047, NO6047+*Avr-Rmg8* and SRA at 22^{o}C suggested that there were two genes responsible for the resistance observed in Arina, Claire, Mattis and Stanley; a weak/moderate resistance effective against NO6047+*Avr-Rmg8* in Arina, and a second more potent

resistance that functions against both NO6047+*Avr-Rmg8* and SRA present in Claire, Mattis and Stanley. Re-phenotyping at 20°C and confirmed that Arina exhibits a moderate, resistance to both NO6047+*Avr-Rmg8* and SRA but that this is temperature sensitive and loses effectiveness at 26°C. In an attempt to identify the moderate temperature sensitive resistance observed in Arina, the 11 accessions with the functional 2A haplotype were removed from the NO6047+*Avr-Rmg8* DLA dataset. The WatRenSeq analysis was rerun with the amended scores however no associations were produced. This suggested that the Watkins panel may not be a useful resource for identifying additional resistance to Brazilian *MoT* isolates using this approach in the future. This highlights a limitation of GWAS based approaches where if the resistance is too rare it may not produce an association strong enough to be detected. It should be noted that a single Watkins accession, WATDE0015 possessed high levels of resistance against both NO6047+*Avr-Rmg8* and SRA isolates. A bi-parental population produced by crossing to the susceptible variety Paragon has been produced and is available in the JIC GRU. This material will be assayed in the future to identify the nature and location of the resistance in this accession. Unexpectedly, both NO6047+*Avr-Rmg8* and SRA Watkins phenotype datasets produced the same positive association on 2AL, corresponding to an interval of approximately 5.3Mb. Sequencing confirmed that SRA contains the eI *Avr-Rmg8* effector so it was assumed that the 2AL interval contained *Rmg7*. Compared to the NO6047+*Avr-Rmg8* assay, a much lower proportion of resistance was observed for SRA, again suggesting that there is limited resistance to *MoT* within the panel and that additional sources of resistance are needed.

Chapter 5 focused on establishing the gene content of the 5.3Mb Mattis interval, and then refining the candidates down to a single gene. Twenty-eight NLR loci were predicted using NLR-Annotator, including 15 complete NLRs. *De novo* gene annotations for Mattis (provided by Ricardo Ramirez-Gonzalez (JIC)) predicted 73 high confidence genes. Thirty-four high confidence genes were considered unlikely to be candidates as they were either linked to retrotransposons or had an unknown function. The interval associated with resistance to the two isolates was then interrogated using the IBSpy haplotype analysis. Two main blocks of similarity were observed, *Region 1* and *Region 2*. *Region 2* was absent in many of the resistant accessions/cultivars so was discounted as containing the candidate gene. By comparing the haplotype/phenotype relationship of accessions WATDE0720, WATDE0056 and WATDE0571, *Region 1* was further refined to a 400kb region. RNAseq analysis combined with polymorphism analysis identified two critical SNPs within a STK that explained the phenotype of 4/5 susceptible accessions that contained the resistant haplotype. Surprisingly, a protein BLAST revealed that the 2AL candidate had previously been identified as the *Bgt R* gene *Pm4* (Sánchez-Martín et al. 2021). Recognition of *Pm4* by *Avr-Rmg8* was confirmed using EMS mutant and

overexpression transgenic material, thus identifying *Rmg7*, the first wheat blast *R* gene to be cloned. *Pm4* also represents the first example within the *MoT*/wheat pathosytem where both the *R* gene and effector are part of an allelic series. Interestingly, the *Pm4b* allele appears to exhibit tissue specific effects against *MoT* and is not effective in the spike. RNAseq experiments to examine if the different *Pm4* alleles are equally expressed on exposure to *MoT*, in different tissues should be performed.

Pm4 encodes a kinase-MCTP protein which likely originated from a gene fusion between a S_TKc and the C terminus of a MCTP (Sanchez-Martin et al. 2021, the present study). Eighteen full length *Pm4* homologues have been identified across various *Triticeae* species including rye (*Secale cereale*), *Ae. tauschii* and barley (*Hordeum vulgare*) and are present on the group two chromosomes (Sanchez-Martin et al. 2021). *Pm4* homologues are not present in other grasses within the *Pooideace* so the identification of a *Pm4* homolog in barley (HORVU2Hr1G126810) suggests that the gene fusion event occurred in a *Triticeae* ancestor. Phylogenetic analysis of the homologues revealed that they do not form clusters representing the group two chromosome they are located on as expected, suggesting that the homologues have undergone complex evolutionary modifications. *Pm4* is not present in the Chinese Spring reference sequence however the closest homologue of the *Pm4b* C2 domain in Chinese Spring, TraesCS2A01G557900, is located near to where *Pm4* maps in Mattis at ~761 Mb on chromosome 2AL. Sanchez-Martin et al. propose multiple steps in the evolution of *Pm4* whereby the C terminus of the ancestor of TraesCS2A01G557900 was duplicated and fused to kinase domain giving rise to an intermediate form of *Pm4* with three 3' C2 domains (2021). The intermediate form was then also duplicated resulting in a *Pm4* ancestor that subsequently lost the first C2 domain within exon 6. The C2 domain donor, *Pm4* intermediary and HORVU2Hr1G126810 are all present in barley in a 1.2 Mb region. The kinase domain within *Pm4* belongs to the receptor-like cytoplasmic kinase (RLCK) family which contains many genes linked to disease resistance (Liang and Zhou 2018). For example RCLKs PBS1 and PBS1-like proteins are bacterial effecter targets and can also transduce immune signals at the plasma membrane (Lu et al. 2010; Zhang et al. 2010; Feng et al. 2012). The kinase domain of *Pm4* may also be targeted by the *Avr-Rmg8* and *Avr-Pm4* effectors directly. Alternatively, in a similar mechanism to sensor/helper NLR interactions, the MCTP domain may detect effector driven changes at the ER, with *Pm4*_V1 and *Pm4*_V2 acting as the helper and sensor proteins respectively (Sánchez-Martín et al. 2021; Liu et al. 2015). Yeast two-hybrid screening or coimmunoprecipitation assays could be performed using the individual *Pm4* transcripts/domains and the *Avr-Rmg8* effector to determine how they interact.

It is becoming increasingly recognised that many proteins designated as effectors occur more commonly than expected for typical virulence effectors and so could be classified as MAMPs (Cook, Mesarich, and Thomma 2015). For example, necrosis and ethylene-inducing peptide 1 (Nep1) was first identified in *Fusarium oxysporum* and several homologs, known as Nep1-like proteins (NLPs) which contribute to virulence have been identified in other fungi, as well as in bacteria and oomycetes (Bailey 1995; Gijzen and Nürnberger 2006; Ottmann et al. 2009). A conserved region of between 20 to 24 amino acids has been identified on NLPs that acts as a strong inducer of plant immune responses and therefore acts as a MAMP (Böhm et al. 2014; Oome et al. 2014). Additionally, two conserved motifs within a 40 amino acid region of the *Botrytis cinerea* effector *BcSp11* are required and sufficient for initiating host defence, including HR (Frías, González, and Brito 2011; Frías et al. 2014). BcSp11 is part of the cerato-platanin family of effector proteins which are encoded by a diverse group of fungi and all the immunogenic cerato-platanins contain the two conserved motifs. It is possible that the dual recognition of *Bgt* and *MoT* by *Pm4* is due to a novel conserved region within both the *Avr-Rmg8* and *Avr-Pm4* effectors that acts as a MAMP. This theory may also reconcile the other examples of *R* genes discussed in the study which provide resistance to both pathogens. This further highlights the importance of identifying *Avr-Pm4* in order to compare effector sequences. The protein structure prediction software AlphaFold could be used to predict the structure of the *Pm4-Avr-Rmg8* and -*Avr-Pm4* complexes and may identify a critical region shared across both effectors that is required for recognition. Work is ongoing within the Keller group to identify the *Bgt Avr-Pm4* effector (personal communication, Beat Keller).

Unlike *Mo* which is a hemi-biotrophic pathogen, *Bgt* is an obligate biotroph (Hückelhoven and Panstruga 2011; Fernandez and Orth 2018). Following conidial germination, in contrast to other mildews, *Blumeria spp* produce a primary sensing germ tube followed by a secondary germ tube that differentiates into an appressorium (Wright et al. 2000; Yamaoka, Matsumoto, and Nishiguchi 2006). As with *Mo* infection, the appressorium uses mechanical pressure (Jankovics et al. 2015). Whilst *Mo* invades the host intracellularly, *Bgt* grows extracellularly and produces intracellular haustoria that are separated from the host cytoplasm by extrahaustorial membrane (Mendgen and Hahn 2002; O'Connell and Panstruga 2006). Having lost the genes encoding primary and secondary metabolism, the haustorium are essential to uptake host nutrients (Frantzeskakis et al. 2018; Panstruga and Dodds 2009). Microscopic observation of wheat leaf tissue inoculated with powdery mildew revealed that *Pm4* mediated resistance is largely due to pre-penetration resistance which suggests a rapid host response once the pathogen is detected (Sanchez-Martin et al. 2021). Both *MoT* and *Bgt* conidia initially colonise the epidermis so an alternative explanation for how *Pm4* gives resistance to both

MoT and *Bgt* is that epidermal cells contain specific PRRs that can detect a MAMP common to both pathogens which triggers a secondary defence response facilitated by *Pm4*.

Pm4 represents the second blast gene identified within the Nicholson group involved in both *Mot* and *Bgt* resistance, the other being *Rwt4* (Arora et al. 2023). Phenotyping CWR for dual *Bgt* and *MoT* resistance or screening known *Bgt R* genes for blast resistance may be fruitful approaches to identify new sources of resistance against isolates of *MoT*. Given that *Rwt4* encodes a WTK (Arora et al. 2023), *Pm4* contains a STK and ongoing work within the Nicholson group suggests that a kinase may also be involved in *Rmg2* mediated blast resistance, *Bgt R* genes with kinase domains should be prioritised for screening. Known *Bgt* genes may already have been selected by breeders and so already be in elite cultivar backgrounds. This was evident in this study where all the adaptive wheat cultivars tested within **Chapter 5** carried functional alleles of *Pm4* and so were resistant to blast. Several of the *Pm4* alleles originate from wild species: the *Pm4a, Pm4b* and *Pm4d* alleles were introgressed into wheat *T. dicoccoides*, *T. carthlicum* and *T. monococum* respectively (Briggle 1966; McIntosh and Bennet 1979; Schmolke et al. 2012). This adds further support for the use of CWR as sources of wheat blast resistance.

The BTJ4P spike test indicated that *Pm4f* has the most potent effect against the Bangladesh isolates however phenotyping is required to establish whether the resistance against BTJ4P is maintained at 26^{o}C. If resistance is expressed at high temperatures this would be highly significant for breeding efforts in Bangladesh where temperatures are high at the time when the crop is in flower. *Pm4f* carriers provide strong resistance to the SRA isolate at 22^{o}C at the both the seedling and spike stages, however resistance is lost in the spike at 26^{o}C. It would be highly advantageous to understand the mechanism behind the loss of resistance. If expression of the gene is decreased in adult plants at high temperatures engineering overexpression may restore resistance. Given the variation in resistance conveyed by the *Pm4* alleles tested so far to *MoT*, it is vital to screen the remaining alleles to establish if they provide more potent resistance. Additionally, utilising the deletion/replacement isogenic series for *Avr-Rmg8* alleles will confirm the differential efficacies of the *Pm4* resistance alleles in the host against the allelic series of the *Avr-Rmg8* effector in the pathogen, which will help inform breeders of the best alleles to incorporate (Wang et al. 2018; Horo et al. 2020). KASP markers for *Pm4* developed in this study have already been shared with CIMMYT. Given that the *Pwt4* effector suppresses *Rmg8* resistance in *rwt4* carriers it would be prudent to maintain both *Pm4* and *Rwt4* within breeding programmes (Inoue et al. 2020).

Additional phenotyping private to this thesis using the BTJ4P isolate against the Watkins core panel has identified several intervals that that may offer additional resistance to isolates in Bangladesh and India. The work carried out within this study demonstrates the power of combining genome-based GWAS with isolate-specific phenotyping of individual host tissues in the identification of loci and genes conferring resistance to *MoT*. This approach has the potential to markedly increase the speed with which additional resistance genes can be identified to ensure that perfect markers (designed to the causal gene/allele) are available to breeders to ensure that varieties contain multiple resistances in order to reduce the risk of breakdown of resistance on mutation within the pathogen population.

7. DATA AVAILIBILITY

The complete *variations* data used for haplotype analysis are available from Zenodo under the DOI zenodo.org/record/8355991. The Mattis gene models discussed in this study are available at DOI zenodo.org/record/8380858.

8. REFERENCES

Aguilar, V, P Stamp, M Winzeler, H Winzeler, G Schachermayr, B Keller, S Zanetti, and MM Messmer. 2005. 'Inheritance of field resistance to Stagonospora nodorum leaf and glume blotch and correlations with other morphological traits in hexaploid wheat (Triticum aestivum L.)', *Theoretical and Applied Genetics*, 111: 325-36.

Anh, V, Yoshihiro Inoue, Soichiro Asuke, Trinh Thi Phuong Vy, Nguyen Tuan Anh, Shizhen Wang, Izumi Chuma, and Yukio Tosa. 2018. 'Rmg8 and Rmg7, wheat genes for resistance to the wheat blast fungus, recognize the same avirulence gene AVR-Rmg8', *Molecular Plant Pathology*, 19: 1252-56.

Anh, V. L;, N. T; Anh, A. G; Tagle, T. T. P; Vy, Y; Inoue, S; Takumi, I; Chuma, and Y; Tosa. 2015. 'Rmg8, a New Gene for Resistance to Triticum Isolates of Pyricularia oryzae in Hexaploid Wheat', *Phytopathology*, 105: 1568-72.

Aoun, Meriem, Xianming Chen, Mohamed Somo, Steven S Xu, Xuehui Li, and Elias M Elias. 2021. 'Novel stripe rust all-stage resistance loci identified in a worldwide collection of durum wheat using genome-wide association mapping', *The Plant Genome*, 14: e20136.

Arora, S., N. Singh, S. Kaur, N. S. Bains, C. Uauy, J. Poland, and P. Chhuneja. 2017. 'Genome-Wide Association Study of Grain Architecture in Wild Wheat Aegilops tauschii', *Front Plant Sci*, 8: 886.

Arora, S., B. Steuernagel, K. Gaurav, S. Chandramohan, Y. Long, O. Matny, R. Johnson, J. Enk, S. Periyannan, N. Singh, M. Asyraf Md Hatta, N. Athiyannan, J. Cheema, G. Yu, N. Kangara, S. Ghosh, L. J. Szabo, J. Poland, H. Bariana, J. D. G. Jones, A. R. Bentley, M. Ayliffe, E. Olson, S. S. Xu, B. J. Steffenson, E. Lagudah, and B. B. H. Wulff. 2019. 'Resistance gene cloning from a wild crop relative by sequence capture and association genetics', *Nature Biotechnology*, 37: 139-43.

Arora, Sanu, Andrew Steed, Rachel Goddard, Kumar Gaurav, Tom O'Hara, Adam Schoen, Nidhi Rawat, Ahmed F Elkot, Andrey V Korolev, and Catherine Chinoy. 2023. 'A wheat kinase and immune receptor form host-specificity barriers against the blast fungus', *Nature plants*: 1-8.

Arruda, M.A., Bueno, C.R.N.C., Zamprogno, K.C., Lavorenti, N.A. and Urashima, A.S., . 2005. 'Reação do trigo à Magnaporthe grisea nos diferentes estádios de desenvolvimento', *Fitopatologia Brasileira*, 30: 121-26.

Ashikawa, Ikuo, Nagao Hayashi, Hiroko Yamane, Hiroyuki Kanamori, Jianzhong Wu, Takashi Matsumoto, Kazuko Ono, and Masahiro Yano. 2008. 'Two adjacent nucleotide-binding site–

leucine-rich repeat class genes are required to confer Pikm-specific rice blast resistance', *Genetics*, 180: 2267-76.

Bailey, Bryan A. 1995. 'Purification of a protein from culture filtrates of Fusarium oxysporum that induces ethylene and necrosis in leaves of Erythroxylum coca', *Phytopathology*, 85: 1250-55.

Bergelson, Joy, Martin Kreitman, Eli A Stahl, and Dacheng Tian. 2001. 'Evolutionary dynamics of plant R-genes', *science*, 292: 2281-85.

Bettgenhaeuser, Jan, and Simon G Krattinger. 2019. 'Rapid gene cloning in cereals', *Theoretical and Applied Genetics*, 132: 699-711.

Bockus, W, C Cruz, B Kalia, B Gill, J Stack, K Pedley, G Peterson, and B Valent. 2012. 'Reaction of selected accessions of Aegilops tauschii to wheat blast, 2011', *Plant Dis. Manage. Rep*, 6.

Böhm, Hannah, Isabell Albert, Stan Oome, Tom M Raaymakers, Guido Van den Ackerveken, and Thorsten Nürnberger. 2014. 'A conserved peptide pattern from a widespread microbial virulence factor triggers pattern-induced immunity in Arabidopsis', *PLoS Pathogens*, 10: e1004491.

Börner, Andreas, Francis Chuks Ogbonnaya, Marion S Röder, Awais Rasheed, Sambasivam Periyannan, and Evans S Lagudah. 2015. 'Aegilops tauschii introgressions in wheat.' in, *Alien introgression in wheat* (Springer).

Bourett, Timothy M, and Richard J Howard. 1990. 'In vitro development of penetration structures in the rice blast fungus Magnaporthe grisea', *Canadian Journal of Botany*, 68: 329-42.

Brabham, Helen Jane, Diana Gómez De La Cruz, Vincent Were, Motoki Shimizu, Hiromasa Saitoh, Inmaculada Hernández-Pinzón, Phon Green, Jennifer Lorang, Koki Fujisaki, and Kazuhiro Sato. 2022. 'Barley MLA3 recognizes the host-specificity determinant PWL2 from rice blast (M. oryzae)', *bioRxiv*: 2022.10. 21.512921.

Brault, Marie L, Jules D Petit, Françoise Immel, William J Nicolas, Marie Glavier, Lysiane Brocard, Amèlia Gaston, Mathieu Fouché, Timothy J Hawkins, and Jean-Marc Crowet. 2019. 'Multiple C2 domains and transmembrane region proteins (MCTP s) tether membranes at plasmodesmata', *EMBO reports*, 20: e47182.

Briggle, LW. 1966. 'Transfer of resistance to Erysiphe graminis f. sp. tritici from Khapli Emmer and Yuma Durum to Hexaploid Wheat 1', *Crop Science*, 6: 459-61.

Brown, Neil Andrew, Sanne Schrevens, Patrick Van Dijck, and Gustavo Henrique Goldman. 2018. 'Fungal G-protein-coupled receptors: mediators of pathogenesis and targets for disease control', *Nature Microbiology*, 3: 402-14.

Brozynska, Marta, Agnelo Furtado, and Robert J Henry. 2016. 'Genomics of crop wild relatives: expanding the gene pool for crop improvement', *Plant Biotechnology Journal*, 14: 1070-85.

Brueggeman, R, A Druka, J Nirmala, T Cavileer, T Drader, N Rostoks, A Mirlohi, H Bennypaul, U Gill, and D Kudrna. 2008. 'The stem rust resistance gene Rpg5 encodes a protein with nucleotide-binding-site, leucine-rich, and protein kinase domains', *Proceedings of the National Academy of Sciences*, 105: 14970-75.

Brueggeman, Royal, N Rostoks, D Kudrna, A Kilian, F Han, J Chen, A Druka, B Steffenson, and A Kleinhofs. 2002. 'The barley stem rust-resistance gene Rpg1 is a novel disease-resistance gene with homology to receptor kinases', *Proceedings of the National Academy of Sciences*, 99: 9328-33.

Büschges, Rainer, Karin Hollricher, Ralph Panstruga, Guus Simons, Marietta Wolter, Adrie Frijters, Raymond Van Daelen, Theo van der Lee, Paul Diergaarde, and John Groenendijk. 1997. 'The barley Mlo gene: a novel control element of plant pathogen resistance', *Cell*, 88: 695-705.

Caldwell, Katherine S, Jan Dvorak, Evans S Lagudah, Eduard Akhunov, Ming-Cheng Luo, Petra Wolters, and Wayne Powell. 2004. 'Sequence polymorphism in polyploid wheat and their D-genome diploid ancestor', *Genetics*, 167: 941-47.

Callaway, Ewen. 2016. 'Devastating wheat fungus appears in Asia for first time', *Nature News*, 532: 421.

Cardoso, Cinara Araújo de Andrade, Erlei Melo Reis, and Eder Novaes Moreira. 2008. 'Development of a warning system for wheat blast caused by Pyricularia grisea', *Summa Phytopathologica*, 34: 216-21.

Castroagudin, Vanina, Anderson Danelli, Silvino Intra Moreira, Juliana Teodora de Assis Reges, Giselle Carvalho, Joao Leodato Nunes Maciel, Ana Lidia Variani Bonato, Carlos Alberto Forcelini, Eduardo Alves, Bruce McDonald, Daniel Croll, and Paulo Ceresini. 2017. 'The wheat blast pathogen *Pyricularia graminis-tritici* has complex origins and a diease cycle spanning multiple grass hosts'.

Castroagudín, Vanina L, Paulo C Ceresini, Samanta C de Oliveira, Juliana TA Reges, João LN Maciel, Ana LV Bonato, Adriano F Dorigan, and Bruce A McDonald. 2015. 'Resistance to QoI fungicides is widespread in Brazilian populations of the wheat blast pathogen Magnaporthe oryzae', *Phytopathology*, 105: 284-94.

Castroagudín, Vanina L, Silvino I Moreira, Danilo AS Pereira, Sávia S Moreira, Patrick C Brunner, João LN Maciel, Pedro W Crous, Bruce A McDonald, Eduardo Alves, and Paulo C Ceresini. 2016. 'Pyricularia graminis-tritici, a new Pyricularia species causing wheat blast', *Persoonia: Molecular Phylogeny and Evolution of Fungi*, 37: 199.

Cazal-Martínez, Cinthia Carolina, Yessica Magaliz Reyes-Caballero, and Man Mohan Kohli. 2022. 'Response of wheat carrying 2NS/2AS, Rmg8 and Rmg7 translocation to Pyricularia oryzae pathotype Triticum from Paraguay', *Summa Phytopathologica*, 48: 32-35.

Ceresini, P. C., V. L. Castroagudin, F. A. Rodrigues, Jonas Alberto Rios, Carlos Eduardo Aucique-Perez, Silvino Intra Moreira, D. Croll, Eduardo Alves, Giselle Carvalho, D., J. L. Maciel, and B. A. McDonald. 2018. 'Wheat blast: from its origins in South America to its emergence as a global threat', *Molecular Plant Patholgy*.

Ceresini, Paulo Cezar, Vanina Lilian Castroagudin, Fabricio Avila Rodrigues, Jonas Alberto Rios, Carlos Eduardo Aucique-Perez, Silvino Intra Moreira, Eduardo Alves, Daniel Croll, and Joao Leodato Nunes Maciel. 2018. 'Wheat Blast: Past, Present, and Future.' in J. E. Leach and S. E. Lindow (eds.), *Annual Review of Phytopathology, Vol 56*.

Cesari, Stella. 2018. 'Multiple strategies for pathogen perception by plant immune receptors', *New Phytologist*, 219: 17-24.

Cesari, Stella, Maud Bernoux, Philippe Moncuquet, Thomas Kroj, and Peter N. Dodds. 2014. 'A novel conserved mechanism for plant NLR protein pairs: the "integrated decoy" hypothesis', *Frontiers in plant science*, 5.

Chaipanya, Chaivarakun, Mary Jeanie Telebanco-Yanoria, Berlaine Quime, Apinya Longya, Siripar Korinsak, Siriporn Korinsak, Theerayut Toojinda, Apichart Vanavichit, Chatchawan Jantasuriyarat, and Bo Zhou. 2017. 'Dissection of broad-spectrum resistance of the Thai rice variety Jao Hom Nin conferred by two resistance genes against rice blast', *Rice*, 10: 1-11.

Chakraborty, Sukumar, Jo Luck, Grant Hollaway, Glenn Fitzgerald, and Neil White. 2011. 'Rust-proofing wheat for a changing climate', *Euphytica*, 179: 19-32.

Chauhan, Harsh, Rainer Boni, Rahel Bucher, Benjamin Kuhn, Gabriele Buchmann, Justine Sucher, Liselotte L Selter, Goetz Hensel, Jochen Kumlehn, and Laurent Bigler. 2015. 'The wheat resistance gene Lr34 results in the constitutive induction of multiple defense pathways in transgenic barley', *The Plant Journal*, 84: 202-15.

Chauhan, Rajinder, Mark Farman, H-B Zhang, and Sally Leong. 2002. 'Genetic and physical mapping of a rice blast resistance locus, Pi-CO39 (t), that corresponds to the avirulence gene AVR1-CO39 of Magnaporthe grisea', *Molecular Genetics and Genomics*, 267: 603-12.

Cheetham, Seth W, Geoffrey J Faulkner, and Marcel E Dinger. 2020. 'Overcoming challenges and dogmas to understand the functions of pseudogenes', *Nature Reviews Genetics*, 21: 191-201.

Chen, Shen, Aiqing Feng, Congying Wang, Junliang Zhao, Jinqi Feng, Bing Chen, Jianyuan Yang, Wenjuan Wang, Meiying Zhang, and Kailing Chen. 2022. 'Identification and fine-mapping of Xo2, a novel rice bacterial leaf streak resistance gene', *Theoretical and Applied Genetics*, 135: 3195-209.

Chen, Shisheng, Matthew N Rouse, Wenjun Zhang, Xiaoqin Zhang, Yan Guo, Jordan Briggs, and Jorge Dubcovsky. 2020. 'Wheat gene Sr60 encodes a protein with two putative kinase domains that confers resistance to stem rust', *New Phytologist*, 225: 948-59.

Chen, Xuewei, Junjun Shang, Dexi Chen, Cailin Lei, Yan Zou, Wenxue Zhai, Guozhen Liu, Jichen Xu, Zhongzhuan Ling, and Gang Cao. 2006. 'AB-lectin receptor kinase gene conferring rice blast resistance', *The Plant Journal*, 46: 794-804.

Cheng, Cheng, Xiquan Gao, Baomin Feng, Jen Sheen, Libo Shan, and Ping He. 2013. 'Plant immune response to pathogens differs with changing temperatures', *Nature communications*, 4: 2530.

Chumley, Forrest G, and Barbara Valent. 1990. 'Genetic analysis of melanin-deficient, nonpathogenic mutants of Magnaporthe grisea', *Mol. Plant-Microbe Interact*, 3: 135-43.

Collemare, Jérôme, Alexis Billard, Heidi U Böhnert, and Marc-Henri Lebrun. 2008. 'Biosynthesis of secondary metabolites in the rice blast fungus Magnaporthe grisea: the role of hybrid PKS-NRPS in pathogenicity', *Mycological Research*, 112: 207-15.

Cook, David E, Carl H Mesarich, and Bart PHJ Thomma. 2015. 'Understanding plant immunity as a surveillance system to detect invasion', *Annual Review of Phytopathology*, 53: 541-63.

Coombes, Benedict, John P Fellers, Surbhi Grewal, Rachel Rusholme-Pilcher, Stella Hubbart-Edwards, Cai-yun Yang, Ryan Joynson, Ian P King, Julie King, and Anthony Hall. 2022. 'Whole genome sequencing uncovers the structural and transcriptomic landscape of hexaploid wheat/Ambylopyrum muticum introgression lines', *Plant Biotechnology Journal*.

Cornell, Michael J, Intikhab Alam, Darren M Soanes, Han Min Wong, Cornelia Hedeler, Norman W Paton, Magnus Rattray, Simon J Hubbard, Nicholas J Talbot, and Stephen G Oliver. 2007. 'Comparative genome analysis across a kingdom of eukaryotic organisms: specialization and diversification in the fungi', *Genome Research*, 17: 1809-22.

Couch, Brett C, Isabelle Fudal, Marc-Henri Lebrun, Didier Tharreau, Barbara Valent, Pham Van Kim, Jean-Loup Nottéghem, and Linda M Kohn. 2005. 'Origins of host-specific populations of the blast pathogen Magnaporthe oryzae in crop domestication with subsequent expansion of pandemic clones on rice and weeds of rice', *Genetics*, 170: 613-30.

Cox, TS. 1997. 'Deepening the wheat gene pool', *Journal of Crop Production*, 1: 1-25.

Cox, TS, RG Sears, BS Gill, and EN Jellen. 1994. 'Registration of KS91WGRC11, KS92WGRC15, and KS92WGRC23 leaf rust-resistant hard red winter wheat germplasms', *Crop science (USA)*.

Cruppe, Giovana, Christian D Cruz, Gary L Peterson, Kerry F Pedley, Asif Mohammad, Allan Fritz, Lidia Calderon, Cristiano Lemes da Silva, Tim Todd, and Paulo Kuhnem. 2019. 'Novel Sources of Wheat Head Blast Resistance in Modern Breeding Lines and Wheat Wild Relatives', *Plant Disease*.

Cruz, C. D., G. L. Peterson, W. W. Bockus, P. Kankanala, J. Dubcovsky, K. W. Jordan, E. Akhunov, F. Chumley, F. D. Baldelomar, and B. Valent. 2016. 'The 2NS Translocation from Aegilops ventricosa Confers Resistance to the Triticum Pathotype of Magnaporthe oryzae', *Crop Science*, 56: 990-1000.

Cruz, C. D., and B. Valent. 2017. 'Wheat blast disease: danger on the move', *Tropical Plant Pathology*, 42: 210-22.

Cruz, CD, J Kiyuna, WW Bockus, TC Todd, JP Stack, and B Valent. 2015. 'Magnaporthe oryzae conidia on basal wheat leaves as a potential source of wheat blast inoculum', *Plant Pathology*, 64: 1491-98.

Cruz, Christian D, William W Bockus, James P Stack, Xiaoyan Tang, Barbara Valent, Kerry F Pedley, and Gary L Peterson. 2012. 'Preliminary assessment of resistance among US wheat cultivars to the Triticum pathotype of Magnaporthe oryzae', *Plant Disease*, 96: 1501-05.

Cruz, Maria Fernanda A, Ariano M Prestes, João LN Maciel, and Pedro L Scheeren. 2010. 'Partial resistance to blast on common and synthetic wheat genotypes in seedling and in adult plant growth stages', *Tropical Plant Pathology*, 35: 024-31.

Cruz-Mireles, Neftaly, Alice Bisola Eseola, Míriam Osés-Ruiz, Lauren S Ryder, and Nicholas J Talbot. 2021. 'From appressorium to transpressorium—Defining the morphogenetic basis of host cell invasion by the rice blast fungus', *PLoS Pathogens*, 17: e1009779.

Cunningham, Fiona, James E Allen, Jamie Allen, Jorge Alvarez-Jarreta, M Ridwan Amode, Irina M Armean, Olanrewaju Austine-Orimoloye, Andrey G Azov, If Barnes, and Ruth Bennett. 2022. 'Ensembl 2022', *Nucleic Acids Research*, 50: D988-D95.

Dagdas, Yasin F, Kae Yoshino, Gulay Dagdas, Lauren S Ryder, Ewa Bielska, Gero Steinberg, and Nicholas J Talbot. 2012. 'Septin-mediated plant cell invasion by the rice blast fungus, Magnaporthe oryzae', *science*, 336: 1590-95.

de Jong, Joke C, Barbara J McCormack, Nicholas Smirnoff, and Nicholas J Talbot. 1997. 'Glycerol generates turgor in rice blast', *Nature*, 389: 244-44.

De Oliveira, Romain, Hélène Rimbert, François Balfourier, Jonathan Kitt, Emeric Dynomant, Jan Vrána, Jaroslav Doležel, Federica Cattonaro, Etienne Paux, and Frédéric Choulet. 2020. 'Structural variations affecting genes and transposable elements of chromosome 3B in wheats', *Frontiers in Genetics*: 891.

de Paula, Igor Gonçalves, Hilda Barbosa Gloria, Adérico Júnior Badaró Pimentel, Guilherme Ribeiro, and Moacil Alves de Souza. 2019. 'Screening wheat genotypes for resistance to wheat blast disease in the vegetative and reproductive stages', *Euphytica*, 215: 59.

Dean, Ralph A, Nicholas J Talbot, Daniel J Ebbole, Mark L Farman, Thomas K Mitchell, Marc J Orbach, Michael Thon, Resham Kulkarni, Jin-Rong Xu, and Huaqin Pan. 2005. 'The genome sequence of the rice blast fungus Magnaporthe grisea', *Nature*, 434: 980.

Deng, Yiwen, Keran Zhai, Zhen Xie, Dongyong Yang, Xudong Zhu, Junzhong Liu, Xin Wang, Peng Qin, Yuanzhu Yang, and Guomin Zhang. 2017. 'Epigenetic regulation of antagonistic receptors confers rice blast resistance with yield balance', *science*, 355: 962-65.

Deppe, Johannes P, Ritta Rabbat, Stefan Hörtensteiner, Beat Keller, Enrico Martinoia, and Rosa L Lopéz-Marqués. 2018. 'The wheat ABC transporter Lr34 modifies the lipid environment at the plasma membrane', *Journal of Biological Chemistry*, 293: 18667-79.

Deslandes, Laurent, Jocelyne Olivier, Nemo Peeters, Dong Xin Feng, Manirath Khounlotham, Christian Boucher, Imre Somssich, Stéphane Genin, and Yves Marco. 2003. 'Physical interaction between RRS1-R, a protein conferring resistance to bacterial wilt, and PopP2, a type III effector targeted to the plant nucleus', *Proceedings of the National Academy of Sciences*, 100: 8024-29.

Deslandes, Laurent, Jocelyne Olivier, Frédéric Theulières, Judith Hirsch, Dong Xin Feng, Peter Bittner-Eddy, Jim Beynon, and Yves Marco. 2002. 'Resistance to Ralstonia solanacearum in Arabidopsis thaliana is conferred by the recessive RRS1-R gene, a member of a novel family of resistance genes', *Proceedings of the National Academy of Sciences*, 99: 2404-09.

Devanna, Basavantraya N, Priyanka Jain, Amolkumar U Solanke, Alok Das, Shallu Thakur, Pankaj K Singh, Mandeep Kumari, Himanshu Dubey, Rajdeep Jaswal, and Deepak Pawar. 2022. 'Understanding the dynamics of blast resistance in rice-Magnaporthe oryzae interactions', *Journal of Fungi*, 8: 584.

Devanna, BN, and TR Sharma. 2018. 'Wheat blast disease management: cues from the advancements in molecular biology of rice-Magnaporthe pathosystem', *Journal of plant biochemistry and biotechnology*, 27: 249-59.

DeZwaan, Todd M, Anne M Carroll, Barbara Valent, and James A Sweigard. 1999. 'Magnaporthe grisea pth11p is a novel plasma membrane protein that mediates appressorium differentiation in response to inductive substrate cues', *The Plant Cell*, 11: 2013-30.

Dievart, Anne, Céline Gottin, Christophe Périn, Vincent Ranwez, and Nathalie Chantret. 2020. 'Origin and diversity of plant receptor-like kinases', *Annual Review of Plant Biology*, 71: 131-56.

Dinh, Hoan X, Davinder Singh, Sambasivam Periyannan, Robert F Park, and Mohammad Pourkheirandish. 2020. 'Molecular genetics of leaf rust resistance in wheat and barley', *Theoretical and Applied Genetics*, 133: 2035-50.

Dong, Liying, Shufang Liu, Peng Xu, Wei Deng, Xundong Li, Didier Tharreau, Jing Li, Jiawu Zhou, Qun Wang, and Dayun Tao. 2017. 'Fine mapping of Pi57 (t) conferring broad spectrum resistance against Magnaporthe oryzae in introgression line IL-E1454 derived from Oryza longistaminata', *PloS one*, 12: e0186201.

Dong, Zhenjie, Chao Ma, Xiubin Tian, Changtao Zhu, Gang Wang, Yuanfeng Lv, Bernd Friebe, Huanhuan Li, and Wenxuan Liu. 2020. 'Genome-wide impacts of alien chromatin introgression on wheat gene transcriptions', *Scientific Reports*, 10: 1-12.

Dreisigacker, Susanne, Masahiro Kishii, Jacob Lage, and Marilyn Warburton. 2008. 'Use of synthetic hexaploid wheat to increase diversity for CIMMYT bread wheat improvement', *Australian Journal of Agricultural Research*, 59: 413-20.

Dyck, PL, and R Johnson. 1983. 'Temperature sensitivity of genes for resistance in wheat to Puccinia recondita', *Canadian Journal of Plant Pathology*, 5: 229-34.

Dyck, PL, and ER Kerber. 1985. 'Resistance of the race-specific type.' in, *Diseases, distribution, epidemiology, and control* (Elsevier).

Erenstein, Olaf, and William Thorpe. 2011. 'Livelihoods and agro-ecological gradients: A meso-level analysis in the Indo-Gangetic Plains, India', *Agricultural Systems*, 104: 42-53.

FAO. 2019. 'Amid generally well-supplied cereal markets in 2018/19, wheat output is seen rebounding in 2019', Accessed 14/3/19. http://www.fao.org/worldfoodsituation/csdb/en/.

Feng, Feng, Fan Yang, Wei Rong, Xiaogang Wu, Jie Zhang, She Chen, Chaozu He, and Jian-Min Zhou. 2012. 'A Xanthomonas uridine 5′-monophosphate transferase inhibits plant immune kinases', *Nature*, 485: 114-18.

Feng, Hao, Wei Liu, Qiong Zhang, Xiaojie Wang, Xiaodong Wang, Xiaoyuan Duan, Feng Li, Lili Huang, and Zhensheng Kang. 2014. 'TaMDHAR4, a monodehydroascorbate reductase gene participates in the interactions between wheat and Puccinia striiformis f. sp. tritici', *Plant Physiology and Biochemistry*, 76: 7-16.

Fernandez, Jessie, and Kim Orth. 2018. 'Rise of a cereal killer: the biology of Magnaporthe oryzae biotrophic growth', *Trends in Microbiology*, 26: 582-97.

Fernandez, Jessie, and Richard A Wilson. 2014. 'Cells in cells: morphogenetic and metabolic strategies conditioning rice infection by the blast fungus Magnaporthe oryzae', *Protoplasma*, 251: 37-47.

Ferreira, Jéssica Rosset, Gisele Abigail Montan Torres, Luciano Consoli, Eliseu Binneck, Gabriela Andriolio Camilotti, Sandra Maria Mansur Scagliusi, Carolina Cardoso Deuner, Alexei de Campos Dianese, Augusto César Pereira Goulart, and Claudine Dinali Santos Seixas. 2020. 'Genetic and molecular basis of wheat–Magnaporthe oryzae Triticum interaction.' in, *Wheat blast* (CRC Press).

Foster, Andrew J , Vincent M Were, Xia Yan, Joe Win, Adeline Harant, Thorsten Langner, Sophien Kamoun, and Nicholas J Talbot. 2021. 'MagnaGenes (v.1.0): an open science database of gene function studies in the blast fungus Magnaporthe oryzae', *Zenodo*.

Foster, Andrew J, Lauren S Ryder, Michael J Kershaw, and Nicholas J Talbot. 2017. 'The role of glycerol in the pathogenic lifestyle of the rice blast fungus Magnaporthe oryzae', *Environmental Microbiology*, 19: 1008-16.

Frantzeskakis, Lamprinos, Barbara Kracher, Stefan Kusch, Makoto Yoshikawa-Maekawa, Saskia Bauer, Carsten Pedersen, Pietro D Spanu, Takaki Maekawa, Paul Schulze-Lefert, and Ralph Panstruga. 2018. 'Signatures of host specialization and a recent transposable element burst in the dynamic one-speed genome of the fungal barley powdery mildew pathogen', *BMC Genomics*, 19: 1-23.

Frías, Marcos, Nélida Brito, Mario González, and Celedonio González. 2014. 'The phytotoxic activity of the cerato-platanin BcSpl1 resides in a two-peptide motif on the protein surface', *Molecular Plant Pathology*, 15: 342-51.

Frías, Marcos, Celedonio González, and Nélida Brito. 2011. 'BcSpl1, a cerato-platanin family protein, contributes to Botrytis cinerea virulence and elicits the hypersensitive response in the host', *New Phytologist*, 192: 483-95.

Fukuoka, S, and K Okuno. 1997. '33. QTL analysis for Field resistance to rice blast using RFLP markers'.

Fukuoka, Shuichi, Norikuni Saka, Hironori Koga, Kazuko Ono, Takehiko Shimizu, Kaworu Ebana, Nagao Hayashi, Akira Takahashi, Hirohiko Hirochika, and Kazutoshi Okuno. 2009. 'Loss of function of a proline-containing protein confers durable disease resistance in rice', *Science*, 325: 998-1001.

Gassmann, Walter, Matthew E Hinsch, and Brian J Staskawicz. 1999. 'The Arabidopsis RPS4 bacterial-resistance gene is a member of the TIR-NBS-LRR family of disease-resistance genes', *The Plant Journal*, 20: 265-77.

Gaurav, Kumar, Sanu Arora, Paula Silva, Javier Sánchez-Martín, Richard Horsnell, Liangliang Gao, Gurcharn S Brar, Victoria Widrig, W John Raupp, and Narinder Singh. 2022. 'Population genomic analysis of Aegilops tauschii identifies targets for bread wheat improvement', *Nature Biotechnology*, 40: 422-31.

GCARD. 2012. "National Food Security – The Wheat Initiative – an International Research Initiative for Wheat Improvement." In *Second Global Conference on Agricultural Research for Development (GCARD)*. Punta del Este, Uraguay.

Ghatak, Abhijeet, Laetitia Willocquet, Serge Savary, and Jatinder Kumar. 2013. 'Variability in aggressiveness of rice blast (Magnaporthe oryzae) isolates originating from rice leaves and necks: a case of pathogen specialization?', *PloS one*, 8: e66180.

Gijzen, Mark, and Thorsten Nürnberger. 2006. 'Nep1-like proteins from plant pathogens: recruitment and diversification of the NPP1 domain across taxa', *Phytochemistry*, 67: 1800-07.

Giles, Rachel J, and Terence A Brown. 2006. 'GluDy allele variations in Aegilops tauschii and Triticum aestivum: implications for the origins of hexaploid wheats', *Theoretical and Applied Genetics*, 112: 1563-72.

Giraud, Tatiana, Pierre Gladieux, and Sergey Gavrilets. 2010. 'Linking the emergence of fungal plant diseases with ecological speciation', *Trends in Ecology & Evolution*, 25: 387-95.

Gladieux, Pierre, Bradford Condon, Sebastien Ravel, Darren Soanes, Joao Leodato Nunes Maciel, Antonio Nhani, Li Chen, Ryohei Terauchi, Marc-Henri Lebrun, and Didier Tharreau. 2018. 'Gene flow between divergent cereal-and grass-specific lineages of the rice blast fungus Magnaporthe oryzae', *MBio*, 9: e01219-17.

Gladieux, Pierre, Sebastien Ravel, Adrien Rieux, Sandrine Cros-Arteil, Henri Adreit, Joelle Milazzo, Maud Thierry, Elisabeth Fournier, Ryohei Terauchi, and Didier Tharreau. 2018. 'Coexistence of multiple endemic and pandemic lineages of the rice blast pathogen', *MBio*, 9: e01806-17.

Goddard, Rachel, Andrew Steed, Catherine Chinoy, Jéssica Rosset Ferreira, Pedro Luiz Scheeren, João Leodato Nunes Maciel, Eduardo Caierão, Gisele Abigail Montan Torres, Luciano Consoli, and Flavio Martins Santana. 2020. 'Dissecting the genetic basis of wheat blast resistance in the Brazilian wheat cultivar BR 18-Terena', *BMC Plant Biology*, 20: 1-15.

Goulart, ACP, F de A Paiva, and AN de Mesquita. 1990. 'Occurrence of wheat blast (Pyricularia oyzae) in the state of Mato Grosso do Sul, Brazil', *Fitopatologia Brasileira (Brazil)*.

Gupta, Sanjiv, Elysia Vassos, Beata Sznajder, Rebecca Fox, Kelvin HP Khoo, Robert Loughman, Kenneth J Chalmers, and Diane E Mather. 2018. 'A locus on barley chromosome 5H affects adult plant resistance to powdery mildew', *Molecular Breeding*, 38: 103.

Gupta, Yogesh K, Yasin F Dagdas, Ana-Lilia Martinez-Rocha, Michael J Kershaw, George R Littlejohn, Lauren S Ryder, Jan Sklenar, Frank Menke, and Nicholas J Talbot. 2015. 'Septin-dependent assembly of the exocyst is essential for plant infection by Magnaporthe oryzae', *The Plant Cell*, 27: 3277-89.

Hamer, John E, Richard J Howard, Forrest G Chumley, and Barbara Valent. 1988. 'A mechanism for surface attachment in spores of a plant pathogenic fungus', *science*, 239: 288-90.

Hao, Ming, Lianquan Zhang, Shunzong Ning, Lin Huang, Zhongwei Yuan, Bihua Wu, Zehong Yan, Shoufen Dai, Bo Jiang, and Youliang Zheng. 2020. 'The resurgence of introgression breeding, as exemplified in wheat improvement', *Frontiers in plant science*, 11: 252.

Hao, Yuanfeng, Aifeng Liu, Yuhai Wang, Deshun Feng, Jurong Gao, Xingfeng Li, Shubing Liu, and Honggang Wang. 2008. 'Pm23: a new allele of Pm4 located on chromosome 2AL in wheat', *Theoretical and Applied Genetics*, 117: 1205-12.

Haudry, Annabelle, Alberto Cenci, Catherine Ravel, Thomas Bataillon, Dominique Brunel, Charles Poncet, Isabelle Hochu, Sebastien Poirier, Sylvain Santoni, and Sylvain Glémin. 2007. 'Grinding up wheat: a massive loss of nucleotide diversity since domestication', *Molecular Biology and Evolution*, 24: 1506-17.

Helguera, Marcelo, IA Khan, James Kolmer, D Lijavetzky, L Zhong-Qi, and Jorge Dubcovsky. 2003. 'PCR assays for the Lr37-Yr17-Sr38 cluster of rust resistance genes and their use to develop isogenic hard red spring wheat lines', *Crop Science*, 43: 1839-47.

Herrera-Foessel, Sybil A, Evans S Lagudah, Julio Huerta-Espino, Matthew J Hayden, Harbans S Bariana, Davinder Singh, and Ravi P Singh. 2011. 'New slow-rusting leaf rust and stripe rust resistance genes Lr67 and Yr46 in wheat are pleiotropic or closely linked', *Theoretical and Applied Genetics*, 122: 239-49.

Herrera-Foessel, Sybil A, Ravi P Singh, Morten Lillemo, Julio Huerta-Espino, Sridhar Bhavani, Sukhwinder Singh, Caixia Lan, Violeta Calvo-Salazar, and Evans S Lagudah. 2014. 'Lr67/Yr46 confers adult plant resistance to stem rust and powdery mildew in wheat', *Theoretical and Applied Genetics*, 127: 781-89.

Hickey, Lee T, Wendy Lawson, Greg J Platz, Mark Dieters, and Jerome Franckowiak. 2012. 'Origin of leaf rust adult plant resistance gene Rph20 in barley', *Genome*, 55: 396-99.

Hickman, Alison B, and Fred Dyda. 2015. 'Mechanisms of DNA transposition', *Microbiology spectrum*, 3: 3.2. 12.

Hiebert, Colin W, Julian B Thomas, Brent D McCallum, D Gavin Humphreys, Ronald M DePauw, Matthew J Hayden, Rohit Mago, Wendelin Schnippenkoetter, and Wolfgang Spielmeyer. 2010. 'An introgression on wheat chromosome 4DL in RL6077 (Thatcher* 6/PI 250413) confers adult plant resistance to stripe rust and leaf rust (Lr67)', *Theoretical and Applied Genetics*, 121: 1083-91.

Hirata, Kenji, Yukio Tosa, Hitoshi Nakayashiki, and Shigeyuki Mayama. 2005. 'Significance of PWT4–Rwt4 interaction in the species specificity of Avena isolates of Magnaporthe oryzae on wheat', *Journal of general plant pathology*, 71: 340-44.

Horo, Jemal Tola, Soichiro Asuke, Trinh Thi Phuong Vy, and Yukio Tosa. 2020. 'Effectiveness of the Wheat Blast Resistance Gene Rmg8 in Bangladesh Suggested by Distribution of an AVR-Rmg8 Allele in the Pyricularia oryzae Population', *Phytopathology®*: PHYTO-03-20-0073-R.

Hossain, Akbar, Khondoker Abdul Mottaleb, Md Farhad, and Naresh Chandra Deb Barma. 2019. 'Mitigating the twin problems of malnutrition and wheat blast by one wheat variety,'BARI Gom 33', in Bangladesh'.

Hossain, Akbar, and Jaime A Teixeira da Silva. 2013. 'Wheat production in Bangladesh: its future in the light of global warming', *AoB Plants*, 5.

Hu, Ke-Ming, De-Yun Qiu, Xiang-Ling Shen, Xiang-Hua Li, and Shi-Ping Wang. 2008. 'Isolation and manipulation of quantitative trait loci for disease resistance in rice using a candidate gene approach', *Molecular plant*, 1: 786-93.

Hückelhoven, Ralph, and Ralph Panstruga. 2011. 'Cell biology of the plant–powdery mildew interaction', *Current Opinion in Plant Biology*, 14: 738-46.

Hulbert, SH, J Bai, JP Fellers, MG Pacheco, and RL Bowden. 2007. 'Gene expression patterns in near isogenic lines for wheat rust resistance gene Lr34/Yr18', *Phytopathology*, 97: 1083-93.

Huot, Bethany, Christian Danve M Castroverde, André C Velásquez, Emily Hubbard, Jane A Pulman, Jian Yao, Kevin L Childs, Kenichi Tsuda, Beronda L Montgomery, and Sheng Yang He. 2017. 'Dual impact of elevated temperature on plant defence and bacterial virulence in Arabidopsis', *Nature communications*, 8: 1808.

Igarashi, S. 1990. "Update on wheat blast (Pyricularia oryzae) in Brazil." In *A Proceeding of the International Conference-Wheat for the Nontaditional Warm Areas*, 480-83.

Igarashi, S, CM Utiamada, LC Igarashi, AH Kazuma, and RS Lopes. 1986. 'Pyricularia in wheat. 1. Occurrence of Pyricularia sp', *Paran state. Fitopatol. Bras*, 11: 351-52.

Inoue, Yoshihiro, Trinh T. P. Vy, Kentaro Yoshida, Hokuto Asano, Chikako Mitsuoka, Soichiro Asuke, Vu L. Anh, Christian J. R. Cumagun, Izumi Chuma, Ryohei Terauchi, Kenji Kato, Thomas Mitchell, Barbara Valent, Mark Farman, and Yukio Tosa. 2017. 'Evolution of the wheat blast fungus through functional losses in a host specificity determinant', *science*, 357: 80-82.

Inoue, Yoshihiro, Trinh Thi Phuoug Vy, Daichi Tani, and Yukio Tosa. 2020. 'Suppression of wheat blast resistance by an effector of Pyricularia oryzae is counteracted by a host specificity resistance gene in wheat', *New Phytologist*, 229: 488-500.

International Wheat Genome Sequencing, Consortium. 2014. 'A chromosome-based draft sequence of the hexaploid bread wheat (Triticum aestivum) genome', *science*, 345: 1251788.

Islam, M. T., D. Croll, P. Gladieux, D. M. Soanes, A. Persoons, P. Bhattacharjee, M. S. Hossain, D. R. Gupta, M. M. Rahman, M. G. Mahboob, N. Cook, M. U. Salam, M. Z. Surovy, V. B. Sancho, J. L. Maciel, A. NhaniJunior, V. L. Castroagudin, J. T. Reges, P. C. Ceresini, S. Ravel, R. Kellner, E. Fournier, D. Tharreau, M. H. Lebrun, B. A. McDonald, T. Stitt, D. Swan, N. J. Talbot, D. G. Saunders, J. Win, and S. Kamoun. 2016. 'Emergence of wheat blast in Bangladesh was caused by a South American lineage of Magnaporthe oryzae', *BMC Biology*, 14: 84.

Islam, M. T., Kwang-Hyung Kim, and Jaehyuk Choi. 2019. 'Wheat Blast in Bangladesh: The Current Situation and Future Impacts', *The Plant Pathology Journal*, 35.

IWGSC, Rudi Appels, Kellye Eversole, Nils Stein, Catherine Feuillet, Beat Keller, Jane Rogers, Curtis J Pozniak, Frederic Choulet, and Assaf Distelfeld. 2018. 'Shifting the limits in wheat research and breeding using a fully annotated reference genome', *science*, 361: eaar7191.

Jahier, J, P Abelard, M Tanguy, F Dedryver, R Rivoal, S Khatkar, HS Bariana, and R Koebner. 2001. 'The Aegilops ventricosa segment on chromosome 2AS of the wheat cultivar 'VPM1'carries the cereal cyst nematode resistance gene Cre5', *Plant Breeding*, 120: 125-28.

Jankovics, Tünde, Judit Komáromi, Attila Fábián, Katalin Jäger, Gyula Vida, and Levente Kiss. 2015. 'New insights into the life cycle of the wheat powdery mildew: direct observation of ascosporic infection in Blumeria graminis f. sp. tritici', *Phytopathology*, 105: 797-804.

Jensen, Cassandra, and Diane GO Saunders. 2023. 'Magnaporthe oryzae pathotype Triticum (MoT) can act as a heterologous expression system for fungal effectors with high transcript abundance in wheat', *Scientific Reports*, 13: 108.

Jensen, Cassandra, Yukio Tosa, M Tofazzal Islam, Nicholas J Talbot, Sophien Kamoun, and Diane GO Saunders. 2019. 'Rmg8 confers resistance to the Bangladeshi lineage of the wheat blast fungus. '.

Johal, Gurmukh S, and Steven P Briggs. 1992. 'Reductase activity encoded by the HM1 disease resistance gene in maize', *science*, 258: 985-87.

Jones, Jonathan D. G., and Jeffery L. Dangl. 2006. 'The plant immune system', *Nature*, 444: 323-29.

Juliana, Philomin, Ravi P Singh, Pawan K Singh, Jose Crossa, Julio Huerta-Espino, Caixia Lan, Sridhar Bhavani, Jessica E Rutkoski, Jesse A Poland, and Gary C Bergstrom. 2017. 'Genomic and pedigree-based prediction for leaf, stem, and stripe rust resistance in wheat', *Theoretical and Applied Genetics*, 130: 1415-30.

Jupe, F., K. Witek, W. Verweij, J. Sliwka, L. Pritchard, G. J. Etherington, D. Maclean, P. J. Cock, R. M. Leggett, G. J. Bryan, L. Cardle, I. Hein, and J. D. Jones. 2013. 'Resistance gene enrichment sequencing (RenSeq) enables reannotation of the NB-LRR gene family from sequenced plant genomes and rapid mapping of resistance loci in segregating populations', *Plant Journal*, 76: 530-44.

Kang, Seogchan, James A Sweigard, and Barbara Valent. 1995. 'The PWL host specificity gene family in the blast fungus Magnaporthe grisea', *MPMI-Molecular Plant Microbe Interactions*, 8: 939-48.

Kankanala, Prasanna, Kirk Czymmek, and Barbara Valent. 2007. 'Roles for rice membrane dynamics and plasmodesmata during biotrophic invasion by the blast fungus', *The Plant Cell*, 19: 706-24.

Kato, Hajime, Masaaki Yamamoto, Tomona Yamaguchi-Ozaki, Hiroyuki Kadouchi, Yutaka Iwamoto, Hitoshi Nakayashiki, Tosa Yukio, Shigeyuki Mayama, and Mori Naoki. 2000. 'Pathogenicity, mating ability and DNA restriction fragment length polymorphisms of Pyricularia populations isolated from Gramineae, Bambusideae and Zingiberaceae plants', *Journal of general plant pathology*, 66: 30-47.

Kema, GHJ, W Lange, and CH Van Silfhout. 1995. 'Differential suppression of stripe rust resistance in synthetic wheat hexaploids derived from Triticum turgidum subsp. dicoccoides and Aegilops squarrosa', *Phytopathology (USA)*.

Kerber, ER. 1987. 'Resistance to Leaf Rust in Hexaploid Wheat: Lr32 a Third Gene Derived from Triticum tauschii 1', *Crop Science*, 27: 204-06.

Khang, Chang Hyun, Romain Berruyer, Martha C Giraldo, Prasanna Kankanala, Sook-Young Park, Kirk Czymmek, Seogchan Kang, and Barbara Valent. 2010. 'Translocation of Magnaporthe oryzae effectors into rice cells and their subsequent cell-to-cell movement', *The Plant Cell*, 22: 1388-403.

Kishii, Masahiro. 2019. 'An update of recent use of Aegilops species in wheat breeding', *Frontiers in plant science*, 10: 585.

Klindworth, Daryl L, Zhixia Niu, Shiaoman Chao, Timothy L Friesen, Yue Jin, Justin D Faris, Xiwen Cai, and Steven S Xu. 2012. 'Introgression and characterization of a goatgrass gene for a high level of resistance to Ug99 stem rust in tetraploid wheat', *G3: Genes| Genomes| Genetics*, 2: 665-73.

Kohli, MM, YR Mehta, E Guzman, L De Viedma, and LE Cubilla. 2011. 'Pyricularia blast-a threat to wheat cultivation', *Czech J. Genet. Plant Breed*, 47: S130-S34.

Kolmer, JA, ES Lagudah, M Lillemo, M Lin, and G Bai. 2015. 'The Lr46 gene conditions partial adult-plant resistance to stripe rust, stem rust, and powdery mildew in Thatcher wheat', *Crop Science*, 55: 2557-65.

Kolodziej, Markus C, Jyoti Singla, Javier Sánchez-Martín, Helen Zbinden, Hana Šimková, Miroslava Karafiátová, Jaroslav Doležel, Julien Gronnier, Manuel Poretti, and Gaétan Glauser. 2021. 'A membrane-bound ankyrin repeat protein confers race-specific leaf rust disease resistance in wheat', *Nature communications*, 12: 956.

Kong, Lingyao, and Cheng Chang. 2018. 'Suppression of wheat TaCDK8/TaWIN1 interaction negatively affects germination of Blumeria graminis f. sp. tritici by interfering with very-long-chain aldehyde biosynthesis', *Plant Molecular Biology*, 96: 165-78.

Kourelis, Jiorgos, and Renier AL Van Der Hoorn. 2018. 'Defended to the nines: 25 years of resistance gene cloning identifies nine mechanisms for R protein function', *The Plant Cell*, 30: 285-99.

Krattinger, Simon G, Evans S Lagudah, Wolfgang Spielmeyer, Ravi P Singh, Julio Huerta-Espino, Helen McFadden, Eligio Bossolini, Liselotte L Selter, and Beat Keller. 2009. 'A putative ABC transporter confers durable resistance to multiple fungal pathogens in wheat', *science*, 323: 1360-63.

Kulkarni, Resham D, Hemant S Kelkar, and Ralph A Dean. 2003. 'An eight-cysteine-containing CFEM domain unique to a group of fungal membrane proteins', *Trends in Biochemical Sciences*, 28: 118-21.

Lagudah, Evans S, Simon G Krattinger, Sybil Herrera-Foessel, Ravi P Singh, Julio Huerta-Espino, Wolfgang Spielmeyer, Gina Brown-Guedira, Liselotte L Selter, and Beat Keller. 2009. 'Gene-specific markers for the wheat gene Lr34/Yr18/Pm38 which confers resistance to multiple fungal pathogens', *Theoretical and Applied Genetics*, 119: 889-98.

Le Roux, Clémentine, Gaëlle Huet, Alain Jauneau, Laurent Camborde, Dominique Trémousaygue, Alexandra Kraut, Binbin Zhou, Marie Levaillant, Hiroaki Adachi, and Hirofumi Yoshioka. 2015. 'A receptor pair with an integrated decoy converts pathogen disabling of transcription factors to immunity', *Cell*, 161: 1074-88.

Lee, Sang-Kyu, Min-Young Song, Young-Su Seo, Hye-Kyung Kim, Seho Ko, Pei-Jian Cao, Jung-Pil Suh, Gihwan Yi, Jae-Hwan Roh, and Sichul Lee. 2009. 'Rice Pi5-mediated resistance to Magnaporthe oryzae requires the presence of two coiled-coil–nucleotide-binding–leucine-rich repeat genes', *Genetics*, 181: 1627-38.

Leonard, Kurt J, and Les J Szabo. 2005. 'Stem rust of small grains and grasses caused by Puccinia graminis', *Molecular Plant Pathology*, 6: 99-111.

Lewis, Jennifer D, Amy Huei-Yi Lee, Jana A Hassan, Janet Wan, Brenden Hurley, Jacquelyn R Jhingree, Pauline W Wang, Timothy Lo, Ji-Young Youn, and David S Guttman. 2013. 'The Arabidopsis ZED1 pseudokinase is required for ZAR1-mediated immunity induced by the Pseudomonas syringae type III effector HopZ1a', *Proceedings of the National Academy of Sciences*, 110: 18722-27.

Li, Chao, Guoxiong Chen, Kohei Mishina, Naoki Yamaji, Jian Feng Ma, Fumiko Yukuhiro, Akemi Tagiri, Cheng Liu, Mohammad Pourkheirandish, and Nadia Anwar. 2017. 'A GDSL-motif esterase/acyltransferase/lipase is responsible for leaf water retention in barley', *Plant Direct*, 1: e00025.

Li, Hao, Karin R Deal, Ming-Cheng Luo, Wanquan Ji, Assaf Distelfeld, and Jan Dvorak. 2017. 'Introgression of the Aegilops speltoides Su1-Ph1 suppressor into wheat', *Frontiers in plant science*, 8: 2163.

Li, Mengmeng, Zige Yang, and Cheng Chang. 2022. 'Susceptibility is new resistance: wheat susceptibility genes and exploitation in resistance breeding', *Agriculture*, 12: 1419.

Li, Na, Haiyan Jia, Zhongxin Kong, Wenbin Tang, Yunxiao Ding, Junchao Liang, Hongqi Ma, and Zhengqiang Ma. 2017. 'Identification and marker-assisted transfer of a new powdery mildew resistance gene at the Pm4 locus in common wheat', *Molecular Breeding*, 37: 1-9.

Li, Weitao, Mawsheng Chern, Junjie Yin, Jing Wang, and Xuewei Chen. 2019. 'Recent advances in broad-spectrum resistance to the rice blast disease', *Current Opinion in Plant Biology*, 50: 114-20.

Li, Weitao, Kang Wang, Mawsheng Chern, Yuchen Liu, Ziwei Zhu, Jiang Liu, Xiaobo Zhu, Junjie Yin, Li Ran, and Jun Xiong. 2020. 'Sclerenchyma cell thickening through enhanced lignification induced by OsMYB30 prevents fungal penetration of rice leaves', *New Phytologist*, 226: 1850-63.

Li, Weitao, Ziwei Zhu, Mawsheng Chern, Junjie Yin, Chao Yang, Li Ran, Mengping Cheng, Min He, Kang Wang, and Jing Wang. 2017. 'A natural allele of a transcription factor in rice confers broad-spectrum blast resistance', *Cell*, 170: 114-26. e15.

Li, Yuxiang, Lu Liu, Meinan Wang, Travis Ruff, Deven R See, Xiaoping Hu, and Xianming Chen. 2023. 'Characterization and Molecular Mapping of a Gene Conferring High-temperature Adult-plant Resistance to Stripe Rust Originally from Aegilops ventricosa', *Plant Disease*: PDIS-06-22-1419-RE.

Li, Zhan, Huimin Liu, Zehong Ding, Jiapei Yan, Huiyun Yu, Ronghui Pan, Jin Hu, Yajing Guan, and Jian Hua. 2020. 'Low temperature enhances plant immunity via salicylic acid pathway genes that are repressed by ethylene', *Plant Physiology*, 182: 626-39.

Liang, Xiangxiu, and Jian-Min Zhou. 2018. 'Receptor-like cytoplasmic kinases: central players in plant receptor kinase–mediated signaling', *Annual Review of Plant Biology*, 69: 267-99.

Lillemo, M, B Asalf, RP Singh, J Huerta-Espino, XM Chen, ZH He, and Å Bjørnstad. 2008. 'The adult plant rust resistance loci Lr34/Yr18 and Lr46/Yr29 are important determinants of partial resistance to powdery mildew in bread wheat line Saar', *Theoretical and Applied Genetics*, 116: 1155-66.

Lin, Min, Beatrice Corsi, Andrea Ficke, Kar-Chun Tan, James Cockram, and Morten Lillemo. 2020. 'Genetic mapping using a wheat multi-founder population reveals a locus on chromosome 2A controlling resistance to both leaf and glume blotch caused by the necrotrophic fungal pathogen Parastagonospora nodorum', *Theoretical and Applied Genetics*, 133: 785-808.

Liu, G, G Lu, L Zeng, and G-L Wang. 2002. 'Two broad-spectrum blast resistance genes, Pi9 (t) and Pi2 (t), are physically linked on rice chromosome 6', *Molecular Genetics and Genomics*, 267: 472-80.

Liu, JQ, and JA Kolmer. 1998. 'Genetics of stem rust resistance in wheat cvs. Pasqua and AC Taber', *Phytopathology*, 88: 171-76.

Liu, Zhi-qin, Ai-lian Qiu, Lan-ping Shi, Jin-sen Cai, Xue-ying Huang, Sheng Yang, Bo Wang, Lei Shen, Mu-kun Huang, and Shao-liang Mou. 2015. 'SRC2-1 is required in PcINF1-induced pepper immunity by acting as an interacting partner of PcINF1', *Journal of Experimental Botany*, 66: 3683-98.

Lu, Dongping, Shujing Wu, Xiquan Gao, Yulan Zhang, Libo Shan, and Ping He. 2010. 'A receptor-like cytoplasmic kinase, BIK1, associates with a flagellin receptor complex to initiate plant innate immunity', *Proceedings of the National Academy of Sciences*, 107: 496-501.

Luo, Ming-Cheng, Yong Q Gu, Daniela Puiu, Hao Wang, Sven O Twardziok, Karin R Deal, Naxin Huo, Tingting Zhu, Le Wang, and Yi Wang. 2017. 'Genome sequence of the progenitor of the wheat D genome Aegilops tauschii', *Nature*, 551: 498.

Ma, H, RP Singh, and A Mujeeb-Kazi. 1995. 'Resistance to stripe rust in Triticum turgidum, T. tauschii and their synthetic hexaploids', *Euphytica*, 82: 117-24.

Ma, Yan, Hailong Guo, Lanxi Hu, Paula Pons Martinez, Panagiotis N Moschou, Volkan Cevik, Pingtao Ding, Zane Duxbury, Panagiotis F Sarris, and Jonathan DG Jones. 2018. 'Distinct modes of derepression of an Arabidopsis immune receptor complex by two different bacterial effectors', *Proceedings of the National Academy of Sciences*, 115: 10218-27.

Maciel, J. L. N., P. C. Ceresini, V. L. Castroagudin, M. Zala, G. H. J. Kema, and B. A. McDonald. 2014. 'Population Structure and Pathotype Diversity of the Wheat Blast Pathogen Magnaporthe oryzae 25 Years After Its Emergence in Brazil', *Phytopathology*, 104: 95-107.

Maciel, Joao L Nunes. 2011. 'Magnaporthe oryzae, the blast pathogen: current status and options for its control', *Plant Sci. Rev*, 264: 233-40.

Malaker, Paritosh K, NC Barma, TP Tiwary, William J Collis, EP Duveiller, K Singh, Arun Kumar Joshi, Ravi P Singh, Hans-Joachim Braun, and Gary L Peterson. 2016. 'First report of wheat blast caused by Magnaporthe oryzae pathotype triticum in Bangladesh', *Plant Disease*, 100: 2330.

Marcel, Sylvain, Ruairidh Sawers, Edward Oakeley, Herbert Angliker, and Uta Paszkowski. 2010. 'Tissue-adapted invasion strategies of the rice blast fungus Magnaporthe oryzae', *The Plant Cell*, 22: 3177-87.

Marchler-Bauer, Aron, and Stephen H Bryant. 2004. 'CD-Search: protein domain annotations on the fly', *Nucleic Acids Research*, 32: W327-W31.

Marchler-Bauer, Aron, Shennan Lu, John B Anderson, Farideh Chitsaz, Myra K Derbyshire, Carol DeWeese-Scott, Jessica H Fong, Lewis Y Geer, Renata C Geer, and Noreen R Gonzales. 2010. 'CDD: a Conserved Domain Database for the functional annotation of proteins', *Nucleic Acids Research*, 39: D225-D29.

Marcussen, Thomas, Simen R Sandve, Lise Heier, Manuel Spannagl, Matthias Pfeifer, Kjetill S Jakobsen, Brande BH Wulff, Burkhard Steuernagel, Klaus FX Mayer, and Odd-Arne Olsen. 2014. 'Ancient hybridizations among the ancestral genomes of bread wheat', *science*, 345: 1250092.

Marone, Daniela, Monica Rodriguez, Sergio Saia, Roberto Papa, Domenico Rau, Ivano Pecorella, Giovanni Laidò, Nicola Pecchioni, Julia Lafferty, and Matthias Rapp. 2020. 'Genome-wide association mapping of prostrate/erect growth habit in winter durum wheat', *International journal of molecular sciences*, 21: 394.

Matsuoka, Yoshihiro. 2011. 'Evolution of polyploid Triticum wheats under cultivation: the role of domestication, natural hybridization and allopolyploid speciation in their diversification', *Plant and cell physiology*, 52: 750-64.

Maxted, Nigel, Brian V Ford-Lloyd, Stephen Jury, Shelagh Kell, and Maria Scholten. 2006. 'Towards a definition of a crop wild relative', *Biodiversity & Conservation*, 15: 2673-85.

Maxted, Nigel, Shelagh Kell, Brian Ford-Lloyd, Ehsan Dulloo, and Álvaro Toledo. 2012. 'Toward the systematic conservation of global crop wild relative diversity', *Crop Science*, 52: 774-85.

McIntosh, RA, and Fiona GA Bennett. 1979. 'Cytogenetical studies in wheat. IX. Monosomic analyses, telocentric mapping and linkage relationships of genes Sr21, Pm4 and Mle', *Australian Journal of Biological Sciences*, 32: 115-26.

McIntosh, Robert Alexander, Colin Ross Wellings, and Robert Fraser Park. 1995. *Wheat rusts: an atlas of resistance genes* (CSIRO publishing).

Mendgen, Kurt, and Matthias Hahn. 2002. 'Plant infection and the establishment of fungal biotrophy', *Trends in Plant Science*, 7: 352-56.

Mentlak, Thomas A, Anja Kombrink, Tomonori Shinya, Lauren S Ryder, Ippei Otomo, Hiromasa Saitoh, Ryohei Terauchi, Yoko Nishizawa, Naoto Shibuya, and Bart PHJ Thomma. 2012. 'Effector-mediated suppression of chitin-triggered immunity by Magnaporthe oryzae is necessary for rice blast disease', *The Plant Cell*, 24: 322-35.

Miranda, L M, J P Murphy, David Marshall, and S Leath. 2006. 'Pm34: a new powdery mildew resistance gene transferred from Aegilops tauschii Coss. to common wheat (Triticum aestivum L.)', *Theoretical and Applied Genetics*, 113: 1497-504.

Mizuno, Nobuyuki, Masanori Yamasaki, Yoshihiro Matsuoka, Taihachi Kawahara, and Shigeo Takumi. 2010. 'Population structure of wild wheat D-genome progenitor Aegilops tauschii Coss.: implications for intraspecific lineage diversification and evolution of common wheat', *Molecular Ecology*, 19: 999-1013.

Monino-Lopez, Daniel, Maarten Nijenhuis, Linda Kodde, Sophien Kamoun, Hamed Salehian, Kyrylo Schentsnyi, Remco Stam, Anoma Lokossou, Ahmed Abd-El-Haliem, and Richard GF Visser. 2021. 'Allelic variants of the NLR protein Rpi-chc1 differentially recognize members of the Phytophthora infestans PexRD12/31 effector superfamily through the leucine-rich repeat domain', *The Plant Journal*, 107: 182-97.

Moore, John W, Sybil Herrera-Foessel, Caixia Lan, Wendelin Schnippenkoetter, Michael Ayliffe, Julio Huerta-Espino, Morten Lillemo, Libby Viccars, Ricky Milne, and Sambasivam Periyannan. 2015. 'A recently evolved hexose transporter variant confers resistance to multiple pathogens in wheat', *Nature Genetics*, 47: 1494-98.

Moreira, Silvino Intra, Paulo Cézar Ceresini, and Eduardo Alves. 2015. 'Sexual reproduction in Pyricularia oryzae', *Summa Phytopathologica*, 41: 175-82.

Mottaleb, K. A., P. K. Singh, K. Sonder, G. Kruseman, T. P. Tiwari, N. C. D. Barma, P. K. Malaker, H. J. Braun, and O. Erenstein. 2018. 'Threat of wheat blast to South Asia's food security: An ex-ante analysis', *PloS one*, 13: e0197555.

Mukhi, Nitika, Hannah Brown, Danylo Gorenkin, Pingtao Ding, Adam R Bentham, Clare EM Stevenson, Jonathan DG Jones, and Mark J Banfield. 2021. 'Perception of structurally distinct effectors by the integrated WRKY domain of a plant immune receptor', *Proceedings of the National Academy of Sciences*, 118: e2113996118.

Murakami, J, Y Tosa, T Kataoka, R Tomita, J Kawasaki, I Chuma, Y Sesumi, M Kusaba, H Nakayashiki, and S Mayama. 2000. 'Analysis of host species specificity of Magnaporthe grisea toward wheat using a genetic cross between isolates from wheat and foxtail millet', *Phytopathology*, 90: 1060-67.

NABIM. 2019. 'Wheat', Accessed 14/3/19. http://www.nabim.org.uk/wheat.

Narusaka, Mari, Satoshi Iuchi, and Yoshihiro Narusaka. 2017. 'Analyses of natural variation indicates that the absence of RPS4/RRS1 and amino acid change in RPS4 cause loss of their functions and resistance to pathogens', *Plant signaling & behavior*, 12: e1293218.

Narusaka, Mari, Yasuyuki Kubo, Katsunori Hatakeyama, Jun Imamura, Hiroshi Ezura, Yoshihiko Nanasato, Yutaka Tabei, Yoshitaka Takano, Ken Shirasu, and Yoshihiro Narusaka. 2013. 'Interfamily transfer of dual NB-LRR genes confers resistance to multiple pathogens', *PloS one*, 8: e55954.

Narusaka, Mari, Ken Shirasu, Yoshiteru Noutoshi, Yasuyuki Kubo, Tomonori Shiraishi, Masaki Iwabuchi, and Yoshihiro Narusaka. 2009. 'RRS1 and RPS4 provide a dual Resistance-gene system against fungal and bacterial pathogens', *The Plant Journal*, 60: 218-26.

Nelson, Andy. 2017. 'Crop pests: Crop-health survey aims to fill data gaps', *Nature*, 541: 464.

Nelson, Rebecca, Tyr Wiesner-Hanks, Randall Wisser, and Peter Balint-Kurti. 2018. 'Navigating complexity to breed disease-resistant crops', *Nature Reviews Genetics*, 19: 21-33.

Nga, NTT, VTB Hau, and Y Tosa. 2009. 'Identification of genes for resistance to a Digitaria isolate of Magnaporthe grisea in common wheat cultivars', *Genome*, 52: 801-09.

Ngou, Bruno Pok Man, Pingtao Ding, and Jonathan DG Jones. 2022. 'Thirty years of resistance: Zig-zag through the plant immune system', *The Plant Cell*, 34: 1447-78.

O'Connell, Richard J, and Ralph Panstruga. 2006. 'Tête à tête inside a plant cell: establishing compatibility between plants and biotrophic fungi and oomycetes', *New Phytologist*, 171: 699-718.

Oerke, E-C. 2006. 'Crop losses to pests', *The Journal of Agricultural Science*, 144: 31-43.

Ogbonnaya, Francis C, Osman Abdalla, Abdul Mujeeb-Kazi, Alvina G Kazi, Steven S Xu, Nick Gosman, Evans S Lagudah, David Bonnett, Mark E Sorrells, and Hisashi Tsujimoto. 2013. 'Synthetic hexaploids: harnessing species of the primary gene pool for wheat improvement', *Plant Breed. Rev*, 37: 35-122.

Oh, HS, Y Tosa, N Takabayashi, S Nakagawa, R Tomita, LD Don, M Kusaba, H Nakayashiki, and S Mayama. 2002. 'Characterization of an Avena isolate of Magnaporthe grisea and identification of a locus conditioning its specificity on oat', *Canadian Journal of Botany*, 80: 1088-95.

Okuyama, Yudai, Hiroyuki Kanzaki, Akira Abe, Kentaro Yoshida, Muluneh Tamiru, Hiromasa Saitoh, Takahiro Fujibe, Hideo Matsumura, Matt Shenton, and Dominique Clark Galam. 2011. 'A multifaceted genomics approach allows the isolation of the rice Pia-blast resistance gene consisting of two adjacent NBS-LRR protein genes', *The Plant Journal*, 66: 467-79.

Olson, Eric L, Matthew N Rouse, Michael O Pumphrey, Robert L Bowden, Bikram S Gill, and Jesse A Poland. 2013. 'Simultaneous transfer, introgression, and genomic localization of genes for resistance to stem rust race TTKSK (Ug99) from Aegilops tauschii to wheat', *Theoretical and Applied Genetics*, 126: 1179-88.

Oome, Stan, Tom M Raaymakers, Adriana Cabral, Simon Samwel, Hannah Böhm, Isabell Albert, Thorsten Nürnberger, and Guido Van den Ackerveken. 2014. 'Nep1-like proteins from three kingdoms of life act as a microbe-associated molecular pattern in Arabidopsis', *Proceedings of the National Academy of Sciences*, 111: 16955-60.

Orozco-Arias, Simon, Gustavo Isaza, and Romain Guyot. 2019. 'Retrotransposons in plant genomes: structure, identification, and classification through bioinformatics and machine learning', *International journal of molecular sciences*, 20: 3837.

Ottmann, Christian, Borries Luberacki, Isabell Küfner, Wolfgang Koch, Frédéric Brunner, Michael Weyand, Laura Mattinen, Minna Pirhonen, Gregor Anderluh, and Hanns Ulrich Seitz. 2009. 'A common toxin fold mediates microbial attack and plant defense', *Proceedings of the National Academy of Sciences*, 106: 10359-64.

Panstruga, Ralph, and Peter N Dodds. 2009. 'Terrific protein traffic: the mystery of effector protein delivery by filamentous plant pathogens', *science*, 324: 748-50.

Papaïx, Julien, Jeremy J Burdon, Jiasui Zhan, and Peter H Thrall. 2015. 'Crop pathogen emergence and evolution in agro-ecological landscapes', *Evolutionary applications*, 8: 385-402.

Park, Chan-Ho, Songbiao Chen, Gautam Shirsekar, Bo Zhou, Chang Hyun Khang, Pattavipha Songkumarn, Ahmed J Afzal, Yuese Ning, Ruyi Wang, and Maria Bellizzi. 2012. 'The Magnaporthe oryzae effector AvrPiz-t targets the RING E3 ubiquitin ligase APIP6 to suppress pathogen-associated molecular pattern–triggered immunity in rice', *The Plant Cell*, 24: 4748-62.

Park, Robert F, Gavin J Ash, and Robert G Rees. 1992. 'Effects of temperature on the response of some Australian wheat cultivars to Puccinia striiformis f. sp. tritici', *Mycological Research*, 96: 166-70.

Park, Robert F, Prashant G Golegaonkar, Lida Derevnina, Karanjeet S Sandhu, Haydar Karaoglu, Huda M Elmansour, Peter M Dracatos, and Davinder Singh. 2015. 'Leaf rust of cultivated barley: pathology and control', *Annual Review of Phytopathology*, 53: 565-89.

Paux, Etienne, Delphine Roger, Ekatherina Badaeva, Georges Gay, Michel Bernard, Pierre Sourdille, and Catherine Feuillet. 2006. 'Characterizing the composition and evolution of homoeologous genomes in hexaploid wheat through BAC-end sequencing on chromosome 3B', *The Plant Journal*, 48: 463-74.

Peng, Zhao, Ely Oliveira-Garcia, Guifang Lin, Ying Hu, Melinda Dalby, Pierre Migeon, Haibao Tang, Mark Farman, David Cook, and Frank F White. 2019. 'Effector gene reshuffling involves dispensable mini-chromosomes in the wheat blast fungus', *PLoS Genetics*, 15: e1008272.

Petersen, Gitte, Ole Seberg, Merete Yde, and Kasper Berthelsen. 2006. 'Phylogenetic relationships of Triticum and Aegilops and evidence for the origin of the A, B, and D genomes of common wheat (Triticum aestivum)', *Molecular Phylogenetics and Evolution*, 39: 70-82.

Pont, Caroline, Thibault Leroy, Michael Seidel, Alessandro Tondelli, Wandrille Duchemin, David Armisen, Daniel Lang, Daniela Bustos-Korts, Nadia Goué, and François Balfourier. 2019. 'Tracing the ancestry of modern bread wheats', *Nature Genetics*, 51: 905-11.

Prabhu, AS, MC Filippi, and N Castro. 1992. 'Pathogenic variation among isolates of Pyricularia oryzae affecting rice, wheat, and grasses in Brazil', *International Journal of Pest Management*, 38: 367-71.

Prestes, AM, PF Arendt, JMC Fernandes, and PL Scheeren. 2007. 'Resistance to Magnaporthe grisea among Brazilian wheat genotypes.' in, *Wheat production in stressed environments* (Springer).

Qin, Peng, Yu Lin, Yaodong Hu, Kun Liu, Shuangshuang Mao, Zhanyi Li, Jirui Wang, Yaxi Liu, Yuming Wei, and Youliang Zheng. 2016. 'Genome-wide association study of drought-related resistance traits in Aegilops tauschii', *Genetics and Molecular Biology*, 39: 398-407.

Rahnama, Mostafa, Bradford Condon, Joao P Ascari, Julian R Dupuis, Emerson M Del Ponte, Kerry F Pedley, Sebastián Martinez, Barbara Valent, and Mark Farman. 2021. 'Recombination of standing variation in a multi-hybrid swarm drove adaptive radiation in a fungal pathogen and gave rise to two pandemic plant diseases', *bioRxiv*.

Reif, Jochen C, Pingzhi Zhang, Susanne Dreisigacker, Marilyn L Warburton, Maarten van Ginkel, David Hoisington, Martin Bohn, and Albrecht E Melchinger. 2005. 'Wheat genetic diversity trends during domestication and breeding', *Theoretical and Applied Genetics*, 110: 859-64.

Rey, Elodie, Michael Abrouk, Gabriel Keeble-Gagnère, Miroslava Karafiátová, Jan Vrána, Sandrine Balzergue, Ludivine Soubigou-Taconnat, Véronique Brunaud, Marie-Laure Martin-Magniette, and Takashi R Endo. 2018. 'Transcriptome reprogramming due to the introduction of a barley telosome into bread wheat affects more barley genes than wheat', *Plant Biotechnology Journal*, 16: 1767-77.

Robinson, James T, Helga Thorvaldsdóttir, Wendy Winckler, Mitchell Guttman, Eric S Lander, Gad Getz, and Jill P Mesirov. 2011. 'Integrative genomics viewer', *Nature Biotechnology*, 29: 24-26.

Ryder, Lauren S, Yasin F Dagdas, Michael J Kershaw, Chandrasekhar Venkataraman, Anotida Madzvamuse, Xia Yan, Neftaly Cruz-Mireles, Darren M Soanes, Miriam Oses-Ruiz, and Vanessa Styles. 2019. 'A sensor kinase controls turgor-driven plant infection by the rice blast fungus', *Nature*, 574: 423-27.

Ryder, Lauren S, and Nicholas J Talbot. 2015. 'Regulation of appressorium development in pathogenic fungi', *Current Opinion in Plant Biology*, 26: 8-13.

Saeidi, Hojjatollah, Badradin Ebrahim Sayed Tabatabaei, Mehdi Rahimmalek, Majid Talebi-Badaf, and Mohammad Reza Rahiminejad. 2008. 'Genetic diversity and gene-pool subdivisions of diploid D-genome Aegilops tauschii Coss.(Poaceae) in Iran as revealed by AFLP', *Genetic Resources and Crop Evolution*, 55: 1231-38.

Sakulkoo, Wasin, Miriam Osés-Ruiz, Ely Oliveira Garcia, Darren M Soanes, George R Littlejohn, Christian Hacker, Ana Correia, Barbara Valent, and Nicholas J Talbot. 2018. 'A single fungal MAP kinase controls plant cell-to-cell invasion by the rice blast fungus', *science*, 359: 1399-403.

Salamini, Francesco, Hakan Özkan, Andrea Brandolini, Ralf Schäfer-Pregl, and William Martin. 2002. 'Genetics and geography of wild cereal domestication in the near east', *Nature Reviews Genetics*, 3: 429.

Saleh, Dounia, Peng Xu, Ying Shen, Chenguyn Li, Henri Adreit, Joelle Milazzo, Virginie Ravigné, Eric Bazin, JEAN-LOUP NOTTÉGHEM, and Elisabeth Fournier. 2012. 'Sex at the origin: an Asian population of the rice blast fungus Magnaporthe oryzae reproduces sexually', *Molecular Ecology*, 21: 1330-44.

Samra, Jagir S, and Kuldip Kumar. 2003. "Managing crop residues in the rice-wheat system of the Indo-Gangetic Plain." In *Improving the productivity and sustainability of rice-wheat systems: issues and impacts. Proceedings of an international symposium, held at the 2001 Annual Meetings of the American Society of Agronomy, Crop Science Society of America, and Soil Science Society of America, Charlotte, NC, USA, 22 October 2001*, 173-95. American Society of Agronomy.

Sánchez-Martín, Javier, Victoria Widrig, Gerhard Herren, Thomas Wicker, Helen Zbinden, Julien Gronnier, Laurin Spörri, Coraline R. Praz, Matthias Heuberger, Markus C. Kolodziej, Jonatan Isaksson, Burkhard Steuernagel, Miroslava Karafiátová, Jaroslav Doležel, Cyril Zipfel, and Beat Keller. 2021. 'Wheat Pm4 resistance to powdery mildew is controlled by alternative splice variants encoding chimeric proteins', *Nature plants*, 7: 327-41.

Sarris, Panagiotis F, Zane Duxbury, Sung Un Huh, Yan Ma, Cécile Segonzac, Jan Sklenar, Paul Derbyshire, Volkan Cevik, Ghanasyam Rallapalli, and Simon B Saucet. 2015. 'A plant immune receptor detects pathogen effectors that target WRKY transcription factors', *Cell*, 161: 1089-100.

Saucet, SB, Y Ma, PF Sarris, OJ Furzer, KH Sohn, and JD Jones. 2015. "Two linked pairs of Arabidopsis TNL resistance genes independently confer recognition of bacterial effector AvrRps4. Nat. Commun. 6: 6338." In.

Savary, Serge, Laetitia Willocquet, Francisco A Elazegui, Nancy P Castilla, and Paul S Teng. 2000. 'Rice pest constraints in tropical Asia: quantification of yield losses due to rice pests in a range of production situations', *Plant Disease*, 84: 357-69.

Schmolke, Michael, Volker Mohler, Lorenz Hartl, Friedrich J Zeller, and Sai LK Hsam. 2012. 'A new powdery mildew resistance allele at the Pm4 wheat locus transferred from einkorn (Triticum monococcum)', *Molecular Breeding*, 29: 449-56.

Seto, Derek, Noushin Koulena, Timothy Lo, Alexandra Menna, David S Guttman, and Darrell Desveaux. 2017. 'Expanded type III effector recognition by the ZAR1 NLR protein using ZED1-related kinases', *Nature plants*, 3: 1-4.

Sharma, TR, MS Madhav, BK Singh, P Shanker, TK Jana, V Dalal, A Pandit, A Singh, K Gaikwad, and HC Upreti. 2005. 'High-resolution mapping, cloning and molecular characterization of the Pi-k h gene of rice, which confers resistance to Magnaporthe grisea', *Molecular Genetics and Genomics*, 274: 569-78.

Shewry, Peter R. 2009. 'Wheat', *Journal of Experimental Botany*, 60: 1537-53.

Silué, D, and Jean-Loup Nottéghem. 1990. 'Production of perithecia of Magnaporthe grisea on rice plants', *Mycological Research*, 94: 1151-52.

Singh, Pawan K, Navin C Gahtyari, Chandan Roy, Krishna K Roy, Xinyao He, B Tembo, Kaijie Xu, Philomin Juliana, Kai Sonder, and Muhammad R Kabir. 2021. 'Wheat blast: a disease spreading by intercontinental jumps and its management strategies', *Frontiers in plant science*, 12: 710707.

Singh, PK, S Thakur, R Rathour, M Variar, SK Prashanthi, AK Singh, UD Singh, V Sharma, NK Singh, and TR Sharma. 2014. 'Transposon-based high sequence diversity in Avr-Pita alleles increases the potential for pathogenicity of Magnaporthe oryzae populations', *Functional & integrative genomics*, 14: 419-29.

Singh, Ravi Prakash, JULIO Huerta-Espino, and HARINDRA WILLIAM. 2005. 'Genetics and breeding for durable resistance to leaf and stripe rusts in wheat', *Turkish journal of agriculture and forestry*, 29: 121-27.

Soanes, Darren M, Intikhab Alam, Mike Cornell, Han Min Wong, Cornelia Hedeler, Norman W Paton, Magnus Rattray, Simon J Hubbard, Stephen G Oliver, and Nicholas J Talbot. 2008. 'Comparative genome analysis of filamentous fungi reveals gene family expansions associated with fungal pathogenesis', *PloS one*, 3: e2300.

Soanes, Darren M, Thomas A Richards, and Nicholas J Talbot. 2007. 'Insights from sequencing fungal and oomycete genomes: what can we learn about plant disease and the evolution of pathogenicity?', *The Plant Cell*, 19: 3318-26.

Song, Wen-Yuan, Guo-Liang Wang, Li-Li Chen, Han-Suk Kim, Li-Ya Pi, Tom Holsten, J Gardner, Bei Wang, Wen-Xue Zhai, and Li-Huang Zhu. 1995. 'A receptor kinase-like protein encoded by the rice disease resistance gene, Xa21', *science*, 270: 1804-06.

Sousa, Paulo Gervini. 2002. 'BR 18Terena: wheat cultivar for Brazil', *Pesquisa Agropecuária Brasileira*, 37: 1039-43.

Spielmeyer, W, RA McIntosh, James Kolmer, and ES Lagudah. 2005. 'Powdery mildew resistance and Lr34/Yr18 genes for durable resistance to leaf and stripe rust cosegregate at a locus on the short arm of chromosome 7D of wheat', *Theoretical and Applied Genetics*, 111: 731-35.

Steuernagel, B., F. Jupe, K. Witek, J. D. Jones, and B. B. Wulff. 2015. 'NLR-parser: rapid annotation of plant NLR complements', *Bioinformatics*, 31: 1665-7.

Steuernagel, B., Witek, K., Krattinger, S.G., Ramirez-Gonzalez, R.H., Schoonbeek, H.J., Yu, G., Baggs, E., Witek, A.I., Yadav, I., Krasileva, K.V. and Jones, J.D. 2020. 'The NLR-Annotator tool enables annotation of the intracellular immune receptor repertoire', *Plant Physiology*, 183(2): 468-82.

Su, Jing, Wenjuan Wang, Jingluan Han, Shen Chen, Congying Wang, Liexian Zeng, Aiqing Feng, Jianyuan Yang, Bo Zhou, and Xiaoyuan Zhu. 2015. 'Functional divergence of duplicated genes results in a novel blast resistance gene Pi50 at the Pi2/9 locus', *Theoretical and Applied Genetics*, 128: 2213-25.

Sweigard, James A, Anne M Carroll, Seogchan Kang, Leonard Farrall, Forrest G Chumley, and Barbara Valent. 1995. 'Identification, cloning, and characterization of PWL2, a gene for host species specificity in the rice blast fungus', *The Plant Cell*, 7: 1221-33.

Tagle, A. G., I. Chuma, and Y. Tosa. 2015. 'Rmg7, a New Gene for Resistance to Triticum Isolates of Pyricularia oryzae Identified in Tetraploid Wheat', *Phytopathology*, 105: 495-9.

Takabayashi, N., Y. Tosa, H. S. Oh, and S. Mayama. 2002. 'A gene-for-gene relationship underlying the species-specific parasitism of Avena/Triticum isolates of Magnaporthe grisea on wheat cultivars', *Phytopathology*, 92: 1182-88.

Talbot, Nicholas J. 2003. 'On the trail of a cereal killer: exploring the biology of Magnaporthe grisea', *Annual Reviews in Microbiology*, 57: 177-202.

Tao, Hui, Xuetao Shi, Feng He, Dan Wang, Ning Xiao, Hong Fang, Ruyi Wang, Fan Zhang, Min Wang, and Aihong Li. 2021. 'Engineering broad-spectrum disease-resistant rice by editing multiple susceptibility genes', *Journal of Integrative Plant Biology*, 63: 1639-48.

Tembo, Batiseba, Rabson M Mulenga, Suwilanji Sichilima, Kenneth K M'siska, Moses Mwale, Patrick C Chikoti, Pawan K Singh, Xinyao He, Kerry F Pedley, and Gary L Peterson. 2020. 'Detection and characterization of fungus (Magnaporthe oryzae pathotype Triticum) causing wheat blast disease on rain-fed grown wheat (Triticum aestivum L.) in Zambia', *PloS one*, 15: e0238724.

Tosa, Yukio, Yoshihiro Inoue, TP Vy Trinh, and Izumi Chuma. 2016. 'Genetic and molecular analyses of the incompatibility between Lolium isolates of Pyricularia oryzae and wheat', *Physiological and Molecular Plant Pathology*, 95: 84-86.

Urashima, A., S. Leite, and R. Galbieri. 2007. 'Efficiency of aerial dissemination of Pyricularia grisea', *Summa Phytopathologica*, 33: 275-79.

Urashima, A. S, Ana. C Bruno, and Norberto. A Lavorenti. 2001. 'Segregation analysis of avirulence of Magnaporthe grisea of wheat', *Fitopatologia Brasileira*, 26: 544-648.

Urashima, Alfredo S, Norberto A Lavorent, Augusto CP Goulart, and Yeshwant R Mehta. 2004. 'Resistance spectra of wheat cultivars and virulence diversity of Magnaporthe grisea isolates in Brazil', *Fitopatologia Brasileira*, 29: 511-18.

Urashima, Alfredo Seiiti, R Galbieri, and A Stabili. 2005. 'DNA fingerprinting and sexual characterization revealed two distinct populations of Magnaporthe grisea in wheat blast from Brazil', *Czech J. Genet. Plant Breed*, 41: 238-45.

Urashima, AS, S Igarashi, and H Kato. 1993. 'Host range, mating type, and fertility of Pyricularia grisea from wheat in Brazil', *Plant Disease*, 77: 1211-16.

Valent, Barbara. 1990. 'Rice blast as a model system for plant pathology', *Phytopathology*, 80: 33-36.

Valent, Barbara, and Chang Hyun Khang. 2010. 'Recent advances in rice blast effector research', *Current Opinion in Plant Biology*, 13: 434-41.

Van de Wouw, Angela P, Anton J Cozijnsen, James K Hane, Patrick C Brunner, Bruce A McDonald, Richard P Oliver, and Barbara J Howlett. 2010. 'Evolution of linked avirulence effectors in Leptosphaeria maculans is affected by genomic environment and exposure to resistance genes in host plants', *PLoS Pathogens*, 6: e1001180.

Van Der Biezen, Erik A, and Jonathan DG Jones. 1998. 'Plant disease-resistance proteins and the gene-for-gene concept', *Trends in Biochemical Sciences*, 23: 454-56.

Velu, Govindan, Leonardo Crespo Herrera, Carlos Guzman, Julio Huerta, Thomas Payne, and Ravi P Singh. 2019. 'Assessing genetic diversity to breed competitive biofortified wheat with enhanced grain Zn and Fe concentrations', *Frontiers in plant science*, 9: 1971.

Veses, Verónica, and Neil AR Gow. 2009. 'Pseudohypha budding patterns of Candida albicans', *Medical Mycology*, 47: 268-75.

Villareal, RL, K Sayre, O Banuelos, and A Mujeeb-Kazi. 2001. 'Registration of four synthetic hexaploid wheat (Triticum turgidum/Aegilops tauschii) germplasm lines tolerant to waterlogging', *Crop Science*, 41: 274-74.

Vlot, A Corina, D'Maris Amick Dempsey, and Daniel F Klessig. 2009. 'Salicylic acid, a multifaceted hormone to combat disease', *Annual Review of Phytopathology*, 47: 177-206.

Voss-Fels, Kai, Matthias Frisch, Lunwen Qian, Stefan Kontowski, Wolfgang Friedt, Sven Gottwald, and Rod J Snowdon. 2015. 'Subgenomic diversity patterns caused by directional selection in bread wheat gene pools', *The Plant Genome*, 8: plantgenome2015.03.0013.

Vy, Trinh Thi Phuong, Gang-Su Hyon, Nguyen Thi Thanh Nga, Yoshihiro Inoue, Izumi Chuma, and Yukio Tosa. 2014. 'Genetic analysis of host–pathogen incompatibility between Lolium isolates of Pyriculariaoryzae and wheat', *Journal of General Plant Pathology*, 80: 59-65.

Walkowiak, Sean, Liangliang Gao, Cecile Monat, Georg Haberer, Mulualem T Kassa, Jemima Brinton, Ricardo H Ramirez-Gonzalez, Markus C Kolodziej, Emily Delorean, and Dinushika Thambugala. 2020. 'Multiple wheat genomes reveal global variation in modern breeding', *Nature*, 588: 277-83.

Wan, Jiangxue, Min He, Qingqing Hou, Lijuan Zou, Yihua Yang, Yan Wei, and Xuewei Chen. 2021. 'Cell wall associated immunity in plants', *Stress Biology*, 1: 3.

Wang, Bao-hua, Daniel J Ebbole, and Zong-hua Wang. 2017. 'The arms race between Magnaporthe oryzae and rice: Diversity and interaction of Avr and R genes', *Journal of integrative agriculture*, 16: 2746-60.

Wang, Cuifen, Guihong Yin, Xianchun Xia, Zhonghu He, Peipei Zhang, Zhanjun Yao, Jinyan Qin, Zaifeng Li, and Daqun Liu. 2016. 'Molecular mapping of a new temperature-sensitive gene LrZH22 for leaf rust resistance in Chinese wheat cultivar Zhoumai 22', *Molecular Breeding*, 36: 1-10.

Wang, Guoxun, Brice Roux, Feng Feng, Endrick Guy, Lin Li, Nannan Li, Xiaojuan Zhang, Martine Lautier, Marie-Françoise Jardinaud, and Matthieu Chabannes. 2015. 'The decoy substrate of a pathogen effector and a pseudokinase specify pathogen-induced modified-self recognition and immunity in plants', *Cell host & microbe*, 18: 285-95.

Wang, Jirui, Ming-Cheng Luo, Zhongxu Chen, Frank M You, Yuming Wei, Youliang Zheng, and Jan Dvorak. 2013. 'Aegilops tauschii single nucleotide polymorphisms shed light on the origins of wheat D-genome genetic diversity and pinpoint the geographic origin of hexaploid wheat', *New Phytologist*, 198: 925-37.

Wang, Ning, Chunlei Tang, Xin Fan, Mengying He, Pengfei Gan, Shan Zhang, Zeyu Hu, Xiaodong Wang, Tong Yan, and Weixue Shu. 2022. 'Inactivation of a wheat protein kinase gene confers broad-spectrum resistance to rust fungi', *Cell*, 185: 2961-74. e19.

Wang, S., S. Asuke, T. T. P. Vy, Y. Inoue, I. Chuma, J. Win, K. Kato, and Y. Tosa. 2018. 'A New Resistance Gene in Combination with Rmg8 Confers Strong Resistance Against Triticum Isolates of Pyricularia oryzae in a Common Wheat Landrace', *Phytopathology*, 108: 1299-306.

Wicker, Thomas, Heidrun Gundlach, Manuel Spannagl, Cristobal Uauy, Philippa Borrill, Ricardo H Ramírez-González, Romain De Oliveira, Klaus FX Mayer, Etienne Paux, and Frédéric Choulet. 2018. 'Impact of transposable elements on genome structure and evolution in bread wheat', *Genome biology*, 19: 1-18.

Wiesner-Hanks, Tyr, and Rebecca Nelson. 2016. 'Multiple disease resistance in plants', *Annual Review of Phytopathology*, 54: 229-52.

Wildermuth, Mary C, Julia Dewdney, Gang Wu, and Frederick M Ausubel. 2001. 'Isochorismate synthase is required to synthesize salicylic acid for plant defence', *Nature*, 414: 562-65.

Williams, Simon J, Kee Hoon Sohn, Li Wan, Maud Bernoux, Panagiotis F Sarris, Cecile Segonzac, Thomas Ve, Yan Ma, Simon B Saucet, and Daniel J Ericsson. 2014. 'Structural basis for assembly and function of a heterodimeric plant immune receptor', *science*, 344: 299-303.

Williamson, Valerie M, Varghese Thomas, Howard Ferris, and Jorge Dubcovsky. 2013. 'An Aegilops ventricosa translocation confers resistance against root-knot nematodes to common wheat', *Crop Science*, 53: 1412-18.

Wilson, Richard A, and Nicholas J Talbot. 2009. 'Under pressure: investigating the biology of plant infection by Magnaporthe oryzae', *Nature Reviews Microbiology*, 7: 185-95.

Winfield, Mark O, Alexandra M Allen, Paul A Wilkinson, Amanda J Burridge, Gary LA Barker, Jane Coghill, Christy Waterfall, Luzie U Wingen, Simon Griffiths, and Keith J Edwards. 2018. 'High-density genotyping of the AE Watkins Collection of hexaploid landraces identifies a large molecular diversity compared to elite bread wheat', *Plant Biotechnology Journal*, 16: 165-75.

Wingen, Luzie U, Simon Orford, Richard Goram, Michelle Leverington-Waite, Lorelei Bilham, Theofania S Patsiou, Mike Ambrose, Jo Dicks, and Simon Griffiths. 2014. 'Establishing the AE Watkins landrace cultivar collection as a resource for systematic gene discovery in bread wheat', *Theoretical and Applied Genetics*, 127: 1831-42.

Witek, Kamil, Florian Jupe, Agnieszka I Witek, David Baker, Matthew D Clark, and Jonathan DG Jones. 2016. 'Accelerated cloning of a potato late blight–resistance gene using RenSeq and SMRT sequencing', *Nature Biotechnology*, 34: 656.

WorldAtlas. 2019. 'Top Wheat Producing Countries', Accessed 03/3/19. https://www.worldatlas.com/articles/top-wheat-producing-countries.html.

Wright, Alison J, Tim LW Carver, Barry J Thomas, Nick ID Fenwick, Hitoshi Kunoh, and Ralph L Nicholson. 2000. 'The rapid and accurate determination of germ tube emergence site by Blumeria graminis conidia', *Physiological and Molecular Plant Pathology*, 57: 281-301.

Wulff, B. B., and M. J. Moscou. 2014. 'Strategies for transferring resistance into wheat: from wide crosses to GM cassettes', *Front Plant Sci*, 5: 692.

Xiao, Gui, Wenjuan Wang, Muxing Liu, Ya Li, Jianbin Liu, Marina Franceschetti, Zhaofeng Yi, Xiaoyuan Zhu, Zhengguang Zhang, and Guodong Lu. 2022. 'The Piks allele of the NLR immune receptor

Pik breaks the recognition of AvrPik effectors of the rice blast fungus', *Journal of Integrative Plant Biology*.

Xiao, Shunyuan, Simon Ellwood, Ozer Calis, Elaine Patrick, Tianxian Li, Mark Coleman, and John G Turner. 2001. 'Broad-spectrum mildew resistance in Arabidopsis thaliana mediated by RPW8', *science*, 291: 118-20.

Xu, Jin-Rong, and John E Hamer. 1996. 'MAP kinase and cAMP signaling regulate infection structure formation and pathogenic growth in the rice blast fungus Magnaporthe grisea', *Genes & Development*, 10: 2696-706.

Xue, Minfeng, Jun Yang, Zhigang Li, Songnian Hu, Nan Yao, Ralph A Dean, Wensheng Zhao, Mi Shen, Haiwang Zhang, and Chao Li. 2012. 'Comparative analysis of the genomes of two field isolates of the rice blast fungus Magnaporthe oryzae'.

Yamaoka, Naoto, Isao Matsumoto, and Masamichi Nishiguchi. 2006. 'The role of primary germ tubes (PGT) in the life cycle of Blumeria graminis: the stopping of PGT elongation is necessary for the triggering of appressorial germ tube (AGT) emergence', *Physiological and Molecular Plant Pathology*, 69: 153-59.

Yan, Xia, Bozeng Tang, Lauren S Ryder, Dan MacLean, Vincent M Were, Alice Bisola Eseola, Neftaly Cruz-Mireles, Weibin Ma, Andrew J Foster, and Miriam Osés-Ruiz. 2023. 'The transcriptional landscape of plant infection by the rice blast fungus Magnaporthe oryzae reveals distinct families of temporally co-regulated and structurally conserved effectors', *The Plant Cell*, 35: 1360-85.

Yang, Qin, Yijian He, Mercy Kabahuma, Timothy Chaya, Amy Kelly, Eli Borrego, Yang Bian, Farid El Kasmi, Li Yang, and Paulo Teixeira. 2017. 'A gene encoding maize caffeoyl-CoA O-methyltransferase confers quantitative resistance to multiple pathogens', *Nature Genetics*, 49: 1364-72.

Yao, Danyu, Waqas Ijaz, Yi Liu, Jinghuang Hu, Wentao Peng, Bowen Zhang, Xiaolan Wen, Juan Wang, Dan Qiu, and Hongjie Li. 2022. 'Identification of a Pm4 allele as a powdery mildew resistance gene in wheat line xiaomaomai', *International journal of molecular sciences*, 23: 1194.

Yates, Andrew D, Premanand Achuthan, Wasiu Akanni, James Allen, Jamie Allen, Jorge Alvarez-Jarreta, M Ridwan Amode, Irina M Armean, Andrey G Azov, Ruth Bennett, Jyothish Bhai, Konstantinos Billis, Sanjay Boddu, José Carlos Marugán, Carla Cummins, Claire Davidson, Kamalkumar Dodiya, Reham Fatima, Astrid Gall, Carlos Garcia Giron, Laurent Gil, Tiago Grego, Leanne Haggerty, Erin Haskell, Thibaut Hourlier, Osagie G Izuogu, Sophie H Janacek, Thomas Juettemann, Mike Kay, Ilias Lavidas, Tuan Le, Diana Lemos, Jose Gonzalez Martinez, Thomas Maurel, Mark McDowall, Aoife McMahon, Shamika Mohanan, Benjamin Moore, Michael Nuhn, Denye N Oheh, Anne Parker, Andrew Parton, Mateus Patricio, Manoj Pandian Sakthivel, Ahamed Imran Abdul Salam, Bianca M Schmitt, Helen Schuilenburg, Dan Sheppard, Mira Sycheva, Marek Szuba, Kieron Taylor, Anja Thormann, Glen Threadgold, Alessandro Vullo, Brandon Walts, Andrea Winterbottom, Amonida Zadissa, Marc Chakiachvili, Bethany Flint, Adam Frankish, Sarah E Hunt, Garth IIsley, Myrto Kostadima, Nick Langridge, Jane E Loveland, Fergal J Martin, Joannella Morales, Jonathan M Mudge, Matthieu Muffato, Emily Perry, Magali Ruffier, Stephen J Trevanion, Fiona Cunningham, Kevin L Howe, Daniel R Zerbino, and Paul Flicek. 2019. 'Ensembl 2020', *Nucleic Acids Research*, 48: D682-D88.

Yu, Guotai, Qijun Zhang, Timothy L Friesen, Matthew N Rouse, Yue Jin, Shaobin Zhong, Jack B Rasmussen, Evans S Lagudah, and Steven S Xu. 2015. 'Identification and mapping of Sr46 from Aegilops tauschii accession Clae 25 conferring resistance to race TTKSK (Ug99) of wheat stem rust pathogen', *Theoretical and Applied Genetics*, 128: 431-43.

Yuan, Bin, Chun Zhai, Wenjuan Wang, Xiaoshan Zeng, Xiaoke Xu, Hanqiao Hu, Fei Lin, Ling Wang, and Qinghua Pan. 2011. 'The Pik-p resistance to Magnaporthe oryzae in rice is mediated by a pair of closely linked CC-NBS-LRR genes', *Theoretical and Applied Genetics*, 122: 1017-28.

Yunoki, T, A Ezuka, T Morinaka, Y Sakurai, and H Shinoda. 1970. 'Studies on the varietal resistance to Rice blast. 4. Variation of field resistance due to fungus strains', *Bull. Chugoku agric. Exp. Stn., Ser. A*: 21-41.

Zenbayashi-Sawata, Kaoru, Taketo Ashizawa, and Shinzo Koizumi. 2005. 'Pi34-AVRPi34: a new gene-for-gene interaction for partial resistance in rice to blast caused by Magnaporthe grisea', *Journal of general plant pathology*, 71: 395-401.

Zhai, Chun, Yu Zhang, Nan Yao, Fei Lin, Zhe Liu, Zhongqiu Dong, Ling Wang, and Qinghua Pan. 2014. 'Function and interaction of the coupled genes responsible for Pik-h encoded rice blast resistance', *PloS one*, 9: e98067.

Zhan, S. W., S. Mayama, and Y. Tosa. 2008. 'Identification of two genes for resistance to Triticum isolates of Magnaporthe oryzae in wheat', *Genome*, 51: 216-21.

Zhang, Chaozhong, Lin Huang, Huifei Zhang, Qunqun Hao, Bo Lyu, Meinan Wang, Lynn Epstein, Miao Liu, Chunlan Kou, and Juan Qi. 2019. 'An ancestral NB-LRR with duplicated 3’ UTRs confers stripe rust resistance in wheat and barley', *Nature communications*, 10: 4023.

Zhang, Haifeng, Xiaobo Zheng, and Zhengguang Zhang. 2016. 'The Magnaporthe grisea species complex and plant pathogenesis', *Molecular Plant Pathology*, 17: 796.

Zhang, Jie, Wei Li, Tingting Xiang, Zixu Liu, Kristin Laluk, Xiaojun Ding, Yan Zou, Minghui Gao, Xiaojuan Zhang, and She Chen. 2010. 'Receptor-like cytoplasmic kinases integrate signaling from multiple plant immune receptors and are targeted by a Pseudomonas syringae effector', *Cell host & microbe*, 7: 290-301.

Zhang, Lei, Yong-Liang Zhao, Li-Feng Gao, Guang-Yao Zhao, Rong-Hua Zhou, Bao-Shi Zhang, and Ji-Zeng Jia. 2012. 'TaCKX6-D1, the ortholog of rice OsCKX2, is associated with grain weight in hexaploid wheat', *New Phytologist*, 195: 574-84.

Zhao, Haijun, Xueyan Wang, Yulin Jia, Bastian Minkenberg, Matthew Wheatley, Jiangbo Fan, Melissa H Jia, Adam Famoso, Jeremy D Edwards, and Yeshi Wamishe. 2018. 'The rice blast resistance gene Ptr encodes an atypical protein required for broad-spectrum disease resistance', *Nature communications*, 9: 2039.

Zheng, Yan, Wenhui Zheng, Fucheng Lin, Ying Zhang, Yunping Yi, Baohua Wang, Guodong Lu, Zonghua Wang, and Weiren Wu. 2011. 'AVR1-CO39 is a predominant locus governing the broad avirulence of Magnaporthe oryzae 2539 on cultivated rice (Oryza sativa L.)', *Molecular Plant-Microbe Interactions*, 24: 13-17.

Zhou, Erxun, Yulin Jia, Pratibha Singh, James C Correll, and Fleet N Lee. 2007. 'Instability of the Magnaporthe oryzae avirulence gene AVR-Pita alters virulence', *Fungal Genetics and Biology*, 44: 1024-34.

Zhou, Yao, Xuebo Zhao, Yiwen Li, Jun Xu, Aoyue Bi, Lipeng Kang, Daxing Xu, Haofeng Chen, Ying Wang, and Yuan-ge Wang. 2020. 'Triticum population sequencing provides insights into wheat adaptation', *Nature Genetics*, 52: 1412-22.

Zhou, Yun, Shenglong Bai, Hao Li, Guiling Sun, Dale Zhang, Feifei Ma, Xinpeng Zhao, Fang Nie, Jingyao Li, and Liyang Chen. 2021. 'Introgressing the Aegilops tauschii genome into wheat as a basis for cereal improvement', *Nature plants*, 7: 774-86.

Zhu, Ying, Weiqiang Qian, and Jian Hua. 2010. 'Temperature modulates plant defense responses through NB-LRR proteins', *PLoS Pathogens*, 6: e1000844.

SUPPLEMENTARY INFORMATION

Supplementary figures

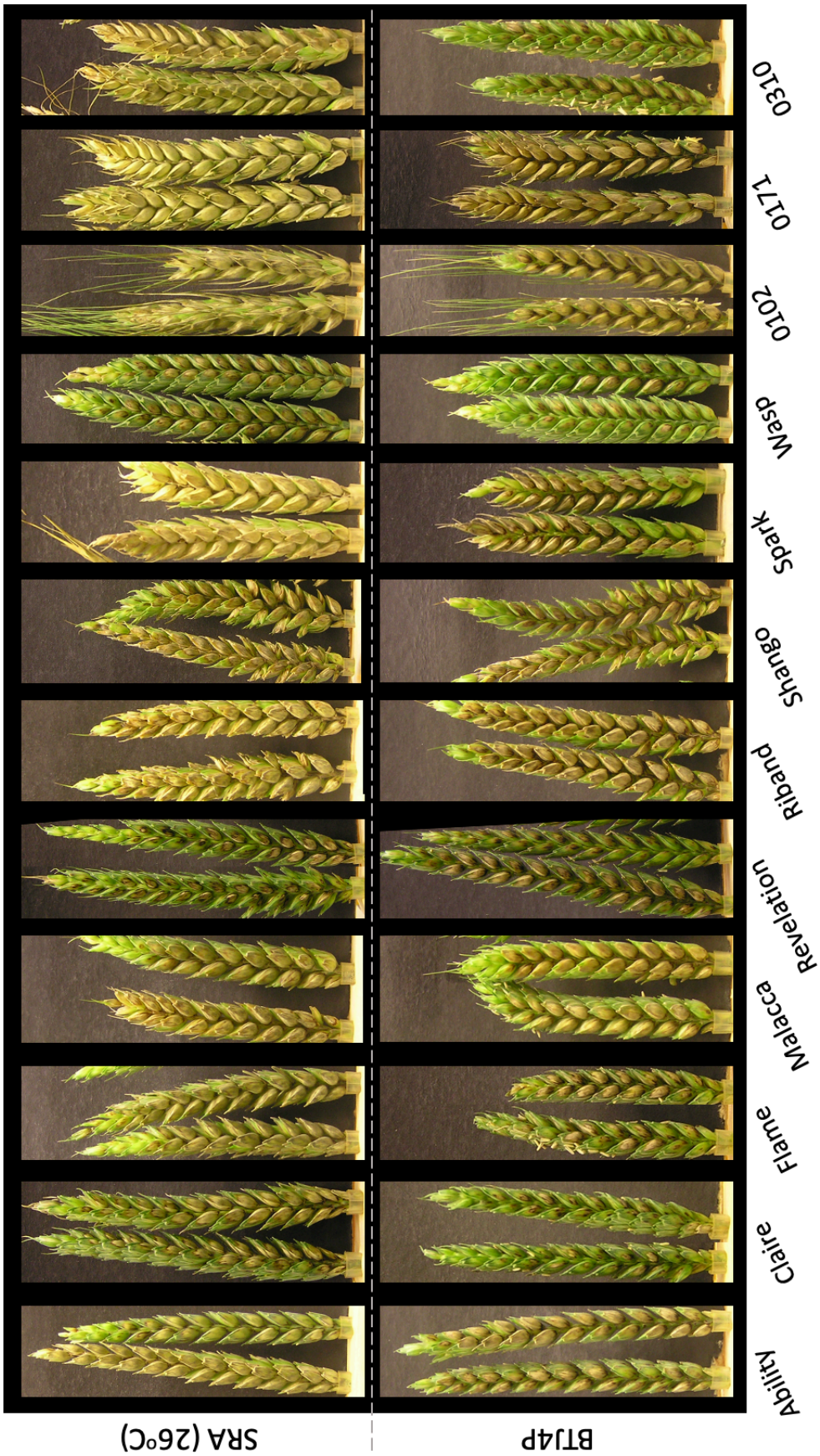

Supplementary Fig. S1: *Pm4b* DSA with SRA and BTJ4P isolates. Spikes were phenotyped at 26°C and 22°C for SRA and BTJ4P respectively. All accessions with numerical codes are Watkins lines that start 'WATDE'. Images were taken at 6 dpi.

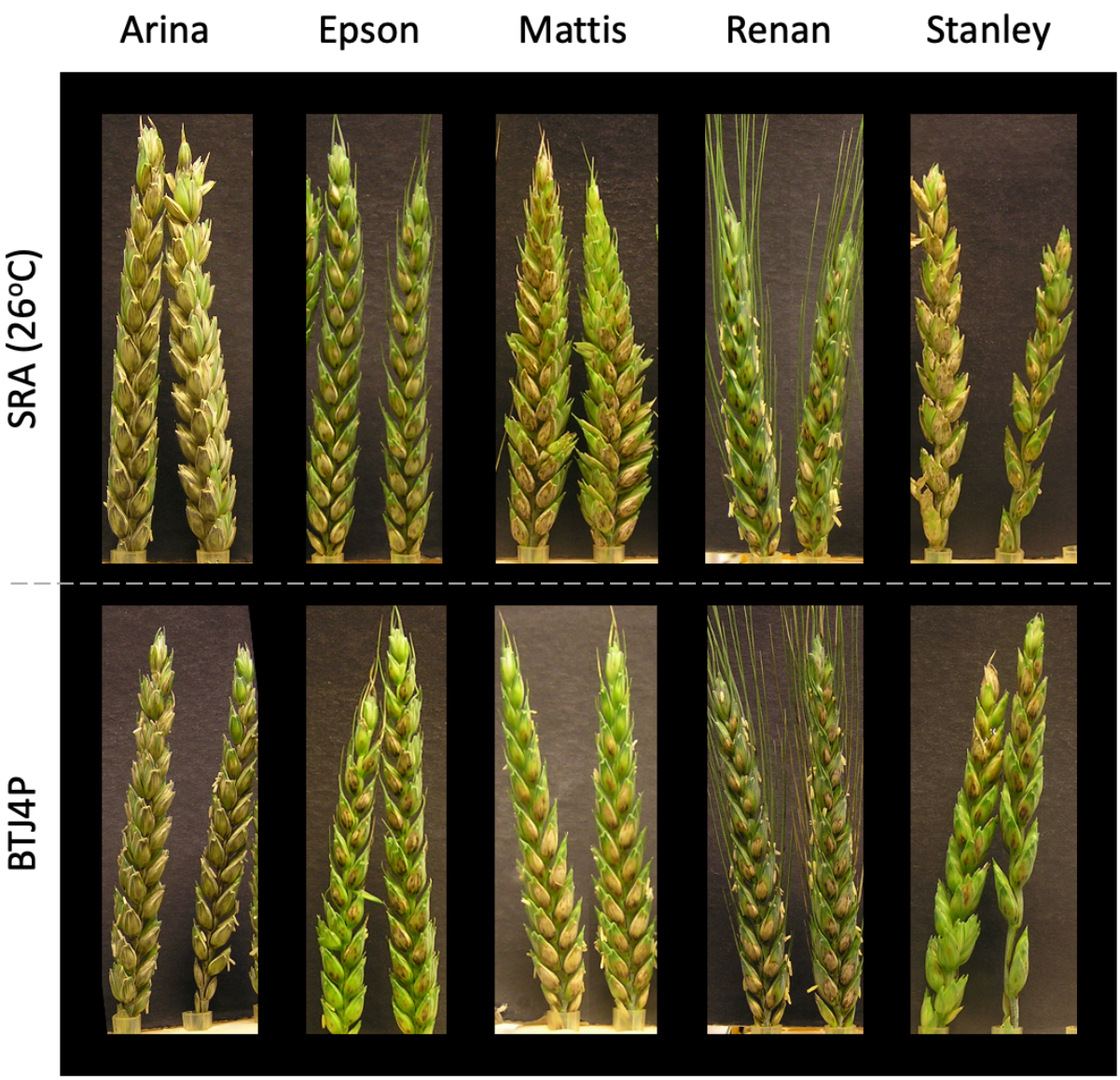

Supplementary Fig. S2: *Pm4d* DSA with SRA and BTJ4P isolates. Spikes were phenotyped at 26°C and 22°C for SRA and BTJ4P respectively. All accessions with numerical codes are Watkins lines that start 'WATDE'. Arina was included as a susceptible control. Images were taken at 6 dpi.

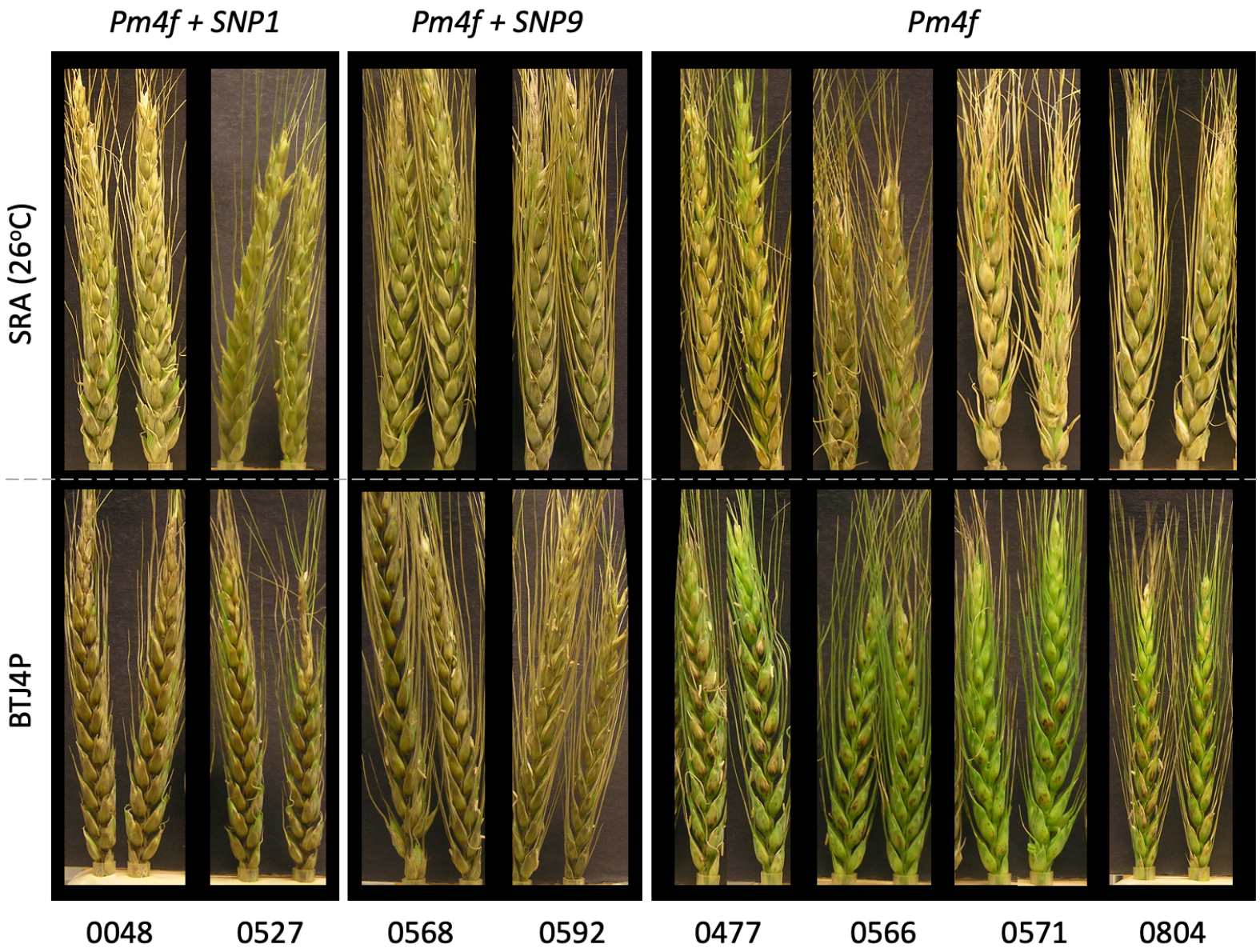

Supplementary Fig. S3: *Pm4f, Pm4f+SNP1* and *Pm4f+SNP9* DSA with SRA and BTJ4P isolates. Spikes were phenotyped at 26°C and 22°C for SRA and BTJ4P respectively. All accessions with numerical codes are Watkins lines that start 'WATDE'. Images were taken

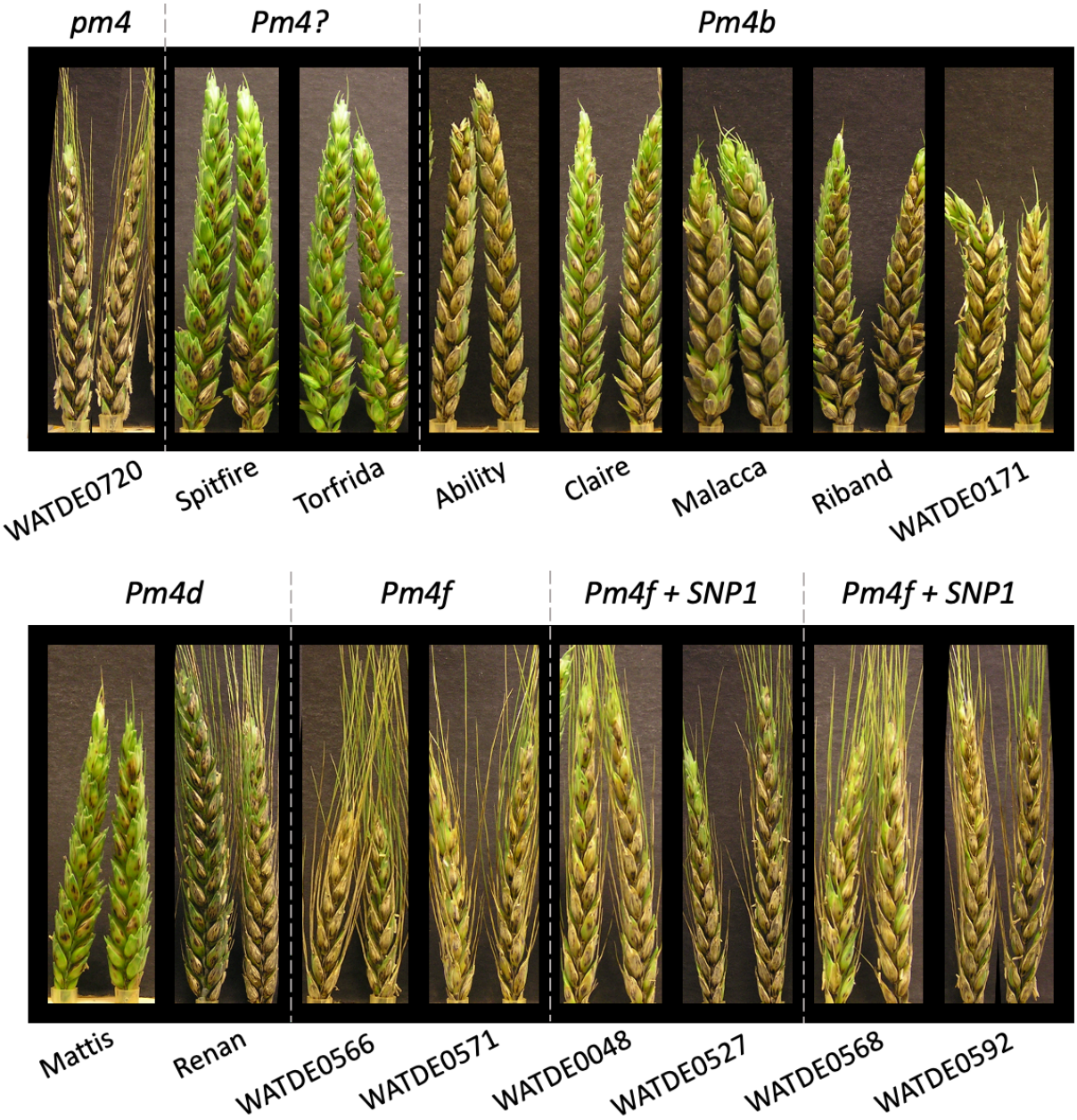

Supplementary Fig. S4: *Pm4* NO6047 DSA. Images were taken at 9 dpi.

Supplementary tables

Supplementary table S1: *Aegilops tauschii* ssp. *strangulata* (Lineage 2) accessions in the diversity panel and their origins.

Project Accession No.	GRU* No.	Original Source	Country of Origin	State/Province/City
BW_01001	TOWWC002	NSGC	Iran	Mazandaran
BW_01002	TOWWC003	NSGC	Iran	Golestan
BW_01003	TOWWC004	NSGC	Iran	Golestan
BW_01004	TOWWC005	NSGC	Iran	Golestan
BW_01005	TOWWC006	NSGC	Iran	Mazandaran
BW_01006	TOWWC007	NSGC	Iran	Mazandaran
BW_01007	TOWWC008	ICARDA	Azerbaijan	Agsu
BW_01008	TOWWC009	ICARDA	Azerbaijan	Askeran
BW_01009	TOWWC010	ICARDA	Azerbaijan	Baku
BW_01010	TOWWC011	ICARDA	Azerbaijan	Aliabad
BW_01011	TOWWC012	ICARDA	Azerbaijan	Lankaran
BW_01019	TOWWC020	IPK	Azerbaijan	
BW_01020	TOWWC021	IPK	Azerbaijan	
BW_01021	TOWWC022	IPK	Azerbaijan	
BW_01022	TOWWC023	IPK	Azerbaijan	
BW_01024	TOWWC025	IPK	Turkmenistan	
BW_01025	TOWWC026	IPK	Armenia	
BW_01026	TOWWC027	IPK	Turkmenistan	
BW_01027	TOWWC028	IPK	Armenia	
BW_01029	TOWWC030	Vavilov Institute	Tajikistan	
BW_01030	TOWWC031	Vavilov Institute	Russia	North Caucasian
BW_01032	TOWWC033	KSU	Turkey	Shemsdin
BW_01033	TOWWC034	KSU	Turkey	Shemsdin
BW_01039	TOWWC040		Azerbaijan	
BW_01041	TOWWC042		Azerbaijan	Shaki
BW_01042	TOWWC043		Azerbaijan	Ismailli
BW_01043	TOWWC044		Azerbaijan	Fizuli
BW_01044	TOWWC045		Azerbaijan	Zangilan
BW_01045	TOWWC046		Azerbaijan	Basut-Chay State Reserve
BW_01046	TOWWC047		Armenia	
BW_01047	TOWWC048		Armenia	
BW_01048	TOWWC049		Armenia	
BW_01049	TOWWC050		Uzbekistan	Zangiota
BW_01050	TOWWC051		Syrian Arab Republic	Ras al-Ayn
BW_01055	TOWWC056			
BW_01056	TOWWC057		Georgia	Kumisi
BW_01057	TOWWC058		Georgia	Kumisi

BW_01058	TOWWC059	Georgia	Signhnaghi
BW_01059	TOWWC060	Georgia	Signhnaghi
BW_01060	TOWWC061	Azerbaijan	Shirvan
BW_01062	TOWWC063	Azerbaijan	Shirvan
BW_01063	TOWWC064	Azerbaijan	Saatly
BW_01065	TOWWC066	Azerbaijan	Shamakhi
BW_01066	TOWWC067	Azerbaijan	Shamakhi
BW_01068	TOWWC069	Azerbaijan	Agsu
BW_01069	TOWWC070	Azerbaijan	Agsu
BW_01070	TOWWC071	Azerbaijan	Agsu
BW_01071	TOWWC072	Azerbaijan	
BW_01072	TOWWC073	Azerbaijan	
BW_01073	TOWWC074	Azerbaijan	
BW_01074	TOWWC075	Azerbaijan	
BW_01076	TOWWC077	Azerbaijan	
BW_01077	TOWWC078	Azerbaijan	
BW_01078	TOWWC079	Azerbaijan	
BW_01079	TOWWC080	Iran	
BW_01081	TOWWC082	Turkey	Hakkari
BW_01082	TOWWC083	Turkey	Hakkari
BW_01083	TOWWC084	Iran	Mazandaran
BW_01084	TOWWC085	Iran	Mazandaran
BW_01085	TOWWC086		
BW_01086	TOWWC087	Iran	Amol
BW_01087	TOWWC088	Former USSR	
BW_01088	TOWWC089	Russian Federation	
BW_01089	TOWWC090	Turkmenistan	Balkan
BW_01091	TOWWC092	Azerbaijan	Shabran
BW_01094	TOWWC095	Iran	Mazandaran
BW_01095	TOWWC096	Iran	Golestan
BW_01096	TOWWC097	Iran	Hamadan
BW_01097	TOWWC098	Iran	Aliabad
BW_01098	TOWWC099	Iran	Mazandaran
BW_01099	TOWWC100	Iran	Guilan
BW_01100	TOWWC101	Iran	Golestan
BW_01102	TOWWC103	Azerbaijan	Goychay
BW_01103	TOWWC104	Azerbaijan	
BW_01104	TOWWC105	Azerbaijan	Sabirabad
BW_01105	TOWWC106	Azerbaijan	
BW_01106	TOWWC107	Azerbaijan	
BW_01107	TOWWC108	Azerbaijan	Masalli
BW_01108	TOWWC109	Azerbaijan	Shamakhi
BW_01109	TOWWC110	Azerbaijan	Shamakhi

BW_01111	TOWWC112	Azerbaijan	Shamakhi
BW_01112	TOWWC113	Azerbaijan	Shamakhi
BW_01113	TOWWC114	Azerbaijan	Kutkashen
BW_01114	TOWWC115	Azerbaijan	Yardymli
BW_01115	TOWWC116	Turkmenistan	
BW_01116	TOWWC117	Azerbaijan	
BW_01117	TOWWC118	Azerbaijan	
BW_01118	TOWWC119	Azerbaijan	Shamakhi
BW_01119	TOWWC120	Azerbaijan	Agsu
BW_01120	TOWWC121	Azerbaijan	Shaki
BW_01121	TOWWC122	Azerbaijan	Kutkashen
BW_01122	TOWWC123	Azerbaijan	Davachi
BW_01123	TOWWC124	Azerbaijan	Ezmarail
BW_01124	TOWWC125	Azerbaijan	Shamakhi
BW_01125	TOWWC126		
BW_01126	TOWWC127		
BW_01128	TOWWC129		
BW_01129	TOWWC130		
BW_01130	TOWWC131	Iran	Gilan
BW_01132	TOWWC133	Iran	Guilan
BW_01133	TOWWC134	Iran	Markazi
BW_01134	TOWWC135	Russian Federation	Dagestan
BW_01135	TOWWC136	Iran	Alborz
BW_01136	TOWWC137	Iran	Tehran
BW_01137	TOWWC138	Iran	Mazandaran
BW_01138	TOWWC139	Iran	Mazandaran
BW_01139	TOWWC140	Iran	Alborz
BW_01140	TOWWC141	Iran	Mazandaran
BW_01141	TOWWC142	Iran	Mazandaran
BW_01142	TOWWC143	Iran	Gorgan
BW_01143	TOWWC144	Iran	Aliabad-e Katul
BW_01144	TOWWC145	Iran	Aliabad-e Katul
BW_01146	TOWWC147	Iran	Golestan
BW_01147	TOWWC148	Iran	Golestan
BW_01148	TOWWC149	Iran	Golestan
BW_01151	TOWWC152	Iran	Mazandaran
BW_01152	TOWWC153	Iran	Mazandaran
BW_01153	TOWWC154	Iran	Mazandaran
BW_01154	TOWWC155	Iran	Mazandaran
BW_01155	TOWWC156	Iran	Mazandaran
BW_01156	TOWWC157	Iran	Mazandaran
BW_01158	TOWWC159	Iran	Mazandaran
BW_01159	TOWWC160	Iran	Mazandaran

BW_01161	TOWWC162		Iran	Guilan
BW_01162	TOWWC163		Iran	Guilan
BW_01163	TOWWC164		Iran	Guilan
BW_01164	TOWWC165		Iran	Gilan
BW_01165	TOWWC166		Iran	Gilan
BW_01166	TOWWC167		Iran	Gilan
BW_01167	TOWWC168		Iran	Ardabil
BW_01168	TOWWC169		Iran	
BW_01170	TOWWC171		Iran	East Azerbaijan
BW_01171	TOWWC172		Iran	Mazandaran
BW_01172	TOWWC173		Iran	Mazandaran
BW_01175	TOWWC176		Iran	Mazandaran
BW_01176	TOWWC177		Iran	Mazandaran
BW_01177	TOWWC178		Iran	Mazandaran
BW_01178	TOWWC179		Iran	Mazandaran
BW_01179	TOWWC180		Azerbaijan	Shamakhi
BW_01181	TOWWC182		Azerbaijan	Shamakhi
BW_01182	TOWWC183		Azerbaijan	
BW_01184	TOWWC185		Armenia	Yerevan
BW_01185	TOWWC186		Georgia	Tbilisi
BW_01186	TOWWC187		Georgia	Gori
BW_01189	TOWWC190		Iran	Gorgan
BW_01190	TOWWC191		Iran	
BW_01192	TOWWC193	UC Davis	Armenia	
BW_01193	TOWWC194	UC Davis	Iran	Mazandaran

*Germplasm Resources Unit, John Innes Centre, Norwich, NR4 7UH, UK

Supplementary table S2: *MoT* isolates used in this study.

Isolate code	Origin	Date collected	Source
NO6047	Brazil	2006	Diane Saunders, JIC
NO6047+*Avr-Rmg8*	-	-	Diane Saunders, JIC
Py 15.1.018	Brazil	2015	Embrapa
BTJ4P-1	Bangladesh	2016	Tofazzal Islam, BSMRU, Bangladesh
BR48ΔeI	-	-	Yukio Tosa, Kobe University
BR48ΔeI+eI	-	-	Yukio Tosa, Kobe University
BR48ΔeI+eII	-	-	Yukio Tosa, Kobe University
BR48ΔeI+eII'	-	-	Yukio Tosa, Kobe University

Supplementary table S3: Mean scores from the *Ae. tauschii* DLAs with NO6047 and NO6047+*Avr-Rmg8*, plus the iso008 spike data collected by Paula Silva.

Accession number	NO6047 (mean of 4 and 5 dpi)	NO6047+*Avr-Rmg8* (5 dpi)		Differential scores**	iso008 spike data***
		Mean	Extreme*		AUDPC
BW_01001	4.10	1.00	6.00	3.10	-
BW_01002	4.25	1.25	6.00	3.00	-
BW_01003	5.50	-	-	-	-
BW_01004	1.50	-	-	-	-
BW_01005	4.20	1.20	6.00	3.00	-
BW_01006	5.10	1.40	6.00	3.70	-
BW_01007	4.63	3.25	0.00	1.38	-
BW_01008	5.10	2.80	0.00	2.30	-
BW_01009	3.00	-	-	-	-
BW_01010	4.63	1.33	6.00	3.29	-
BW_01011	4.25	5.20	0.00	-0.95	-
BW_01012	2.50	-	-	-	-
BW_01015	4.70	2.80	0.00	1.90	-
BW_01016	4.00	4.00	0.00	0.00	-
BW_01019	5.00	4.80	0.00	0.20	-
BW_01020	4.60	2.50	-	2.10	-
BW_01021	4.70	2.20	-	2.50	-
BW_01022	4.60	1.00	6.00	3.60	-
BW_01024	3.90	-	-	-	-
BW_01025	5.60	1.00	6.00	4.60	-
BW_01026	4.80	3.20	0.00	1.60	-
BW_01027	5.10	3.50	0.00	1.60	-
BW_01031	4.20	1.00	6.00	3.20	-
BW_01032	3.88	-	-	-	-
BW_01033	3.00	-	-	-	-
BW_01039	2.40	-	-	-	456.27
BW_01040	-	-	-	-	547.03
BW_01041	2.25	-	-	-	507.38
BW_01042	3.38	-	-	-	619.25
BW_01043	4.90	1.00	6.00	3.90	239.13
BW_01044	4.00	3.00	0.00	1.00	675.82
BW_01045	2.60	-	-	-	441.52
BW_01046	3.90	-	-	-	209.03
BW_01047	3.75	-	-	-	199.34
BW_01048	2.60	-	-	-	198.33
BW_01049	2.00	-	-	-	47.60
BW_01050	1.13	-	-	-	175.89
BW_01055	4.60	2.00	-	2.60	371.90

BW_01056	4.00	2.60	-	1.40	615.21
BW_01057	4.80	3.00	0.00	1.80	691.85
BW_01058	5.00	3.80	0.00	1.20	652.50
BW_01059	4.90	4.60	0.00	0.30	664.60
BW_01060	5.50	1.00	6.00	4.50	67.62
BW_01061	-	-	-	-	221.84
BW_01062	3.60	-	-	-	522.85
BW_01063	2.00	-	-	-	-
BW_01064	-	-	-	-	673.78
BW_01065	5.20	-	-	-	636.89
BW_01066	5.10	3.40	0.00	1.70	652.72
BW_01067	-	-	-	-	512.80
BW_01068	4.80	1.00	6.00	3.80	47.57
BW_01069	5.30	3.67	0.00	1.63	517.30
BW_01070	2.50	-	-	-	451.81
BW_01071	5.50	-	-	-	-
BW_01072	4.60	3.50	0.00	1.10	618.13
BW_01073	2.80	-	-	-	-
BW_01074	3.00	-	-	-	247.82
BW_01076	4.15	4.00	0.00	0.15	751.90
BW_01077	5.60	3.00	0.00	2.60	-
BW_01078	5.70	3.50	0.00	2.20	659.88
BW_01079	3.50	-	-	-	24.21
BW_01080	-	-	-	-	694.16
BW_01081	3.00	-	-	-	644.13
BW_01082	4.80	-	-	-	617.37
BW_01083	3.50	-	-	-	-
BW_01084	5.10	1.00	6.00	4.10	17.99
BW_01085	2.70	-	-	-	418.10
BW_01086	5.50	3.80	0.00	1.70	-
BW_01087	4.70	4.00	0.00	0.70	552.64
BW_01088	4.70	-	-	-	67.02
BW_01089	4.30	1.00	6.00	3.30	88.15
BW_01090	-	-	-	-	41.36
BW_01091	4.38	2.20	-	2.18	-
BW_01092	-	-	-	-	192.64
BW_01093	-	-	-	-	161.42
BW_01094	5.50	-	-	-	351.63
BW_01095	4.70	1.20	6.00	3.50	181.45
BW_01096	4.20	2.00	-	2.20	-
BW_01097	4.80	1.00	6.00	3.80	46.52
BW_01098	4.70	-	-	-	166.45
BW_01099	4.90	1.40	6.00	3.50	339.39

BW_01100	5.63	1.67	6.00	3.96	73.45
BW_01101	-	-	-	-	329.13
BW_01102	4.40	1.00	6.00	3.40	-
BW_01103	3.63	-	-	-	-
BW_01104	3.40	-	-	-	68.68
BW_01106	4.60	1.00	6.00	3.60	452.43
BW_01107	5.90	1.00	6.00	4.90	75.81
BW_01108	4.80	1.25	6.00	3.55	291.88
BW_01109	5.20	4.00	0.00	1.20	622.98
BW_01111	5.40	1.00	6.00	4.40	394.80
BW_01112	-	-	-	-	31.90
BW_01113	3.90	-	-	-	337.90
BW_01114	3.80	-	-	-	541.23
BW_01115	3.90	-	-	-	23.50
BW_01116	4.20	1.00	6.00	3.20	132.64
BW_01117	5.80	-	-	-	311.21
BW_01118	5.40	2.40	-	3.00	693.63
BW_01119	5.30	3.40	0.00	1.90	745.97
BW_01120	5.60	4.00	0.00	1.60	657.13
BW_01121	5.10	2.80	0.00	2.30	-
BW_01122	5.40	3.00	0.00	2.40	610.90
BW_01123	3.50	-	-	-	-
BW_01124	2.20	-	-	-	-
BW_01125	5.20	-	-	-	270.59
BW_01126	4.40	2.80	0.00	1.60	219.33
BW_01127	-	-	-	-	23.15
BW_01128	5.40	1.00	6.00	4.40	92.84
BW_01129	4.60	2.60	-	2.00	570.24
BW_01130	5.00	-	-	-	37.90
BW_01131	-	-	-	-	366.40
BW_01132	4.60	1.40	6.00	3.20	203.18
BW_01133	4.60	4.00	0.00	0.60	621.64
BW_01134	5.20	3.60	0.00	1.60	580.27
BW_01135	5.30	4.00	0.00	1.30	723.97
BW_01136	5.30	3.00	0.00	2.30	680.99
BW_01137	4.70	1.00	6.00	3.70	198.90
BW_01138	4.50	2.80	0.00	1.70	16.69
BW_01139	4.70	4.00	0.00	0.70	584.43
BW_01140	4.90	3.00	0.00	1.90	142.63
BW_01141	5.40	2.00	-	3.40	188.77
BW_01142	5.20	1.40	6.00	3.80	78.19
BW_01143	4.50	1.00	6.00	3.50	115.99
BW_01144	5.40	2.00	-	3.40	63.84
BW_01145	-	-	-	-	98.46

BW_01146	4.80	1.00	6.00	3.80	251.47
BW_01147	4.00	5.80	0.00	-1.80	538.35
BW_01148	2.10	-	-	-	33.83
BW_01149	-	-	-	-	116.86
BW_01150	-	-	-	-	101.50
BW_01151	5.00	1.00	6.00	4.00	489.00
BW_01152	3.00	-	-	-	266.75
BW_01153	5.75	1.00	6.00	4.75	50.67
BW_01154	5.70	-	-	-	-
BW_01155	4.80	1.00	6.00	3.80	130.48
BW_01156	4.40	1.00	6.00	3.40	19.37
BW_01158	3.60	-	-	-	19.50
BW_01159	5.20	3.00	0.00	2.20	19.67
BW_01160	-	-	-	-	253.47
BW_01161	4.60	3.20	0.00	1.40	161.32
BW_01162	4.50	3.60	0.00	0.90	544.25
BW_01163	4.30	3.80	0.00	0.50	482.92
BW_01164	4.50	-	-	-	233.37
BW_01165	2.63	-	-	-	11.35
BW_01166	-	-	-	-	439.71
BW_01167	5.30	5.80	0.00	-0.50	780.14
BW_01168	5.38	6.00	0.00	-0.63	690.60
BW_01170	4.60	3.80	0.00	0.80	461.59
BW_01171	5.10	4.60	0.00	0.50	281.22
BW_01172	3.90	-	-	-	52.16
BW_01174	-	-	-	-	705.40
BW_01175	5.20	4.00	0.00	1.20	457.96
BW_01176	5.40	3.20	0.00	2.20	296.19
BW_01177	4.38	1.20	6.00	3.18	106.63
BW_01178	4.70	2.60	-	2.10	487.11
BW_01179	5.70	0.80	6.00	4.90	232.44
BW_01181	4.20	3.40	0.00	0.80	646.12
BW_01182	5.70	-	-	-	130.13
BW_01184	3.80	-	-	-	562.94
BW_01185	4.20	3.40	0.00	0.80	403.51
BW_01186	3.38	-	-	-	499.43
BW_01189	4.20	-	-	-	-
BW_01190	4.30	1.00	6.00	3.30	-
BW_01192	5.40	3.20	0.00	2.20	-
BW_23925	-	-	-	-	215.40

* Extreme scores: Mean score of ≥ 2 and ≤ 2.6 were removed. Remaining scores reclassed as either resistant or susceptible and given a score of 6 or 0 respectively.

** NO6047+*Avr-Rmg8* DLA scores subtracted from NO6047 DLA scores

*** data provided by Paula Silva, KSU.

Supplementary table S4: Mean scores for the NIAB RIL population A DLA and DSA. Green = resistant, red = susceptible. Salmon = genotyped as susceptible.

Population A				
Accession	DLA		DSA Mean (6/7 dpi)	Melt-curve marker genotype
	Number of replicates	Mean (6 dpi)		
A2	1	2.00	3.67	82-sus
A3	1	5.00	5.00	82-sus
A4	1	3.00	4.00	82-sus
A5	1	5.00	4.67	82-sus
A6*	2	1.00	2.50	86-res
A7	1	5.00	4.33	86-res
A8	1	6.00	5.50	86-res
A9	1	6.00	5.33	82-sus
A10	1	3.00	3.00	82-sus
A11*	2	3.00	4.80	82-sus
A12	2	3.00	4.00	86-res
A13*	2	5.50	5.00	82-sus
A14	1	6.00	5.00	82-sus
A15	1	5.00	5.33	82-sus
A17	1	5.00	4.00	82-sus
A18	1	2.00	4.00	-
A19*	2	5.00	5.17	82-sus
A21*	2	3.50	4.78	86-res
A22*	2	5.50	5.83	86-res
A23*	2	5.00	5.50	82-sus
A24	1	2.00	-	-
A25*	2	5.00	5.83	82-sus
A26*	2	5.00	5.83	86-res
A27*	2	6.00	5.50	82-sus
A30	1	6.00	5.67	82-sus
A31	1	6.00	4.67	82-sus
A32	1	4.00	5.00	86-res
A33*	2	4.00	5.17	86-res
A34	1	2.00	5.00	86-res
A35*	2	6.00	5.17	82-sus
A36*	2	5.00	4.67	86-res
A37*	2	2.00	4.00	82-sus
A38*	2	6.00	5.40	82-sus
A39	1	2.00	4.00	86-res
A40	1	6.00	6.00	82-sus

A41	1	6.00	6.00	82-sus
A42	1	1.00	5.00	86-res
A43*	2	3.00	3.71	86-res
A44*	1	3.00	4.00	86-res
A46*	3	1.67	3.00	82-sus
A49*	2	2.00	4.83	82-sus
A50*	2	1.00	3.83	82-sus
A51	1	5.00	5.00	82-sus
A52	1	5.00	5.67	82-sus
A53*	2	3.00	4.60	82-sus
A54	1	4.00	6.00	86-res
A55	1	6.00	6.00	86-res
A56*	3	4.00	5.60	82-sus
A57*	1	4.00	5.00	82-sus
A59*	-	-	4.67	82-sus
A60	-	-	6.00	82-sus
A61	-	-	5.00	82-sus

* Sampled more than once in the DSA

Supplementary table S5: Mean scores for the NIAB RIL population B DLA and DSA. Green = resistant, red = susceptible. Salmon = genotyped as susceptible.

Population B				
Accession	DLA		DSA Mean (6/7 dpi)	Melt-curve marker genotype
	Number of replicates	Mean (6 dpi)		
B1*	-	-	3.13	82-sus
B2*	-	-	2.67	82-sus
B3	1	1.00	1.00	82-sus
B4	1	4.00	5.33	82-sus
B6*	3	6.00	4.67	82-sus
B7	1	4.00	4.67	86-res
B8	1	4.00	4.33	82-sus
B9*	1	5.00	3.67	82-sus
B10	1	5.00	5.00	82-sus
B11*	3	5.00	5.67	82-sus
B12	1	4.00	4.67	86-res
B13*	3	4.00	4.20	82-sus
B14	1	5.00	4.67	86-res
B15	1	5.00	5.00	-
B16*	2	5.00	4.75	82-sus
B17*	2	4.00	5.25	86-res
B18*	2	5.00	4.00	86-res
B19*	2	5.00	5.50	82-sus
B20*	2	1.50	3.00	86-res
B21*	1	2.00	4.33	82-sus
B22	1	2.00	4.67	82-sus
B23*	3	2.00	3.80	86-res
B24*	2	3.00	4.00	82-sus
B25	1	5.00	5.00	-
B27	1	6.00	5.67	82-sus
B28*	3	6.00	5.25	86-res
B29*	2	6.00	5.80	86-res
B30*	1	5.00	4.80	86-res
B31*	3	5.67	5.00	82-sus
B32	1	5.00	5.67	82-sus
B33*	1	5.00	5.00	82-sus
B34*	3	5.33	5.50	82-sus
B35*	2	5.50	5.80	82-sus
B36	1	4.00	4.33	82-sus
B37*	2	4.00	4.67	82-sus
B38*	3	6.00	5.00	82-sus

B39*	2	5.50	5.17	82-sus
B40*	2	4.50	5.50	86-res
B42*	2	1.00	3.40	86-res
B43*	3	5.67	5.50	86-res
B44*	2	2.00	5.00	82-sus
B45*	2	2.00	4.17	86-res
B46*	3	1.33	3.75	86-res
B49*	1	3.00	4.00	86-res
B50	1	4.00	3.67	86-res
B51*	2	3.50	4.75	82-sus

* Sampled more than once in the DSA

Supplementary table S6: Watkins landraces included in *M. oryzae* assays and their origin. Ancestral groups are as described in Wingen *et al.* (2014).

GRU^ No.	ID	Country of Origin	Ancestral Group	Group Code
WATDE0001	Wat1190004	Iraq	1.3.C-E-Asia	1.3
WATDE0002	Wat1190007	Australia	2.4.S-Med-Afr	2.4
WATDE0003	Wat1190023	Australia	2.5.N-Med	2.5
WATDE0004	Wat1190032	India	1.4.Eur-Asia	1.4
WATDE0005	Wat1190034	India	1.4.Eur-Asia	1.4
WATDE0007	Wat1190042	France	2.2.N-Eur-Asia	2.2
WATDE0008	Wat1190044	Morocco	2.4.S-Med-Afr	2.4
WATDE0009	Wat1190045	Syria	2.4.S-Med-Afr	2.4
WATDE0010	Wat1190079	India	2.4.S-Med-Afr	2.4
WATDE0011	Wat1190081	India	2.3.E-Eur	2.3
WATDE0013	Wat1190103	Italy	2.5.N-Med	2.5
WATDE0015	Wat1190126	India	1.4.Eur-Asia	1.4
WATDE0016	Wat1190127	India	1.1.USSR	1.1
WATDE0017	Wat1190139	France	2.5.N-Med	2.5
WATDE0018	Wat1190141	China	2.4.S-Med-Afr	2.4
WATDE0019	Wat1190145	Spain	2.4.S-Med-Afr	2.4
WATDE0020	Wat1190149	United Kingdom	2.2.N-Eur-Asia	2.2
WATDE0021	Wat1190160	Spain	Mix 2.1:5	2.1
WATDE0022	Wat1190181	Poland	2.2.N-Eur-Asia	2.2
WATDE0023	Wat1190199	India	Mix 1.3:4	1.4
WATDE0024	Wat1190209	Egypt	1.3.C-E-Asia	1.3
WATDE0025	Wat1190216	Morocco	2.4.S-Med-Afr	2.4
WATDE0026	Wat1190218	Tunisia	2.4.S-Med-Afr	2.4
WATDE0027	Wat1190219	Spain	2.4.S-Med-Afr	2.4
WATDE0028	Wat1190223	Burma	2.4.S-Med-Afr	2.4
WATDE0029	Wat1190224	China	2.4.S-Med-Afr	2.4
WATDE0030	Wat1190231	Hungary	2.2.N-Eur-Asia	2.2
WATDE0031	Wat1190238	Iran	1.4.Eur-Asia	1.4
WATDE0032	Wat1190239	Spain	Mix 2.4:5	2.5
WATDE0033	Wat1190246	India	1.3.C-E-Asia	1.3
WATDE0034	Wat1190254	Morocco	2.5.N-Med	2.5
WATDE0035	Wat1190264	Canary Islands	Mix 2.4:5	2.4
WATDE0036	Wat1190273	Spain	1.3.C-E-Asia	1.3
WATDE0037	Wat1190291	Cyprus	Mix 2.3:4	2.4
WATDE0038	Wat1190292	Cyprus	2.3.E-Eur	2.3
WATDE0039	Wat1190299	Turkey	1.3.C-E-Asia	1.3
WATDE0040	Wat1190300	Turkey	1.3.C-E-Asia	1.3
WATDE0041	Wat1190305	Egypt	2.4.S-Med-Afr	2.4
WATDE0042	Wat1190308	Iran	1.4.Eur-Asia	1.4
WATDE0046	Wat1190349	Bulgaria	2.5.N-Med	2.5
WATDE0047	Wat1190352	Yugoslavia	1.4.Eur-Asia	1.4
WATDE0048	Wat1190355	Yugoslavia	2.2.N-Eur-Asia	2.2
WATDE0049	Wat1190360	Yugoslavia	1.1.USSR	1.1
WATDE0050	Wat1190387	Spain	2.4.S-Med-Afr	2.4
WATDE0051	Wat1190396	Portugal	2.5.N-Med	2.5
WATDE0052	Wat1190397	Portugal	2.5.N-Med	2.5
WATDE0053	Wat1190398	Palestine	2.4.S-Med-Afr	2.4

WATDE0054	Wat1190406	India	1.3.C-E-Asia	1.3
WATDE0055	Wat1190420	India	1.3.C-E-Asia	1.3
WATDE0056	Wat1190433	India	1.4.Eur-Asia	1.4
WATDE0057	Wat1190440	China	1.2.Chi-Ind	1.2
WATDE0058	Wat1190444	China	2.4.S-Med-Afr	2.4
WATDE0060	Wat1190460	Afghanistan	2.2.N-Eur-Asia	2.2
WATDE0061	Wat1190468	Afghanistan	2.2.N-Eur-Asia	2.2
WATDE0062*	Wat1190471	Afghanistan	2.1.S-Eur-Asia	2.1
WATDE0063**	Wat1190474	Afghanistan	1.3.C-E-Asia	1.3
WATDE0064**	Wat1190475	Afghanistan	1.4.Eur-Asia	1.4
WATDE0066	Wat1190483	Poland	2.5.N-Med	2.5
WATDE0067	Wat1190496	Morocco	2.4.S-Med-Afr	2.4
WATDE0068	Wat1190507	Australia	2.1.S-Eur-Asia	2.1
WATDE0069	Wat1190546	Spain	2.4.S-Med-Afr	2.4
WATDE0070	Wat1190551	Spain	2.5.N-Med	2.5
WATDE0071	Wat1190560	Greece	2.4.S-Med-Afr	2.4
WATDE0072	Wat1190562	Greece	2.3.E-Eur	2.3
WATDE0073	Wat1190566	Greece	1.3.C-E-Asia	1.3
WATDE0074	Wat1190568	China	1.3.C-E-Asia	1.3
WATDE0075	Wat1190579	Iran	1.4.Eur-Asia	1.4
WATDE0076	Wat1190580	Iran	1.4.Eur-Asia	1.4
WATDE0077	Wat1190591	Portugal	1.3.C-E-Asia	1.3
WATDE0078	Wat1190605	Greece	1.1.USSR	1.1
WATDE0080	Wat1190627	Iran	1.2.Chi-Ind	1.2
WATDE0081	Wat1190629	Iran	1.2.Chi-Ind	1.2
WATDE0082	Wat1190637	Turkey	2.3.E-Eur	2.3
WATDE0083	Wat1190639	Crete	2.5.N-Med	2.5
WATDE0086	Wat1190662	Romania	2.3.E-Eur	2.3
WATDE0087	Wat1190670	Poland	Mix 2.3:5	2.3
WATDE0088	Wat1190671	USSR	1.4.Eur-Asia	1.4
WATDE0089	Wat1190680	Italy	1.4.Eur-Asia	1.4
WATDE0090	Wat1190683	Spain	2.5.N-Med	2.5
WATDE0091	Wat1190685	Spain	Mix 2.4:5	2.5
WATDE0092	Wat1190690	Greece	2.5.N-Med	2.5
WATDE0093	Wat1190694	India	1.2.Chi-Ind	1.2
WATDE0094	Wat1190698	China		
WATDE0095	Wat1190700	China	1.1.USSR	1.1
WATDE0096	Wat1190704	Iran	1.3.C-E-Asia	1.3
WATDE0097	Wat1190705	Iran		
WATDE0098	Wat1190707	India	1.2.Chi-Ind	1.2
WATDE0099	Wat1190722	China	2.2.N-Eur-Asia	2.2
WATDE0100	Wat1190729	Iran		
WATDE0101	Wat1190731	India	1.4.Eur-Asia	1.4
WATDE0102	Wat1190732	India	1.4.Eur-Asia	1.4
WATDE0104	Wat1190742	Algeria	2.4.S-Med-Afr	2.4
WATDE0105	Wat1190746	USSR	1.1.USSR	1.1
WATDE0106	Wat1190747	Ethiopia	1.1.USSR	1.1
WATDE0107	Wat1190749	USSR	1.1.USSR	1.1
WATDE0108	Wat1190750	USSR		
WATDE0110	Wat1190771	USSR	1.2.Chi-Ind	1.2
WATDE0111	Wat1190777	Finland	1.2.Chi-Ind	1.2

WATDE0112	Wat1190784	Italy	1.2.Chi-Ind	1.2
WATDE0113	Wat1190788	USSR	1.1.USSR	1.1
WATDE0114	Wat1190789	USSR	1.1.USSR	1.1
WATDE0115	Wat1190811	Tunisia	1.2.Chi-Ind	1.2
WATDE0116	Wat1190814	Tunisia	1.3.C-E-Asia	1.3
WATDE0117	Wat1190816	Italy	Mix 1.2:4	1.4
WATDE0118	Wat1190827	China	1.2.Chi-Ind	1.2
WATDE0126	Wat1190008	Portugal	2.4.S-Med-Afr	2.4
WATDE0133	Wat1190012	India	2.3.E-Eur	2.3
WATDE0138	Wat1190015	Yugoslavia	2.3.E-Eur	2.3
WATDE0149	Wat1190024	Australia	2.2.N-Eur-Asia	2.2
WATDE0156	Wat1190030	Australia	Mix 1.2:4	1.2
WATDE0171	Wat1190046	Crete	Mix 2.2:3	2.2
WATDE0180	Wat1190053	Spain	2.4.S-Med-Afr	2.4
WATDE0192	Wat1190063	Spain	2.3.E-Eur	2.3
WATDE0196	Wat1190066	Spain	2.4.S-Med-Afr	2.4
WATDE0198	Wat1190067	Spain	2.3.E-Eur	2.3
WATDE0215	Wat1190082	India	2.2.N-Eur-Asia	2.2
WATDE0216	Wat1190083	Spain	2.4.S-Med-Afr	2.4
WATDE0222	Wat1190088	Poland	1.3.C-E-Asia	1.3
WATDE0228	Wat1190094	India	2.5.N-Med	2.5
WATDE0238	Wat1190104	Italy	2.1.S-Eur-Asia	2.1
WATDE0241	Wat1190106	France	2.5.N-Med	2.5
WATDE0249	Wat1190114	Yugoslavia	1.1.USSR	1.1
WATDE0250	Wat1190115	Yugoslavia	2.4.S-Med-Afr	2.4
WATDE0253	Wat1190117	Spain	2.5.N-Med	2.5
WATDE0262	Wat1190124	India	1.4.Eur-Asia	1.4
WATDE0263	Wat1190125	India	Mix 2.1:3	2.3
WATDE0266	Wat1190129	India	2.3.E-Eur	2.3
WATDE0268	Wat1190130	Spain	2.5.N-Med	2.5
WATDE0276	Wat1190136	Australia	2.4.S-Med-Afr	2.4
WATDE0278	Wat1190138	Australia	2.2.N-Eur-Asia	2.2
WATDE0290	Wat1190151	Portugal	2.5.N-Med	2.5
WATDE0292	Wat1190153	Portugal	1.3.C-E-Asia	1.3
WATDE0294	Wat1190155	Portugal	1.1.USSR	1.1
WATDE0305	Wat1190164	India	2.1.S-Eur-Asia	2.1
WATDE0308	Wat1190166	India	1.4.Eur-Asia	1.4
WATDE0310	Wat1190167	India	2.4.S-Med-Afr	2.4
WATDE0335	Wat1190186	Italy	2.3.E-Eur	2.3
WATDE0336	Wat1190187	Italy	2.5.N-Med	2.5
WATDE0339	Wat1190189	France	2.2.N-Eur-Asia	2.2
WATDE0359	Wat1190206	India	Mix 2.1:2:3	2.3
WATDE0369	Wat1190213	Morocco	2.3.E-Eur	2.3
WATDE0375	Wat1190222	Crete	2.4.S-Med-Afr	2.4
WATDE0381	Wat1190228	Spain	2.4.S-Med-Afr	2.4
WATDE0382	Wat1190229	Portugal	2.5.N-Med	2.5
WATDE0385	Wat1190232	India	2.5.N-Med	2.5
WATDE0386	Wat1190233	India	2.3.E-Eur	2.3
WATDE0392	Wat1190237	Iran	1.4.Eur-Asia	1.4
WATDE0394	Wat1190240	Iran	2.5.N-Med	2.5
WATDE0396	Wat1190241	India	1.1.USSR	1.1

WATDE0397	Wat1190242	India	1.4.Eur-Asia	1.4
WATDE0405	Wat1190248	India	2.5.N-Med	2.5
WATDE0420	Wat1190260	Canary Islands	2.4.S-Med-Afr	2.4
WATDE0422	Wat1190262	Canary Islands	2.4.S-Med-Afr	2.4
WATDE0427	Wat1190268	Spain	2.5.N-Med	2.5
WATDE0430	Wat1190271	Spain	1.3.C-E-Asia	1.3
WATDE0435	Wat1190277	Spain	2.1.S-Eur-Asia	2.1
WATDE0445	Wat1190286	Greece	2.4.S-Med-Afr	2.4
WATDE0450	Wat1190290	Crete	1.3.C-E-Asia	1.3
WATDE0451	Wat1190293	Turkey	2.4.S-Med-Afr	2.4
WATDE0455	Wat1190297	Turkey	1.1.USSR	1.1
WATDE0456	Wat1190298	Turkey	1.4.Eur-Asia	1.4
WATDE0457	Wat1190301	Turkey	2.5.N-Med	2.5
WATDE0459	Wat1190302	Syria	1.1.USSR	1.1
WATDE0461	Wat1190304	Syria	2.4.S-Med-Afr	2.4
WATDE0476	Wat1190315	China	2.1.S-Eur-Asia	2.1
WATDE0477	Wat1190316	China	1.2.Chi-Ind	1.2
WATDE0479	Wat1190317	China	Mix 1.1:3	1.1
WATDE0486	Wat1190321	China	1.2.Chi-Ind	1.2
WATDE0509	Wat1190339	Portugal	2.5.N-Med	2.5
WATDE0518	Wat1190346	Bulgaria	2.3.E-Eur	2.3
WATDE0519	Wat1190347	Bulgaria	2.3.E-Eur	2.3
WATDE0521	Wat1190351	Yugoslavia	2.3.E-Eur	2.3
WATDE0526	Wat1190356	Yugoslavia	2.2.N-Eur-Asia	2.2
WATDE0532	Wat1190361	Yugoslavia	2.3.E-Eur	2.3
WATDE0534	Wat1190363	Yugoslavia	Mix 1.3:4	1.4
WATDE0542	Wat1190370	Yugoslavia	2.5.N-Med	2.5
WATDE0550	Wat1190376	Iran	1.1.USSR	1.1
WATDE0555	Wat1190379	Iran	1.3.C-E-Asia	1.3
WATDE0557	Wat1190381	India	1.3.C-E-Asia	1.3
WATDE0558	Wat1190382	India	1.1.USSR	1.1
WATDE0571	Wat1190394	Portugal	Mix 1.3:4	1.4
WATDE0574	Wat1190399	China	1.2.Chi-Ind	1.2
WATDE0576	Wat1190400	China	1.2.Chi-Ind	1.2
WATDE0577	Wat1190401	Portugal	2.4.S-Med-Afr	2.4
WATDE0579	Wat1190403	Spain	1.1.USSR	1.1
WATDE0581	Wat1190404	Iran	1.1.USSR	1.1
WATDE0582	Wat1190405	Iran	1.4.Eur-Asia	1.4
WATDE0585	Wat1190407	India	1.3.C-E-Asia	1.3
WATDE0588	Wat1190409	India	1.4.Eur-Asia	1.4
WATDE0592	Wat1190412	India	2.5.N-Med	2.5
WATDE0594	Wat1190413	India	1.3.C-E-Asia	1.3
WATDE0596	Wat1190414	India	2.3.E-Eur	2.3
WATDE0601	Wat1190419	India	1.3.C-E-Asia	1.3
WATDE0604	Wat1190423	India	1.3.C-E-Asia	1.3
WATDE0606	Wat1190424	India	1.4.Eur-Asia	1.4
WATDE0609	Wat1190426	India	1.4.Eur-Asia	1.4
WATDE0611	Wat1190428	India	1.3.C-E-Asia	1.3
WATDE0612	Wat1190429	India	1.4.Eur-Asia	1.4
WATDE0613	Wat1190430	India	1.3.C-E-Asia	1.3
WATDE0617	Wat1190435	China	1.3.C-E-Asia	1.3

WATDE0631	Wat1190446	China	1.2.Chi-Ind	1.2
WATDE0634	Wat1190448	Romania	1.2.Chi-Ind	1.2
WATDE0635	Wat1190449	Romania	1.2.Chi-Ind	1.2
WATDE0639	Wat1190453	Afghanistan	2.4.S-Med-Afr	2.4
WATDE0643	Wat1190456	Afghanistan	1.4.Eur-Asia	1.4
WATDE0646	Wat1190458	Afghanistan	2.4.S-Med-Afr	2.4
WATDE0651	Wat1190463	Afghanistan	2.5.N-Med	2.5
WATDE0653	Wat1190465	Afghanistan	1.4.Eur-Asia	1.4
WATDE0659	Wat1190470	Afghanistan	2.3.E-Eur	2.3
WATDE0661	Wat1190473	Afghanistan	1.1.USSR	1.1
WATDE0664	Wat1190478	Afghanistan	1.4.Eur-Asia	1.4
WATDE0668	Wat1190484	Italy	2.3.E-Eur	2.3
WATDE0669	Wat1190485	Algeria	1.4.Eur-Asia	1.4
WATDE0670	Wat1190486	USSR	1.1.USSR	1.1
WATDE0671	Wat1190487	USSR	1.4.Eur-Asia	1.4
WATDE0678	Wat1190492	Spain	Mix 2.2:5	2.2
WATDE0679	Wat1190493	Tunisia	1.1.USSR	1.1
WATDE0694	Wat1190505	Iran	1.3.C-E-Asia	1.3
WATDE0699	Wat1190509	Portugal	1.3.C-E-Asia	1.3
WATDE0702	Wat1190512	India	1.4.Eur-Asia	1.4
WATDE0703	Wat1190513	Iran	1.4.Eur-Asia	1.4
WATDE0705	Wat1190515	Iran	2.5.N-Med	2.5
WATDE0708	Wat1190517	India		
WATDE0712	Wat1190520	India	2.1.S-Eur-Asia	2.1
WATDE0714	Wat1190522	India	1.1.USSR	1.1
WATDE0725	Wat1190528	China	1.4.Eur-Asia	1.4
WATDE0727**	Wat1190530	Afghanistan	2.1.S-Eur-Asia	2.1
WATDE0732	Wat1190534	Morocco	2.3.E-Eur	2.3
WATDE0737	Wat1190538	Tunisia	Mix 2.4:5	2.4
WATDE0740	Wat1190541	Spain	2.5.N-Med	2.5
WATDE0743	Wat1190543	Spain	2.5.N-Med	2.5
WATDE0747	Wat1190547	Spain	1.3.C-E-Asia	1.3
WATDE0749	Wat1190549	Spain	2.5.N-Med	2.5
WATDE0751	Wat1190552	Canary Islands	2.4.S-Med-Afr	2.4
WATDE0758	Wat1190557	Canary Islands	1.4.Eur-Asia	1.4
WATDE0761	Wat1190561	Crete	1.3.C-E-Asia	1.3
WATDE0762	Wat1190563	Crete	2.4.S-Med-Afr	2.4
WATDE0765	Wat1190565	Greece	1.3.C-E-Asia	1.3
WATDE0770	Wat1190571	Turkey	2.5.N-Med	2.5
WATDE0771	Wat1190572	Syria	1.4.Eur-Asia	1.4
WATDE0773	Wat1190573	Turkey	1.4.Eur-Asia	1.4
WATDE0774	Wat1190574	Turkey	1.3.C-E-Asia	1.3
WATDE0776	Wat1190576	Iran	1.4.Eur-Asia	1.4
WATDE0779	Wat1190578	Iran	2.4.S-Med-Afr	2.4
WATDE0782	Wat1190583	China	1.2.Chi-Ind	1.2
WATDE0788	Wat1190587	China	1.3.C-E-Asia	1.3
WATDE0791	Wat1190590	Portugal	2.1.S-Eur-Asia	2.1
WATDE0795	Wat1190594	Portugal	1.3.C-E-Asia	1.3
WATDE0798	Wat1190596	Portugal	1.3.C-E-Asia	1.3
WATDE0801	Wat1190598	Portugal	2.5.N-Med	2.5
WATDE0808	Wat1190604	Spain	1.4.Eur-Asia	1.4

WATDE0811	Wat1190607	Yugoslavia	2.5.N-Med	2.5
WATDE0816	Wat1190611	Yugoslavia	1.1.USSR	1.1
WATDE0819	Wat1190614	Yugoslavia	2.1.S-Eur-Asia	2.1
WATDE0827	Wat1190619	Yugoslavia	2.1.S-Eur-Asia	2.1
WATDE0831	Wat1190622	Bulgaria	2.3.E-Eur	2.3
WATDE0833	Wat1190623	Bulgaria	2.3.E-Eur	2.3
WATDE0835	Wat1190625	Iran	1.3.C-E-Asia	1.3
WATDE0843	Wat1190633	India	1.1.USSR	1.1
WATDE0857	Wat1190644	India	1.3.C-E-Asia	1.3
WATDE0861	Wat1190646	India	1.2.Chi-Ind	1.2
WATDE0863	Wat1190648	China	1.3.C-E-Asia	1.3
WATDE0864	Wat1190649	China	1.2.Chi-Ind	1.2
WATDE0865	Wat1190650	China	1.1.USSR	1.1
WATDE0868	Wat1190653	China	1.2.Chi-Ind	1.2
WATDE0871	Wat1190655	China	1.2.Chi-Ind	1.2
WATDE0873	Wat1190657	China	1.2.Chi-Ind	1.2
WATDE0882	Wat1190667	Afghanistan	2.4.S-Med-Afr	2.4
WATDE0883	Wat1190668	Yugoslavia	1.4.Eur-Asia	1.4
WATDE0888	Wat1190673	USSR	1.3.C-E-Asia	1.3
WATDE0892	Wat1190676	Tunisia	2.3.E-Eur	2.3
WATDE0895	Wat1190678	Iran	1.4.Eur-Asia	1.4
WATDE0898	Wat1190681	Iran	2.4.S-Med-Afr	2.4
WATDE0909	Wat1190695	China	1.4.Eur-Asia	1.4
WATDE0911	Wat1190697	India	1.1.USSR	1.1
WATDE0919	Wat1190711	India	1.3.C-E-Asia	1.3
WATDE0929	Wat1190719	China	1.3.C-E-Asia	1.3
WATDE0932	Wat1190721	China	1.3.C-E-Asia	1.3
WATDE0934	Wat1190724	India	2.2.N-Eur-Asia	2.2
WATDE0937	Wat1190726	China	1.2.Chi-Ind	1.2
WATDE0938	Wat1190727	China		
WATDE0939	Wat1190728	Iraq	1.2.Chi-Ind	1.2
WATDE0950	Wat1190737	Italy	2.3.E-Eur	2.3
WATDE0954	Wat1190743	USSR		
WATDE0963	Wat1190752	USSR		
WATDE0971	Wat1190759	USSR	Mix 2.1:5	2.5
WATDE0973	Wat1190760	USSR	Mix 1.1:4	1.1
WATDE0984	Wat1190769	Algeria	1.1.USSR	1.1
WATDE0986	Wat1190770	USSR	Mix 2.4:5	2.5
WATDE0989	Wat1190773	USSR	1.3.C-E-Asia	1.3
WATDE0991	Wat1190774	Ethiopia	1.3.C-E-Asia	1.3
WATDE0993	Wat1190775	USSR	1.1.USSR	1.1
WATDE1012	Wat1190794	USSR	1.4.Eur-Asia	1.4
WATDE1025	Wat1190802	USSR	1.1.USSR	1.1
WATDE1026	Wat1190803	India	1.2.Chi-Ind	1.2
WATDE1027	Wat1190804	USSR	2.2.N-Eur-Asia	2.2
WATDE1030	Wat1190806	Italy	1.4.Eur-Asia	1.4
WATDE1051	Wat1190823	China	1.2.Chi-Ind	1.2
WATDE1052	Wat1190824	China	1.2.Chi-Ind	1.2
WATDE1060	Wat1190903	India	1.1.USSR	1.1
Baj	Baj			
Becard /Kachu	Becard /Kachu			

Chinese Spring	Chinese Spring
CIMCOG 03	CIMCOG 03
CIMCOG 26	CIMCOG 26
CIMCOG 32	CIMCOG 32
CIMCOG 47	CIMCOG 47
CIMCOG 49	CIMCOG 49
CIMCOG 53	CIMCOG 53
CIMCOG 56	CIMCOG 56
MISR1	MISR1
Pamyat Azieva	Pamyat Azieva
Paragon	Paragon
Pfau**	Pfau
Reedling**	Reedling
Sears Synth Type*	Sears Synth Type
Super 152	Super 152
Waxwing	Waxwing
Weebill	Weebill
Wyalkatchem*	Wyalkatchem

⊥Germplasm Resources Unit, John Innes Centre, Norwich, NR4 7UH, UK

* WATDE0062, Sears Synth Type and Wyalkatchem were excluded from *Arv8* DLA

** WATDE0063, WATDE0064 and WATDE0727 were excluded from SRA DLA

Supplementary table S7: Mean scores from the Watkins core NO6047+*Avr-Rmg8* and SRA DLAs.

GRU store code	Mean (5 dpi)	
	NO6047+*Avr-Rmg8*	SRA
WATDE0001	3.67	4.50
WATDE0002	4.33	3.50
WATDE0003	3.33	3.67
WATDE0004	2.67	3.33
WATDE0005	3.67	5.00
WATDE0007	4.00	5.33
WATDE0008	3.33	4.00
WATDE0009	4.33	3.67
WATDE0010	3.33	4.33
WATDE0011	3.33	5.33
WATDE0013	4.67	5.00
WATDE0015	2.33	0.50
WATDE0016	5.33	5.67
WATDE0017	5.67	4.00
WATDE0018	4.67	3.33
WATDE0019	2.33	3.67
WATDE0020	4.33	5.00
WATDE0021	4.33	4.33
WATDE0022	4.33	5.67
WATDE0023	4.50	6.00
WATDE0024	4.67	5.33
WATDE0025	4.00	4.00
WATDE0026	3.00	1.67
WATDE0027	3.67	4.33
WATDE0028	5.67	4.33
WATDE0029	3.00	3.33
WATDE0030	4.67	4.67
WATDE0031	5.00	5.33
WATDE0032	4.00	3.33
WATDE0033	4.00	3.67
WATDE0034	3.00	4.00
WATDE0035	4.33	6.00
WATDE0036	6.00	5.33
WATDE0037	4.00	5.00
WATDE0038	3.67	5.67
WATDE0039	4.33	6.00
WATDE0040	4.00	5.33
WATDE0041	4.67	5.33
WATDE0042	3.67	5.33
WATDE0046	1.33	2.33
WATDE0047	4.33	5.00
WATDE0048	4.33	5.33

WATDE0049	3.33	4.33
WATDE0050	3.67	3.33
WATDE0051	1.67	2.67
WATDE0052	3.67	5.00
WATDE0053	5.67	5.00
WATDE0054	5.00	5.67
WATDE0055	4.33	5.67
WATDE0056	5.33	4.67
WATDE0057	4.67	4.67
WATDE0058	0.33	4.33
WATDE0060	5.33	5.33
WATDE0061	5.67	5.33
WATDE0062	-	2.00
WATDE0063	4.00	-
WATDE0064	5.33	-
WATDE0066	1.67	4.67
WATDE0067	3.00	4.33
WATDE0068	4.67	4.33
WATDE0069	5.33	3.00
WATDE0070	4.00	3.33
WATDE0071	4.67	2.00
WATDE0072	3.67	5.00
WATDE0073	3.67	3.67
WATDE0074	4.00	3.67
WATDE0075	2.67	3.67
WATDE0076	4.00	4.00
WATDE0077	3.67	2.67
WATDE0078	4.67	4.33
WATDE0080	6.00	6.00
WATDE0081	4.33	4.67
WATDE0082	4.67	4.00
WATDE0083	3.67	4.67
WATDE0086	4.00	3.00
WATDE0087	6.00	6.00
WATDE0088	5.33	5.50
WATDE0089	4.67	4.00
WATDE0090	2.33	2.00
WATDE0091	5.33	6.00
WATDE0092	4.67	6.00
WATDE0093	5.67	6.00
WATDE0094	5.67	5.67
WATDE0095	4.67	6.00
WATDE0096	4.33	5.00
WATDE0097	5.67	6.00
WATDE0098	5.33	4.67
WATDE0099	3.67	5.50

WATDE0100	5.00	5.33
WATDE0101	4.33	6.00
WATDE0102	1.00	1.00
WATDE0104	3.33	5.33
WATDE0105	6.00	5.67
WATDE0106	5.67	5.67
WATDE0107	4.00	6.00
WATDE0108	5.33	4.67
WATDE0110	5.33	6.00
WATDE0111	5.67	6.00
WATDE0112	5.33	5.33
WATDE0113	5.00	6.00
WATDE0114	6.00	6.00
WATDE0115	6.00	6.00
WATDE0116	5.33	6.00
WATDE0117	6.00	6.00
WATDE0118	6.00	6.00
WATDE0126	1.00	2.50
WATDE0133	3.67	6.00
WATDE0138	5.00	6.00
WATDE0149	4.00	6.00
WATDE0156	4.33	4.00
WATDE0171	0.33	1.33
WATDE0180	4.33	4.67
WATDE0192	3.00	4.00
WATDE0196	4.33	4.00
WATDE0198	2.67	3.67
WATDE0215	5.00	6.00
WATDE0216	2.00	3.33
WATDE0222	3.00	4.67
WATDE0228	4.67	6.00
WATDE0238	2.67	4.33
WATDE0241	2.33	4.33
WATDE0249	4.67	5.33
WATDE0250	4.67	3.67
WATDE0253	5.00	3.67
WATDE0262	6.00	5.33
WATDE0263	4.33	6.00
WATDE0266	2.33	5.67
WATDE0268	2.67	2.33
WATDE0276	6.00	3.67
WATDE0278	6.00	4.00
WATDE0290	5.00	3.33
WATDE0292	5.00	6.00
WATDE0294	4.67	4.33
WATDE0305	3.00	4.67

WATDE0308	5.67	5.00
WATDE0310	0.67	0.00
WATDE0335	4.33	5.67
WATDE0336	4.00	4.67
WATDE0339	5.00	4.67
WATDE0359	4.67	5.33
WATDE0369	3.00	1.33
WATDE0375	6.00	4.33
WATDE0381	1.33	2.67
WATDE0382	5.67	4.67
WATDE0385	4.33	3.67
WATDE0386	2.33	2.67
WATDE0392	4.00	4.33
WATDE0394	5.67	6.00
WATDE0396	6.00	6.00
WATDE0397	6.00	6.00
WATDE0405	2.00	4.00
WATDE0420	5.33	6.00
WATDE0422	4.67	6.00
WATDE0427	1.00	0.00
WATDE0430	4.33	5.67
WATDE0435	4.67	4.33
WATDE0445	4.67	4.67
WATDE0450	4.00	3.33
WATDE0451	4.67	5.67
WATDE0455	5.67	5.67
WATDE0456	4.67	5.50
WATDE0457	3.33	5.00
WATDE0459	4.67	6.00
WATDE0461	5.67	4.67
WATDE0476	4.00	4.67
WATDE0477	0.00	0.00
WATDE0479	5.67	5.67
WATDE0486	6.00	6.00
WATDE0509	4.00	5.67
WATDE0518	4.33	4.33
WATDE0519	2.00	3.33
WATDE0521	4.33	6.00
WATDE0526	1.00	0.67
WATDE0532	2.67	3.67
WATDE0534	5.33	6.00
WATDE0542	3.67	4.33
WATDE0550	3.67	6.00
WATDE0555	4.67	4.00
WATDE0557	5.33	6.00
WATDE0558	4.67	4.33

WATDE0571	0.67	0.00
WATDE0574	5.33	5.00
WATDE0576	4.67	4.67
WATDE0577	5.67	6.00
WATDE0579	3.33	3.67
WATDE0581	3.33	4.00
WATDE0582	3.67	5.00
WATDE0585	5.33	5.67
WATDE0588	4.67	5.33
WATDE0592	4.33	6.00
WATDE0594	4.00	5.33
WATDE0596	2.67	5.67
WATDE0601	1.67	4.00
WATDE0604	3.33	4.00
WATDE0609	5.33	6.00
WATDE0611	3.33	5.67
WATDE0612	5.00	5.67
WATDE0613	3.00	5.33
WATDE0617	5.67	6.00
WATDE0631	5.33	6.00
WATDE0634	4.33	4.33
WATDE0635	6.00	5.67
WATDE0639	5.00	6.00
WATDE0643	5.00	5.67
WATDE0646	4.67	5.67
WATDE0651	3.67	6.00
WATDE0653	6.00	6.00
WATDE0659	5.67	6.00
WATDE0661	5.33	6.00
WATDE0664	4.33	5.33
WATDE0668	3.00	5.00
WATDE0669	2.67	4.33
WATDE0670	3.67	6.00
WATDE0671	5.33	6.00
WATDE0678	4.00	5.67
WATDE0679	2.33	5.00
WATDE0694	4.00	4.33
WATDE0699	5.67	5.00
WATDE0702	2.33	4.33
WATDE0703	3.00	4.00
WATDE0705	3.67	4.33
WATDE0708	3.33	5.00
WATDE0712	6.00	4.67
WATDE0714	5.00	5.33
WATDE0725	4.00	4.00
WATDE0727	5.00	-

WATDE0732	3.33	4.67
WATDE0737	4.00	5.00
WATDE0740	4.33	5.00
WATDE0743	4.33	4.67
WATDE0747	2.00	4.00
WATDE0749	1.67	3.67
WATDE0751	3.00	5.00
WATDE0758	3.00	5.67
WATDE0761	4.67	3.00
WATDE0762	4.00	3.33
WATDE0765	3.33	3.00
WATDE0770	3.67	4.00
WATDE0771	2.67	2.67
WATDE0773	4.33	3.33
WATDE0774	6.00	4.33
WATDE0776	4.00	3.67
WATDE0779	1.67	2.00
WATDE0782	5.33	4.33
WATDE0788	5.00	3.33
WATDE0791	6.00	5.00
WATDE0795	2.33	2.33
WATDE0798	4.33	3.00
WATDE0801	5.00	5.00
WATDE0808	4.67	3.67
WATDE0811	2.67	3.00
WATDE0816	4.67	3.50
WATDE0819	3.33	4.00
WATDE0827	3.00	3.33
WATDE0831	4.67	4.67
WATDE0833	4.67	5.67
WATDE0835	6.00	5.67
WATDE0843	4.00	4.67
WATDE0857	5.33	5.67
WATDE0861	5.33	5.00
WATDE0863	5.00	5.00
WATDE0864	5.33	4.50
WATDE0865	4.00	4.00
WATDE0868	4.67	2.67
WATDE0871	5.00	5.33
WATDE0873	5.33	1.67
WATDE0882	4.33	6.00
WATDE0883	5.67	6.00
WATDE0888	6.00	6.00
WATDE0892	4.33	4.33
WATDE0895	6.00	6.00
WATDE0898	3.33	3.67

WATDE0909	5.00	6.00
WATDE0911	6.00	5.50
WATDE0919	5.00	4.67
WATDE0929	3.00	3.67
WATDE0932	6.00	5.00
WATDE0934	5.33	4.33
WATDE0937	6.00	5.00
WATDE0938	6.00	5.67
WATDE0939	5.33	5.00
WATDE0950	4.67	4.67
WATDE0954	4.67	5.33
WATDE0963	4.67	5.00
WATDE0971	0.67	0.00
WATDE0973	0.33	0.33
WATDE0984	2.00	4.67
WATDE0986	5.67	5.67
WATDE0989	4.33	6.00
WATDE0991	4.33	5.00
WATDE0993	5.00	6.00
WATDE1012	4.33	6.00
WATDE1025	5.67	6.00
WATDE1026	6.00	6.00
WATDE1027	4.67	6.00
WATDE1030	5.67	6.00
WATDE1051	4.33	5.33
WATDE1052	5.33	5.00
WATDE1060	6.00	6.00
Baj	5.33	6.00
Chinese Spring	5.33	6.00
CIMCOG 03	4.67	6.00
CIMCOG 12	5.00	6.00
CIMCOG 26	4.67	4.67
CIMCOG 32	4.33	4.33
CIMCOG 47	3.67	5.67
CIMCOG 49	5.67	6.00
CIMCOG 53	5.67	6.00
CIMCOG 56	4.67	6.00
CIMCOG33	5.67	6.00
CIMCOG39	5.00	5.33
Fielder	5.00	6.00
Pamyat Azieva	6.00	6.00
Paragon	5.33	6.00
Pfau	6.00	-
Reedling	5.00	-
Sears Synth Type	-	1.33
Waxwing	5.33	6.00

Weebil	5.00	5.33
Wyalkatchem	-	5.00

Supplementary table S8: All regions within the Mattis 2A resistant haplotype that show expression.

Gene code*	Coordinates (orientation)	Function (NLR-Annotator prediction)	RNAseq read coverage**	TOH code
TraesSYM2A03G00828360	788728552 - 788738447(+)	Receptor-like kinase	good coverage, 7 exons	MA4
TraesSYM2A03G00828400	788828264 - 788832085(+)	methyltransferases superfamily protein	good coverage, 8 exons**	MA5
TraesSYM2A03G00828410	788833791 - 788837343(+)	RNase P 1	good coverage	MA6
TraesSYM2A03G00828420	788837936 - 788839387(+)	STAY-GREEN LIKE, chloroplastic	very high coverage, 3 exons	MA7
-	788878849 - 788879888(-)	-	very high coverage, 2 exons	MA8
TraesSYM2A03G00828460	788885045 - 788890732(+)	resistance protein RGA2 (complete NLR)	very poor coverage	NLR2
TraesSYM2A03G00828620*	789199752 - 789200675(+)	*unknown*	very high coverage, ~2 exons	MA9
TraesSYM2A03G00828720	789284536 - 789289459(+)	resistance protein RGA2 (complete NLR)	only a few reads	NLR8
TraesSYM2A03G00829500*	792396765 - 792399256(-)	*unknown*	moderate coverage, 3 exons**	MA11
TraesSYM2A03G00829510	792400216 - 792404527(-)	N-methyltransferase SUVR4	moderate coverage, 8 exons	MA12
TraesSYM2A03G00829540	792410750 - 792414847(-)	glycosyltransferase subunit 1	good coverage, 8 exons	MA13
TraesSYM2A03G00829580	792519361 - 792525805(-)	toxin-like protein Hfr-2	very high coverage, 2 exons	MA14
TraesSYM2A03G00829620	792554319 - 792557912(+)	domain-containing protein 78	moderate coverage, 5 exons	MA15
TraesSYM2A03G00829630	792559869 - 792562916(+)	protein Rab-18	very high coverage, 6 exons	MA16
TraesSYM2A03G00829660	792670265 - 792673854(+)	resistance protein RGA2	poor coverage, 2 exons	MA17
TraesSYM2A03G00829810	792928596 - 792934980(+)	peptidase	poor coverage	MA18
TraesSYM2A03G00829820	792935138 - 792938913(-)	transporter NIPA (DUF803)	high coverage, 9 exons	MA19
TraesSYM2A03G00830300	793618964 - 793626781(+)	excision repair protein	moderate coverage, 16 exons	MA24
TraesSYM2A03G00830320*	793666286 - 793669583(+)	Receptor-like kinase (complete NLR)	poor coverage	MA25/NLR26
TraesSYM2A03G00830440	793864325 - 793867928(-)	transcription factor 28	moderate coverage, 6 exons	MA28

* Indicates low confidence genes

** Shows expression in only one dataset